A LITHOGEOCHEMICAL STUDY OF THE HOST ROCKS OF THE STRICKLAND SHOWING

PAULA JANE WYNNE

A LITHOGEOCHEMICAL STUDY OF THE HOST ROCKS OF THE STRICKLAND SHOWING

© PAULA JANE WYNNE, B.Sc.

A thesis submitted in partial fulfillment

of the requirements for the degree of

Master of Science

Department of Earth Sciences

Memorial University of Newfoundland

May, 1983

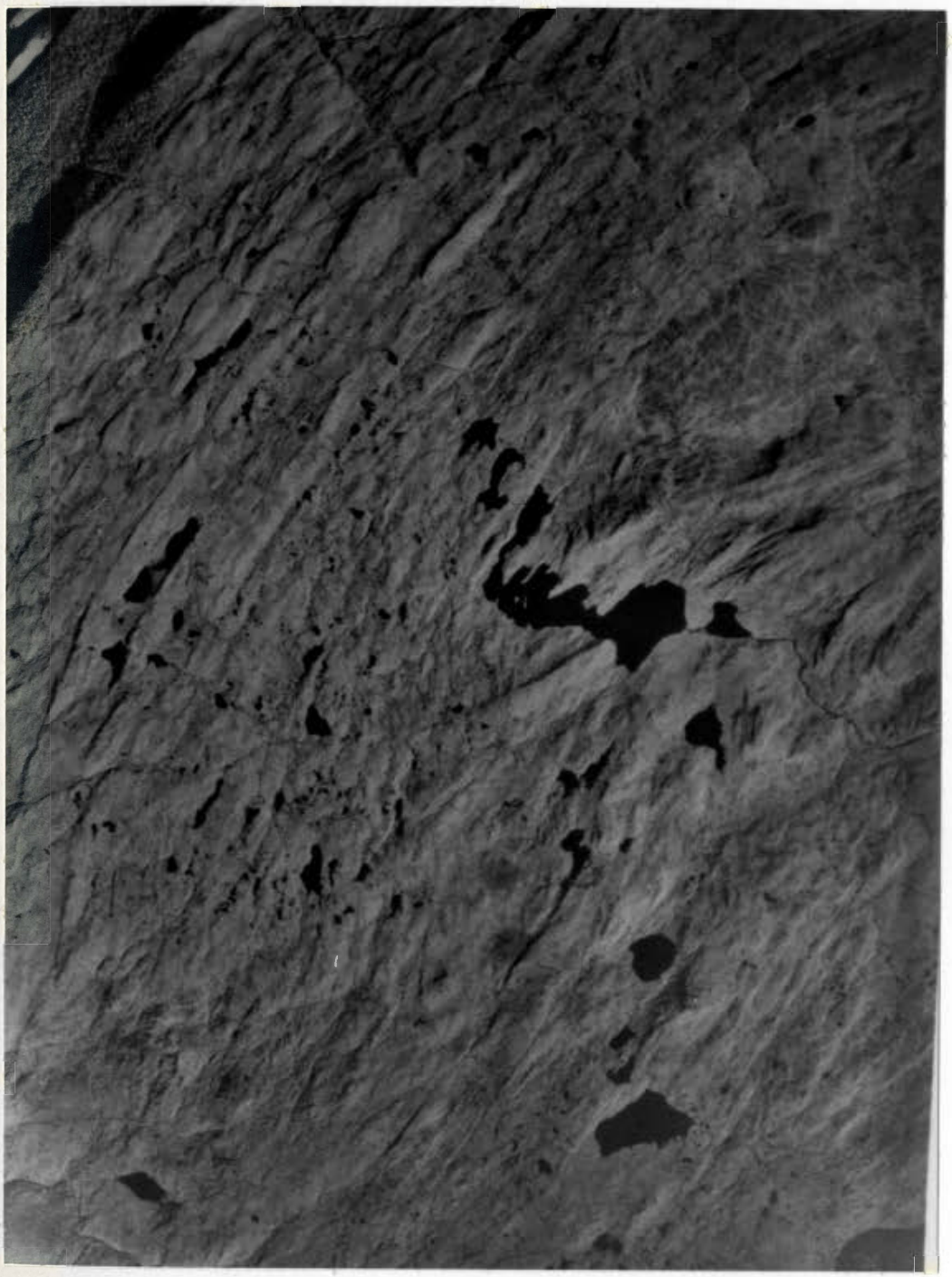

Frontispiece: The Strickland area, approximate scale 1:198,000, north is parallel to the side margin.

ABSTRACT

The Strickland showing consists of several zones of Zn-Pb-Cu-Ag mineralization hosted in a sequence of volcanic, volcaniclastic and sedimentary rocks which form a coherent belt stretching for 100 km along the south coast of Newfoundland. The sequence has been metamorphosed to upper greenschist facies and subjected to inhomogeneous cataclastic deformation. The mineralization identified in five principle zones (Main, Bog, Silver Hill, Copper and Carrot Brook) is interpreted to have been emplaced synvolcanically. This investigation is concerned with the identification of lithogeochemical signatures in the host rocks, produced by the mineralizing events.

A total of 294 surface and 292 diamond drill core samples were collected in the Strickland area. They were analyzed for SiO_2, TiO_2, Al_2O_3, FeO, MnO, MgO, CaO, K_2O, Na_2O, P_2O_5 and LOI (loss on ignition). Most were also analysed for Cu, Pb, Zn and Ag and a selected number of surface samples for Zn, Sr, Rb, U, Th, Ga and Y.

Two statistical approaches were taken in which regression techniques were used to generate residual values for elements in an effort to remove the effects of the rocks' primary composition, i.e. to define anomalies related to mineralization irrespective of lithology. In the first approach discriminant analysis showed that the elements

TiO_2, Al_2O_3 and FeO contributed most to the discrimination between lithologies. These elements were then used as independent variables in curvilinear regression equations with which residual values were calculated. A second more refined approach was taken where the data were divided into three groups based on lithology (igneous, sedimentary and mixed) and TiO_2 (an index of differentiation) was used as the independent variable in curvilinear regression equations to generate residuals for the igneous and mixed groups. Anomalous residual values combined with anomalous analyses from the sedimentary group are referred to as the second pass anomalies. These were found to be more effective in identifying anomalous samples irrespective of lithology than plots of the raw data or first approach residuals.

The surface distribution of the anomalies from the second approach tend to be in sporadic, elongate, strike-parallel clusters except for a single cluster which stretches southeast across strike from the Copper Zone. It is marked by a lithogeochemical signature typical of hydrothermal conduits as observed beneath other massive sulphide deposits (positive SiO_2 and negative Na_2O, Al_2O_3 and CaO anomalies). Mineralization, typically silver rich, associated with carbonate-tremolite gangue (Main Zone and especially in the Silver Hill Zone) is marked by persistant positive MgO, CaO, FeO and negative Na_2O and SiO_2 anomalies.

A horizon 25 m stratigraphically below the Silver Hill Zone characterized by negative Na_2O anomalies and positive

K_2O anomalies is interpreted to be a stratiform hydrothermal conduit.

The Strickland showing is analogous in some respects (age, host lithology, mineralization, Pb-isotopes) to the Bathurst camp of New Brunswick and it is therefore reasonable to speculate that, as in the Bathurst camp, other sulphide accumulations lay, as yet undiscovered, in the sequence of rocks which hosts the Strickland.

When compared with regionally correlative rocks, those associated with the Strickland rocks (felsic flows in particular) are clearly anomalously low in sodium. The low sodium concentration of the Strickland volcanics, typical of the host rocks of many other volcanogenic massive sulphide deposits may prove to be a useful exploration tool in identifying such mineralized areas on a regional basis.

ACKNOWLEDGEMENTS

This thesis has truly been a group effort. As thesis advisor Dr. D.F. Strong struck the perfect and delicate balance of guidance and suppport without interference. His patience, encouragement and optimism have been unfailing - thank you sir. This thesis was supported in part by a Memorial University Graduate Fellowship. The project received the financial and logistical support of Falconbridge Nickel Mines Ltd. I thank Falconbridge geologists Denis Prince and Neil Briggs who were always available with advice and suggestions.

My thanks are extended to Deanna Purvis for her cheerful and able assistance in the field; to the technical staff of the Earth Sciences Department at Memorial University of Newfoundland, in particular Dave Press and Gertrude Andrews for their help in the lab and to Foster Thornhill and Lloyd Warford who prepared all the petrographic sections.

Many thanks to Dr. Wm. Shaw and the members of the Geology Department at St. Francis Xavier University who very generously provided office space during the writing up stage of this thesis. I am grateful to the professional skills of Cathy Mason who typed the thesis and Brenda Randall who assisted with the drafting. Without the cooperation of the staff at the Memorial and St. F.X. computing centers this thesis would not be; I thank them all.

Finally, I wish to thank my husband Alan, to whom I owe a lasting debt of gratitude for his understanding and forbearance during this project.

TABLE OF CONTENTS

Table of Contents continued

Table of Contents continued

Table of Contents continued

Table of Contents continued

LIST OF TABLES

List of Tables continued

LIST OF FIGURES

... Continued

LIST OF FIGURES (continued)

... Continued

LIST OF FIGURES (continued)

... Continued

LIST OF FIGURES (continued)

... Continued

LIST OF FIGURES (continued)

... Continued

LIST OF FIGURES (continued)

.... Continued

LIST OF FIGURES (continued)

... Continued

LIST OF FIGURES (continued)

... Continued

LIST OF FIGURES (continued)

POCKET MAPS

CHAPTER 1

INTRODUCTION

1.1 Characteristics of volcanogenic massive sulphide deposits

1.1.1 Physical characteristics

Volcanogenic massive sulphide deposits (V.M.S.) share many similar features which are the product of their common genesis (see recent reviews by Ishihara, 1974; Sangster, 1972a; Scott and Sangster, 1976; Franklin, Lydon and Sangster, 1981). They are formed by the emanation onto the sea floor of hydrothermal brines, rich in metals. They are associated with rock types ranging from purely volcanic (dominantly calc-alkaline and explosive) to purely sedimentary. They are characteristically represented by the trinity of (i) a thin chert horizon conformably overlying (ii) a stratiform lense of massive base/precious metal sulphides, which in turn is underlain by (iii) a funnel shaped "stockwork" zone of veined and disseminated mineralization which transects the underlying lithologies. (These features and others described below are summarized in Figure 1.1).

The ore minerals are commonly zonally distributed, with chalcopyrite and pyrite more concentrated near the base and sphalerite with galena concentrated towards the top of the stratiform ore body. Some Phanerozoic deposits contain a significant amount of sulphate gangue which may also be

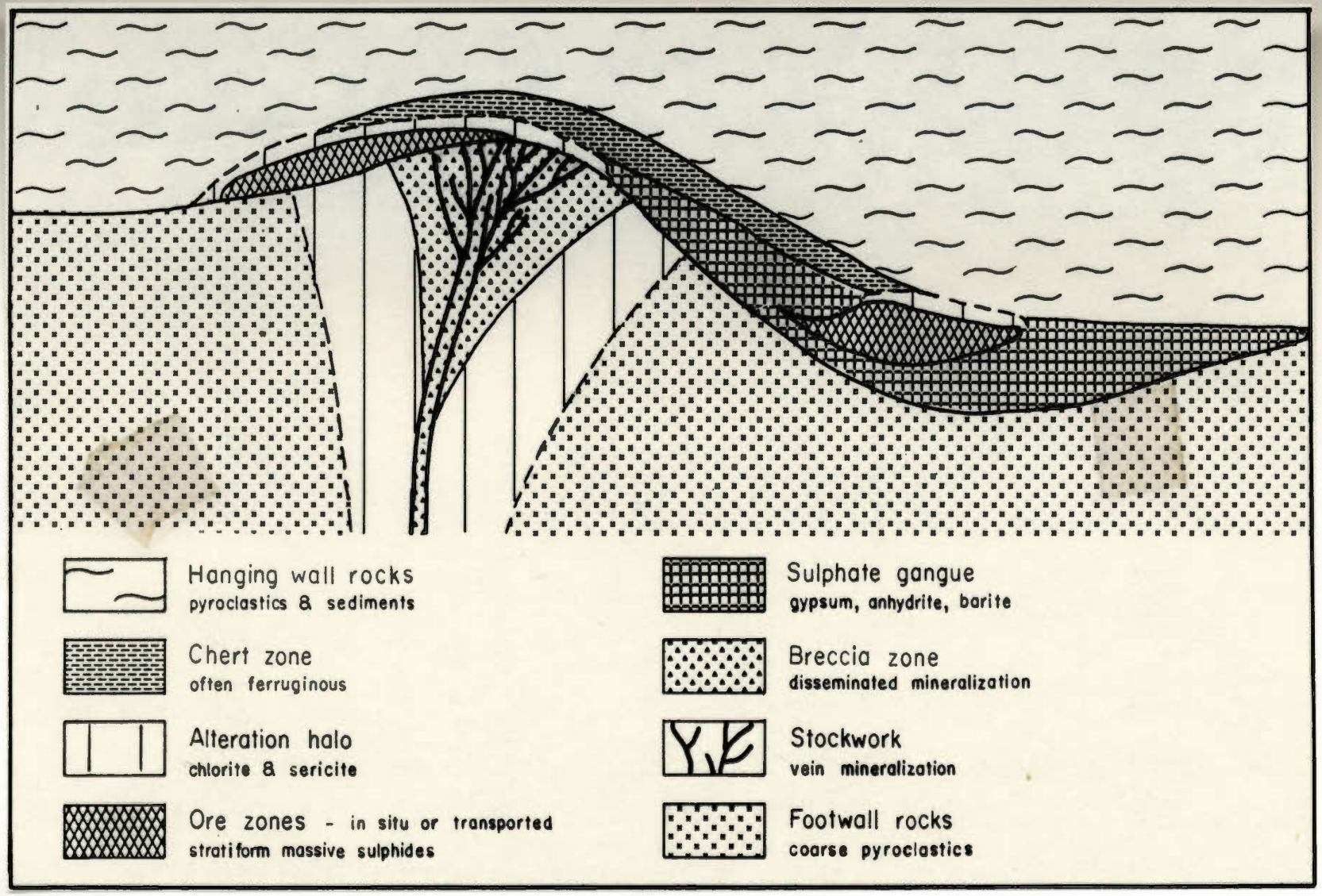

Figure 1.1 An idealized cross section showing the main features of a typical volcanogenic massive sulphide (V.M.S.) deposit (taken from Sato, 1977).

zoned, e.g. with stratabound gypsum and anhydrite towards the base and bedded barite at the top of the ore body (Izawa, 1980).

The footwall rocks adjacent to and containing the stockwork zone are variably affected by the convecting hydrothermal solutions, and alteration zones are produced which may be rich is silica, clays and sericite (e.g. the Kuroko deposits, Lambert and Sato, 1974) or chlorite (e.g. Canadian Archean deposits, Sangster, 1972a). In some Japanese deposits alteration is also observed in the hangingwall rocks, presumably caused by the continued circulation of hydrothermal solutions after the mineralizing event and after the deposit is buried (Sangster, 1972). The distribution of alteration assemblages of the Canadian Archean and Japanese Kuroko deposits are summarized in Figure 1.2.

Sato (1972) has suggested that the salinity and temperature (hence density) of the ascending metal-bearing brines determine the site of sulphide precipitation. The most dense ore fluids flow down-slope from the source vent and precipitate the sulphides in depressions at some distance from the vent (Type I, Figure 1.3).

Ore solutions with an intermediate density flow down-slope but mix with sea water fairly rapidly and precipitate sulphides close to, but down-slope from the vent (Type IIa, Figure 1.3). Less dense brines will float up from the vent, mix with sea water, cool rapidly and sink, depositing sulphides anywhere in the vicinity of the vent

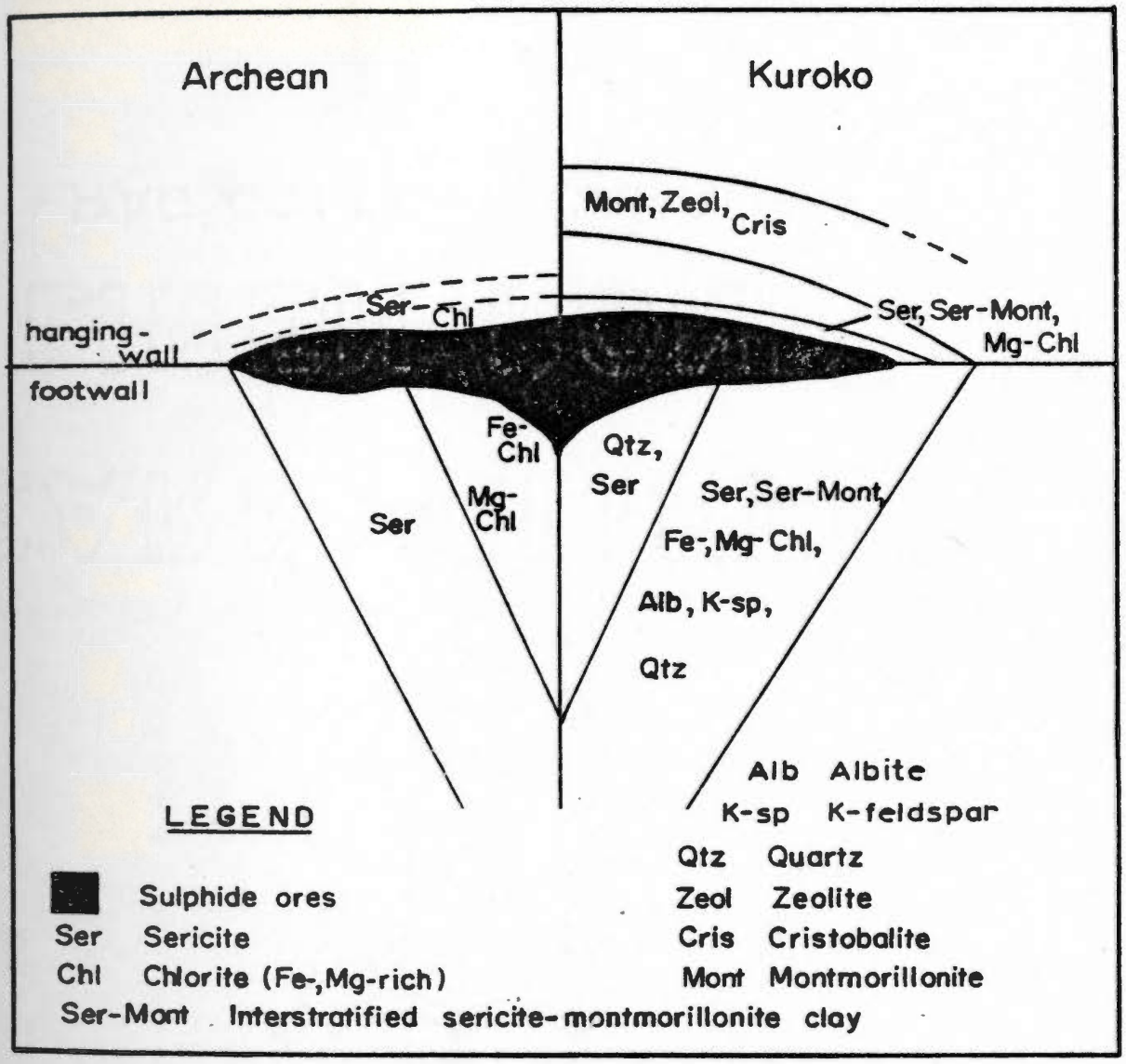

Figure I.2. An idealized cross section comparing the alteration zones associated with Archean (Franklin et al., 1981) and Kuroko (Shirozo, 1974) V.M.S. deposits.

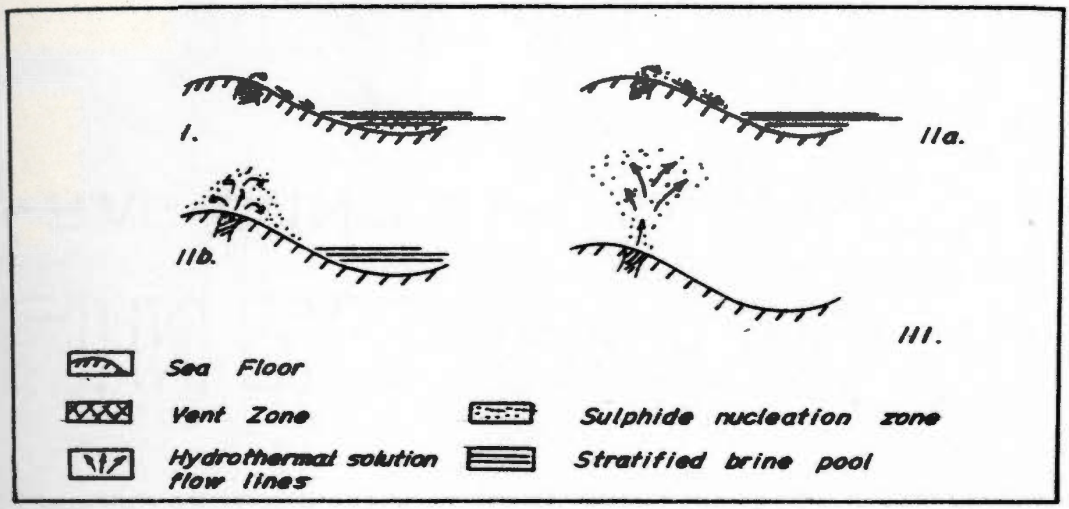

a)

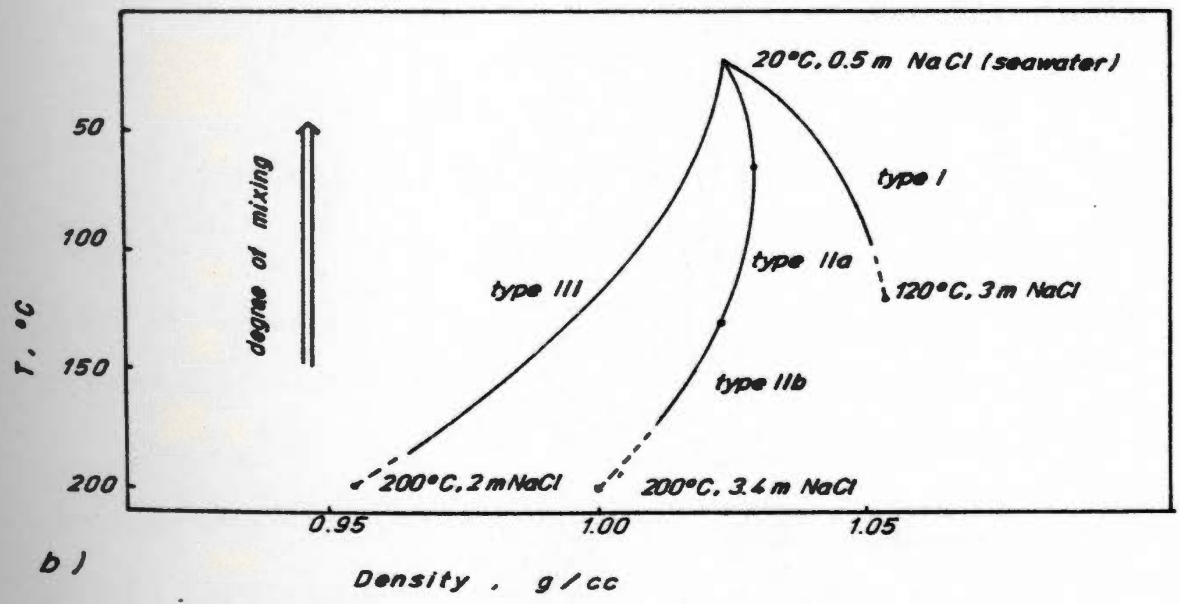

b)

Figure 1.3. a) Probable behaviours of four types of hydrothermal solutions discharging into a submarine environment, defined according to their initial temperature and salinity relationships of Figure 1.3.b. b) Four patterns of density due to the mixing of two NaCl solutions (both a and b are from Sato, 1972).

(Type IIb, Figure 1.3). Ascending brines lighter than sea water will float up and disperse quickly, depositing a thin widespread layer of sulphides far from the vent (Type III, Figure 1.3).

Near-vent accumulations of sulphides may be subject to slumping or transportation down-slope by subaqueous density flows. Sulphide breccias (sulphide and/or silicate clasts in a sulphide matrix), soft sediment deformation structures and a lack of ore mineral zonation or underlying stockwork and alteration zones characterize these transported ore deposits (Thurlow and Swanson, 1981).

Those features of V.M.S. deposits more extensive than the massive sulphide ore itself (the chert horizon, stockwork zone and footwall alteration patterns) are useful exploration guides.

1.1.2 Chemical characteristics

Zones of intense alteration beneath relatively unmetamorphosed, and even strongly metamorphosed V.M.S. deposits can be identified in routine geological mapping. For example, the metamorphosed alteration zone of "dalmationite" (knots of chlorite, sericite and anthophyllite) beneath the Millenbach deposit is not easily missed (Simmons, 1973). On the other hand, chemical alteration of the host rocks may vary in intensity, e.g. with distance from the hydrothermal conduit, without obvious visable changes. For example, mineral assemblages may

remain constant despite a change in their composition. These more subtle patterns of alteration must be detected by chemical analysis of the host rocks, ie. by lithogeochemistry.

Govett and Nichol (1979) in their review of the application of lithogeochemistry in mineral exploration, define lithogeochemistry as "the determination of the chemical composition of bedrock material with the objective of detecting distribution patterns of elements that are spatially related to mineralization". This approach is applicable on a regional scale to identify broad belts of rocks with mineral potential (as opposed to belts which are barren) or on a mine scale (1-2 km) to isolate an area within a favourable horizon which is potentially mineralized (Govett and Nichol, 1979).

Numerous lithogeochemical surveys over known deposits have been successful in outlining element enrichment or depletion haloes produced by mineralizing events. The results of these surveys are summarized in Tables 1.1 and 1.2 which are taken, with a few additions, from Govett and Nichol (1979). Iron and magnesium are typically enriched in the footwall rocks adjacent to mineralization, whereas sodium and calcium are typically depleted. Potassium, silica and manganese have been reported as variably enriched or depleted in different deposits. Dispersion haloes of trace elements close to V.M.S. deposits show a concentration of zinc and, to a lesser extent, copper and/or sulphur. Barium enrichment is a reliable indicator of proximity to the Buchans ore zones (Thurlow et al., 1975).

Table 1.1

Summary of major element dispersions in relation to volcanogenic massive sulphide deposits (modified from Govett and Nichol, 1979)

Deposit	Alteration mineralogy	Elements enriched	Elements depleted	Elements unchanged	Age
Fukazawa, Japan Izawa et al. (1978)	Chl, Ser, Zeol, Mon	Mg	Na, Ca		Cenozoic
Kuroko, Japan Lambert & Sato (1974)	Mon, Ser, Chl, Kaol	K, Mg, Fe, Si	Ca		Cenozoic
Kuroko, Japan Tatsumi & Clark (1972)	Ser, Qtz, Cal	Mg, K	Na, Ca, Fe	Al	Cenozoic
Hitachi, Japan Kuroda (1961)	Cord, Anthoph	Mg, Fe, Ba	Na, Ca, Sr		Cenozoic
Britannia District, Canada Payne, et al. (1980)	Qtz, Ser, Chl	K, Si	Ca, Fe, Mn	Ti, Al	Mesozoic
Buchans, Canada Thurlow et al. (1975)	Chl, Ser, Qtz	Mg, Fe, Si	Na, Ca, K		Paleozoic
Heath Steele, Canada Wahl et al. (1975)	Chl, Ser	Mg	Na, Ca		Paleozoic
Brunswick No. 12, Canada Goodfellow (1975)	Chl, Ser, Qtz	Mg, Fe (Mn), (K)	Na, Ca (Mn), (K)	Al	Paleozoic
Killingdal, Norway Rui (1973)	Chl, Bio, Qtz	Mg, K, Mn	Na, Ca, Si	Al, Ti, Fe (total)	Paleozoic
Skorovass, Norway Gjelsvik (1968)	Chl, Ser	Mg	Na, Ca		Paleozoic
Boliden, Sweden Nilsson (1968)	Chl, Ser, Qtz, Andal	Mg, K, Al, Ti	Na, Ca		Proterozoic

Table 1.1 continued

Deposit	Alteration mineralogy	Elements enriched	Elements depleted	Elements unchanged	Age
Flin Flon, Canada Koo & Mossman (1975)	Talc, Chl, Ser	Fe, Mg, Ca	Na, Si		Proterozoic
Mattabi, Canada Franklin et al. (1975)	Qtz, Carb, Ser, Chld, Chl, Andal, Gar, Kyan, Bio	Fe, Mg, Mn, K	Na, Ca		Archean
Mattagami Lake, Canada Roberts & Reardon (1978)	Talc, Actin, Chl, Carb, Qtz	Fe, Mg, Ca	Na, K, Si, Ti, Al		Archean
Millenbach, Canada Simmons et al. (1973)	Chl, Ser, Anthoph, Cord.	Mg, Fe	Na, Ca, Si		Archean
Millenbach, Canada Riverin & Hodgson (1980)	Anthoph, Chl, Ser, Bio, Cord.	Fe, Mg	Ca, Na		Archean
Mines de Poirier, Canada Descarreaux (1973)	Chl, Ser,	Mg, K	Na, Ca	Si	Archean
Lac Dufault, Canada Sakrison (1966)	Chl, Ser	Mg, Fe, Mn	Na, Ca	Al, Ti K, Si	Archean
East Waite, Mobrun, Joutel, Poirier, Agnico-Eagle, Mattabi, Sturgeon Lake, South Bay, Canada McConnell (1976)	Qtz, Ser, Chl, Carb, Sauss, Epidote	Mg, Fe	Na, Ca	Si, Al	Archean

NOTES: Chl = chlorite, Ser = sericite, Zeol = zeolite, Mon = Montmorillite, Kaol = kaolinite, Qtz = quartz, Cord = cordierite, Anthoph = anthophyillite, Bio = biotite, Andal = andalusite, Gar = garnet, Kyan = kyanite, Chld = chloritoid, Carb = carbonate, Actin = actinolite, Sauss = saussurite

Table 1.2

Summary of trace-element dispersion in relation to volcanogenic massive sulphide deposits (from Govett and Nichol, 1979)

Deposit	Ore mineralogy	Metal dispersion	Age
Kuroko type, Japan Lambert & Sato (1974)	py, cpy, sph, ga, bar	Zn, Cu, Pb	Cenozoic
Buchans, Canada Thurlow et al. (1975)	sph, ga, cpy, (py; tet, bo, cov)	Zn, Pb, Ba, (Ag) (Cu)	Paleozoic
Brunswick No. 12, Canada Goodfellow (1975)	py, sph, ga, po cpy, tet, bo	Zn, Pb	Paleozoic
Heath Steele, Canada Whitehead and Govett (1974)	py, sph, ga, cpy	Pb, Zn	Paleozoic
Killingdal, Norway Rui (1973)	py, sph, cpy	Cu, Zn	Paleozoic
Mattabi, Canada Franklin et al. (1975)	cpy, py, sph	Cu, Zn, S	Archean
Millenbach, Canada Simmons et al. (1973)	cpy, py, sph	Zn	Archean
East Waite Mobrun, Joutel, Poierier, Agnico-Eagle Mattabi, Sturgeon Lake, South Bay Mines, McConnell (1976)	py, sph, cpy (po)	Zn, Cu, S	Archean

NOTES: py = pyrite, cpy = chalcopyrite, sph = sphalerite, ga = galena, bar = barite, tet = tetrahedrite, bo = bornite, cov = covellite, po = pyrrhotite

If regional metamorphism does not significantly affect the bulk composition of a rock although the mineral assemblages of an alteration zone may change, then the chemical signature of the zone should remain intact and identifiable after metamorphism. This has indeed been proven in Canadian Archean greenstone deposits where alteration pipes have been identified below massive sulphide deposits which have been metamorphosed to upper greenschist facies (Mattabi; McConnell, 1976) and hornblende hornfels with retrograde greenschist facies (Millenbach; Riverin and Hodgson, 1980).

1.2 Approaches to evaluating lithogeochemical data

The identification of alteration haloes in massive sulphide host rocks requires that samples enriched or depleted in given elements (anomalous samples) be separated from those with normal (unaltered or background) compositions. In dealing with a known deposit the change in concentration of a single element can be evaluated as a function of distance to the ore body, e.g. increases of S and As with proximity to the Kuroko deposit noted by Izawa, et al., (1978). Ratios of two or more elements plotted with respect to distance from the ore body have been used to highlight multi-element patterns, e.g. the Alteration Index:

AI = $100 \times (MgO + K_2O)/(MgO + CaO + Na_2O + K_2O)$ proposed by Ishikawa et al. (1976) and used by Izawa et al. (1978); Zn/Pb ratio of Pwa (1977); Mg/Fe ratio of Goodfellow (1975) and Wahl (1977).

Where alteration patterns might not be so systematic samples might be arbitrarily divided into groups (or populations) on the basis of their location relative to known ore deposits. Those close to the deposit are most likely to be altered by the mineralizing event and therefore be chemically anomalous. Those samples far from the deposit are most likely to represent unaltered or background samples. The comparison of simple statistical parameters between the two populations may show the expected enrichment or depletion patterns, e.g. the mean zinc concentrations for two sample populations on Cyprus is 83.4 ppm for the anomalous group and 59.7 ppm for the background group (Govett and Pantazis, 1971; Govett, 1972). However, the difference between the means of the two populations is commonly quite small and the range of values may show considerable overlap. To maximize the differences between the two groups more sophisticated computer based statistical techniques can be used.

Discriminant analysis uses the combined covariance of several elements to generate a function which best characterizes each group (the anomalous and background groups), and a sample of unknown significance may then be classified as belonging to either the anomalous or background population using the discriminant functions. For example Whitehead and Govett (1974) used discriminant functions to outline a subtle alteration halo above and along strike from the Heath Steele mine.

Although discriminant functions may be an effective way of dealing with the geochemical analyses from deposits hosted in rocks of fairly uniform lithology, most V.M.S. deposits occur in association with igneous rocks which range in composition from mafic to felsic. It might be necessary to detect the effects of hydrothermal alteration superimposed on an andesite by comparing its chemistry with that of an unaltered rhyolite. In order to do this the primary compositional differences of the two rocks must first be considered.

Regression techniques might use SiO_2 and/or TiO_2 as indices to the degree of fractionation of a sample. By subtracting the component of an element content due to fractionation (estimated by the SiO_2 and/or TiO_2 content of a given sample) from the observed element concentration of that sample a residual element value is generated which may reflect the effects of alteration. McConnell (1976) used samples from unmineralized areas to generate curvilinear regression equations which expressed the behaviour of each element with respect to (SiO_2 + TiO_2). These equations were then used to generate element residuals for samples collected from potentially mineralized areas. By standardizing and combining the residuals of MgO, CaO, FeO, and Na_2O, McConnell was able to identify zones of alteration related to mineralization previously missed in plots of the raw data or simple ratios (Na_2O/K_2O).

Sopuck *et al.* (1980) combined the use of both discriminant analysis and residual techniques in the interpretation of lithogeochemical data. They used element residuals from an area of known mineralization and from barren areas to generate discriminant functions. These were then used to successfully assign other samples into mineralized or barren groups. They found that the discriminant scores were more useful than the raw data of regression residuals in classifying, on a regional scale, cycles of felsic volcanism as potentially mineralized or barren.

1.3 The Strickland showings - a test for lithogeochemistry

The Strickland property of southwestern Newfoundland affords an excellent opportunity to evaluate lithogeochemical approaches in a massive sulphide deposit which has been subjected to intense deformation and metamorphism. The mineralization is rich in iron, zinc, lead, copper and silver and is interpreted to be synvolcanic. It is hosted in a well exposed sequence of sheared, metamorphosed and moderately dipping volcanic, volcaniclastic and sedimentary rocks which extend for 100 km along strike. Possibly because of the tectonic effects few of the "standard" features of volcanogenic massive sulphides, e.g. mineralized stockwork, pipe-like alteration zones, etc. are visually apparent. A graphitic shale

horizon intimately associated with the main sulphide body limits the effectiveness of electrical geophysical methods to detect sulphides along that horizon.

The identification of a unique lithogeochemical signature produced by the mineralizing event and more extensive than the exposed ore would provide a useful exploraion tool, both at the Strickland property and further along strike. It was with this aim that this study was undertaken.

CHAPTER 2

REGIONAL GEOLOGY

2.1 Introduction

The Strickland property is located in the La Poile River area of southwestern Newfoundland which has been mapped by government and industry geologists (Figure 2.1a) (Cooper, 1954; Chorlton, 1980; Gillis, 1972; Prince, 1977).

The geology of the La Poile (110/9) and La Poile River (110/16) map areas, as described by Chorlton (1978a, 1978b, 1979a, 1979b, 1980) can be described in terms of four structural blocks separated by three major east-northeast to east-trending fault zones (Figure 2.1b). From north to south, the Cape Ray Fault, the Bay d'Est Fault, and the Grand Bruit Fault transect a terrain of polydeformed and metamorphosed sedimentary and volcanic rocks which have been intruded by several generations of granitoid rocks (Chorlton, 1978a, 1980). The stratigraphic and lithologic sequences of the area are summarized in Table 2.1.

2.2 Pretectonic rocks

2.2.1 Keepings Gneiss and unnamed gabbro unit

The oldest rocks in the area are inferred to be the Keepings Gneiss and an unnamed metagabbro-metapyroxenite unit both of which have been affected by the first two of four periods of regional deformation (Chorlton, 1980) (Figure 2.1b).

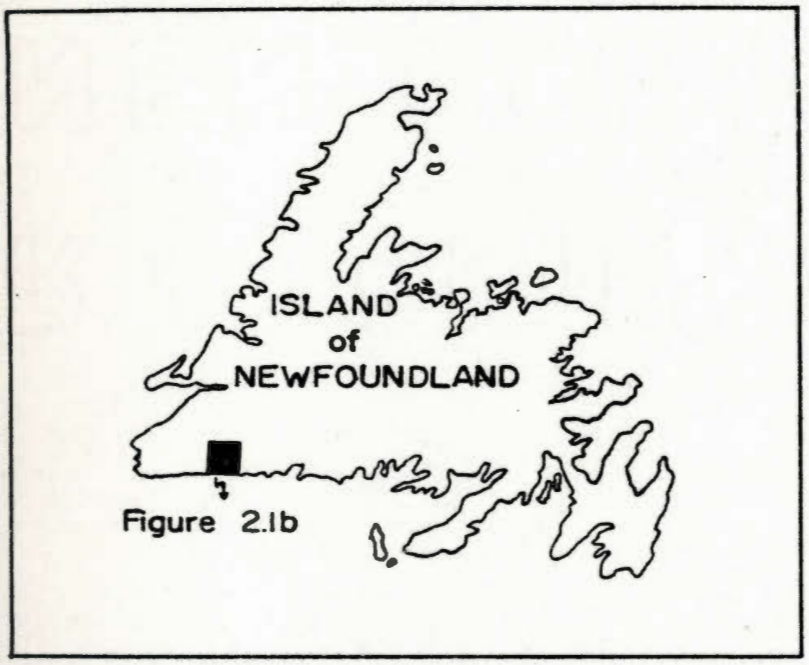

Figure 2.1a. Index map.

Table 2.1

Table of formations compiled from Chorlton 1978a, 1980 and written communication

Period	Formation	Lithology	Fig 2.1b Map Unit
DEVONIAN OR YOUNGER	LATE LEUCOGRANITE	Equigranular, garnet bearing leucogranite	21
	CHEIWYND GRANITE	Coarse grained, equigranular with rapikivi phases and rhyolite dykes	20
	Intrusive contact		
	UNNAMED GRANITE	Porphyritic granite, granodiorite, monzodiorite, quartz diorite	19
	NITTY GRITTY BROOK GRANITE	Fine grained alaskite granite, granite dyke	18
	BILLIARDS BROOK FORMATION	Terrestrial mafic and felsic volcanic and sedimentary rocks	17
	QUARTZ GABBRO	Quartz gabbro, diorite, diabase minor pyroxenite	16
	Deformation		
SILURIAN	HAWKS NEST POND PORPHYRY	Porphyritic microgranite	15
	LA POILE BATHOLITH	Porphyritic (megacrystic) granite — granodiorite with pegmatite and aplite	14a
	OTTER POINT GRANITE	Coarse grained, porphyritic granite, pegmatite, aplite	14b
	Intrusive contact		

Table 2.1 continued

Period	Formation	Lithology	Fig 2.1b Map Unit
	ROSE BLANCHE GRANITE	Foliated two-mica granite granodiorite, tonalite, muscovite granite	13
SILURIAN? OR ORDOVICIAN?	NORTHERN GRANITE	Foliated tonalite, trondhjemite, granodiorite, granite, two-mica granite	12
	No contact exposed		
	CINQ CERF COMPLEX	Equigranular, grey granodiorite, mafic to felsic amphibolite facies schists/gneisses	11
	Intrusive contact, Deformation		
	ERNIE POND GABBRO	Coarse grained, altered gabbro, peridotite, pyroxenite, diorite	10
	LA POILE GROUP: GEORGES BROOK FORMATION	Felsic and mafic volcanic rocks, sedimentary rocks	9
	ROTI GRANITE	Medium grained, equigranular granite, granodiorite, qtz porphyry, qtz-feldspar porphyry	8
	Fault contact		
	DOLMAN FORMATION	Deformed felsic volcanic rocks, mostly pyroclastic	7
	METADIABASE DYKES	Mafic dykes	6
ORDOVICIAN	BAGGS HILL GRANITE	Foliated granite, granophyre, qtz-feldspar porphyry	5
	PIGLET BROOK RHYOLITE	Sparsely porphyritic pink rhyolite	4

Table 2.1 continued

Period	Formation	Lithology	Fig 2.1b Map Unit
	BAY DU NORD GROUP	Semi-pelitic schist Graphitic phyllite Felsic metavolcanic rocks	3a 3b 3c
ORDOVICIAN	GABBRO	Metagabbro, metapyroxenite	2
	No contact exposed		
	KEEPINGS GNEISS	Felsic paraschist or gneiss amphibolite	1

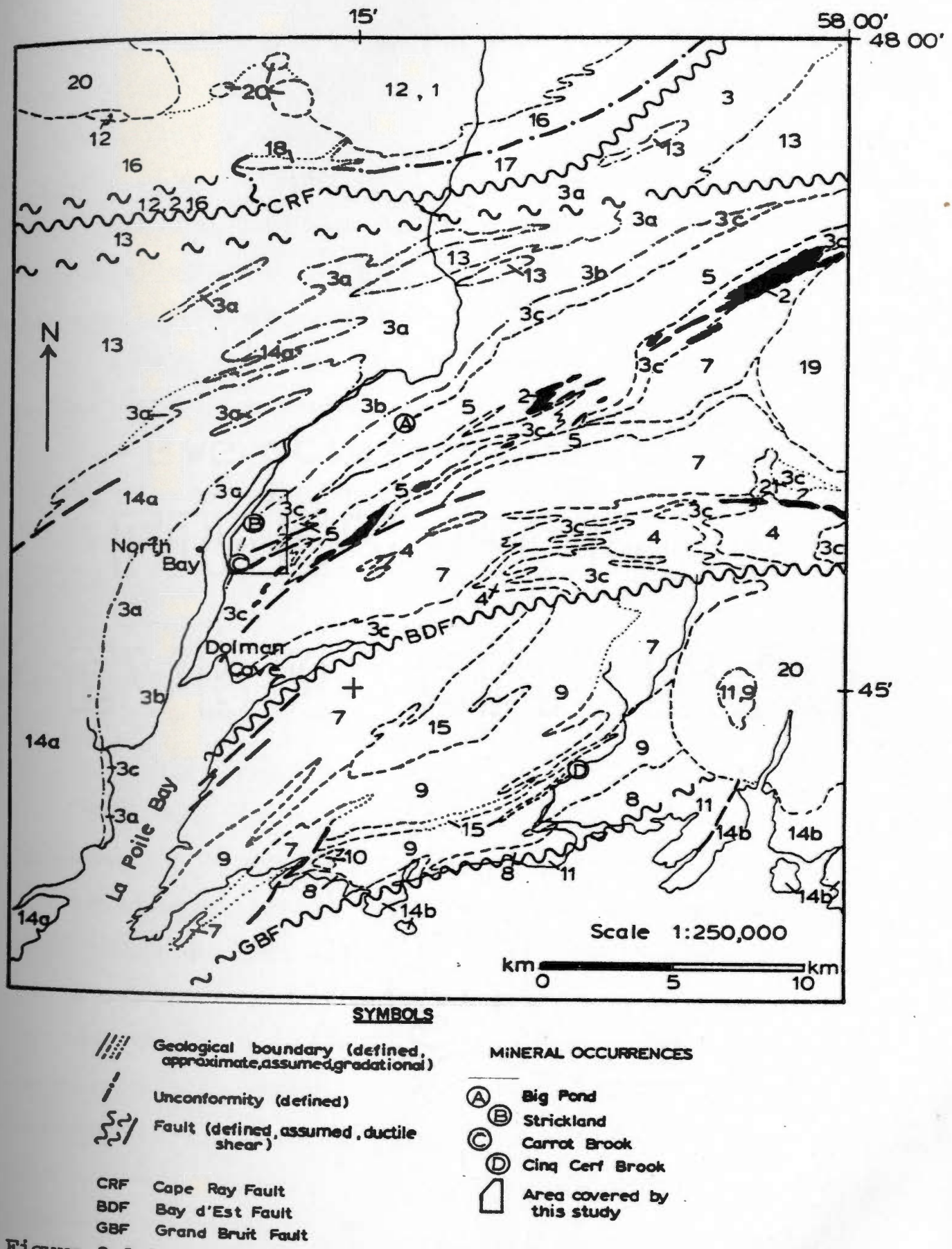

Figure 2.1.b. Generalized geology of the LaPoile River, LaPoile Bay area after maps by Chorlton (1978b, 1979b). A key to the lithologies is given in Table 2.1 .

The Keepings Gneiss is exposed north of the Cape Ray Fault and comprises felsic paragneiss and orthogneiss with minor amphibolite. The metagabbro-metapyroxenite unit is exposed in a series of isolated whaleback outcrops stretching from Dolman Cove northwestward to 2.5 km south of the Cape Ray Fault. Nebulous, folded (cumulate?) layering is locally present in the gabbro. Chorlton (1980) suggested that these mafic to ultramafic rocks may represent tectonically emplaced fragments of basement material.

2.2.2 Metamorphosed sedimentary and volcanic rocks

The metasedimentary and metavolcanic rocks of the area have been divided into three units; the contemporaneous Bay du Nord and La Poile Groups and a third sequence termed the Dolman formation (Figure 2.1b).

2.2.2.1 Bay du Nord Group

The Bay du Nord Group, which hosts the Strickland showings, arcs northeastward and then east for approximately 100 km (Smyth, 1979). The Group extends in a broad 10-15 km wide belt through North Bay and the headwaters of the La Poile River, bounded to the north by the Cape Ray Fault and to the south by the Bay d'Est Fault (Figure 2.1b). It comprises polydeformed and metamorphosed graphitic shale, siltstone, graywacke, conglomerate, felsic volcaniclastics and flows. Pelitic to semipelitic schists and migmatitic schists lie within the 2-3 km wide shear zone associated with the Cape Ray Fault.

The Dolman Gneiss (Cooper, 1954) has been renamed the

Dolman formation by Chorlton (1980) and is considered by her to be part of the Bay du Nord Group. It comprises a belt of schistose crystal-lithic tuff, feldspar porphyry and felsic schist which extends to the northeast from Dolman Cove. Zircons from the Dolman formation have yielded a U/Pb date of 449 ∓ 20 Ma (O'Driscoll and Gibbons, 1980).

The Piglet Brook Rhyolite, Baggs Hill Granite, and several mafic dykes are believed to have been emplaced during the deposition of the Bay du Nord volcanics and sediments and have therefore been informally included in it (Chorlton, 1980).

The Piglet Brook Rhyolite is a series of sugary rhyolite flows, dykes or sills emplaced within the Bay du Nord sediments and volcanics north of the contact between the Bay du Nord Group rocks and the Dolman formation (Figure 2.1b). The Piglet Brook Rhyolite is typically slightly radioactive (three to four times regional background count). The Baggs Hill Granite (Cooper, 1954) and the associated network of dykes and sills is thought to be a subvolcanic stock. It is locally porphyritic, commonly granophyric and grades into an equigranular light-coloured biotite granite (Figure 2.1b). Mafic dykes intrude both the Bay du Nord volcanic and sedimentary rocks as well as the Baggs Hill Granite.

The predominance of metamorphosed shales, greywackes, coarse pyroclastics and reworked volcanics have led Chorlton (1980) to suggest that the sedimentary and volcanic rocks of

the Bay du Nord Group were deposited in a marine basin, possibly associated with an island arc system.

2.2.2.2 The La Poile Group

The La Poile Group, thought to be correlative with the Bay du Nord Group (Chorlton, 1980), is bounded by the Bay d'Est Fault to the north, the Cinq Cerf Complex and Grand Bruit Fault to the south and the Chetwynd Granite to the east (Figure 2.1b). The La Poile Group has been subdivided into at least two units: the Georges Brook Formation, a sequence of volcanic and sedimentary rocks and the Roti Granite, a granitoid instrusion with variable texture and composition (Chorlton, 1978a, 1980). A Silurian zircon U/Pb date of 410 ± 20 Ma for the Hawks Nest Pond Porphyry (Chorlton, 1980) suggests that it not be included in the La Poile Group which is believed to be Ordovician and it is therefore described below. The Georges Brook Formation is a sequence of subaerial and marine volcanics and associated sedimentary rocks which are exposed over much of the area underlain by the La Poile Group. Chorlton (1978a) noted a change in the volcanic component of the Georges Brook Formation with time, and identified three general phases of volcanism.

The earliest phase, exposed in the south, consists of fine-grained rhyolite tuff, felsic to mafic pyroclastic rocks, flow-banded rhyolite, siltstone, arkose and pebbly conglomerate. Felsic and mafic volcanics with intercalated

sedimentary rocks were deposited during the second phase of volcanism (Chorlton, 1978a). These rocks occupy the central portion of the area underlain by the La Poile Group and are richer in sedimentary rocks than the first phase. These pass upwards(?) (Chorlton, 1978) to the northwest into rocks of the third phase of volcanism which produced crystal-lithic tuff, sparsely porphyrftic rhyolite, quartz- and feldspar-porphyry and welded tuff with intercalated sedimentary lenses.

The Roti Granite forms the southern margin of the La Poile Group (Figure 2.1b). The main body is a medium-grained granodiorite with dykes of fine-grained leucogranite or quartz porphyry. The rock is generally foliated.

2.3 Syntectonic and post-tectonic rocks

2.3.1 Billiards Brook formation

The Billiards Brook formation contains the youngest sequence of volcanic and sedimentary rocks in the La Poile area. It is a group of subaerial felsic and mafic volcanic and associated sedimentary rocks deposited unconformably in the Cape Ray Fault zone. On the basis of field relations, Chorlton (1980) has separated these rocks from the Bay du Nord Group to which they had originally been assigned (Cooper, 1954). Devonian plant fossils have been identified in the sedimentary strata (Dorf and Cooper, 1943). This formation is believed to be correlative with the Windsor Point Group (Brown, 1972; Chorlton, 1980).

2.3.2 Granitoid rocks

Several syn- and post-tectonic plutons ranging in composition from gabbro to granite intrude the Bay du Nord and La Poile Groups (Chorlton, 1978a, 1980). The intrusions in approximate order of decreasing age (based on field relationships), include Ernie Pond Gabbro (mafic to ultramafic plugs); the Cinq Cerf Complex (a granodiorite rich in metasedimentary and amphibolite inclusions with associated dykes - exposed south of the Grand Bruit Fault, (see Figure 2.1b); the weakly schistose and gneissose Northern Granite (tonalite, trondhjemite and granodiorite); the schistose Rose Blanche Granite (tonalite and granodiorite); the Otter Point Granite (a coarse grained porphyritic granite); the La Poile Batholith (a large body of porphyritic granite to granodiorite, lithologically similar to the Otter Point Granite); the Hawks Nest Pond Porphyry (a pink-weathering porphyritic microgranite, intrusive into the Georges Brook Formation as a sill or laccolith which has yielded a U/Pb zircon date of 410 ± 20 Ma (O'Driscoll and Gibbons, 1980); and an unnamed quartz gabbro and diabase unit (exposed north of the Cape Ray Fault).

Granitoid rocks younger than the Billiard Brook formation include; the Nitty Gritty Brook Granite (a pink, high level granite with associated dykes); an unnamed porphyritic granite to monzodiorite (exposed just north of the Cape Ray Fault); the Chetwynd Granite and related plutons (an undeformed, coarse grained equigranular biotite granite with rapikivi phases and rhyolite dykes exposed

south of, and truncated by, the Bay d'Est Fault; related plutons are exposed north of the Cape Ray Fault) (Figure 2.1b); and an unnamed, post-tectonic leucogranite with two feldspars and two micas which intrudes the Bay du Nord metasediments and the Dolman formation.

2.4 Deformation

The deformational history of the La Poile area has been analysed in some detail by Chorlton (1978a, 1980), and the major features are summarized below.

The rocks of the Keepings Gneiss, the Bay du Nord and La Poile Groups have undergone four periods of deformation. The younger Billiards Brook formation and granitic intrusions including the Cinq Cerf Complex were affected by only the last two periods of deformation (Chorlton, 1978a, 1980).

The first deformation, D1, produced tight folds and an early schistosity in the Bay du Nord and La Poile Groups. This was accompanied by the initiation of major slide or shear zones (Cape Ray, Bay d'Est and Grand Bruit Faults). The D1 event was partly responsible for placing the Bay du Nord Group at a deeper tectonic level than the La Poile Group. The Keeping Gneiss was sheared and thrusted during the D1 event.

The second phase of deformation, D2, produced the prominent northeast-trending schistosity in the metasediments and metavolcanics of the Bay du Nord Group. A

linear fabric (marked by stretched pebbles and aligned, prismatic hornblende crystals) trending northeasterly and gently to moderately plunging, parallels the D2 fold hinges.

During D2 shear zones in the La Poile block (bounded by the Cape Ray and Bay d'Est Faults) were active and minor folds were produced in the Georges Brook Formation (Chorlton, 1978a, 1980).

In the Keepings Gneiss block (north of the Cape Ray Fault zone) banding and granite stringers were probably folded by the D2 event.

The deposition of the Billiards Brook formation was followed by the third phase of deformation in the Bay du Nord Group and Billiards Brook formation. D3 was active after or during emplacement of the late plutonic rocks. This phase is characterized by drag folding and intense shearing inside the Cape Ray Fault zone, and movement along pre-existing shear zones outside of the Cape Ray Fault zone. Dip-slip movement along the Cape Ray and Bay d'Est faults uplifted the Bay du Nord group relative to the La Poile Group.

The affects of D3 on the rocks of the La Poile block and south of the Grand Bruit Fault are believed to be restricted to shear zones. Similarly, shears parallel to the Cape Ray Fault in the Keepings Gneiss block may have been active during the D3 event (Chorlton, 1980).

The last recognizable deformation event, D4, inhomogenously affected all the rocks in the area and produced kink folds, crenulation cleavage and north-striking

block or strike-slip faults. Significant strike-slip movement was produced on the major east-trending fault zones (Chorlton, 1980).

2.5 Metamorphism

The mineral assemblages of the Bay du Nord Group, Keepings Gneiss and Cinq Cerf Complex indicate that they were metamorphosed to lower to middle amphibolite facies (Chorlton, 1980). The Bay du Nord Group rocks contain staurolite, kyanite, almandine, sillimanite locally, and ubiquitous muscovite. There is local evidence of partial melting. All these factors suggest peak metamorphic temperatures between 600°C and 750°C and pressures from 600 to 700 MPa which corresponds to a depth of 20 to 25 km (Chorlton, 1980 from Miyashiro, 1973).

The La Poile Group was metamorphosed to greenschist facies. The best estimate of peak metamorphic temperature and pressure fall around 300 to 400°C and 200 MPa or 8 km depth (Chorlton, 1980).

The Billiards Brook formation and associated rocks reached a metamorphic peak of lower greenschist facies.

2.6 Major Faults

The first movement along the Cape Ray Fault is thought by Chorlton (1980) to have begun before or early in the premetamorphic stages of deformation affecting the Bay du Nord Group and the Keepings Gneiss. The fault zone includes a belt of thin mylonite bands and metamorphically retrogressed shear zones which cut a wider band of blasto-mylonitic Bay du Nord Group rocks and intrusions of the Rose Blanche Granite. The Cape Ray Fault zone splays near the center of the map area (Figure 2.1b).

Late movement on the fault is both dip-slip and strike-slip (Chorlton, 1980).

Movement along the Bay d'Est Fault was predominantly vertical and was initiated late in the tectonic history of the area. Fractured country rocks, a siliceous mylonite zone and strong micaceous schistosity are locally present in association with the Bay d'Est Fault. The fault brings greenschist facies La Poile Group rocks to the south into contact with the middle amphibolite facies rocks of the Bay du Nord Group to the north.

The Grand Bruit Fault forms the contact between the rocks of the La Poile Group to the north and the Cinq Cerf Complex to the south. Metasedimentary inclusions in the Cinq Cerf Complex granodiorite have been metamorphosed to lower amphibolite facies (Chorlton, 1978a). The juxtaposition of greenschist (La Poile Group) and amphibolite facies (Cinq Cerf Complex) sequences separated by shear planes with steeply plunging mineral lineations has led Chorlton (1978a) to suggest that movement on the Grand Bruit Fault was at least in part vertical, with the south (Cinq Cerf) side being uplifted.

2.7 Geochemistry

Chorlton (1980) analysed volcanic and subvolcanic rocks of the La Poile and Bay du Nord Groups for major and trace elements. She concluded that the Georges Brook Formation is

a calc-alkaline suite generated in a plate margin setting, probably oceanic.

The higher metamorphic grade of the Bay du Nord Group make it difficult to assess, using geochemistry, its original tectonic setting. Chorlton (1980) did note evidence of alkali exchange in felsites and the Dolman tuffs as well as significant sodium enrichment in the Baggs Hill Granite. The Bay du Nord Group is also enriched in silica relative to the La Poile Group.

2.8 Economic Geology

The mineral prospects of the La Poile area have been described by Cooper (1954), Stackhouse (1976), Chorlton (1978a, 1980) and Swinden (1981). The geology of the most signficiant showings is summarized below.

2.8.1 Bay du Nord Group

The Strickland showings comprise the largest of three base metal/precious metal showings hosted in a single felsic volcanic horizon of the Bay du Nord Group (See Figure 2.1b). It is described in detail in Chapter 4.

The Carrot Brook prospect (Figure 2.1b), approximately 2 km southwest of the Strickland showings, is a cluster of mineral showings composed of pyrite with minor sphalerite and galena contained in altered rhyolite. The mineralization lies exposed in the creek bed and to varying extents in five

trenches just north of Carrot Brook (Cooper 1954; Prince, 1977b; Swinden, 1981). At the same stratigraphic horizon and 700m south of Carrot Brook minor sulphides (pyrite mainly) hosted in silicified felsic tuffs are exposed in several old trenches (Swinden 1981).

Near Big Pond, approximately 6 km along strike northeast of the Strickland showing (Figure 2.1b) are two showings of 5% disseminated sulphides contained in silicified felsic tuff (Cooper, 1954; Prince, 1977b; Swinden, 1981). The reported sulphides include pyrite, chalcopyrite, cuprite (Prince, 1977b) as well as tetrahedrite, pyrrhotite, and marcasite (Cooper, 1954).

The Carrot Brook prospect, the Big Pond prospect and the Strickland showing are all interpreted to be the product of hydrothermal activity related to felsic volcanism (Prince, 1977b; Swinden, 1981).

2.8.2 La Poile Group

The La Poile Group hosts five copper-gold mineral occurrences in the Cinq Cerf Brook area (Figure 2.1b). They are the Chetwynd, Copper shafts, Hope Brook and Woodmans Droke prospects. Four of the five (excluding the Woodmans Droke prospect) are contained in two conformable horizons of sheared and altered felsic rock. They have been variably silicified, sericitized, pyritized and pyrophyllitized and are heavily iron-stained and appear deeply leached (Swinden, 1981). These two horizons may be granitic sills or rhyolite flows. Exposed mineralization includes moderately to heavily disseminated pyrite with some bornite and chalcocite. Veins of nearly massive bornite reach a thickness of 2 cm parallel to shear planes (Swinden, 1981). Underground workers reported lenses of bornite up to two or three feet thick in the exploration shafts sunk on the Chetwynd prospect (Reading, 1933 from Swinden, 1981). Gold has been identified in hand specimen and polished section by earlier workers (Snelgrove, 1935; Reading, 1933). Chalcopyrite and tetrahedrite have also been previously reported (Cooper, 1954; Snelgrove, 1935). Accessory minerals include barite and fluorite.

Swinden (1981) has proposed that, on the basis of the epithermal to hypothermal mineral assemblage (tetrahedrite, bornite, chalcopyrite, gold, fluorite and barite) that the mineralization is the product of late magmatic degassing related to the crystallization of granitic sills associated

with La Poile Group igneous activity (possibly the Roti Granite).

2.9 Regional correlations and tectonic interpretation

The deformed and metamorphosed volcanic and sedimentary rocks of the La Poile and Bay du Nord Groups have been traced as far east as the Salmon River (Smyth, 1979, 1980) where they lie on strike with the western end of the Baie d'Espoir Group (Swinden, 1980). The two groups of rocks are separated by 20 kilometres of the North Bay Granite and were originally probably part of a single continuous belt (Prince, 1977a; Smyth 1979, 1980; Chorlton, 1980; Swinden, 1981).

The Baie d'Espoir Group of south central Newfoundland ha in turn been correlated with the Gander and Davidsville Groups of central northeast Newfoundland (Colman-Sadd, 1980; Colman-Sadd and Swinden, 1980; Prince, 1977a). This extensive belt of rocks stretching from the La Poile area to north of Gander, is contained in the tectonostratigraphic Gander Zone (Williams, 1979). Common lithologies (volcanics-dominantly felsic, and sedimentary rocks), depositional environment (marine) and isotopic and fossil dates (middle Ordovician) persist along the entire length of the belt. Several authors (Stevens et al., 1974, Strong et al., 1974; Colman-Sadd, 1980) have suggested that the volcanic and sedimentary rocks of the Baie d'Espoir, Gander and Davidsville Groups were deposited in a back-arc basin, formed behind an island arc sequence produced by an easterly dipping

subduction zone (first suggested by Church and Stevens, 1971). This basin paralleled the eastern margin of the proto-Atlantic Iapetus Ocean. The presence of volcanic rocks in the Isle Galet Formation close to and largely derived from the Avalon Platform has led Colman-Sadd to propose that the island arc may have coalesced with the Avalon Platform pinching out the back-arc basin southwest of Baie d'Espoir (Colman-Sadd, 1980).

An extension of this tectonic interpretation to the La Poile area would suggest that the La Poile and Bay du Nord Groups were deposited subaqueously, adjacent to an island-arc system emplaced on continental (Avalon) crust. On the basis of petrochemical studies Chorlton favours the interpretation that the La Poile and Bay du Nord Groups represent a mature island arc sequence emplaced on oceanic crust (Chorlton, 1980). A similar ensialic back-arc basin environment has been suggested for the deposition of Tetagouche Group of northeastern New Brunswick which hosts the Bathurst V.M.S. deposits (McBride, 1976). The Bathurst camp and the Strickland showing are of comparable ages (Ordovician), share a similar type of mineralization (V.M.S. rich in Pb, Zn, Ag, poor in Cu), and similar host rocks (felsic metavolcanics, metasediments with subordinate mafic metavolcanics) as well as a possible common interpretation of their original tectonic setting (ensialic, back-arc basin). Comparison of the Pb-isotopes for galena from the two areas supports the ensialic origin of the deposits and

and further underlines the similarities of the two areas.

Unpublished data from R.A. Thorpe (personal communication, 1982) for Strickland galena plot remarkably close to Bathurst isotope ratios (Strickland $^{208}Pb/^{204}Pb$ = 38.209, $^{207}Pb/^{204}Pb$ = 15.663, $^{206}Pb/^{204}Pb$ = 18.333; see Figure 2.2). They plot above the orogene evolution curve in $^{207}Pb/^{204}Pb$ which Doe and Zartman (1979) suggests may indicate an unusually high input of continental-erosional material in the Pb source area. This is consistent with the tectonic interpretation of an ensialicly emplaced arc system in contrast with the ensimatic (low radiogenic lead) signature of the Buchans galena (Figure 2.2, $^{207}Pb/^{204}Pb$ vs $^{206}Pb/^{204}Pb$).

The Pb-isotope signature of the Strickland galena is similar to the two largest Phánerozoic V.M.S. deposits (high $^{207}Pb/^{204}Pb$; Bathurst, N.B. and Cobar, New South Wales, Australia) which Doe and Zartman (1979) speculate might indicate that the big V.M.S. deposits of this age are found not in ensimatic orogens but ensialic orogens. The tendency of these V.M.S. deposits to cluster has been noted elsewhere, e.g. there are 30 major deposits in the Bathurst camp (Davies and McAllister, 1980). This coupled with the similar Pb-isotope signature of the Strickland galenas might suggest by analogy that the volcanic horizon of the La Poile

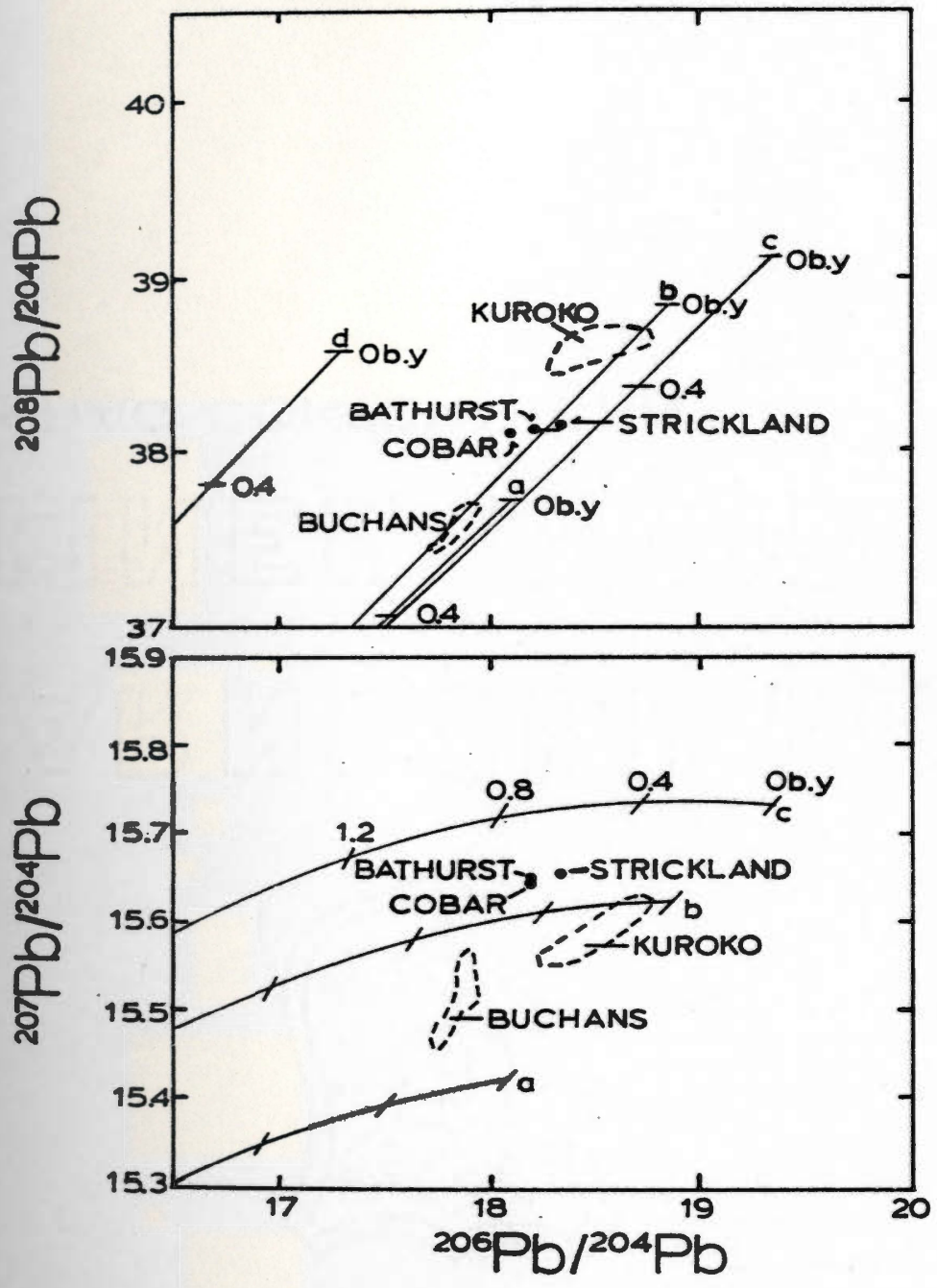

Figure 2.2. Lead isotope diagrams for various volcanogenic massive sulphide deposits. Data for Bathurst, Cobar and Kuroko deposits is from Doe and Zartman (1979); Buchans from Bell and Blenkinsop (1982) and Strickland from R.A. Thorpe (personal communication, 1982). Lead isotope evolution curves for a) the mantle, b) orogene, c) upper crust contributed to orogene and d) lower crust contributed to the orogene are taken from Doe and Zartman (1979).

Group has potential for hosting a major V.M.S. deposit (e.g. Brunswick 12 of the Bathurst camp which has ore reserves of 109.2 million metric tons [Sangster, 1980]).

CHAPTER 3

LOCATION AND PREVIOUS WORK

3.1 General

The Strickland showing is located in southwestern Newfoundland on the highland plateau east of the La Poile River and 2 km east of the abandoned settlement of North Bay (Figure 2.1b). The property is accessible by helicopter from Pasadena or by boat from Rose Blanche. Big Pond, 7 km to the northeast, is the closest lake large enough to accommodate a float plane.

This lead-zinc-silver showing was discovered in 1936 by Alex Strickland. It has been the subject of detailed description and mapping by Cooper (1954), Stackhouse (1976), and Swinden (1981). Chorlton (1980) briefly described the showing geology and the previous work on the property.

Falconbridge Nickel Mines Limited undertook an extensive reconnaissance mapping program in 1977, covering the entire Hermitage Flexure, and staked claim blocks surrounding the showing. In 1978 Falconbridge, in joint venture with Giant Yellowknife Mines Limited and United Keno Hill Mines Limited, optioned the two adjacent fee-simple crown grants which contain the Strickland showings. Previous work on the property is summarized in Table 3.1. The work done on the fee-simple grants and the claim blocks immediately surrounding the showing by Falconbridge Nickel Mines Limited (as operator of the joint venture) between 1977 and 1980 is summarized in Table 3.2.

Table 3.1

Previous work on the Strickland Showing

Year	Participant	Work Done
1936	Alex Strickland	- discovery - initial prospecting and trenching
1937	Venture Limited	- regional geology map - 10 diamond drill holes - trenching
1937-1941	J. R. Cooper	- regional geology map (scale 1:63,360) for the Newfoundland Geological Survey (published 1954) - detailed map and description of the Strickland showing
1956	Kopan Developments Ltd.	- 10 diamond drill holes
1968-1969	Long Lac Mineral Exploration Limited	- 18 diamond drill holes - VLF EM 16 survey - limited soil sampling
1976	J. Stackhouse (Cominco)	- geology map and study of ore/host rock geochemistry (B.Sc. Honours thesis Memorial University of Newfoundland)
1977-1980	Falconbridge Nickel Mines Ltd.	- geophysical geochemical (rock and soil) and geological surveys, diamond drilling (see Table 3.2 for more detail)
1980	L. Chorlton (Newfoundland and Labrador Department of Mines & Energy)	- regional geology (map scale 1:50,000)
1980	P. J. Wynne	- collection of surface and drill core samples for geochemistry

Table 3.1 continued

Year	Participant	Work Done
1981	H.S. Swinden (Newfoundland and Labrador Department of Mines & Energy)	- described the mineralization and host rocks - proposed a genetic model for the deposit

Table 3.2

Work done by Falconbridge Nickel Mines Limited
on the Strickland Showing and surrounding claim blocks

Year	Work Performed
1977	- examination of the property during reconnaissance mapping of the Hermitage Flexure - staking of claims adjacent to the showings (the fee simple crown grants)
1978	- optioned the fee simple crown grants containing the showing - airborne geophysical survey - established a grid - detailed geological mapping (1:1250 scale of the fee simple area by P. Snadjr; 1:2500 scale mapping of the claim blocks) - sampling for assay old trench - soil sampling survey, followed by analysis for Cu Pb Zn Ag - ground geophysical survey (VLF EM-16, magnetometer)
1979	- lake sediment survey, followed by analysis for Cu, Pb, Zn, Ag, Co, Fe and Mn - detailed soil sampling over 1978 soil anomalies - geological mapping in areas of soil anomalies - mapping and sampling of old trenches completed - 23 diamond drill holes - surface and core rock samples collected and analysed for 10 major elements plus Cu, Pb, Zn, Ag
1980	- 14 diamond drill holes - collection of surface and new core rock samples for geochemistry

CHAPTER 4

GEOLOGY OF THE STRICKLAND SHOWINGS

4.1 Introduction

The generalized stratigraphy of the area around the Strickland showings can be summarized as a sequence of volcanic, volcaniclastic and clastic sedimentary rocks (termed here the "mixed sequence") in conformable contact to the northwest with a sequence dominated by clastic sedimentary rocks (termed here the "sedimentary sequence") (Figure 4.1). These rocks are polydeformed, metamorphosed to upper greenschist facies and strike to the north-northeast. The Baggs Hill Granite is interpreted to be a subvolcanic pluton (Prince and Briggs, 1978) which intrudes the mixed sequence.

Several felsic dykes or sills are associated with the Baggs Hill Granite. A few small and variably deformed diabase dykes cut the mixed sequence. One spectacular outcrop of layered metagabbro (a dyke or sill) is exposed in the southeast corner of the project area.

The mixed sequence plus the Baggs Hill Granite have been informally referred to as the Baggs Hill formation (Stackhouse, 1976) and the Top Pond formation (Prince, 1977a). The sedimentary sequence has been informally called the La Poile River formation (Stackhouse, 1976) and the Cuspid Lake formation (Prince, 1977a). Both the mixed and the sedimentary sequences are included in the Bay du Nord Group by Chorlton (1980).

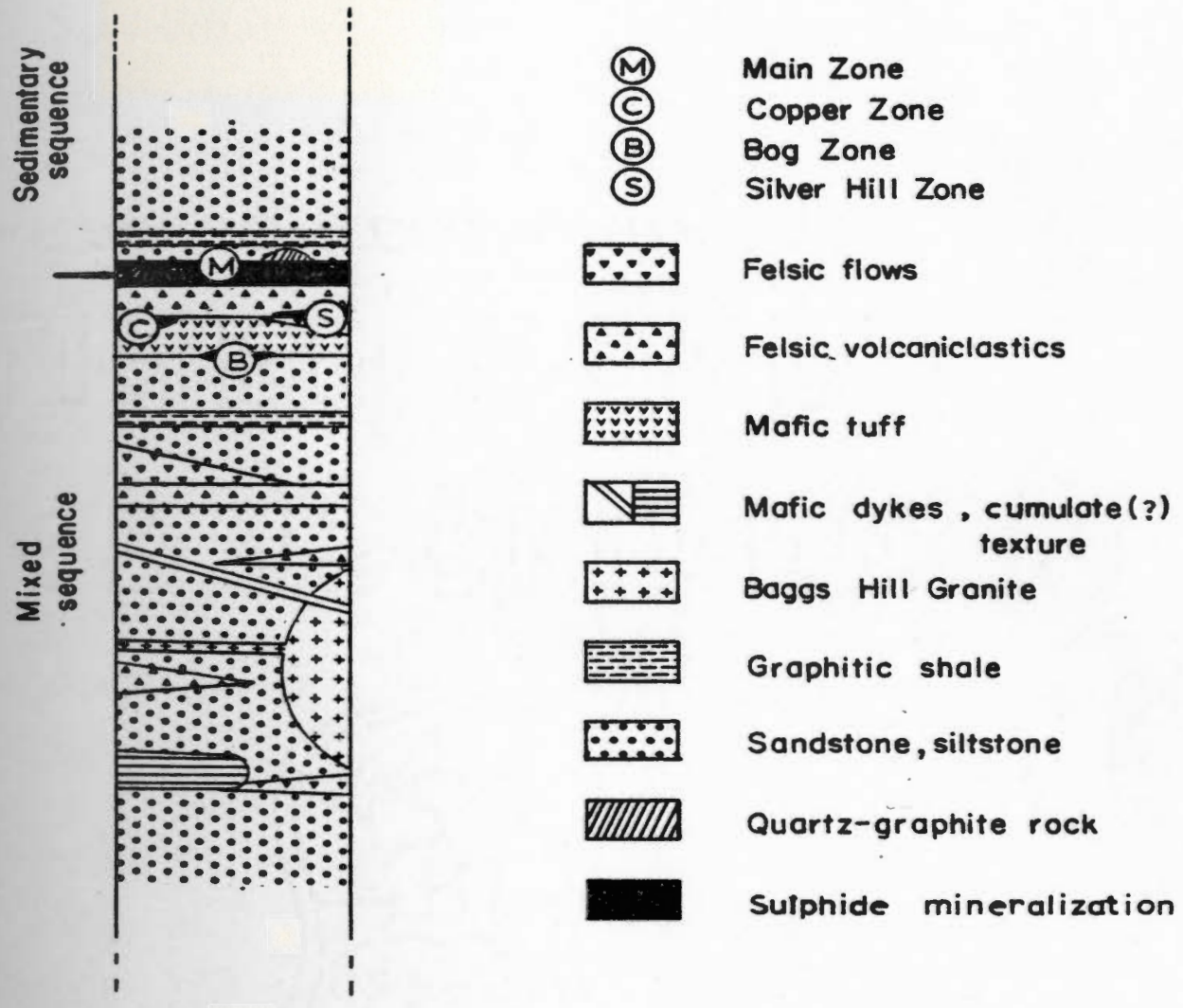

Figure 4.1. Schematic "cross section" of the Strickland area.
Approximate vertical scale is 1:10000.

The entire sequence is believed to be overturned and younging to the northwest on the basis of regional evidence (Prince, 1977a) and deposit morphology (Swinden, 1981). Chorlton (1980) has interpreted the sequence to be upright and younging to the southeast.

Seven mineralized zones identified by Falconbridge in the Strickland area are included in the region studied in this project. They are the Main Zone, Copper Zone, Silver Hill Zone, Bog Zone, Bison Fault Zone, Road Zone and the northern portion of the Carrot Brook Showing. The Main Zone, which contains the largest concentration of sulphide in the area, lies at the contact between the mixed and sedimentary sequences. This horizon is also marked by a discontinuous string of podiform outcrops of a quartz and graphite rock. Four of the other six zones of mineralization are less than 200m from the contact between the two sequences (Figure 4.1).

4.2 Map units and nomenclature

The geological map of the Strickland area (Pocket map no. 1) is adapted with some addition from maps by Falconbridge Nickel Mines Ltd. personnel at scales of 1:2500 and 1:1250. Their coverage was considered adequate and the area was not remapped by the present author except to fill in the area around Baggs Hill. Falconbridge geologists have used igneous and sedimentary rock names (protolithic names) instead of metamorphic rock names, and to maintain consistancy this practice was adopted in this study.

The rock units are discontinuous and intergradational along strike. This is a result of both the original depositional environment and the rock's subsequent history of extensive quartz veining, metamorphism and polyphase deformation. As these were not the focus of this study no formal stgratigraphic order is proposed here. Instead, the units shown on the map are described in the following order; felsic, intermediate then mafic flows and volcaniclastics, sedimentary rocks, Baggs Hill Granite, felsic dykes, mafic dykes and the quartz-graphite rock. Tuffs, lapilli tuffs and agglomerates are represented as separate units on the map but are described together in the text under the common heading of volcaniclastics (felsic, intermediate and mafic). The volcaniclastics have been assigned to one of the three units on the basis of grain size. Lithological terms used by Falconbridge in their 1977 rock sampling program (and in the data of this study) which do not appear as map units and were not later used by this author are not described (they include tuffaceous sediment and sedimentary rock). Each lithology was assigned a numerical code from 1 to 21 which was subsequently used in the computer manipulation of the data. The map units, the lithological terms and their corresponding computer code are presented in Table 4.1.

Table 4.1

A summary of the map unit numbers
(Pocket Map #1), lithologies and computer codes

Map Unit	Lithology	Computer Code Alphabetic	Computer Code Numeric
1	felsic flow	F:FL	10
2	felsic tuff	F:TF	7
3	felsic lapilli tuff	F:LT	8
4	felsic agglomerate	F:AG	9
5	intermediate flow	I:FL	6
6	intermediate tuff	I:TF	3
7	intermediate lapilli tuff	I:LT	4
8	mafic tuff	M:TF	1
9	chlorite schist	S#CH	2
10	sandstone	SSST	12
11	siltstone	SSLT	11
12	shale	SHAL	13
13	quartz-graphite rock		
14	Baggs Hill Granite	GRAN	14
15	felsic dykes	D/F:	15
16	mafic dykes	D/M:	16
	tuffaceous sediment	TFSD	18
	sedimentary rock	SEDM	19
	carbonate	CARB	20
	mafic lapilli tuff	M:LT	21

4.2.1 Felsic flows

The felsic flows form prominent ridges throughout the southwest portion of the map area. Individual flows range in thickness from 10cm to 25m and are commonly interbedded with felsic volcaniclastics. Outcrops and hand samples of the felsic flows are riddled with quartz veins. The flow material is aphanitic to very finely granular. It weathers to a light pink or beige and is beige, light to dark grey or black on the fresh surface. It is foliated (possibly relict flow banding) and in places strongly lineated, commonly breaking into elongate rhombic blocks (Figures 4.2a,b).

The felsic flows consist of isolated (up to 15%), subhedral plagioclase and quartz phenocrysts in a sutured mosaic of very fine grained quartz and orthoclase (Figure 4.3). Separate domains (bands or lenses) of medium grained polygonized quartz and the sutured mosaic variety are common. The phenocrysts are commonly corroded, fractured and pulled apart, with very fine grained quartz filling in between the fragments. Minor mineral constituents include muscovite (commonly as fine grained sericite), biotite, chlorite, epidote and blebs of sphalerite (Figure 4.4). The original pilotaxitic (felty) texture is partly obscured by recrystallization. The biotite and sericite in some sections concentrated in thin anastomosing bands giving the rock a lensoid or particulate appearance.

a.

b.

Figure 4.2. Felsic flows a) riddled with quartz veins, b) strongly foliated.

Figure 4.3. A sutured mosaic of fine grained quartz and orthoclase which is the common groundmass of the felsic flows. (Photo width is approximately 1mm).

Figure 4.4. A felsic flow cut by quartz veins with an inclusion of sphalerite which contains fan-shaped clusters of prochlorite. (Photo width is approximately 2mm).

4.2.2 Felsic volcaniclastics

The felsic volcaniclastics are concentrated at the north and south ends of the map area. These two zones are joined by a 20 m zone of northeast striking felsic volcaniclastic rocks which host the Main Zone mineralization. Discontinuous lenses of felsic volcaniclastics outcrop within the dominantly sedimentary rocks in the center of the map area.

The felsic volcaniclastics consist of intercalated and discontinuous beds of tuff, lapilli tuff and agglomerates from one centimetre to tens of metres thick. In outcrop they are weathered light pink and grey. The tuffs commonly contain up to 20% quartz and feldspar crystals. They are gritty or particulate in appearance, well foliated and contain 5 to 10% mafic minerals. These characteristics aid in distinguishing fine-grained tuffs from massive felsic flows. The lapilli tuffs and agglomerates contain strongly lineated and aligned fragments of rhyolite porphyry, silicified volcanic material and sedimentary rocks (shales, siltstone) (Figure 4.5a,b) in a matrix that is variably tuffaceous, silty or rich in biotite and garnet porphyroblasts. The agglomerate is restricted to small discontinuous lenses no larger than 20 X 100 m (Prince and Briggs, 1978). The largest bomb - sized fragments measure 25 cm x 8 cm x 5 cm (Figure 4.6). The tuffs contain phenocrysts, one to two millimetres in diameter, of albite or perthite, orthoclase or microline and quartz in a matrix of

a.

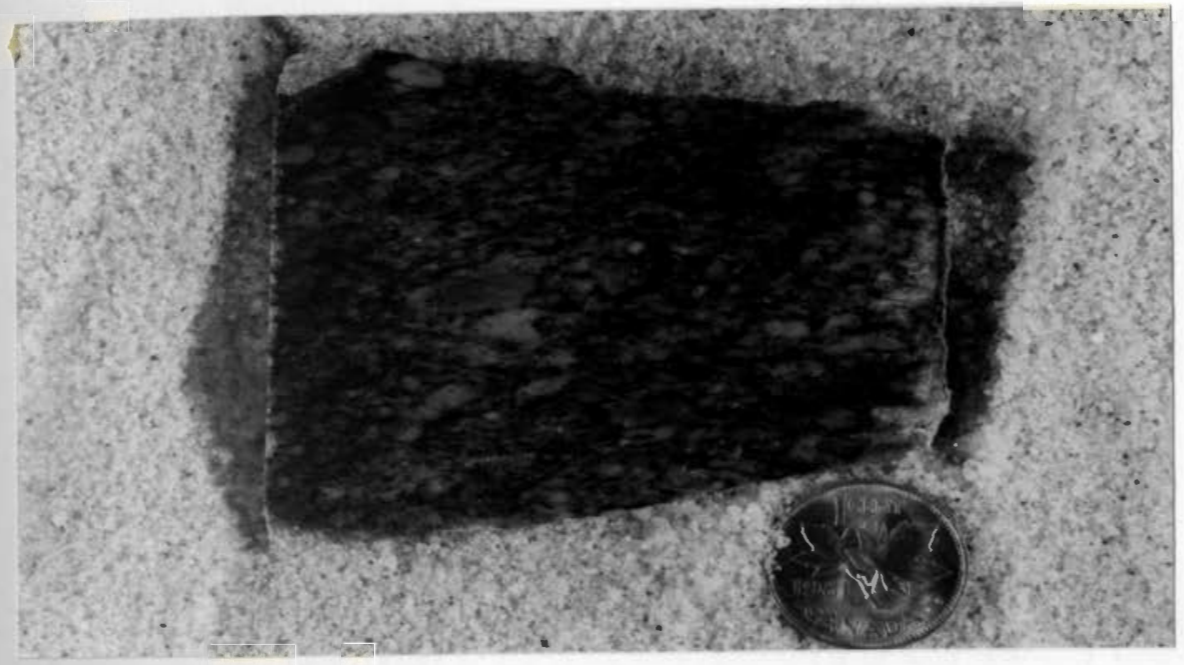

b.

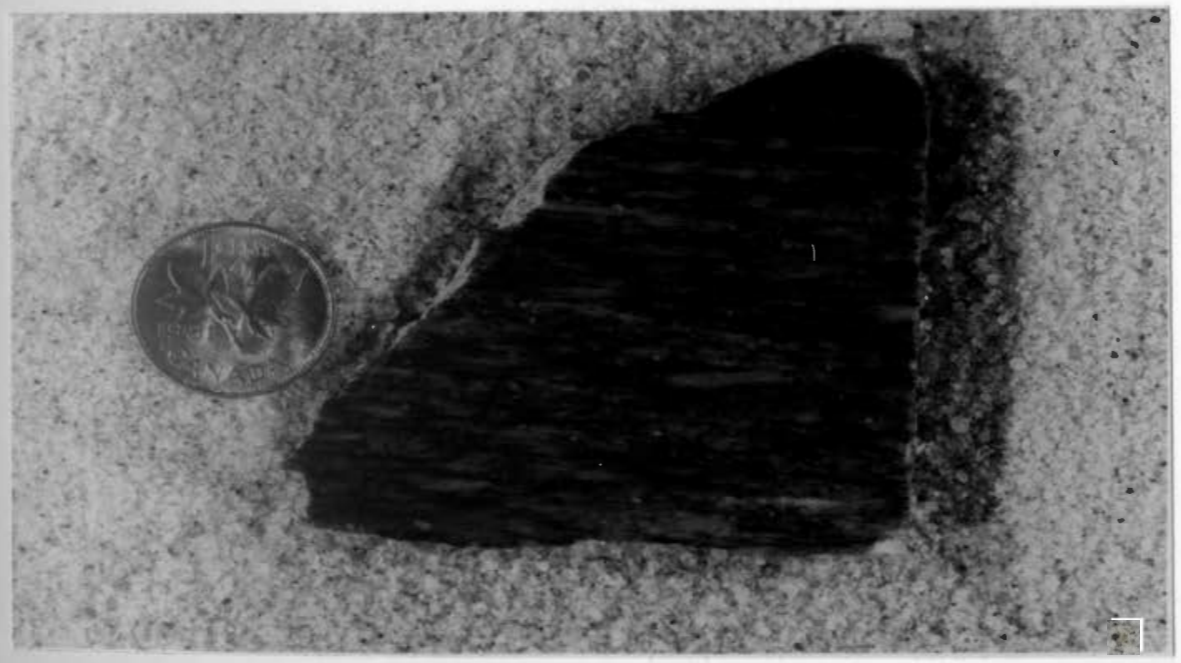

Figure 4.5. Felsic tuff/lapilli tuff showing the lineation of fragments in a) end view and b) longitudinal view.

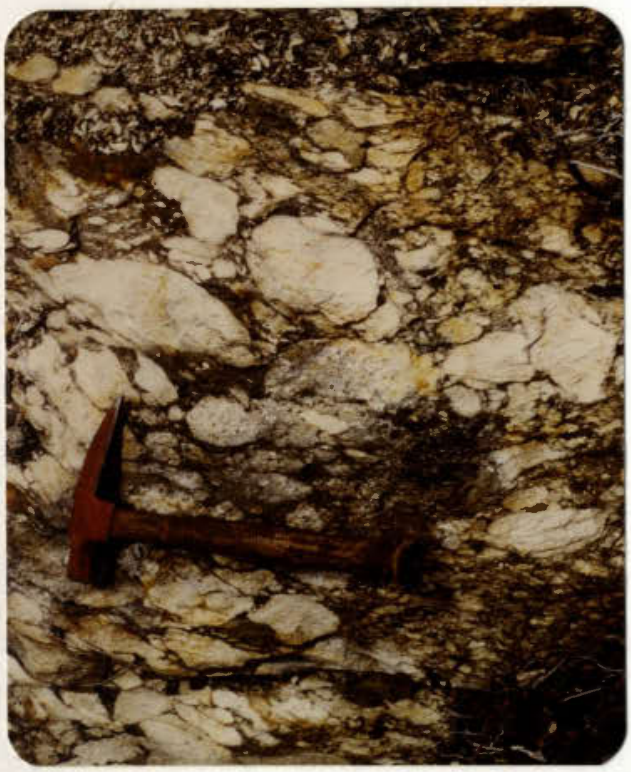

Figure 4.6. An outcrop of felsic agglomerate with slightly flattened bombs up to 20cm long.

Figure 4.7. a crystal-rich felsic tuff cut by a fine grained mylonitized domain - photo width is approximately 3mm .

fine grained quartz, sericite, minor biotite and chlorite (Figure 4.7).

Accessory minerals include epidote, sphene, pyrite and pyrrhotite with rare zircon. The quartz crystals commonly show the euhedral outline of high temperature volcanic beta-quartz. The feldspar and quartz crystals are invariably broken, pulled apart, augened (Figures 4.8a,b) and finely recrystallized in pressure shadows. Deformation twinning in the quartz phenocrysts and bent albite twins in the plagioclase phenocrysts are common. Fragments in the lapilli tuffs are similarly augened and fractured. The lapilli consist of shale, siltstone, granitic clasts and felsic flow material (complete with felty texture) (Figure 4.9) rich in K-feldspar.

Unaltered crystals of brown biotite in places poikilitic, overgrow the main foliation and are weakly aligned parallel to the axial plane of a second cleavage (crenulation cleavage). Epidote and orthoclase porphyroblasts were noted in volcaniclastics rich in sericite. Small (2 mm) euhedral garnet porphyroblasts were noted in the pelitic matrix of one agglomerate outcrop.

4.2.3. Intermediate flows

Massive, homogeneous, aphanitic, mesocratic rocks too rich in mafics to be termed felsic are described here as intermediate flows. This lithology was rarely encountered and does not appear in mappable thicknesses on surface.

a.

b.

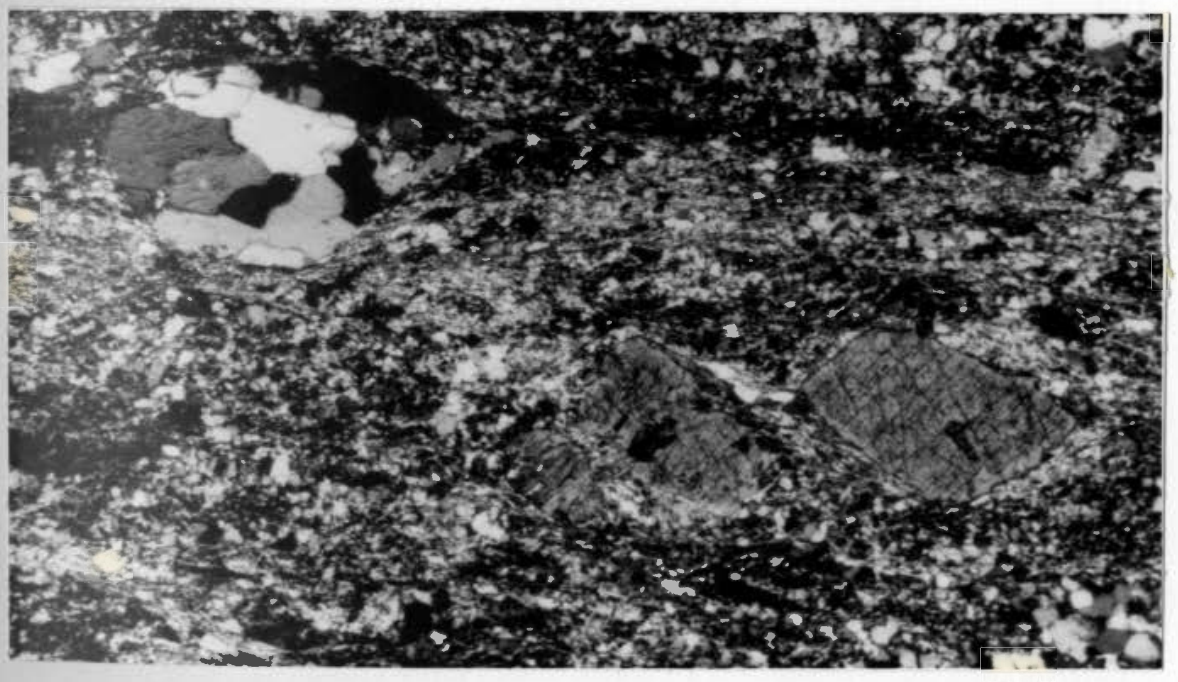

Figure 4.8. a) An albite phenocryst which is pulled apart, rotated and has polyganized quartz grains filling the space between fragments contained in a felsic tuff - photo width is approximately 1mm . b) An augened and recrystallized quartz phenocryst and pulled apart albite phenocryst contained in a felsic tuff - photo width is approximately 3mm .

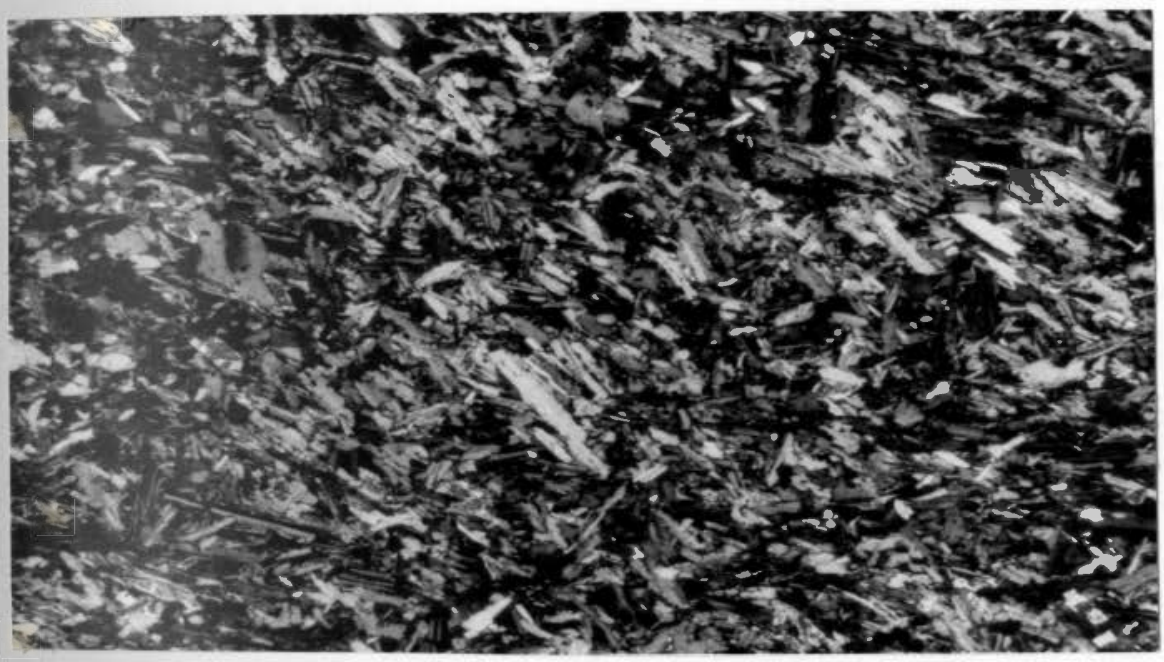

Figure 4.9. Delicate pilotaxitic texture of a volcanic clast in a lapilli tuff - photo width is approximately 1mm .

The rock is composed of fine grained quartz-plagioclase lathes and up to 20% combined biotite and chlorite. Small isolated phenocrysts of plagioclase are also present. The mesocratic appearance of the rock in one section was produced by anastomosing bands concentrated in biotite. These bands cut the rock into lensoid domains within which the primary pilotaxitic texture of the flow is preserved (Figures 4.10a,b)

4.2.4 Intermediate volcaniclastics

The most prominent horizon of intermediate tuff and lapilli tuff underlies the Main Zone. It is 5 to 20 m thick, with a strike length of 1200 m. Smaller discontinuous intervals of intermediate volcaniclastics, commonly intercalated with siltstone, are scattered throughout the property.

The intermediate volcaniclastics are crystal-poor to crystal-rich, dark grey to brown on the fresh surface and generally well foliated (Figure 4.11a,b). The groundmass is composed dominantly of fine grained quartz which is flattened and elongate parallel to the foliation (quartz crystals are often three times as long as they are wide). The rocks contain 5 to 30% sericite and ubiquitous brown biotite which comprises 15 to 20% of the rock. Chlorite (dull grey green and blue under crossed nicols) is a minor component. Calcite is present in veins, pockets and as scattered disseminations throughout some intermediate tuffs.

a.

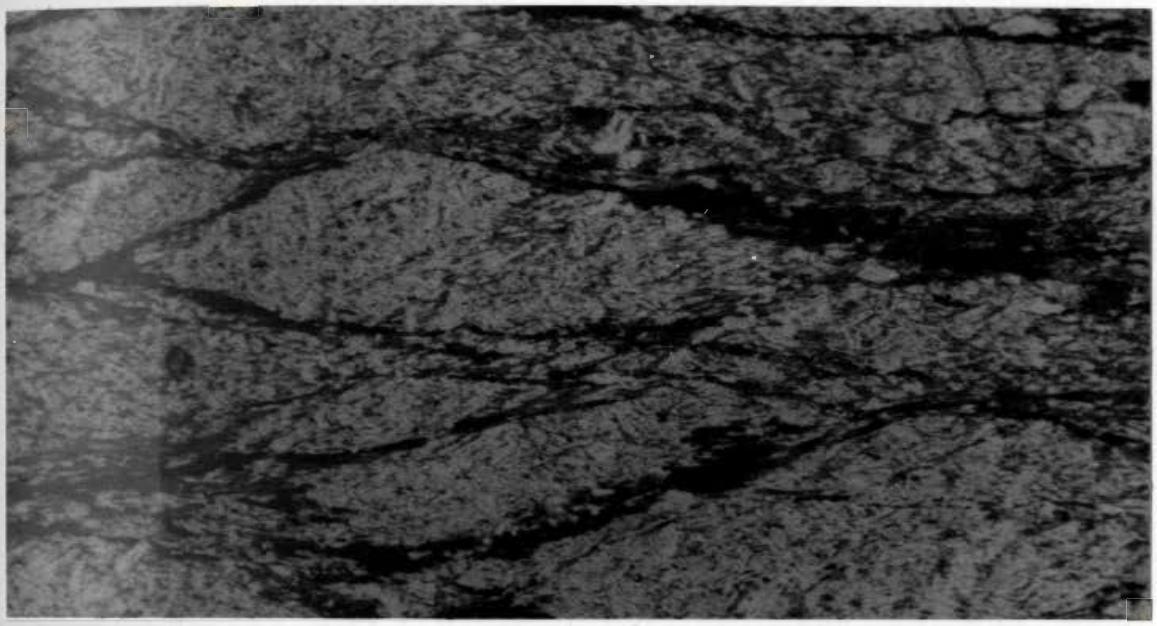

b.

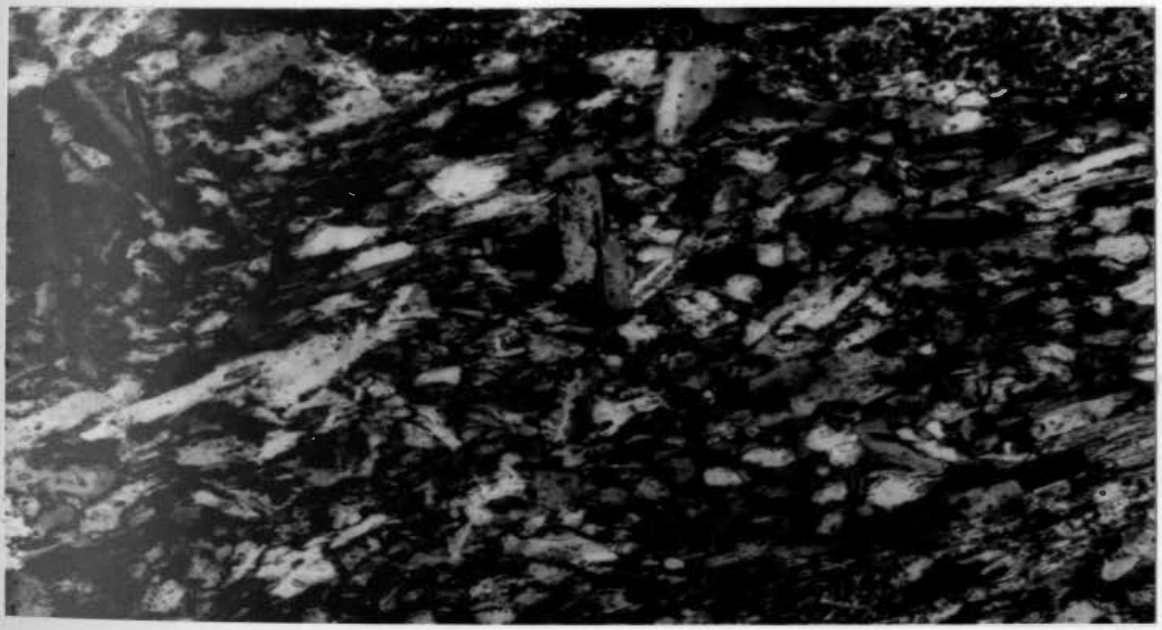

Figure 4.10. a) Anastomosing bands rich in biotite cut an intermediate flow into lensoid domains - photo width is approximately 3mm . b)The trachytic texture of the flow is preserved within these lensoid domains - photo width is approximately 1mm .

a.

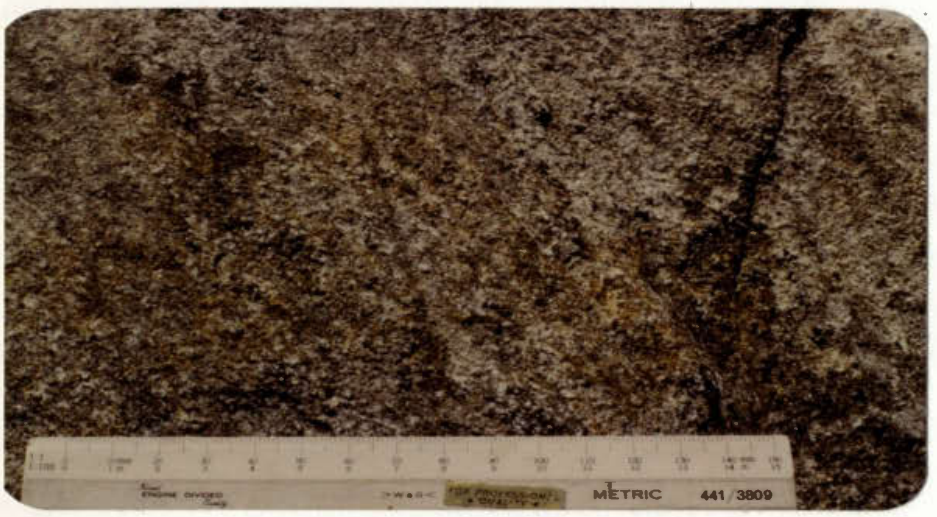

b.

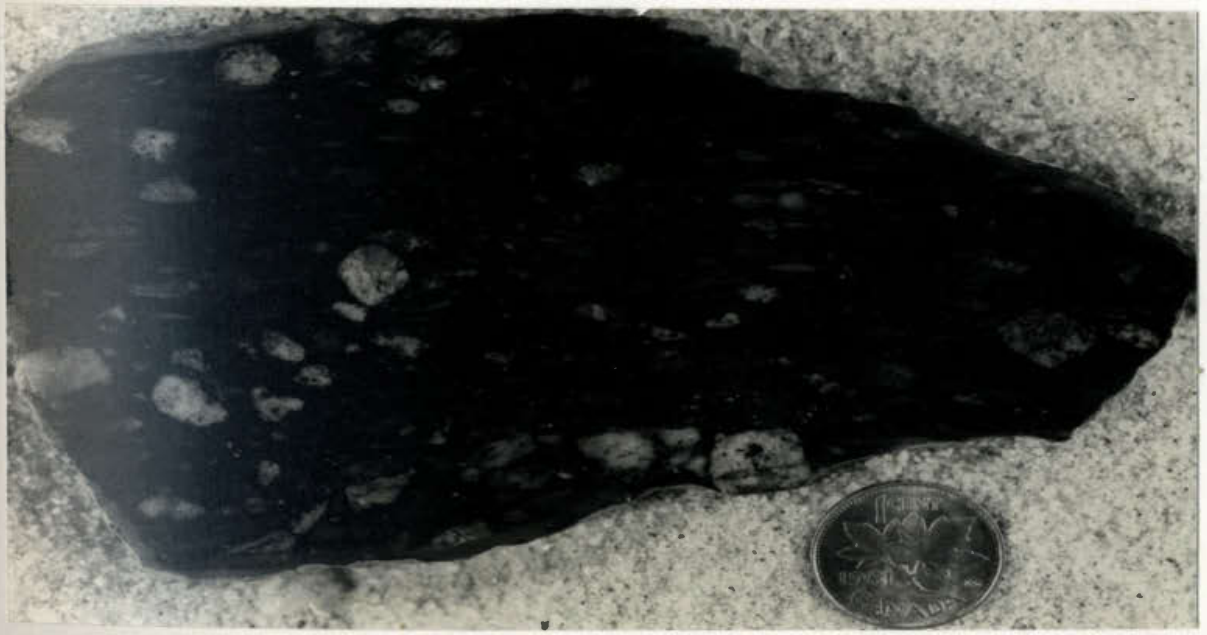

Figure 4.11. a) An intermediate tuff with crystals and clast which are resistant to erosion and stand in positive relief on the weathered surface of this outcrop. b) An intermediate lapilli tuff with a silty matrix.

One sphalerite-rich sample contains up to 20% calcite. Other accessory minerals include epidote, zircon, capillary rutile and disseminated flakes of pyrite, pyrrhotite and sphalerite. The intermediate volcaniclastics contain augened, fractured, embayed, recrystallized, and rarely euhedral phenocrysts of quartz, orthoclase or microcline, perthite and albite. Some individual tuff horizons contain phenocrysts of only one or two minerals, e.g. only quartz and orthoclase phenocrysts. This characteristic might be useful as a correlation tool in a detailed stratigraphic study of the property.

Examples of the intermediate lapilli tuff are rare. The lapilli are invariably strongly augened and contained in a matrix of fine-grained quartz and biotite which wraps around the lapilli. The lapilli consist of sedimentary and igneous rock fragments displaying granophyric or trachytic textures, as well as aggregates of quartz or feldspar crystals (Figure 4.12). Lensoid structures, which appear to be siliceous lapilli in hand samples, are seen in thin sections to be boudined quartz veins in a siltstone or silty tuff.

4.2.5 Mafic volcaniclastics

The unit described as a mafic tuff or chlorite schist by Falconbridge geologists remains enigmatic. It is poorly exposed on surface but where intersected in drill core it is conformable with adjacent lithologies. Metamorphism and

Figure 4.12. An intermediate lapilli tuff with scattered , flattened recrystallized quartz phenocrysts and a single lithic fragment (bottom half of the photo) - photo width is approximately 3mm .

Figure 4.13. A mafic tuff with light coloured blades of actinolite in a matrix dominated by chlorite and flattened grains of quartz - photo width is approximately 3mm .

deformation have obscured primary textures in the rock which might identify it conclusively as a tuff instead of a mafic flow or sill. No mafic flows or mafic lapilli tuffs were observed.

Two 20-30 m thick horizons of the mafic tuff separated by felsic volcaniclastics lie between the Main Zone and the Bog Zone mineralization. These horizons are intercalated with more intermediate tuffs and siltstone. Other discontinuous lenses have been mapped in association with the Road Zone, Copper Zone and Carrot Brook mineralization.

The rock is typically dark grey-green, well foliated with 2 to 3% sulphides (pyrite, pyrrhotite and sphalerite). Sprays of actinolite (2 mm across) and quartz-calcite veins are abundant (Figure 4.13). The mafic tuffs are composed predominantly of chlorite and quartz. The quartz crystals are strongly flattened and aligned (with aspect ratios up to 5:1) and are overgrown by a dense mat of chlorite. Much of the chlorite appears to have replaced weakly pleochroic brown biotite. Biotite is also present as poikilitic porphyroblasts. Actinolite occurs as coarse-grained poikilioblastic sprays. The mafic tuffs may contain up to 20% calcite in veins, pockets (which are possibly flattened amygdules?) and, disseminations. Epidote and sphene are present in small amounts (5%) in most sections of the mafic tuff, with restricted bands containing up to 15% epidote and sphene. The epidote usually occurs as irregular aggregates of very fine crystals but coarse-grained columnar crystals

are also present. Feldspar was absent from the fine grained groundmass of most sections, however, isolated untwinned phenocrysts (never more than 5% of the section) were noted rarely. Lensoid, very fine grained rock fragments (2 mm) were observed in one section supporting the interpretation of these rocks as tuffs.

Porphyroblasts of magnetite with biotite collars are present locally (Figure 4.14). The growth of biotite porphyroblasts preceded the kinking (or crenulation) of the main foliation as they too are bent. The sprays of actinolite are only slightly flattened in the plane of the main foliation and show no evidence of any brittle deformation.

4.2.6 Sedimentary rocks - sandstone, siltstone and shale

The most continuous and prominent sequence of sedimentary rocks in the thesis area lies adjacent to the Main Zone. There is a marked transition at the Main Zone horizon from the sequence to the southeast dominated by felsic volcanic/volcaniclastic rocks intercalated with sedimentary rocks into a sequence of sandstone, siltstones and graphitic shales with only a minor volcaniclastic component to the northwest. The sediments widely exposed in the center of the map area are mainly greywacke sandstones interbedded with subordinate finely laminated siltstone (Figure 4.15) and minor shale. Drill holes in the north end of the property encountered large thicknesses (20 to 40 m) of intercalated fine grained sandstone, siltstone and intermediate tuff. No

Figure 4.14. Porphyroblasts of magnetite with collars of biotite in a mafic tuff (under plane polarized light). The matrix is composed mainly of quartz, chlorite (green) and disseminated pyrite. Photo width is approximately 1mm .

Figure 4.15. An outcrop of sandstone and interbedded siltstone. Note the foliation developed in the recessively weathered siltstone layer.

convincing primary sedimentary structures other than laminar to massive bedding were noted in outcrops of the sedimentary rocks. No conclusive indication of the facing direction of the sequence was noted by the author in the showing area. Falconbridge geologists believe the sequence to be overturned and younging to the northwest. This conclusion is based on regional observations, where to the east along the same stratigraphic horizon the sedimentary sequence is seen to clearly overlie the mixed sequence (and dip gently north; Prince, 1977a). This is in contrast to Chorlton (1980) who maintains on the basis of structural evidence that the sequence at Strickland is not overturned, but is upright and younging to the southeast.

The sandstones are generally fine grained and well sorted with a bimodal grain size distribution. Compositionally they range from quartz arenites to plagioclase arkoses, the latter being more abundant. The sand grains are rounded to subrounded or augened. The coarser grains are commonly fractured and recrystallized into aggregates of smaller subgrains. Grains of quartz, albite, perthite, orthoclase and granophyre were noted. Sericite and biotite with finer grained quartz comprise the matrix. Chlorite, epidote, sulphides (pyrite, pyrrhotite, sphalerite) and a trace of tourmaline occur as accessory minerals (Figure 4.16a, b).

The siltstone is well bedded (laminated to thinly bedded) and very fine grained, usually interbedded with more

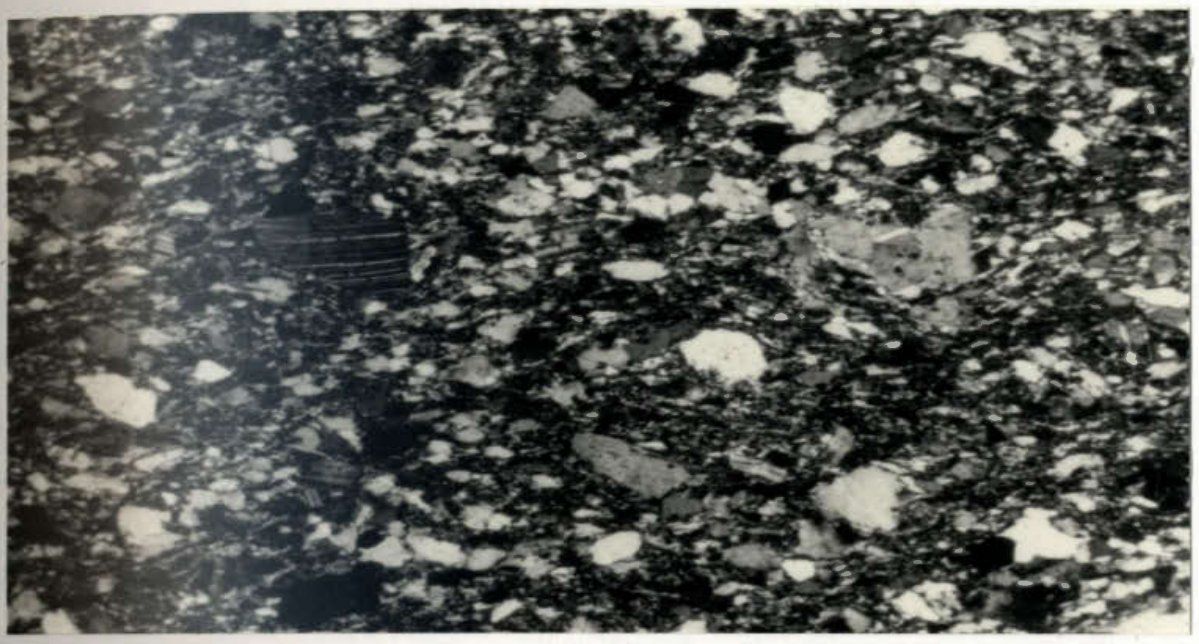

Figure 4.16. An immature sandstone (note the albite grain, center left) typical of the Strickland area. Photo width is approximately 2.5mm .

Figure 4.17. Sandstone and siltstone interbedded on a microscopic scale - photo width is approximately 3mm . Note the flattened shape of many of the grains and the mylonitized appearence of some of the bands.

arenaceous bands (Figure 4.17). Strongly flattened quartz grains (3:1 to 5:1 aspect ratios) are contained in a matrix dominated by sericite or biotite (± chlorite). Flakes of opaques (pyrite, pyrrhotite) are ubiquitous and comprise 2 to 3% of most of the siltstones. Isolated lenses with scattered feldspar and quartz euhedra indicate sporadic and minor volcanic input. The presence of tourmaline is a diagnostic feature of the siltstones. Tourmaline comprises 1 to 3% of these rocks and occurs as coarse grained euhedra which are zoned and greenish-yellow to yellow in plane polarized light (Figure 4.18). Calcite, epidote and sphene are accessory minerals except locally where bands may be concentrated in up to 10% small sphene euhedra. The main foliation varies from being subparallel to 15 to 20 degrees to the bedding (Figure 4.19). Diffuse pumpellyite porphyroblasts were noted in one section. A single peculiar 3 cm thick siltstone horizon was noted in association with the Bog Zone mineralization. It consists of 0.5 mm clots of sericite in a biotite-rich matrix. The sericite clusters give the rock a spotted appearance and may represent altered porphyroblasts of orthoclase or possibly cordierite. This horizon is mineralogically similar to the spotted facies described by Riverin and Hodgson (p. 431, 1980) below the Millenbach deposit.

The shale units are typically graphitic, well foliated, crenulated and rich in disseminated sulphide flakes (3 to 5% pyrrhotite) (Figure 4.20). Shale and siltstone are commonly

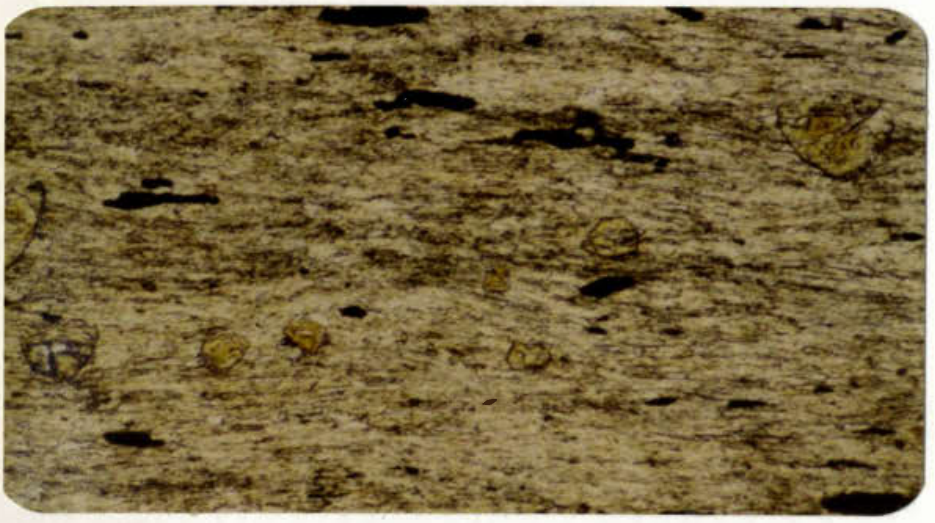

Figure 4.18. A cross sectional view of authigenic tourmaline crystals in a siltstone (under plain polarized light). The groundmass is composed of sericite, biotite, quartz and flakes of pyrite and pyrrhotite. Photo width is approximately 1mm .

Figure 4.19. Foliated micas and sulphides "stepping" across the primary sandstone/siltstone bedding. The foliation is at an apparent angle of 20° to the bedding which is horizontal in this photograph. Photo width is approximately 2.5mm .

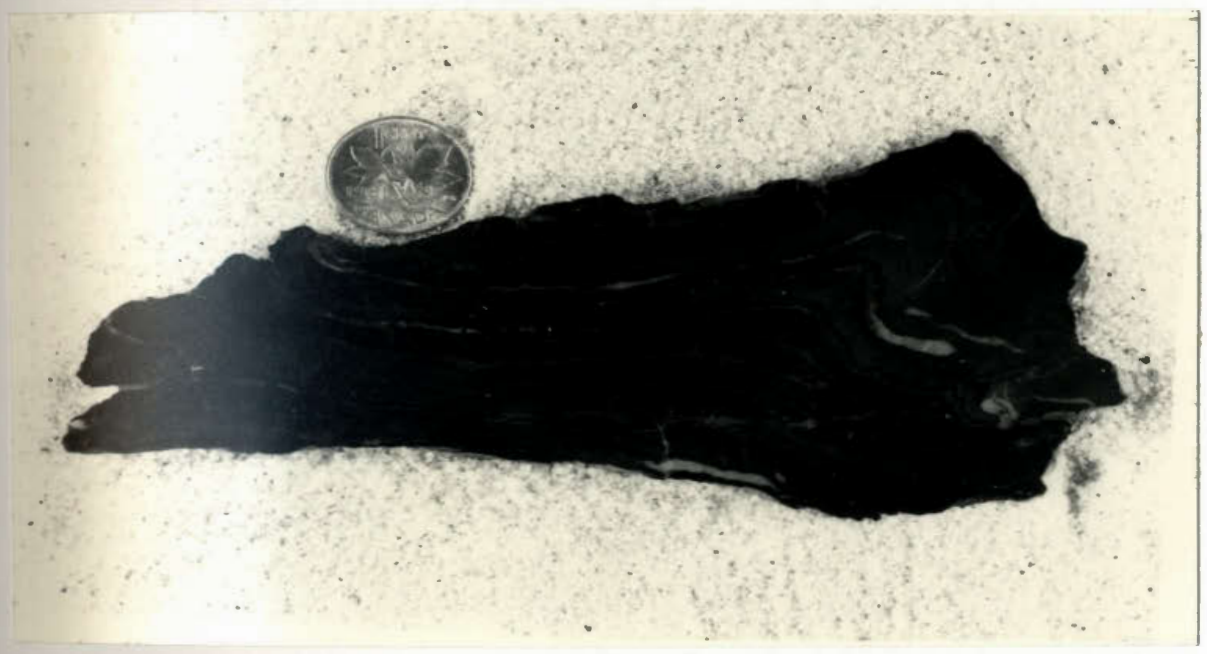

Figure 4.20. Folded graphitic shale with quartz veins.

found interbedded. The shale is composed of flattened quartz (3:1 to 4:1 aspect ratios) with abundant sericite, accessory biotite, chlorite and trace amounts of tourmaline. Graphite is present as a dust of extremely fine grained material.

4.2.7 Quartz-graphite rock

This lithology outcrops in striking, isolated, blue-grey weathering knobs. On close inspection the rock is seen to be composed of porous, saccharoidal, white quartz riddled with randomly cross-cutting and contorted graphite filled veins and graphite-lined vugs (Figure 4.21a). No comparable lithology was encountered in the core although it outcrops at the same stratigraphic horizon (between the main ore zone and the overlying sediments) as a carbonate-tremolite zone intersected in drill hole 16-023-1. The quartz-graphite rock rapidly pinches and swells to a maximum width of four metres creating a string of four isolated outcrops, resembling large boudins. It is composed of fine to medium grained quartz which is variably polygonized, strained or in elongate crystals. Graphite occurs as very fine grained wispy patches, concentrated where the quartz groundmass shows minimum grain size, maximum strain and incomplete recrystallization. The graphitic concentrations are only very weakly foliated (Figure 4.21b). This horizon is interpreted to be a metamorphosed and deformed chert horizon overlying the ore body.

a.

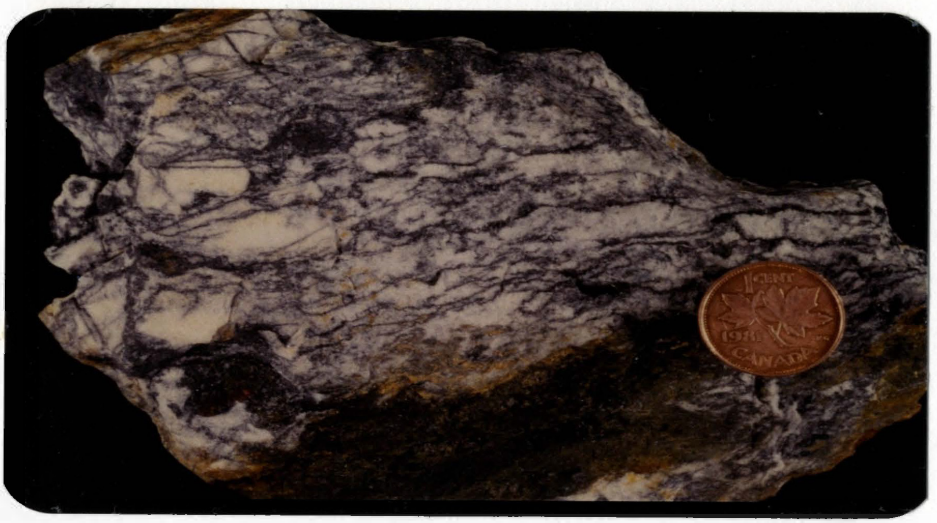

b.

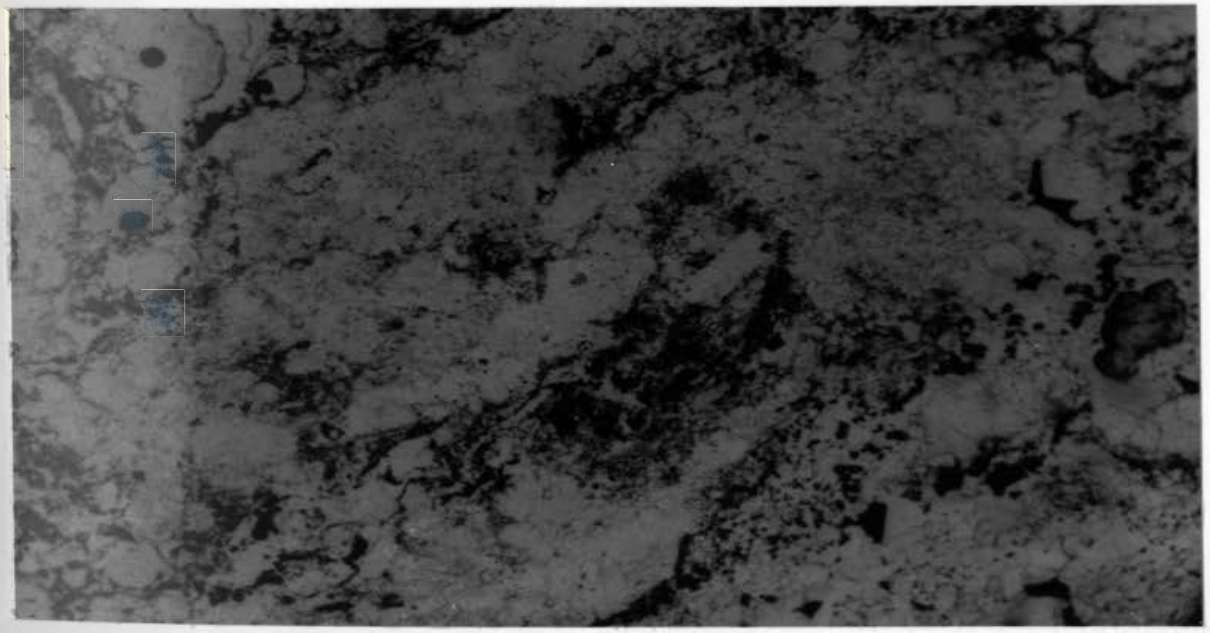

Figure 4.21. Quartz-graphite rock a) veinlets and vugs filled with graphite in a sugary, white quartz rock; b) nebulous patches of graphite are evident in thin section (plain polarized light). Photo width is approximately 2mm .

4.2.8 Baggs Hill Granite

The Baggs Hill Granite is exposed in a 180m high hill in the northeast corner of the property and in apophyses which stretch to the northeast parallel to the regional foliation. The granite weathers a buff to pinkish-grey and is light pinkish-grey on the fresh surface (see Figure 4.22a). It is equigranular, fine to medium grained and contains 5 to 10% of one to two millimetre aggregates of biotite. Granophyric texture, both finely and coarsely developed, is present in all but a few thin sections (Figure 4.22). Perthite, albite and quartz are the dominant mineral phases. Microcline is rare. Perthite with clear albite margins and patch perthite are common (see also Chorlton, 1980). Euhedral feldspars and rare quartz crystals are contained in a granophyric groundmass. No well-developed porphyritic phases were noted. Allanite, zircon, minor biotite and hastingsite occur as primary mineral phases interstitial to quartz and feldspar. Biotite, epidote and chlorite occur as secondary minerals. All these mafic minerals occur as clusters peppered with minor opaques and comprise 5% of the granite. Late stage veins of quartz (1-10 mm wide) cut the rock and are in turn cut by sericite filled fractures and calcite veins.

a.

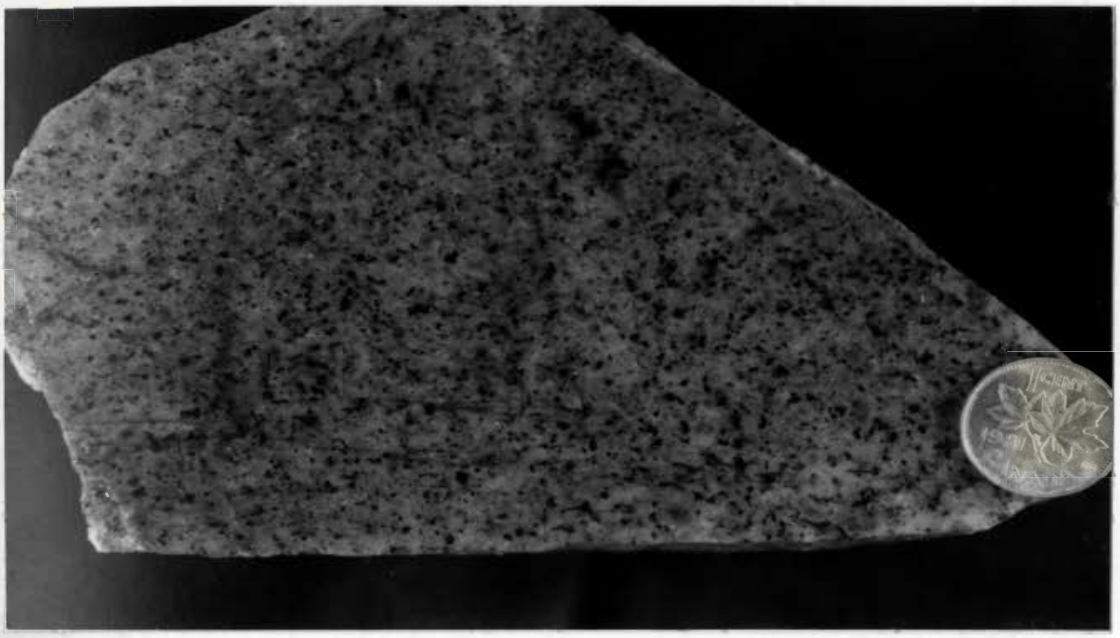

b.

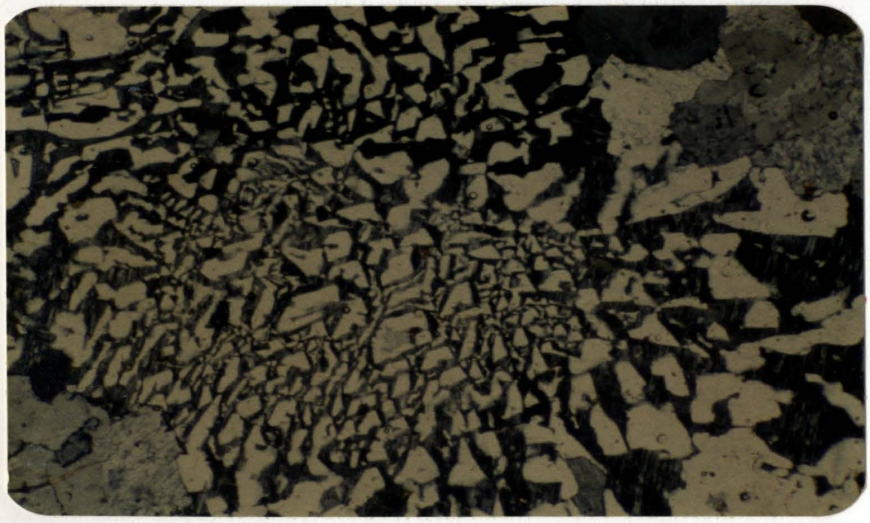

Figure 4.22. Baggs Hill Granite a) an equigranular and leucocratic granite; b) granophyric texture which is typical of the Baggs Hill Granite. Photo width is approximately 3mm .

4.2.9 Felsic dykes

Three felsic dykes 3 to 15 m wide have been identified on the property. Two are parallel northeast-trending extensions of the Baggs Hill Granite. The third lies in the extreme southeast corner of the property and is probably related to an intrusion also mapped as Baggs Hill Granite (Chorlton, 1980). Two of the dykes are high level porphyritic intrusions. One has delicate granophyric textures and quench-textured, skeletal plagioclase with belt-buckle and swallow-tail shapes in a very fine grained, orthoclase-rich groundmass (Figure 4.23).

The other dyke is composed of subhedral to euhedral quartz, albite, and orthoclase phenocrysts set in a fine grained quartz-rich groundmass. The dykes contain 5% secondary biotite, muscovite, and epidote as well as thin quartz veins. A weakly developed fabric marked by zones of recrystallized quartz and aligned biotite flakes was noted in one of the dykes.

The third dyke may be a felsic flow. Preserved in large oval domains (2 to 15 mm across, Figure 24a) are radiating clusters of small simply twinned plagioclase crystals nucleating off fine-grained cores (this is possibly a spherulitic devitrification structure). These clusters are contained in a very fine grained groundmass with sutured grain boundaries. Phenocrysts are scarce. The lensoid domains are separated by .1 to 1 mm bands, rich in K-feldspar, which show strong optical alignment (see Figure

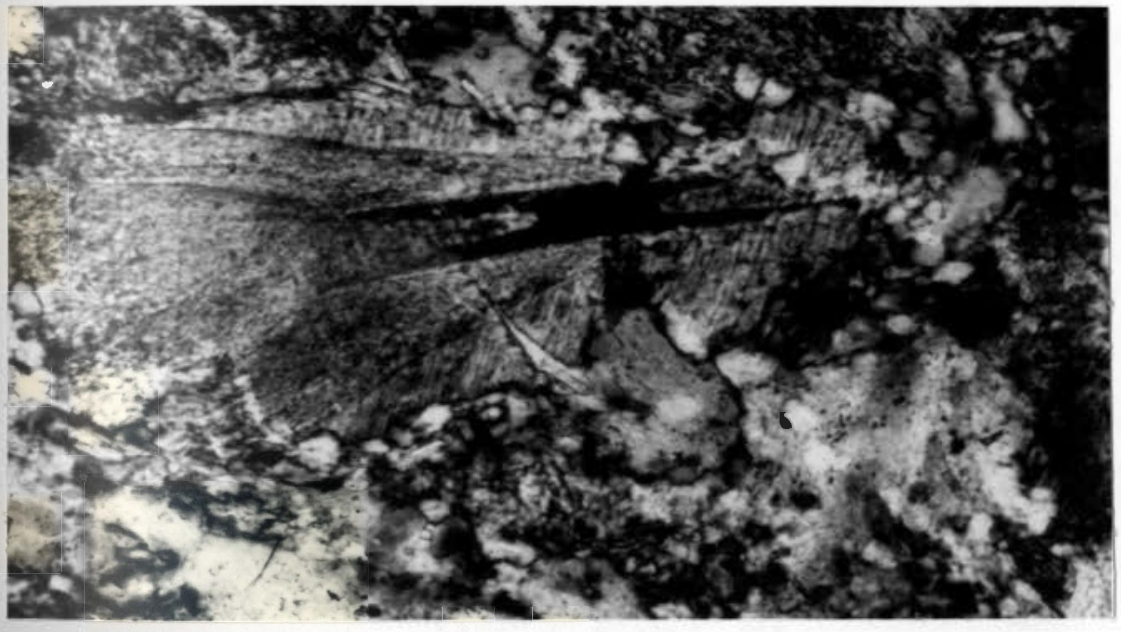

Figure 4.23. A swallowtail (quench texture) plagioclase surrounded by very fine grained granophyric material in a felsic dyke. Photo width is approximately 1mm .

a.

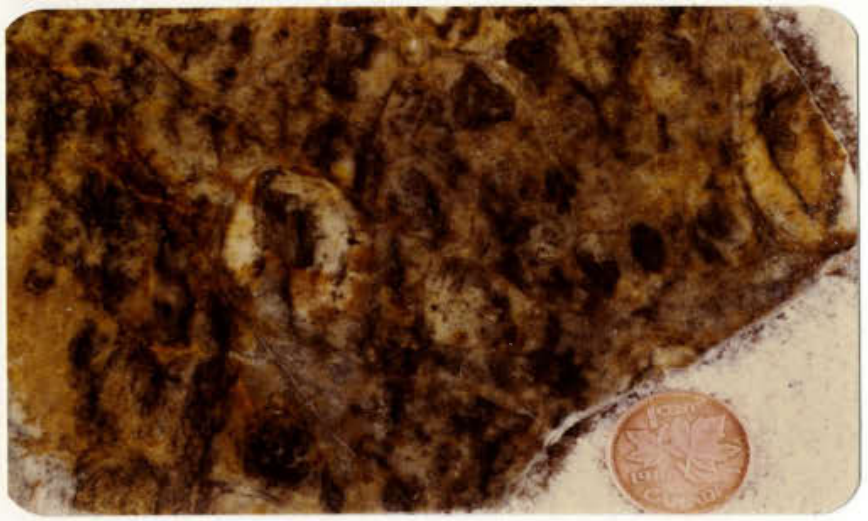

b.

c.

Figure 4.24. A felsic dyke (flow?) with a) peculiar oval shapes which are up to 1.5cm across; b) fine grained domains mark the boundaries of these ovals (seen here under crossed nicols) which are optically aligned (seen in photo c) under crossed nicols with the quartz plate in place). The lengths of photos b) and c) represent approximately 3mm .

4.24b,c). The oval, lensoid shapes prominent in this rock may either be perlitic fractures or evidence of cataclastic deformation.

4.2.10 Mafic dykes

Mafic dykes, 10 to 30 m wide and generally subparallel to the trend of the regional foliation, outcrop throughout the study area. They are typically dark green-grey on the weathered surface and moderate green-grey on the fresh surface. Sprays of actinolite are a diagnostic feature of the dykes (Figure 4.25). In one whaleback-shaped outcrop in the southeast corner of the study area the actinolite sprays are almost 1 cm across and are concentrated in shallowly dipping contorted (folded) bands alternating with bands relatively free of actinolite (Figure 4.26). This banding is interpreted to represent a relict primary cumulate texture of a gabbroic sill. This outcrop is included in Chorlton's (1979b) map unit 2 which she speculates may be tectonically emplaced fragments of oceanic crust (unit 2 in Figure 2.1, page 21).

In thin section the rocks are dominated (35 to 40% of the rock) by bladed and acicular crystals of actinolite (Figure 4.27). Biotite may or may not be present (0 to 15% of the rock) and was noted in one section to show two preferred orientations across the main foliation which is defined by bands alternatingly rich or poor in actinolite. Chlorite and very fine grained quartz with sutured mosaic

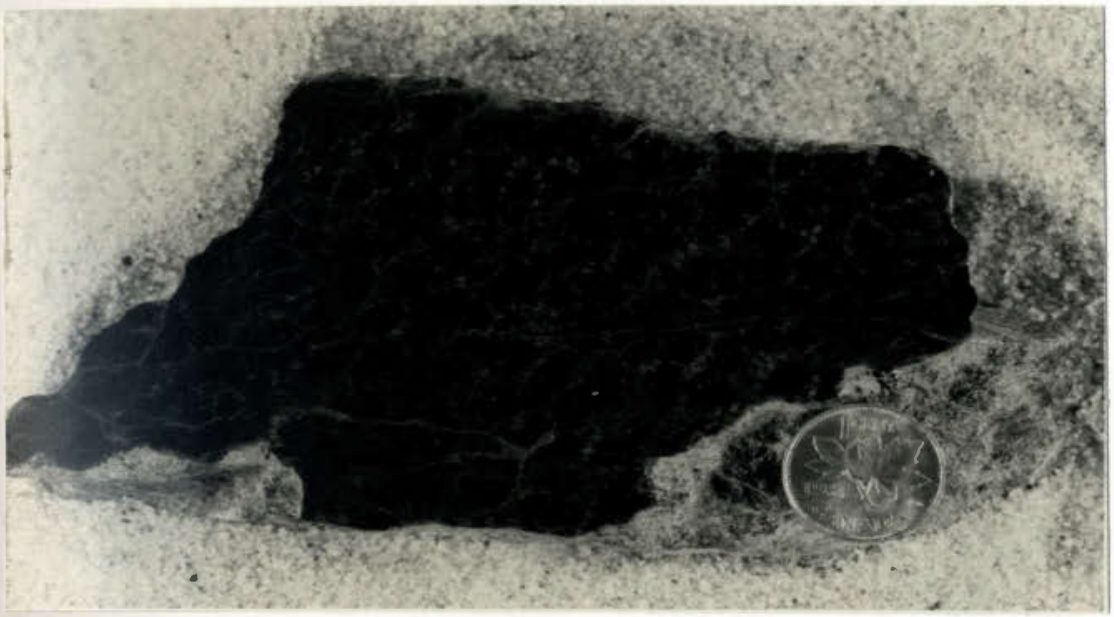

Figure 4.25. A mafic dyke hand sample with diagnostic ovoid knots of actinolite.

Figure 4.26. Folded banding observed in an outcrop of a mafic dyke belonging to Chorlton's (1980) unit 2. The banding may be a relict cumulate texture.

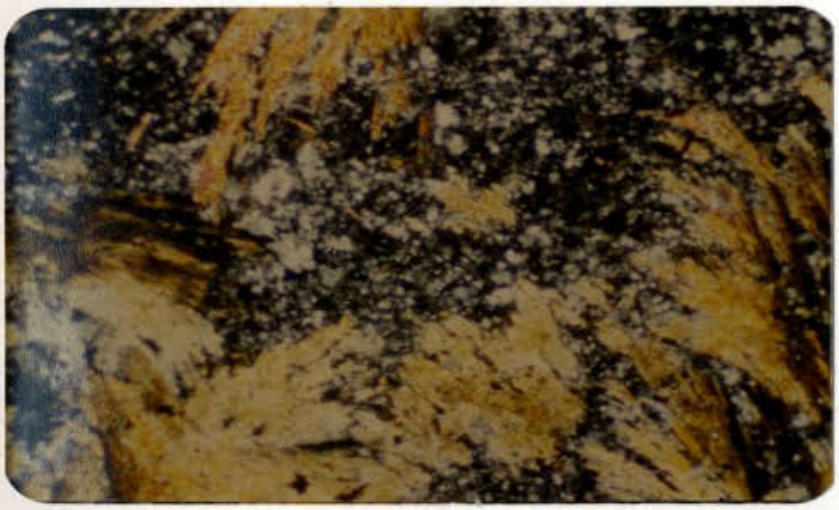

Figure 4.27. Radiating sprays of actinolite in a groundmass of chlorite and quartz typical of the mafic dykes. Photo width is approximately 3mm .

grain boundaries comprise the groundmass interstitial to actinolite. Rare, isolated and relict zoned feldspar phenocrysts were noted. Pyrite, sphene, calcite and tourmaline are common accessory minerals. The mafic dykes are all weakly to moderately foliated and lineated. The growth of the actinolite sprays appears to have been largely post-deformational.

4.3 The metamorphic history

The effects of two distinct periods of metamorphism have been preserved in the rocks of the Strickland area. The earliest metamorphism was coeval with the hydrothermal emplacement of the synvolcanic sulphide mineralization. Abundant sericite, scattered orthoclase porphyroblasts in a sericite or biotite-dominated matrix (Figure 4.28a) and a single tuff containing andalusite (Figure 4.28b) are found only in close proximity to sulphide mineralization. This suggests that these are relicts of, or the metamorphosed equivalent of the products of that earliest period of low pressure, moderate temperature metamorphism (hydrothermal alteration). Sericite and K-feldspar are typical alteration or "metamorphic" products found in the wall rocks adjacent to unmetamorphosed Kuroko-type deposits (Shirozo, 1974). Andalusite is found in the footwall rocks of many of the metamorphosed Archean massive sulphide deposits (Millenbach, Riverin and Hodgson, 1980; Mattabi and Sturgeon Lake Mines, Franklin, et al., 1977) where it probably represents the metamorphic equivalent of an intensely leached argillic alteration zone. Early andalusite-K-feldspar and andalusite-sericite assemblages also occur in alteration zones associated with porphyry copper deposits (El Salvador, Chile, Gustafson and Hunt, 1975).

The effects of regional metamorphism were subsequently superimposed on the alteration and metamorphism related to mineralization in the Strickland area. The rocks reached

a.

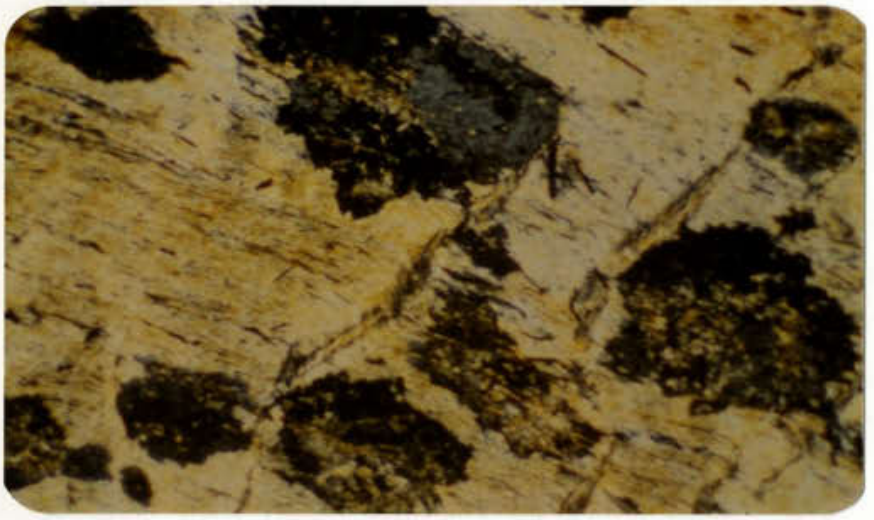

b.

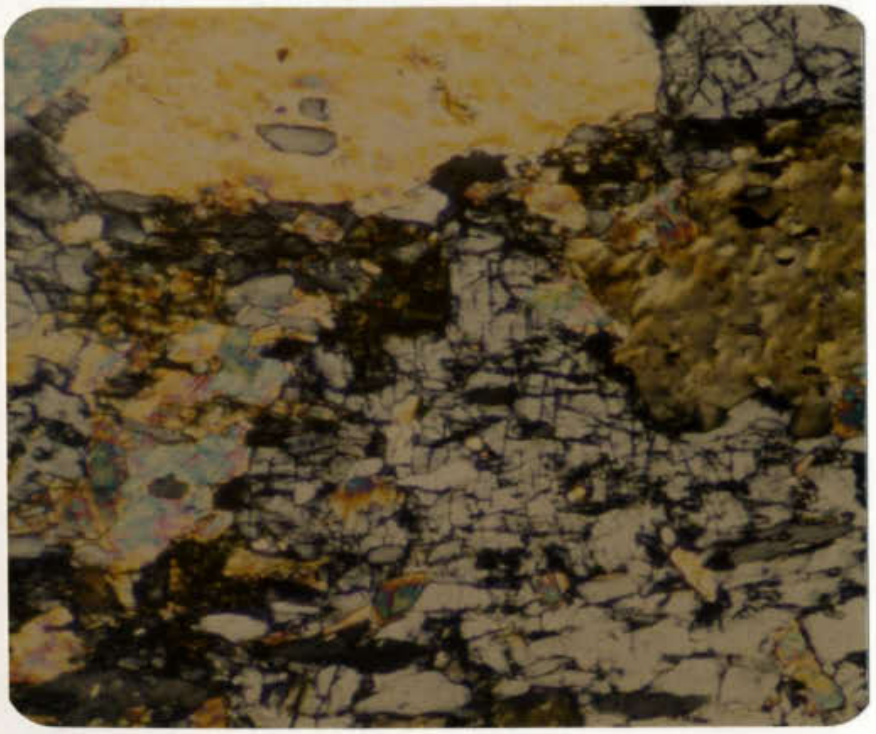

Figure 4.28. Porphyroblasts of a) orthoclase in a sericitized siltstone and b) andalusite (the first order grey material with the two poor cleavages) in an intermediate tuff with biotite. Photo widths are approximately a) 3mm and b) 1mm .

upper greenschist facies and are partially retrogressed to prehnite-pumpellyite facies assemblages. Mineral assemblages in the pelitic rocks include biotite partly replaced by chlorite, quartz, sericite and tourmaline. Garnets with quartz inclusion trains were found in siltstones with brown biotite, quartz and epidote. Poikiloblastic biotites in subparallel alignment to the crenulation cleavage are common in almost all rock types (Figure 4.29a, b). The mineral assemblages of metabasic rocks typically includes chlorite, quartz, actinolite, calcite, +/- biotite, sphene and epidote. The feldspar phenocrysts contained in tuffs and flows are invariably fresh and unaltered - possibly reflecting a low hydrogen ion activity during greenschist facies metamorphism (Hemley and Jones, 1964). Chlorite replacing biotite and the isolated occurrence of irregular pumpellyite porphyroblasts are interpreted as features of retrograde metamorphism. Standard ACF, AKF plots of mineral assemblages and bulk composition of these rocks were not possible because the individual ionic species of iron (ferrous, ferric) were not analysed.

The mineral assemblages present, and the absence of others (staurolite, sillimanite/kyanite), the preservation of delicate primary volcanic textures (trachytic, quench and perlitic(?) textures) as well as the relatively undisturbed nature of the volcaniclastics (lapillii and bombs are easily recognizable, no development of mafic/felsic segregations)

a.

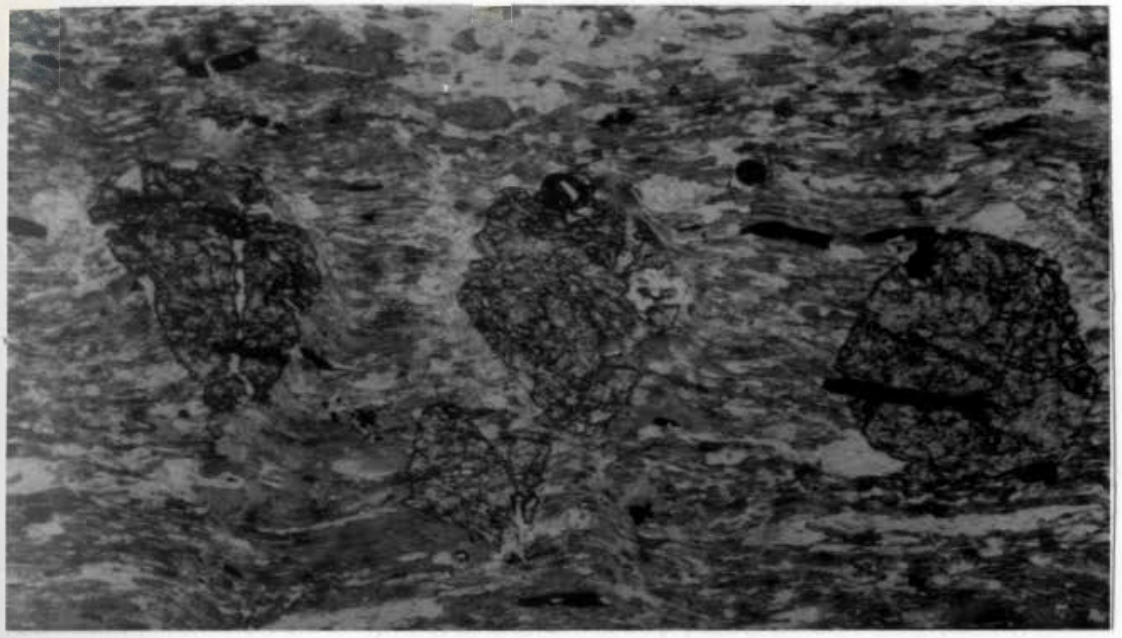

b.

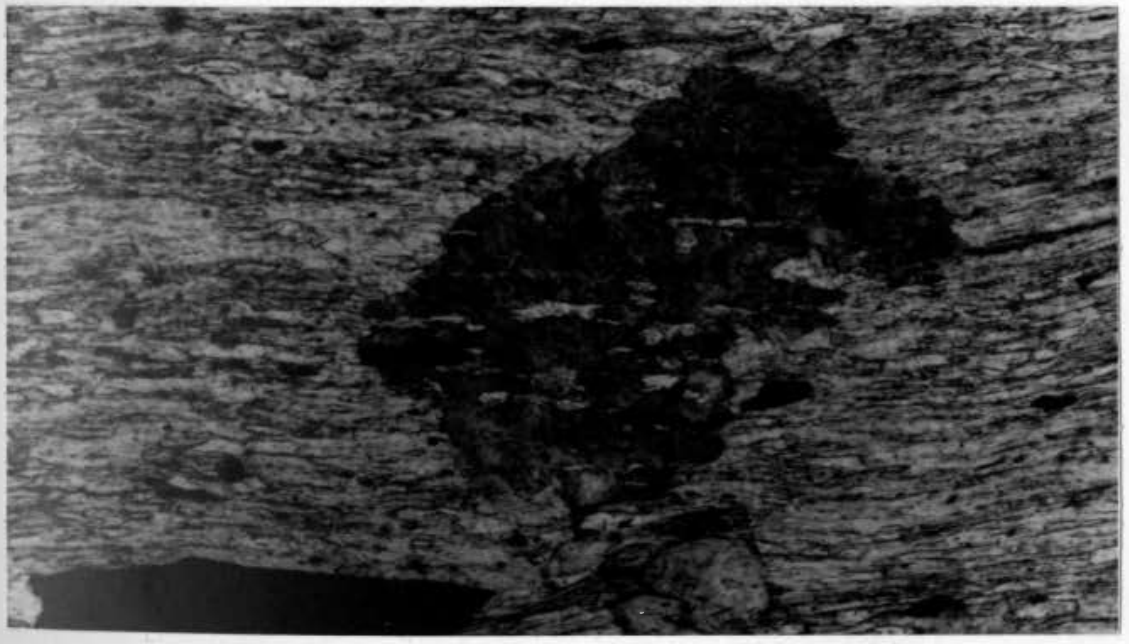

Tourmaline

Figure 4.29. Porphyroblasts of a) garnet and b) brown biotite in siltstone. Note the tourmaline at the center bottom of the photo. Photo widths are approximately a) 2mm and b) 1mm .

argue against Chorlton's conclusions that these rocks have been metamorphosed to middle amphibolite facies (Chorlton, 1980), although elsewhere in the Bay du Nord Group almandine garnet and kyanite are abundant (Chorlton, 1980).

4.4 The deformational history

The effects of at least two periods of deformation are evident in the rocks of the Strickland area. The earliest deformational episode produced a prominent penetrative regional schistosity which strikes between 040° and 050° and dips to the southeast at 50° to 60°. This is approximately subparallel to the bedding, but the bedding dips more shallowly (40° to 50° southeast). Aligned clasts, stretched into cigar shapes (Figure 4.30), lineated aggregates of mafic minerals and disseminated sulphides all aligned in the plane of schistosity are prominent. The lineation trends at 060° with a plunge of 30° and coincides with the fold axis of small drag folds. There is abundant evidence in thin section for extensive inhomogeneous cataclastic deformation of these rocks, recorded in the juxtaposition of domains of finely granulated quartz-rich material with sutured mosaic grain boundaries and domains showing well-developed polygonally recrystallized grain boundaries. Elsewhere domains of randomly oriented muscovite occur millimetres from domains of strongly foliated muscovite. The fine grained, granulated bands are frequently optically aligned. Thin, anastomosing micaceous bands cut rocks of most

Figure 4.30. Strongly stretched and aligned clasts in a felsic agglomerate.

lithologies into millimetre-sized augen-shaped domains, which were probably the locus for the accommodation of shear stresses in these rocks.

Phenocrysts, lithic fragments, and pyrite porphyroblasts are invariably broken, pulled apart, rotated and augened with recrystallized quartz in pressure shadows (Figure 4.31a). Quartz crystals nucleating off phenocrysts in pressure shadows are generally gently bent (Fgure 4.31b, 4.32a, b).

Porphyroblast growth (garnet, andalusite) appears to have taken place between the two phases of deformation (as interkinematic crystal growth) or late in the first phase of deformation.

The latest phase of deformation produced a weak crenulation cleavage which is best developed in the more micaceous units (Figure 4.33). Polygonal arcs, micas with two preferred orientations in some sections and the weak alignment of late stage poikilitic biotite porphyroblasts are related to this period of deformation (Figures 4.34a, b).

The fabric in one section suggested that the penetrative foliation here described as a product of the earliest phase of deformation might in fact be a crenulation fabric of an even earlier foliation. This observation could not be reproduced in other thin sections, but it is possible that the intensity of deformation which produced the prominent schistosity and parallel cataclastic deformation may have obliterated evidence of earlier phases of deformation. Indeed, Stackhouse (1976) proposed a three-stage

a.

b.

Figure 4.31. a) Bent albite twinning in plagioclase and b) bent quartz crystals nucleating on a grain of pyrite. Photo widths are approximately a) 1mm and b) 2mm .

a.

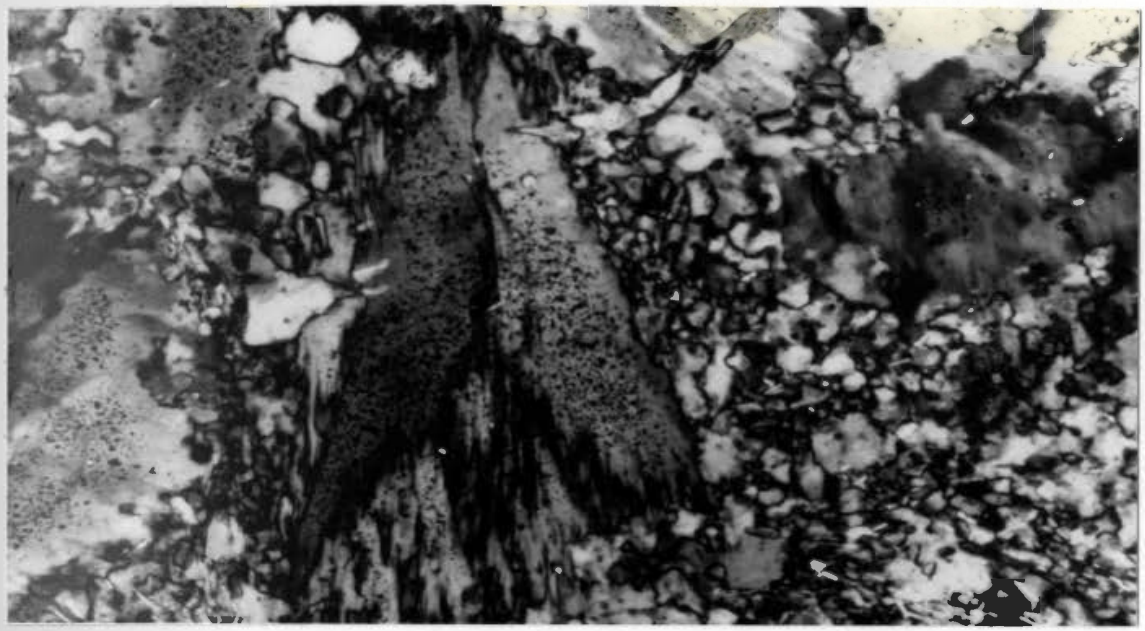

b.

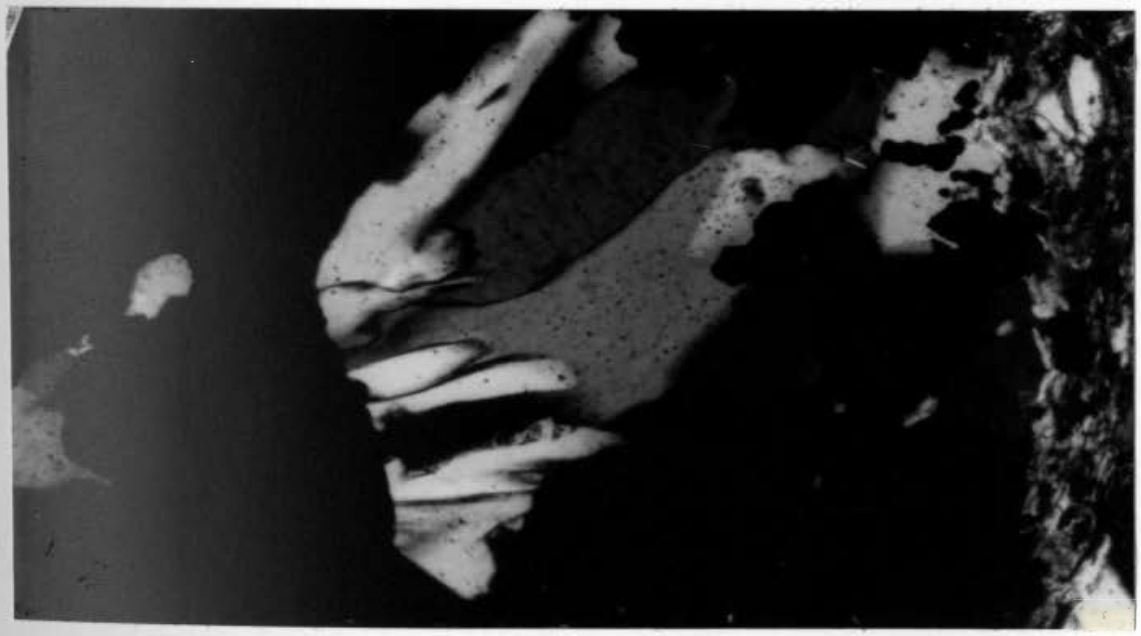

Figure 4.32. Examples of the effect of deformation on quartz grains; a) corroded quartz phenocrysts in a sutured mosaic groundmass of quartz and b) bent quartz subgrains nucleating off pyrite in a pressure shadow. Photos widths are approximately a) 1mm and b) 8mm .

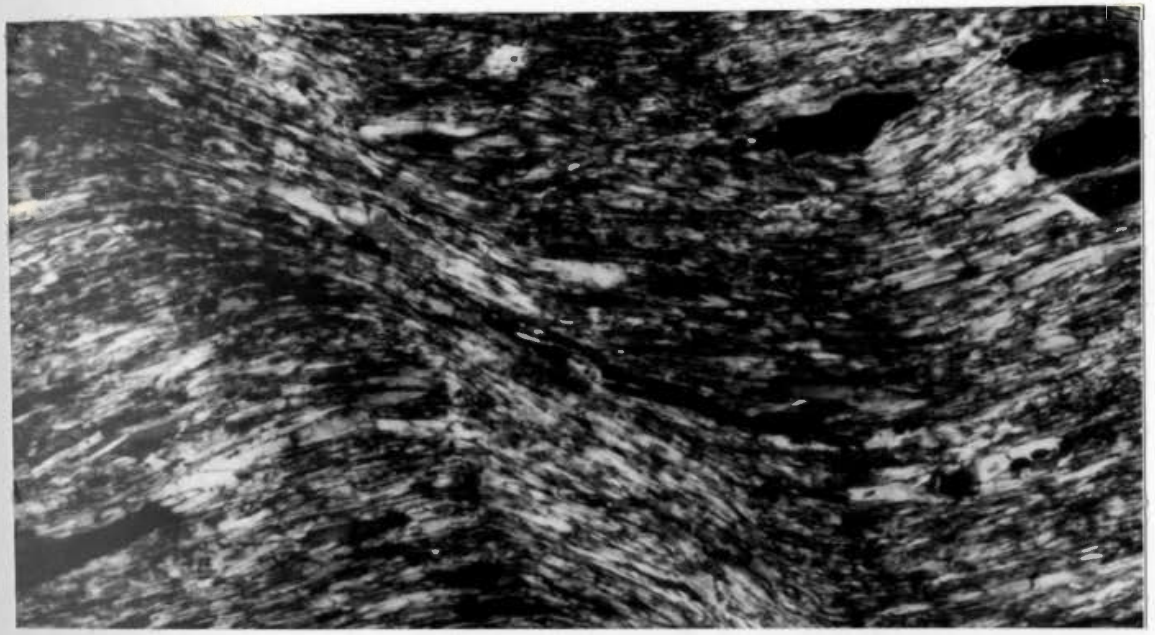

Figure 4.33. Crenulated foliation in a siltstone. Photo width is approximately 1mm .

a.

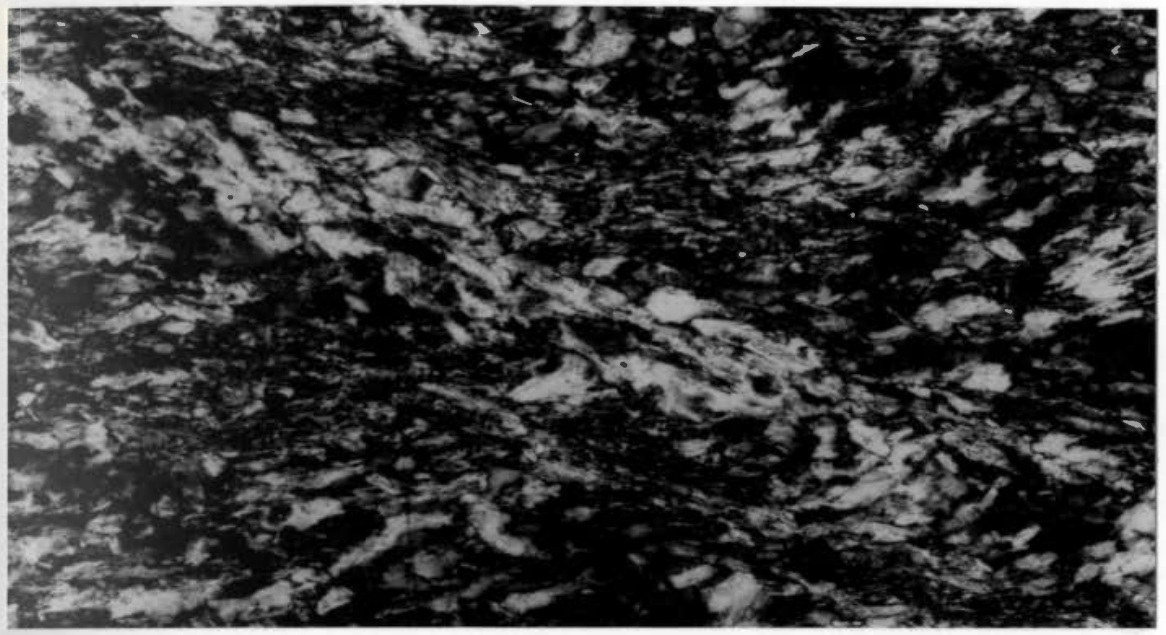

b.

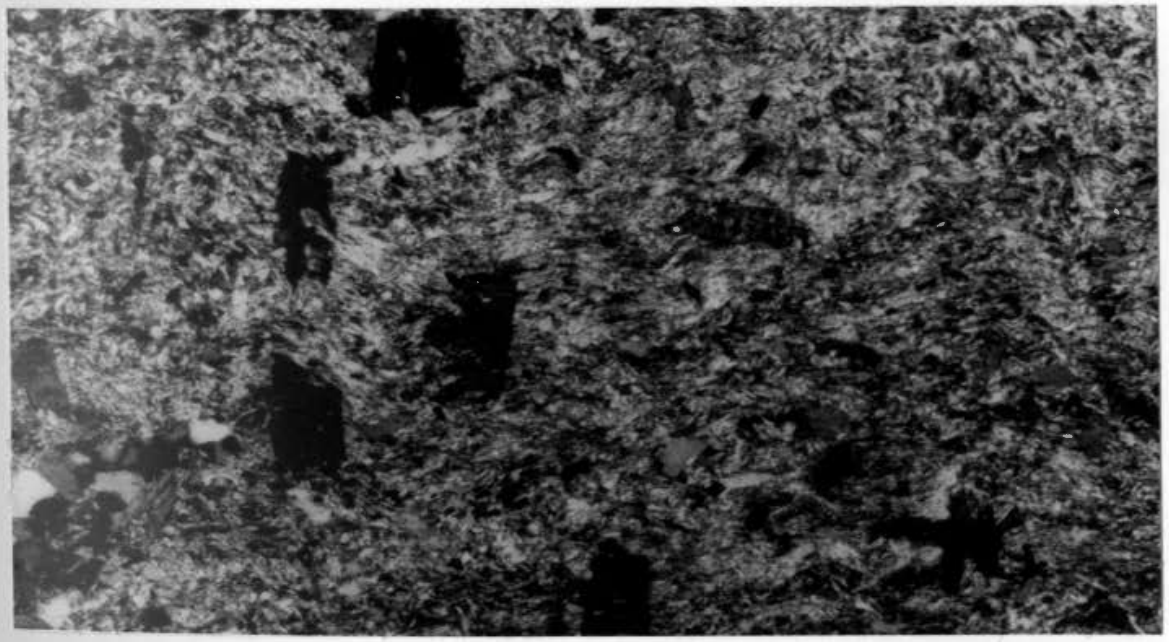

Figure 4.34. a) development of polygonal arcs partially obscuring the first foliation in a siltstone. b) Biotite poikiloblasts aligned parallel to the axial plane of the crenulation cleavage. Photo widths are approximately a) 1mm and b) 2mm .

deformational history for the Strickland area and Chorlton (1980) at least four stages for the Bay du Nord Group.

The Baggs Hill Granite was not strongly affected by these periods of deformation. Marginal phases of the granite appear to be slightly finer grained and contain few straight, equilibrated grain boundaries. Aggregates of mafic minerals are somewhat lineated on subhorizontal joint surfaces in the granite. This fabric is not penetrative and is thought to be a late stage phenomenon. Chorlton (1980) reports that the Baggs Hill Granite is highly sheared locally. A prominent set of near vertical joints cut the granite at 220° which is approximately at right angles to the regional northeast-trending fabric.

A number of prominent faults trending west northwest and east northeast cross cut the regional strike in the Strickland area (Figure 6.1, page 113). Little or no offset of the major units (sedimentary sequence, mixed sequence) is evident along these faults. The Blue Star fault truncates the Main Zone and forms the southern boundary of the Copper Zone. The Dominion fault slightly offsets the Main Zone and the Blackhorse fault is a prominent air photo linear which does not appear to offset the rock units.

The concentration of faults in the Strickland area is anomalously high relative to elsewhere along the Hermitage Flexure (D. Prince, personal communication). Falconbridge geologists (Prince and Briggs, 1978) have suggested that some

of these may be reactivated synvolcanic faults. Many fan out around the south end of Baggs Hill and may be related to the accomodation of regional stresses around the buttress-like Baggs Hill Granite. The coincidence of sulphide mineralization and major fault systems has been documented in the Noranda and Kuroko camps (Sangster, 1972; Knuckley, 1975; Sangster and Scott, 1976 ; Scott, 1978, 1980). Previous authors have proposed that these faults provided a focus for the discharge of mineralizing hydrothermal fluids (Hodgson and Lydon, 1977; Parry and Hutchinson, 1981). The occurrence of extensive faulting in the Strickland area may also be responsible for the focusing of hydrothermal solutions which produced the observed sulphide mineralization.

CHAPTER 5

MINERAL CHEMISTRY

5.1 Silicate and carbonate mineral chemistry

5.1.1 Chlorite

Some authors (e.g. Shirozu, 1974; Henley and Thornley, 1981) have noted an increase in the magnesium content of chlorite with increased proximity to the stockwork zone or pipe of certain volcanogenic massive sulphide deposits. This has been interpreted to have been produced by magnesium metasomatism which is consistent with their formation in the path of a seawater-charged hydrothermal convection system (Henley and Thornley, 1981). Riverin (1977) noted at Lens 14 of the Millenbach mine a zonation from Fe-rich chlorites in the core of the alteration pipe to Mg-rich chlorites in the outer portions of the chlorite zone (a range of Mg/(Mg+Fe) ratios from .23 to .64).

In the present study three types of chlorite were optically identified (1) pennite with berlin blue interference colours and strong pleochroism; (2) a chlorite with olive-green to purple interference colours, moderate to strong pleochroism (green) and parallel extinction which is commonly found replacing biotite; (3) prochlorite (Kerr, 1959) with pale grey to green-grey interference colours and no pleochroism. Examples of each type of chlorite were probed. The change in interference colours (blue to olive-green and purple to pale grey) and pleochroic tendencies

(strongly pleochroic to nonpleochroic) were found to correspond to an increase in the magnesium content of the chlorite with Mg/(Mg+Fe) ratios ranging from .27 to .94 (see Table 5.1 and Figure 5.1). Most of the chlorites probed were associated with minor to massive amounts of sphalerite-pyrite-galena mineralization.

Iron-enriched chlorites were found in samples from the Road Zone and Bog Zone (samples 1,2,3, with Mg/(Mg+Fe) ratios of .27 to .41). Chlorites from one weakly mineralized mafic tuff sample from the Copper Zone (4) as well as samples of the mafic tuff between the Main and Bog Zones (5,6,7), straddle an intermediate range of Fe-Mg concentrations (Mg/(Mg+Fe) ratios of .51 to .66). Samples from the Main Zone (8,9,10,11,13,14) and one Silver Hill Zone sample (12) contains chlorite which is moderately to strongly enriched in magnesium (Mg/(Mg+Fe) ratios .70 to .94).

Therefore, magnesium-enriched chlorites in the Strickland area are associated with sulphide mineralization, but mineralization is not necessarily accompanied by magnesium-rich chlorites.

5.1.2. Carbonates

Carbonate was noted as a major phase associated with massive sulphide mineralization and the Silver Hill carbonate-tremolite alteration zone (see Section 6.2.3.1, page 125). Carbonate occurs as a minor phase in the mafic tuffs and some siltstones. Semi-quantitative probing of eight thin sections containing carbonate indicates that it is

Table 5.1

Partial mineral analyses—chlorites

Interference Colours	Blue			Olive-green/purple			
Reference No.	1	2	3	4	5	6	7
Sample No.	W5071	W5079	W6282	W5031	W5083	W5074	W5064
SiO_2	24.87	23.73	23.70	24.20	25.34	26.43	27.21
TiO_2	0.14	0.02	0.07	0.09	0.10	0.11	0.0
Al_2O_3	20.96	21.93	21.93	21.41	20.98	21.04	20.1
Fe_2O_3	—	—	—	—	—	—	—
FeO	36.37	29.20	29.01	24.95	24.45	20.86	19.30
MnO	0.59	1.19	0.52	0.76	0.43	0.47	0.41
MgO	7.61	10.81	11.44	14.65	16.45	18.71	20.70
CaO	0.06	0.03	0.04	0.03	0.00	0.02	0.04
Na_2O	0.00	0.00	0.02	0.00	0.04	0.01	0.01
K_2O	0.02	0.00	0.02	0.02	0.00	0.01	0.03
Cr_2O_3	0.02	0.00	0.01	0.03	0.00	0.00	0.02
Ni	0.00	0.00	0.01	0.00	0.00	0.03	0.01
Total	90.63	86.91	86.75	86.14	87.80	87.69	87.95
Formula based on 28 oxygens ignoring H_2O^+							
Si	5.38	5.19	5.17	5.22	5.32	5.44	5.53
Ti	0.02	0.00	0.01	0.01	0.01	0.01	0.01
Al	5.35	5.66	5.64	5.44	5.19	5.11	4.82
Fe^{2+}	6.58	5.35	5.30	4.50	4.30	3.59	3.28
Mn	0.11	0.22	0.10	0.13	0.07	0.08	0.06
Mg	2.45	3.53	3.72	4.71	5.15	5.74	6.28
Ca	0.01	0.01	0.01	0.01	0.00	0.00	0.01
Na	0.00	0.00	0.01	0.00	0.01	0.00	0.00
K	0.00	0.00	0.00	0.00	0.00	0.00	0.01
(OH)	16.00	16.00	16.00	16.00	16.00	16.00	16.00
Mg/Mg + Fe	.27	.40	.41	.51	.54	.62	.66

NOTES on the lithology/mineralogy of the analysed slides.

W5071 Mafic tuff

W5079 Intermediate to mafic tuff with chalcopyrite

W6282 Felsic tuff with arsenopyrite in a late quartz vein

W5031 Mafic tuff, crenulated

W5083 Mafic tuff with knots of magnetite

W5074 Mafic tuff, strongly foliated, with .1mm pockets of calcite

W5064 Mafic tuff with actinolite

Table 5.1 continued.

Interference Colours	Pale grey/pale green-grey						
Reference No.	8	9	10	11	12	13	14
Sample No.	W6234	W6241A	W6216	W6235	W6223	W5059	W5075
SiO_2	26.52	27.49	27.13	27.95	26.57	30.49	28.91
TiO_2	0.05	0.03	0.04	0.07	0.09	0.04	0.04
Al_2O_3	21.99	21.75	21.56	21.33	21.24	19.51	21.04
Fe_2O_3	—	—	—	—	—	—	—
FeO	15.89	15.13	13.04	11.20	10.33	6.06	2.92
MnO	1.16	0.84	0.79	1.07	0.35	0.48	0.14
MgO	20.78	22.04	23.65	24.01	25.90	29.53	30.64
CaO	0.05	.02	0.02	0.06	0.05	0.00	0.04
Na_2O	0.03	.03	0.02	0.00	0.02	0.02	0.00
K_2O	0.01	.00	0.00	0.10	0.05	0.01	0.00
Cr_2O_3	0.00	.00	0.05	0.00	0.00	0.05	0.00
Ni	0.00	.05	0.00	0.03	0.05	0.02	0.00
Total	86.48	87.36	86.30	85.82	84.78	86.22	83.73
Formula based on 28 oxygens ignoring H_2O^+							
Si	5.40	5.50	5.44	5.59	5.36	5.88	5.64
Ti	0.01	0.00	0.01	0.00	0.01	0.01	0.01
Al	5.28	5.13	5.10	5.03	5.05	4.43	4.84
Fe^{2+}	2.70	2.53	2.19	1.87	1.74	0.97	0.48
Mn	0.20	0.14	0.13	0.18	0.07	0.07	0.02
Mg	6.31	6.58	7.08	7.16	7.79	8.48	8.91
Ca	0.01	0.00	0.00	0.12	0.01	0.00	0.01
Na	0.01	0.01	0.01	0.00	0.01	0.01	0.00
K	0.00	0.00	0.00	0.02	0.01	0.00	0.00
(OH)	16.00	16.00	16.00	16.00	16.00	16.00	16.00
Mg/Mg + Fe	.70	.72	.76	.79	.82	.90	.94

NOTES on the lithology/mineralogy of the analysed slides.

W6234 Silicified felsic flow
W6241A Massive sphalerite with chlorite
W6216 Massive sphalerite with sericite, chlorite and quartz
W6235 Intermediate tuff with calcite and minor sphalerite
W6223 Tremolitic rock with calcite and minor sphalerite
W5059 Massive sphalerite, calcite, chlorite
W5075 Calcite, sericite, sphalerite

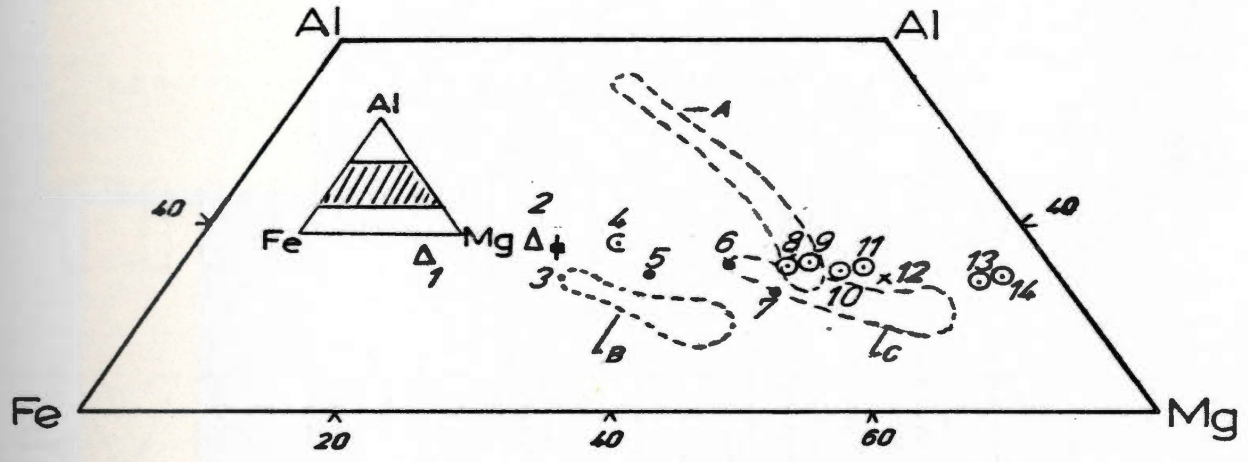

Location of Strickland Chlorites

- ⊙ Main Zone
- × Silver Hill Zone
- Δ Bog Zone
- ✚ Road Zone
- ⓒ Copper Zone (mafic tuff)
- • Mafic Tuff

Henley and Thornley (1981) Buchans chlorite compositions

- A Felsic rocks
- B Mafic rocks
- C ore samples

Figure 5.1. Chlorite compositions from the Strickland area rocks compared with those of the Buchans rocks shown on a portion of the system Al-Fe-Mg (mole percent) from Henley and Thornley (1981). The analyses of the Strickland chlorites (1-14) are given in Table 5.1 .

calcite with 1-5% combined magnesium, manganese and iron (see Table 5.2).

5.1.3 Actinolite-tremolite

Acicular sprays and blades of pleochroic actinolite are invariably associated with the mafic tuffs and dykes of the study area. The occurrence of tremolite with calcite is restricted to the Silver Hill and Main Zones of mineralization. Microprobe analyses of these two minerals are given in Table 5.3.

5.1.4 Tourmaline

Slack (1981) has noted that abundant Mg-rich dravite is commonly found as clots, fracture fillings or disseminations in wallrocks adjacent to and within the ore of many stratabound massive sulphide deposits. He suggests that the tourmaline may have been formed by boron-charged hydrothermal fluids which also deposited the sulphide ores. A local abundance of Mg-rich tourmaline in a metamorphic terrain might then indicate proximity to a former discharge vent.

The tourmaline found in the Strickland area was never observed intimately associated with massive sulphides or to comprise more than 3% of any rock. Slack (1981), reports tourmaline comprising up to 30% of total gangue in the sedimentary hosted Black Hawk (Maine), and Elizabeth Mines (Vermont). The Strickland tourmalines occur almost

Table 5.2
Semi-quantative partial carbonate analyses

Sample No.	5075	5075	5074	6235	5083	5059	5064	6223A	6232
MgO	1.25	.99	1.01	1.18	.72	.69	.91	.08	1.12
CaO	69.49	56.75	60.75	63.16	68.41	67.56	61.16	66.46	65.84
MnO	.66	.63	2.12	3.40	1.52	1.32	1.59	.74	1.30
FeO	.20	.03	2.00	.81	1.25	.15	1.29	.14	.62
Total	71.64	58.71	66.14	68.76	72.06	69.90	65.11	67.45	69.36
Formula based on 6 oxygens									
Mg	.048	.026	.042	.048	.028	.028	.038	.002	.044
Ca	1.934	1.930	1.852	1.850	1.908	1.854	1.890	1.974	1.90
Mn	.014	.016	.05	.078	.032	.030	.038	.016	.028
Fe	.002	—	.046	.018	.026	.002	.030	.002	.012

NOTES on the lithology/mineralogy of the analysed slides not previously described in Table 5.1 .

W6232 Tremolite, calcite, biotite and sphalerite

Table 5.3

Partial analyses of actinolite-tremolite

Sample Number	5064	6223	6227	6232
SiO_2	50.93	54.80	53.93	55.37
TiO_2	.18	.11	.02	.02
Al_2O_3	4.35	2.00	2.80	2.17
FeO	12.04	4.61	6.34	4.73
MnO	.47	.35	.59	.48
MgO	15.70	20.56	19.07	21.25
CaO	12.51	15.43	13.69	12.44
Na_2O	.79	.18	.20	.13
K_2O	.00	.05	.01	.00
Total	96.98	98.09	96.64	96.60
Formula based on 24 oxygens				
Si	7.74	7.97	7.99	8.09
Ti	.02	.01	.00	.00
Al	.77	.34	.49	.37
Fe	1.53	.56	.78	.57
Mn	.05	.04	.07	.05
Mg	3.56	4.45	4.22	4.63
Ca	2.03	2.41	2.17	1.95
Na	.23	.05	.05	.03
K	.00	.00	.00	.00
	Actinolite	(	Tremolite	)

NOTES on the lithology/mineralogy of the slides analysed not previously described in Tables 5.1 and 5.2 .

W6227 Tremolite rock with calcite

exclusively in the pelitic sediments of both the footwall and the hanging wall sequences. They are typically euhedral, authigenic grains one millimetre in diameter displaying colour zones with yellow to greenish-yellow pleochroism.

Analyses of several grains from one shale sample are presented in Table 5.4. The zoned crystal is more iron-rich and silica-poor in the center than at the rim. The overall composition of the tourmaline is intermediate between schorl and dravite. The paucity and chemistry of the tourmalines in the Strickland area do not seem to correspond to the patterns noted elsewhere by Slack (1980, 1981).

5.2 Sphalerite mineral chemistry and geobarometry

5.2.1 The sphalerite geobarometer

It has been demonstrated (Scott and Barnes, 1971; Scott, 1973, 1974, 1976; Hutchison and Scott, 1981) that the FeS content of sphalerite in equilibrium with iron sulphides is controlled by pressure, temperature and the activity of FeS (aFeS). The activity of FeS is buffered when sphalerite is in equilibrium with pyrite and hexagonal pyrrhotite. Experimentally derived and thermodynamically calculated T-X projections of phase relations in part of the FeS-ZnS-S system (see Figure 5.2) show that the sphalerite-pyrite-hexagonal pyrrhotite solvus (s.p.hp. solvus) is temperature independent over a wide range of temperatures (245° C to 502° C at 1 bar, 300° C to 700° C at 20 kb). It is, however, very sensitive to any change in confining pressure (Barton

Table 5.4

Semi-quantitative partial tourmaline analyses

Sample Number	W6225				
Probe site	1A edge of zoned crystal	1B centre of zoned crystal	2	3	4
Na_2O	2.60	2.66	2.59	1.79	2.10
MgO	5.89	5.73	7.31	6.57	7.09
Al_2O_3	29.75	29.21	31.26	33.68	31.13
SiO_2	41.38	36.34	36.07	38.08	36.16
K_2O	.00	.05	.00	.03	.00
CaO	.23	.27	.66	.08	.96
TiO_2	.57	2.01	1.35	.29	1.23
Cr_2O_3	.05	.00	.00	.10	.08
MnO	.05	.03	.02	.07	.07
FeO	7.11	9.96	7.26	6.71	6.42
Ni	.00	.07	.01	.00	.00
Total	87.62	86.30	87.16	87.39	85.23
Formula based on 29 oxygens					
Na	.95	1.01	.96	.65	.79
Mg	1.65	1.68	2.09	1.85	2.07
Al	6.61	6.78	7.08	7.49	7.17
Si	7.80	7.16	7.05	7.19	7.07
K	.00	.01	.00	.00	.00
Ca	.04	.05	.14	.01	.20
Ti	.08	.29	.19	.04	.18
Cr	.00	.00	.00	.01	.11
Mn	.00	.00	.00	.01	.11
Fe	1.12	1.64	1.16	1.06	1.04
Ni	.00	.00	.00	.00	.00

NOTES on the lithology/mineralogy of the analysed slides not previously described in Tables 5.1, 5.2 and 5.3 .

W6225 Shale, crenulated with sericite and quartz

and Toulmin, 1966; Scott, 1973). The data of several studies have been combined by Hutchison and Scott (1981) in the following equation expressing sphalerite composition as a function of pressure for the temperature independent portion of the s.p.hp. solvus;

$P = 42.30 - (32.10 \log \text{mole \% FeS})$ in Kbar.

Experimentally determined isobars as functions of temperature and sphalerite compositions along the s.p.hp. solvus are also shown in Figure 5.2. Note that with increasing confining pressure the FeS content of the sphalerite on the solvus decreases.

The sphalerite geobarometer is only useful to estimate pressure for rocks which have equilibrated at temperatures within the temperature independent portions of the isobars. Temperature estimates can be inferred from metamorphic silicate assemblages.

Sphalerite in equilibrium with just pyrite (or lying to the right of the solvus in the T-X diagram) should be less rich in iron than sphalerite in the same rock coexisting with pyrite and hexagonal pyrrhotite. Therefore, the FeS content in pyrite-sphalerite pairs should give an estimate of the maximum (or upper limit of) metamorphic pressures (Hutchison and Scott, 1980).

Peak metamorphic pressures are generally attained close to the same time as peak metamorphic temperatures which are conducive to the recrystallization of pyrite. Blebs of sphalerite poikiloblastically enclosed within pyrite

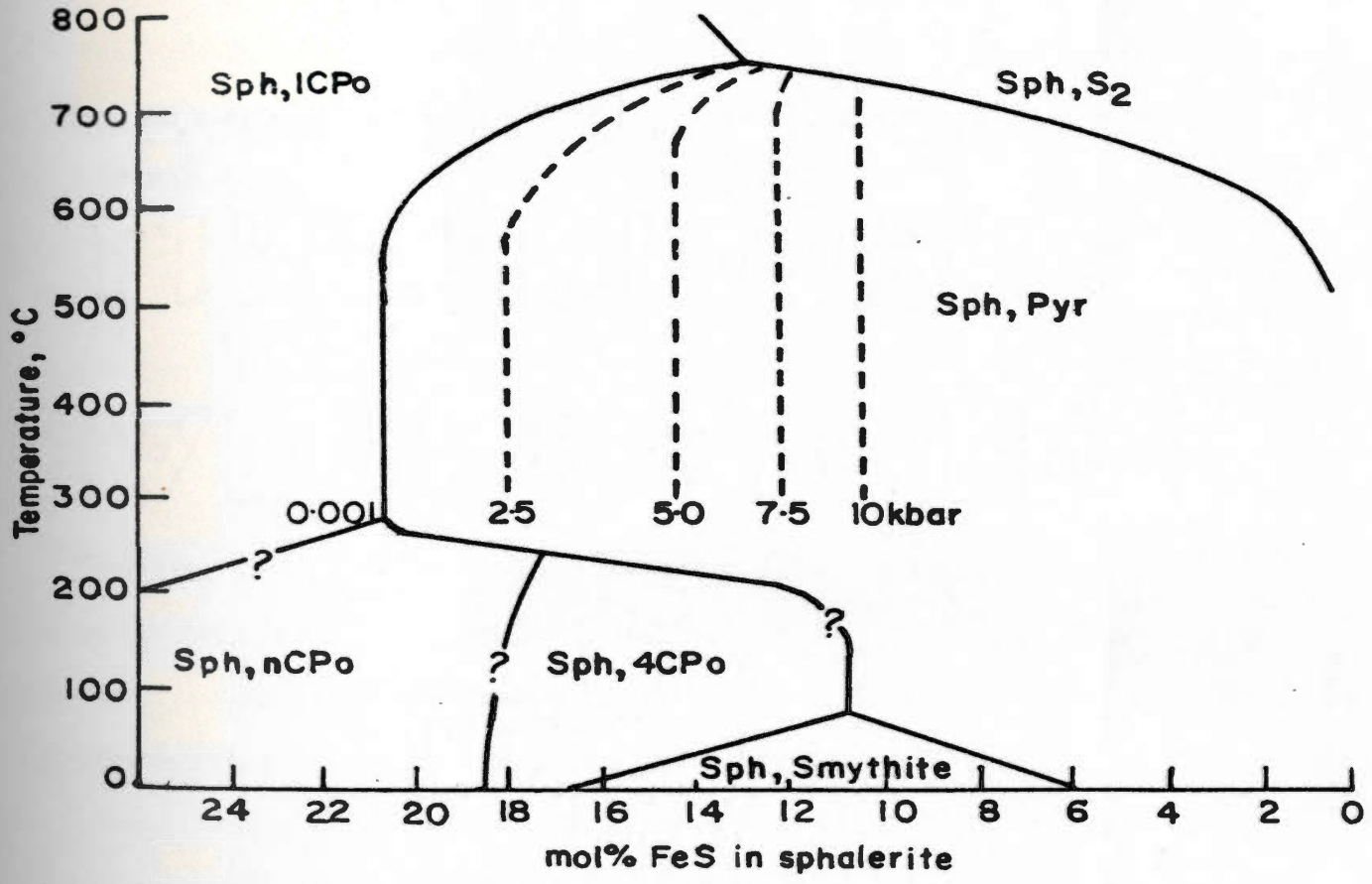

Figure 5.2. FeS in sphalerite, mol%, coexisting with pyrite and pyrrhotite as a function of temperature and confining pressure. Numbered isobars from experimental data (from Willan & Hall, 1980). Pyr - pyrite, Po - pyrrhotite, Sph - sphalerite.

crystals are effectively removed from subsequent processes (low temperature reequilibration, etc.) and should compositionally record the effects of maximum metamorphic pressures.

5.2.2. Application

The Main Zone sulphide assemblage is dominated by sphalerite, pyrite and lesser amounts of galena, pyrrhotite and chalcopyrite. Sphalerite occurs as a medium grained aggregate which hosts broken and embayed euhedral pyrite porphyroblasts and interstitial galena and chalcopyrite. The sphalerite is free of any oriented blebs of exsolved chalcopyrite and is frequently observed as poikiloblastic inclusions in pyrite. The equilibrium assemblage of sphalerite, pyrite and hexagonal pyrrhotite was not observed.

Three varieties of sphalerite were noted in sections observed under transmitted light; (1) roughly-textured red-brown sphalerite commonly as inclusions in pyrite and as a groundmass; (2) clear red-brown sphalerite seen only as small subgrains in the textured red-brown spalerite; and (3) a few isolated grains of pale yellow sphalerite which occur both as inclusions in pyrite and in the silicate groundmass (Figures 5.3a, b). Examples of these three varieties were probed and their textural relations (inclusions, groundmass) within the section carefully noted. The results of these analyses are summarized in Table 5.5 and Figure 5.4. The full analyses are listed in Appendix A.

a.

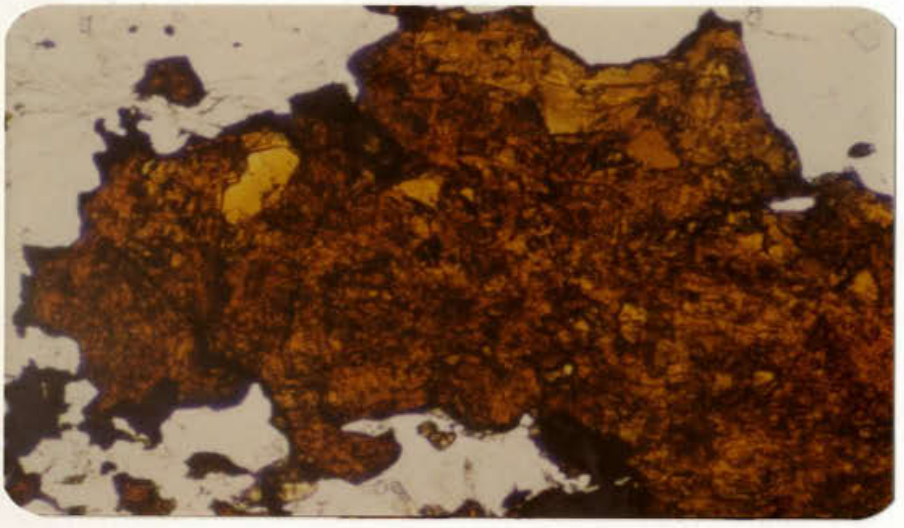

b.

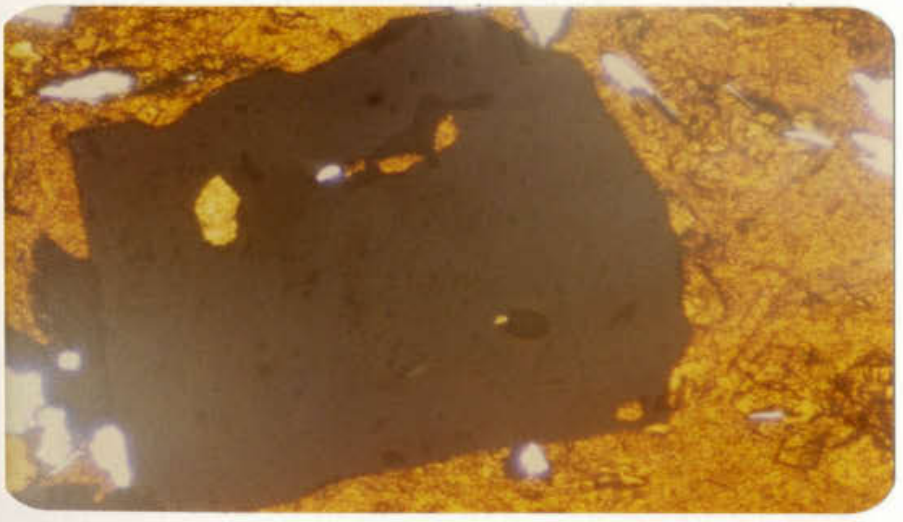

Figure 5.3. a) Textured red-brown sphalerite as a groundmass with clear red-brown sphalerite as subgrains (located in the top left corner and along the top edge of the sphalerite mass). b) Yellow sphalerite and red-brown textured sphalerite poikiloblasticly enclosed in pyrite contained in a groundmass of textured red-brown sphalerite. Photo widths are approximately 1mm .

Table 5.5
FeS in sphalerite from the Strickland mineralization
- microprobe analyses

Sphalerite description	n	weight % range	weight % $\bar{x}$	weight % σ	mole % range	mole % $\bar{x}$	mole % σ
Textured red-brown, as inclusions in py	24	7.75–9.22	8.50	0.44	6.71–7.97	7.35	0.38
Textured red-brown matrix	8	7.54–8.51	8.06	0.31	6.49–7.29	6.88	0.26
Clear red-brown	5	7.07–8.48	7.76	0.55	6.20–7.40	6.74	0.47
Pale yellow as inclusions in py	5	4.20–5.30	4.87	0.45	3.60–4.70	4.22	0.42
Pale yellow, as free grains in silicate gangue	2	3.80–3.69	3.74	0.05	3.30–3.00	3.15	0.15

n - number of analyses, where each analysis is the ave. of 3 point analyses of one sphalerite grain.
$\bar{x}$ - arithmetic mean
σ - standard deviation
py- pyrite

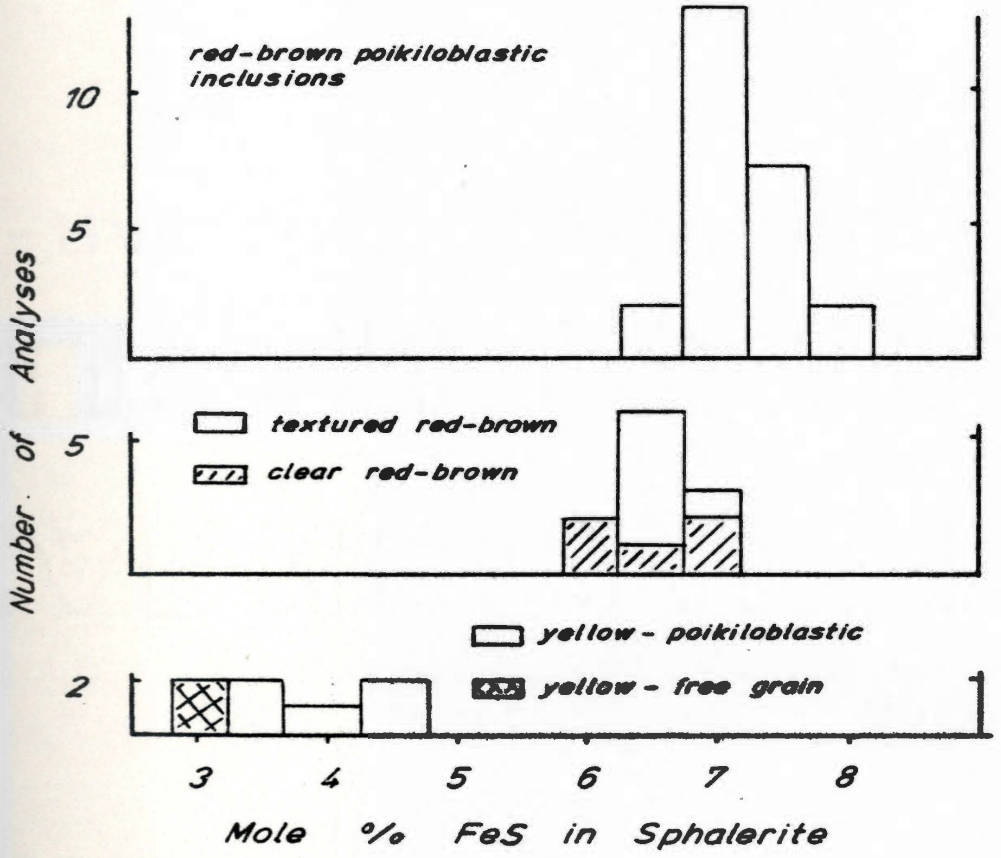

Figure 5.4. FeS content of sphalerites from the Strickland zones of mineralization

All the sphalerites probed are relatively low in iron. The textured red-brown matrix sphalerites and the clear red-brown sphalerite it contains have similar Fe contents (5.7-5.8 mole%). The clear red-brown sphalerite is interpreted to be a strain-free recrystalized equivalent of the textured red-brown matrix sphalerite. The pale yellow sphalerite is uniformly depleted in iron relative to the other sphalerites, whether as inclusions in pyrite or as free grains in a silicate matrix. Textured red-brown sphalerite inclusions in pyrite yielded the highest iron content of all the sphalerites probed.

Silicate assemblages indicate a peak metamorphism of upper greenschist facies. Temperatures at these grades of metamorphism range from 500 to 600° C (Winkler, 1976) which are near the top end of the temperature independent portion of the s.p.hp. solvus. This temperature estimate and the absence of chalcopyrite inclusions in the sphalerite should make it amenable to the application of the sphalerite geobarometer.

The low iron content of the sphalerite included in pyrite yield geologically extraordinary pressures of 17 Kbars which are clearly incompatible with pressure estimates based on the metamorphic grade of the host rock. The iron content of the included sphalerites (both textured red-brown and pale yellow varieties) is higher than their matrix equivalents.

The low iron content of the sphalerites can be explained in two ways. The temperature estimates (hence metamorphic

grade) may actually be higher than upper greenschist facies where at a given pressure the solvus composition of sphalerite is much lower than it is within the temperature independent portion of the solvus (and therefore the sphalerite geobarometer would not be applicable to this deposit). Alternatively, the low iron sphalerites could be produced by low temperature reequilibration of sphalerite in the presence of a fluid phase (Willan and Hall, 1980; Hutchison and Scott, 1980). The slightly higher iron content of the included sphalerites might indicate that they were partially protected from this fluid fluxing and reequilibration.

CHAPTER 6

ORE PETROLOGY AND ORE RELATED ALTERATION

6.1 Ore petrology

Four main types of mineralization were examined during this study. They include sulphides dominated by sphalerite, hosted in siliceous or calcite gangue from the Main Zone, sulphides dominated by chalcopyrite from the Copper Zone and weak sphalerite-galena, high silver mineralization associated with carbonate-tremolite gangue of the Silver Hill Zone.

6.1.1 Main Zone

The mineralization of the Main Zone extends 1.2 km along strike and is conformably contained in a section of felsic pyroclastics and flows at the contact between the sedimentary sequence and mixed sequence (Figure 6.1). It is offset slightly by several faults. What is interpreted to be the stratigraphically lowest (therefore earliest) mineralization in the Main Zone is strongly foliated (Figure 6.2) and composed dominantly of close packed, fine-grained aggregates of pyrite (Figures 6.3, 6.4). Galena never constitutes more than 5% of the total sulphides and occurs as xenoblastic grains interstitial to sphalerite. Small wedge-shaped inclusions of tetrahedrite are rarely present in the galena (Figure 6.5). Areas rich in pyrrhotite show late stage alteration to marcasite along grain margins and fractures (Figure 6.6a). Rounded clasts of felsic volcanic material are contained in massive sphalerite near the top of the ore zone (Figure 6.6b). Stackhouse (1976) identified

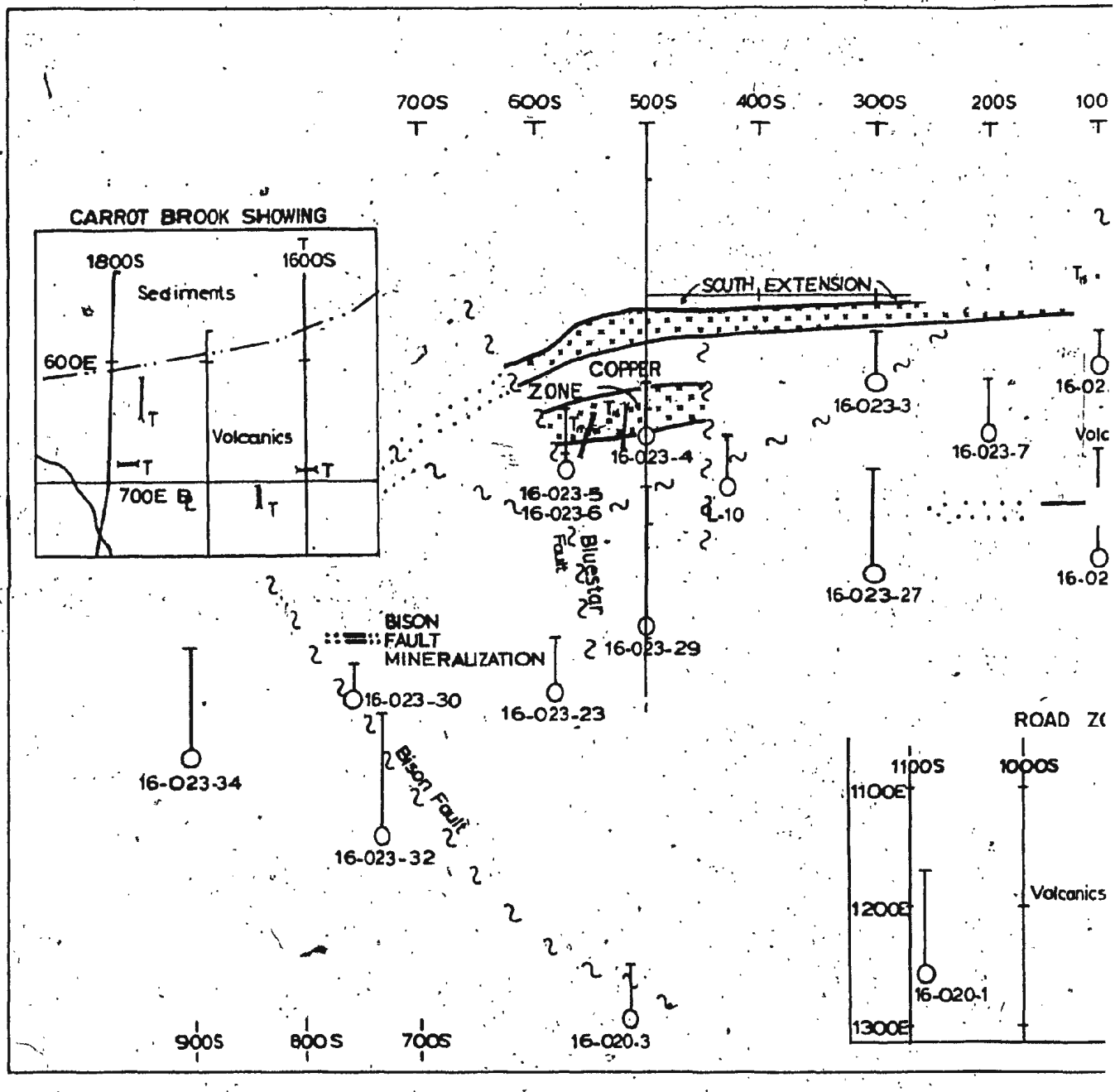
700S
600S
500S
400S
300S
200S
100
CARROT BROOK SHOWING
1800S
1600S
Sediments
600E
Volcanics
700E
SOUTH EXTENSION
COPPER
ZONE
16-023-3
16-023-4
16-023-5
16-023-6
16-023-7
16-023-27
Bluestar Fault
BISON
FAULT
MINERALIZATION
16-023-29
16-023-30
16-023-23
16-023-34
Bison Fault
16-023-32
ROAD
1100S
1000S
1100E
1200E
1300E
Volcanics
16-020-1
16-020-3
900S
800S
700S

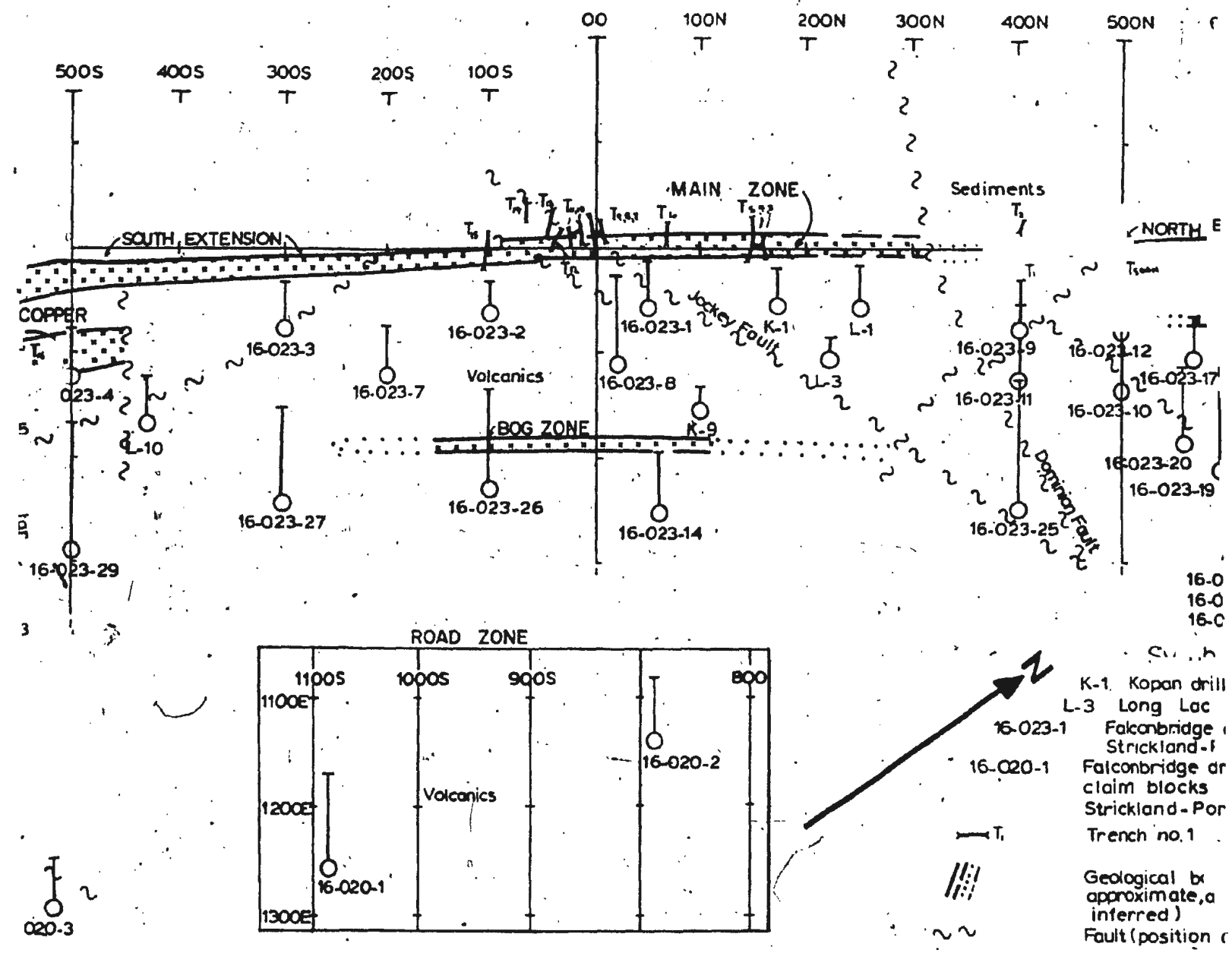
00
100N
200N
300N
400N
500N
500S
400S
300S
200S
100S
MAIN ZONE
Sediments
SOUTH EXTENSION
NORTH E
COPPER
16-023-2
16-023-1
16-023-3
16-023-7
16-023-8
Volcanics
BOG ZONE
K-1
L-1
L-3
K-9
16-023-9
16-023-12
16-023-17
16-023-11
16-023-10
16-023-20
16-023-19
16-023-26
16-023-27
16-023-14
16-023-25
16-023-29
Jockey Fault
Dorrington Fault
ROAD ZONE
1100S
1000S
900S
800
1100E
1200E
1300E
16-020-2
16-020-1
020-3
N
K-1 Kopan drill
L-3 Long Lac
16-023-1 Falconbridge
Strickland-
16-020-1 Falconbridge dr
claim blocks
Strickland-Por
Trench no.1
Geological b
approximate,a
inferred)
Fault (position

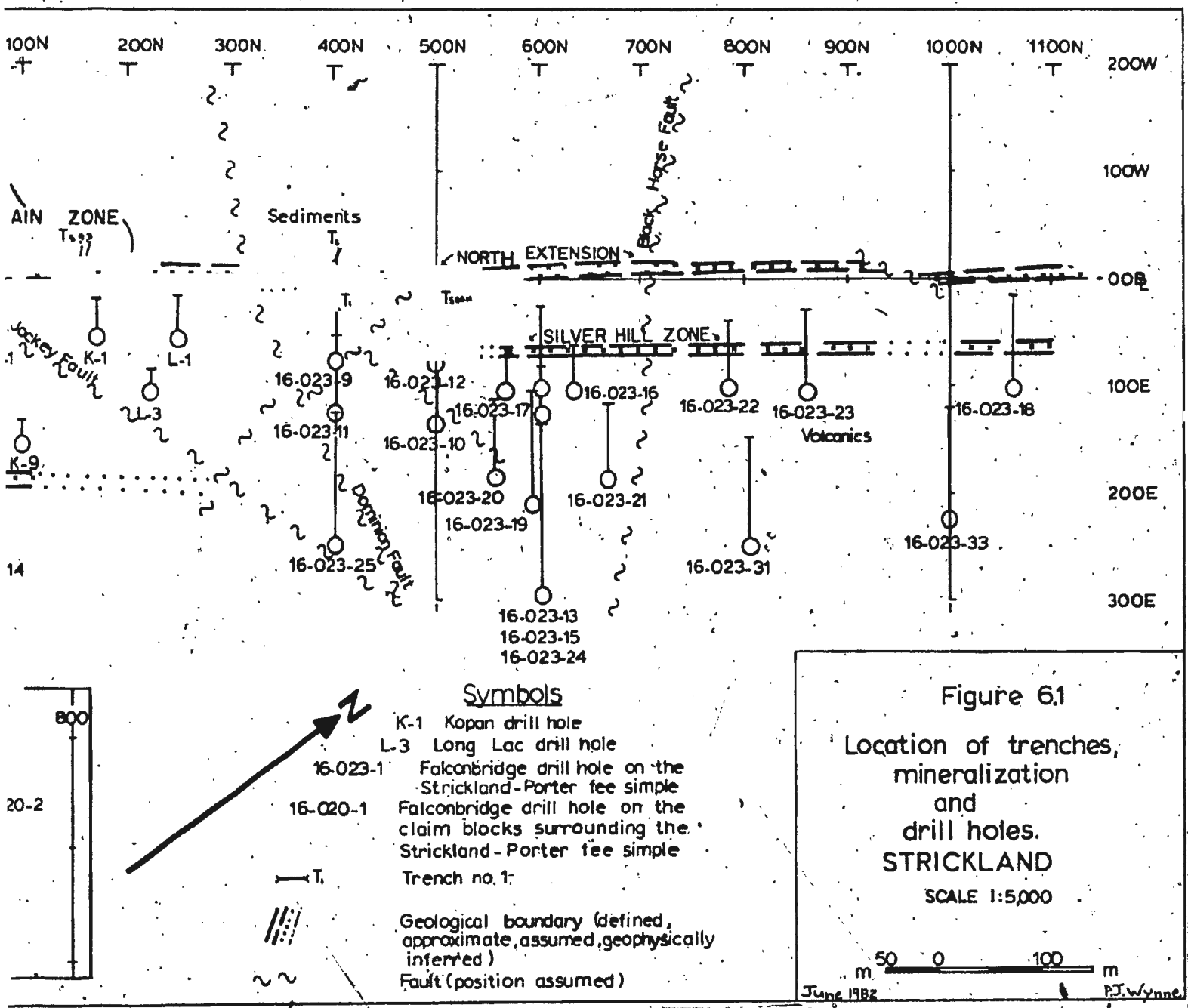
100N
200N
300N
400N
500N
600N
700N
800N
900N
1000N
1100N
200W
100W
00E
100E
200E
300E
AIN ZONE
Sediments
NORTH EXTENSION
Black Horse Fault
SILVER HILL ZONE
Jockey Fault
Dorrington Fault
K-1
L-1
L-3
K-9
16-023-9
16-023-11
16-023-12
16-023-10
16-023-17
16-023-16
16-023-22
16-023-23
Volcanics
16-023-18
16-023-20
16-023-19
16-023-21
16-023-25
16-023-31
16-023-33
16-023-13
16-023-15
16-023-24
14
800
20-2
Symbols
K-1 Kopan drill hole
L-3 Long Lac drill hole
16-023-1 Falconbridge drill hole on the Strickland-Porter fee simple
16-020-1 Falconbridge drill hole on the claim blocks surrounding the Strickland-Porter fee simple
Trench no. 1
Geological boundary (defined, approximate, assumed, geophysically inferred)
Fault (position assumed)
N
Figure 6.1
Location of trenches, mineralization and drill holes.
STRICKLAND
SCALE 1:5,000
50 0 100
m m
June 1982
P.J. Wynne

3 of 3

Figure 6.2. Well foliated pyrite, sphalerite and quartz gangue typical of the Main Zone mineralization.

Figure 6.3. Contorted folds of sericite contained in sphalerite (under crossed nicols, in transmitted light). Photo width is approximately 3mm .

Figure 6.4. Pyrite euhedra impinging on each other in a matrix of sphalerite (medium grey) and silicate gangue (black). Photo width is approximately 6mm .

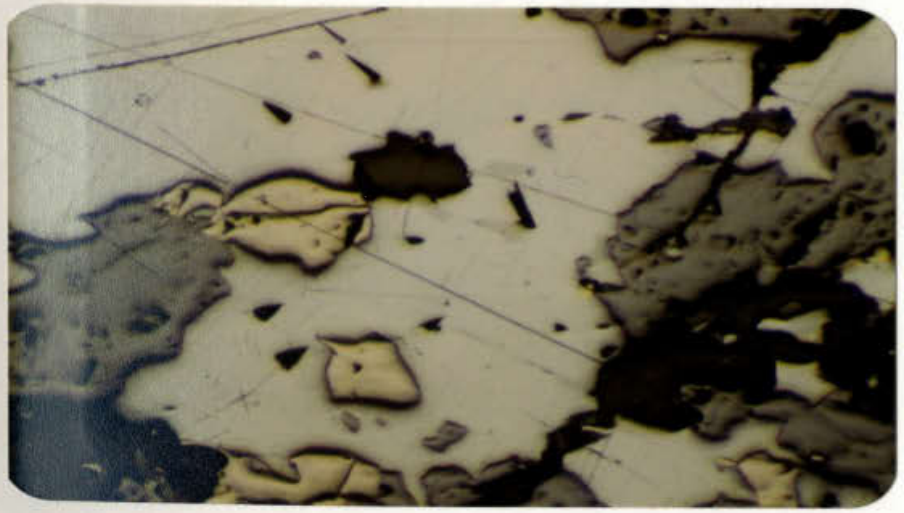

Figure 6.5. Small wedge-shaped inclusions of tetrahedrite (photo center) contained in galena (light grey) with minor chalcopyrite (yellow) and surrounded by sphalerite (medium grey). Photo width is approximately 1.2mm .

a.

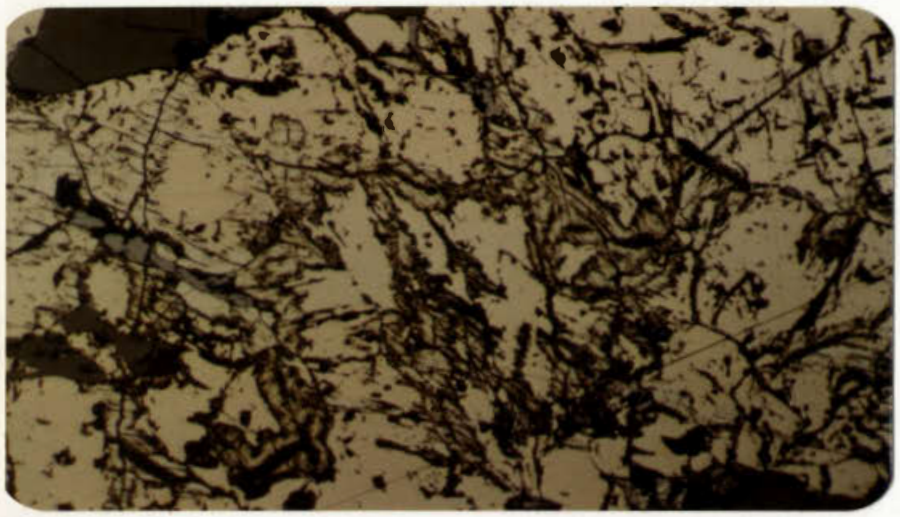

b.

Figure 6.6. a) Fractures through pyrrhotite bordered by irregular margins of marcasite (polished section in reflected light). Photo width is approximately 2mm . b) Felsic clasts in a matrix of sphalerite.

the clasts as being similar to silicified felsic volcanics which underlie the Main Ore Zone to the southeast and may represent ejecta from a phreatic explosion or slump-breccia material incorporated into a pocket of sulphides.

No primary textures were observed in the Main Zone ores (e.g. colloform textures). The banding in the ore may be relict bedding or a foliation produced during the metamorphism and deformation of the ore (which produced fractured pyrite porphyroblasts and folded micas included in sulphides). Indeed, the silicate clasts may have been produced by deformational processes where fragments of wallrock are detached and incorporated into the sulphides as a consequence of plastic flow of the sulphides during metamorphism (Vokes, 1969 "Durchbewegung" fabric).

Scattered rare pods of mineralization with carbonate (± tremolite) gangue occur near the top of the massive sphalerite horizon. These have been described by Cooper (1954) and Stackhouse (1976). The sulphide mineralization comprises 30-60% banded aggregates of medium-grained sphalerite, pyrite euhedra and minor galena with coarsely crystalline calcite, minor quartz ± tremolite. In at least one drill hole mineralization with carbonate-tremolite gangue assayed high in silver (DDH 16-023-1, 7.5 oz/ton, Briggs and Prince, 1979). Similar mineralization is characteristic of the Silver Hill Zone. The high silver assays of the upper sulphide horizon of the Main Zone are believed to be (by this author) related to the occurrence of those portions of the ore with carbonate-tremolite gangue.

6.1.2 Copper Zone

The sulphide mineralization of the Copper Zone is contained in a conformable interval of mafic tuff which lies stratigraphically below the Main Zone. It is bounded to the north and south by faults (the Bluestar fault to the south) and represents the principal occurrence of significant copper mineralization in the Strickland area (Figure 6.1).

Sulphide mineralization in the Copper Zone occurs as pyrite, chalcopyrite, sphalerite in quartz veins and veinlets in chlorite-rich mafic tuffs and as sphalerite-galena blebs conformable with the foliation of interbedded felsic tuffs. Remobilized chalcopyrite fills fractures in the quartz gangue (Figure 6.7a). Inclusions of chalcopyrite in the gangue are rimmed by sphalerite (reaction rims?) (see Figure 6.7b). Thin wedges and flames of tetrahedrite are included in the chalcopyrite. Supergene malachite and azurite were noted in the surface exposures of the Copper Zone.

6.1.3 Silver Hill Zone

The Silver Hill Zone lies stratigraphically below the Main Zone mineralization north of the Dominion fault (Figure 6.1). It is a conformable interval of carbonate-tremolite gangue material overgrowing 3-5% sphalerite and galena. While no discrete silver-bearing minerals were identified in this study Falconbridge geologists believe it to be present as a native silver-antimony alloy, allargentum. Tremolite in this section occurs as spectacular radiating sprays up to

a.

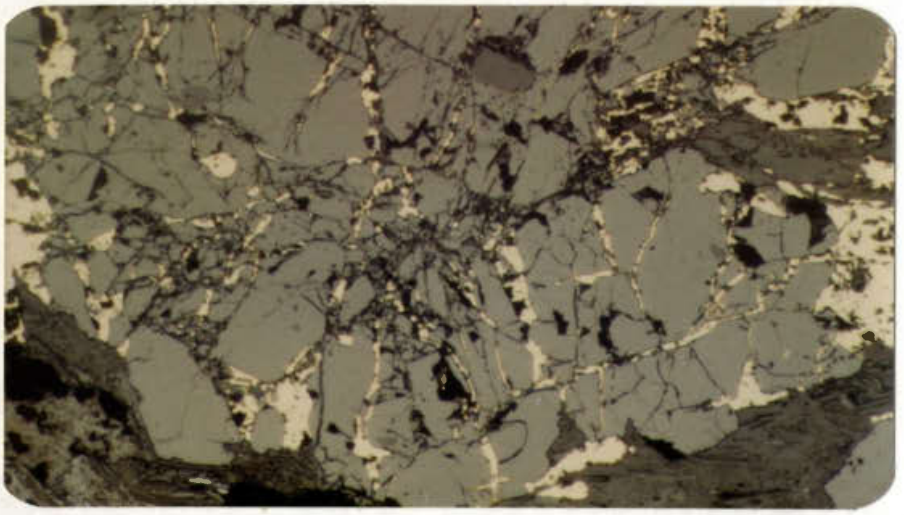

b.

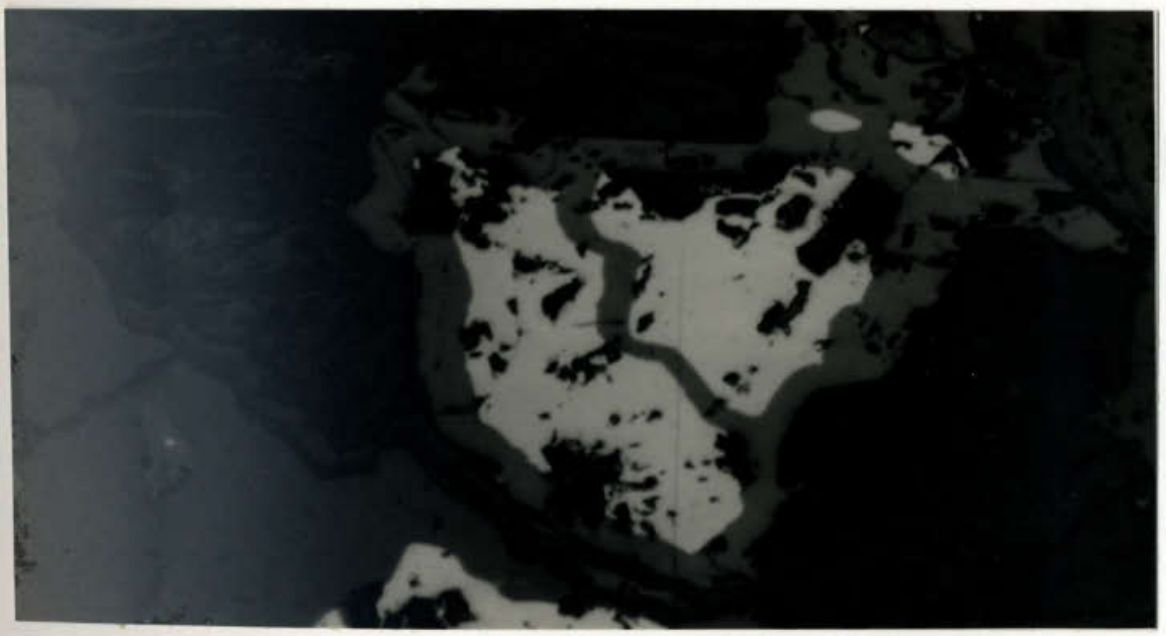

Figure 6.7. Copper Zone mineralization a) fractured quartz gangue (medium grey) with remobilized chalcopyrite (light grey) filling the fractures. b) Chalcopyrite (light grey) rimmed with sphalerite (dark grey) in quartz gangue (black). Photo widths are approximately a) 2mm and b) .8mm .

2 cm across (Figure 6.8). The carbonate-tremolite nature of this horizon fades laterally (to the north) and down-dip into a chloritic intermediate tuff-siltstone. This unit is overlain by graphitic shales and underlain by siliceous felsic pyroclastics and flows.

6.1.4 Bog Zone

The Bog Zone (Figure 6.1) is a roughly conformable 9 m thickness of low grade disseminated pyrite, sphalerite, galena, minor chalcopyrite and pyrrhotite associated with quartz veins in a horizon of mafic to intermediate tuff. It lies 200m stratigraphically below the Main Zone and has been traced for a strike length of 200-300m.

6.1.5 Carrot Brook

Mineralization exposed in old trenches just north of Carrot Brook and in the brook itself (Figure 6.1) is composed of rusty weathering disseminated pyrite with minor amounts of galena and sphalerite. The sulphides occur as blebs and fracture-controlled stringers (with epidote) in a silicified and sericitized rhyolite which lies on strike with the Main Zone horizon (Briggs and Prince, 1979; Swinden, 1981). The Carrot Brook area was not examined by this author but was sampled for lithogeochemistry by Falconbridge personnel and is therefore included here.

Figure 6.8. Coarse sprays of tremolite characteristic of the Silver Hill Zone gangue.

6.1.6 The Road Zone, Anomaly Hole and Bison Fault Mineralization

The Road Zone, Anomaly Hole and Bison Fault mineralization occur stratigraphically below and geographically to the south of the Copper Zone (Figure 6.1). They were intersected by diamond drill holes collared on the basis of multi-element soil geochemical anomalies. Arsenopyrite euhedra are found in quartz veins through a lapilli tuff outcrop north of the Road Zone (the Road Zone area extends from 700S to 1200S and 1000E to 1300E). Minor disseminations of sphalerite, galena, chalcopyrite and pyrite contained in an intermediate lapilli tuff were intersected in the Road Zone holes (16-020-1, 16-020-2). Similar weak mineralization was intersected in intercalated intermediate tuff and sandstone by the Anomaly hole (16-020-3) to the north. In a single drill hole (16-023-30) a sulphide matrix breccia (5-8% chalcopyrite with sphalerite) was intersected in a felsic-intermediate pyroclastic. The Bison Fault was intersected at the start of the hole and this mineralization will be referred to as the Bison Fault mineralization. The relationship of this mineralization to the Copper Zone is unknown.

6.2 Alteration related to mineralization

6.2.1 Silicification

Falconbridge geologists have identified a sequence of three conformable felsic volcanic/volcaniclastic lithologies

beneath and intimately associated with the Main Zone mineralization. The lowest unit is a silicified felsic lapilli tuff (estimated 8.5m thick) with up to 5% disseminated pyrite and 3-5% scattered and flattened blebs (1 cm long) of sphalerite and minor galena (Prince, 1978). This constitutes the low grade mineralization of the Main Zone. The unit is riddled with fine-grained quartz veins and it is locally finely brecciated (Figure 6.9a,b). Lapilli are sparse and invariably stretched. This horizon grades upwards into an increasingly sericitized lapilli tuff which is described below.

6.2.2 Potassic Alteration

6.2.2.1 Sericitization

The rocks associated with the Main Zone mineralization are by far the most sericitic rocks of the Strickland property. The pyrite-rich sericitized felsic lapilli tuff (approximately 2.5m thick) immediately below the massive sulphide horizon of the Main Zone contains little sphalerite or galena, but assays up to .5 oz/ton silver (Prince, 1978). It is strongly foliated and would be more accurately described as a sericite schist. It breaks easily in flaggy fragments with a characteristic pearly luster and orange-beige weathered surfaces. The contained blebs of pyrite and pyrrhotite are stretched and aligned. A similar strongly sericitized lapilli tuff containing up to 2% pyrite overlies the massive ore. This horizon is discontinuous, but where present is up to 2m thick (Prince, 1978).

a.

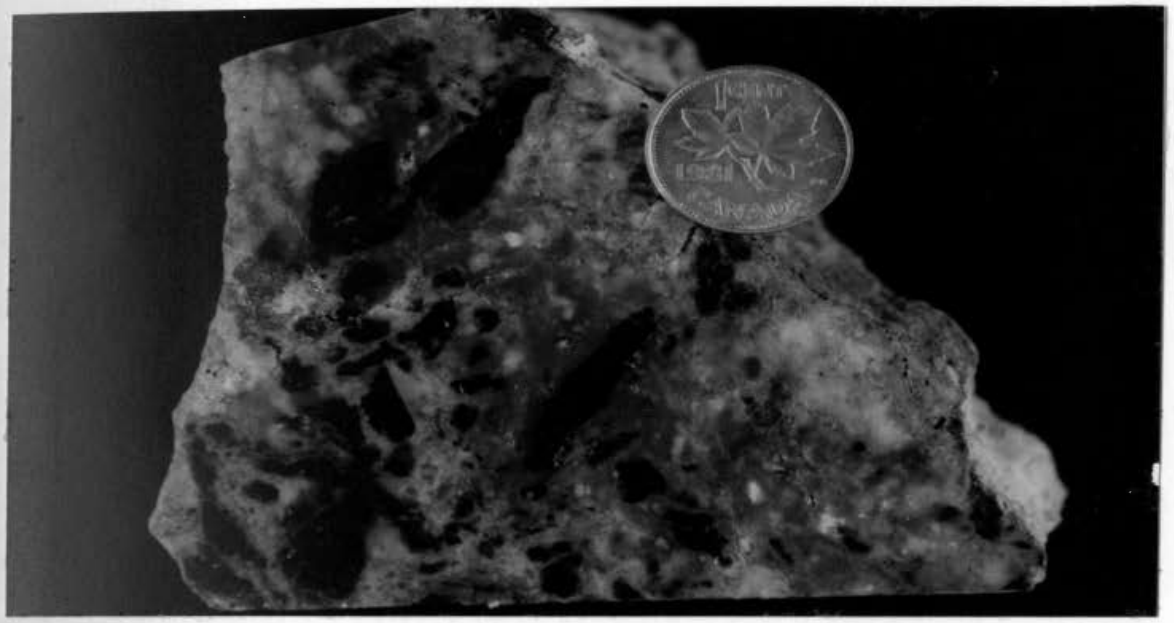

b.

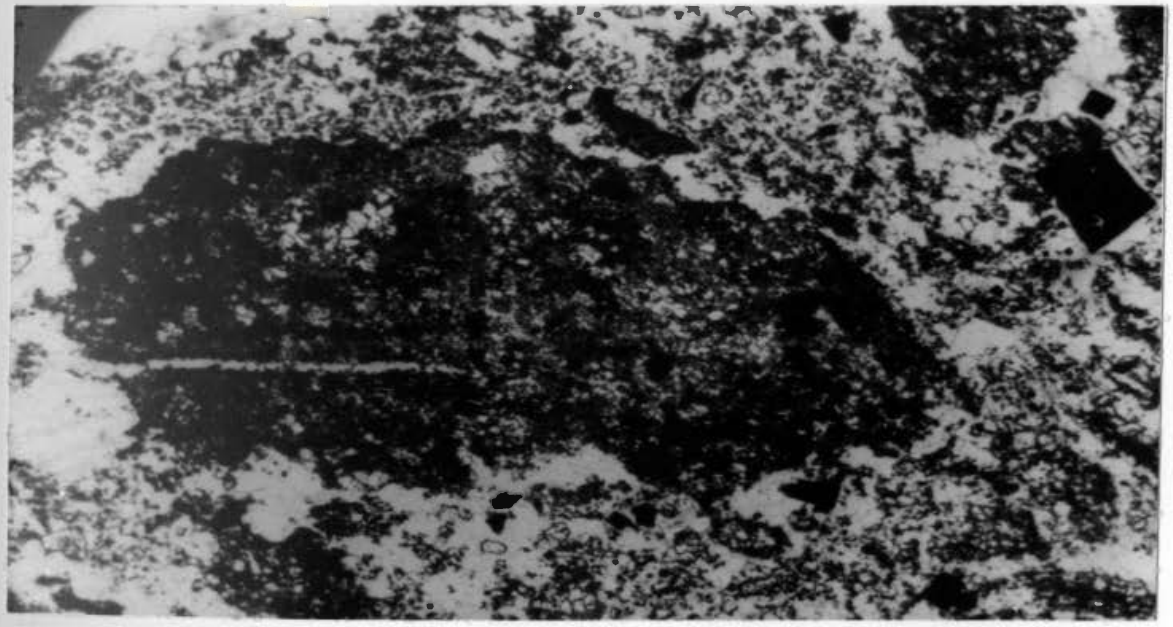

Figure 6.9. a) Brecciated volcanic material from the Main Zone, cemented with a quartz-rich matrix. b) Breccia fragment, under crossed nicols, shows a strong reaction with sodium cobaltinitrite stain for K-feldspar. Photo width is approximately 2mm .

The host rocks of the Copper Zone mineralization are also locally sericitized and silicified (Briggs and Prince, 1979).

6.2.2.2 Orthoclase porphyroblasts

Porphyroblasts of orthoclase were noted in intermediate and mafic tuffs, siltstones and shales associated with the Main Zone, Copper Zone, Road Zone and Silver Hill mineralization. The porphyroblasts are typically contained in a matrix rich in sericite or biotite (Figure 4.28a). Their presence in more felsic rocks might go unnoticed because of the small size of the porphyroblasts and the lack of an optical contrast in a quartz-rich matrix. These porphyroblasts (as well as much of the sericite/biotite matrix material) are interpreted to have been formed during the emplacement of the ore and reflect potassium enrichment of the host rocks by the mineralizing fluids.

6.2.3 Magnesium alteration

6.2.3.1 Carbonate-tremolite

Two zones of intense carbonate-tremolite "alteration" not exposed in mappable widths on surface were intersected by drill holes. The first is found at the top of the Main Zone mineralization where drill hole 16-023-1 intersected 3.7m of carbonate, tremolite and sulphide mineralization (sphalerite, pyrite, galena) with minor felsic tuff intervals. This interval is immediately overlain by the hanging wall sediments. Thin sections show xenoblastic and polygonized quartz in weakly flattened calcite, where

calcite comprises 60% of the slide (Figure 6.10). Other thin sections contain more varied mineralogy-coarse grained muscovite, chlorite, calcite, tremolite and up to 10% sphalerite. Drill hole 16-023-26 intersected a similar calcite-sericite-tremolite- chlorite-lithology at the same stratigraphic horizon but with no associated sulphide mineralization. The tremolite blades in this interval are bent, fractured and pulled apart indicating some deformation after crystal growth.

The other zone of carbonate-tremolite material is that of the Silver Hill Zone. A two to three metre thickness of spectacular pale-green sprays of tremolite up to 1.5cm across was intersected in holes 16-023-13, 16-023-15 and 16-023-19 (Figures 6.11). Sphalerite and galena comprise 3 to 5% of this interval which is rich in silver. The sulphides occur interstitial to and overgrown by fine acicular and coarsely bladed tremolite. Foliated brown biotite may also be present (up to 25% of the rock) and is overgrown by tremolite.

There are at least 3 possible interpretations of the origins of the carbonate-tremolite material: 1) it is the metamorphosed equivalent of Mg-rich alteration of the host rock produced by a synvolcanic mineralizing event; 2) it is the metamorphosed equivalent of an Mg-rich mineral (talc?) which was precipitated on the sea floor from the synvolcanic mineralizing fluids (so it is not an alteration product but a meta-chemical sediment); or 3) it is the product of a metasomatic mineralizing event (possibly metamorphic) later

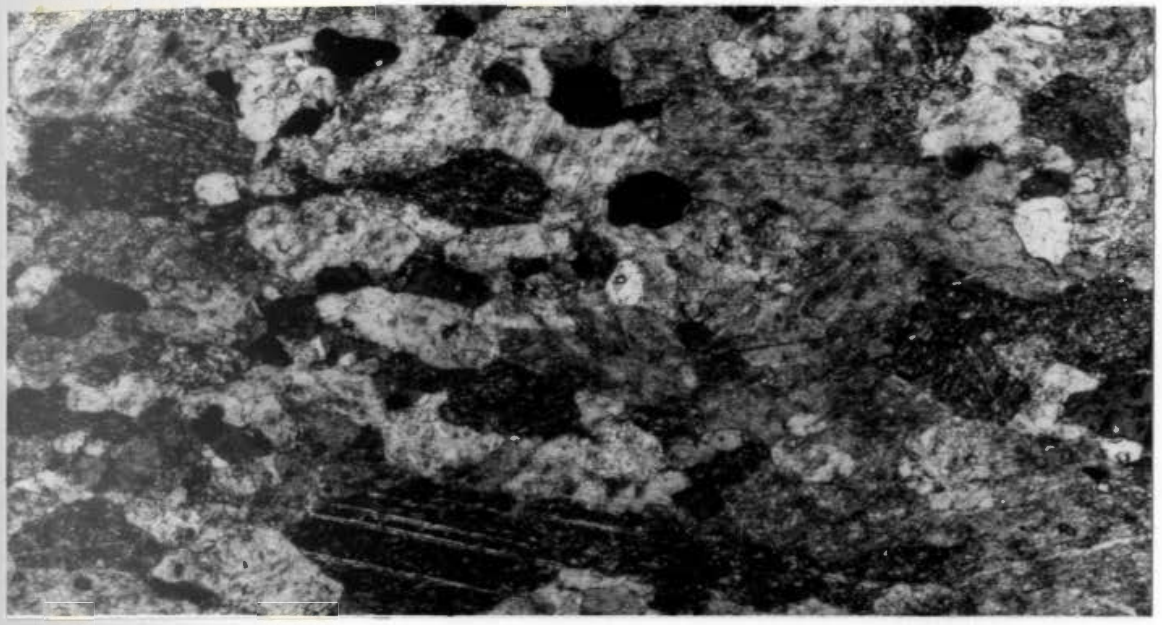

Figure 6.10. A section from the carbonate zone of drill hole 16-023-1 which is composed of calcite plus minor quartz. Photo width is approximately 3mm .

Figure 6.11. Sprays of tremolite typical of the Silver Hill Zone. Photo width is approximately 3mm .

than the emplacement of the sulphides. The close association of the carbonate-tremolite material with the massive sulphides of the Main Zone and similar low grade mineralization of the Silver Hill Zone argues that its depositional history is analogous to and closely linked with that of the sulphides. It is, therefore, interpreted to have been emplaced synvolcanically.

6.2.3.2 Magnesium-rich chlorite

The magnesium-rich chlorites detected in the limited number of slides analyzed were from the Main Zone and Silver Hill mineralized horizons. Chlorites with similar optical characteristics were found in thin sections of a wide range of lithologies, the majority of which, but not all, are associated with the Copper Zone, Main Zone and Silver Hill mineralization (within 10m of sulphides, either stratigraphically above, below or down dip from mineralization).

These magnesium-rich chlorites, coupled with the occurrence of tremolite in close association with sulphide mineralization, suggest that the emplacement of much of the ore in the Strickland area was accompanied by magnesium-rich fluids.

6.3 Summary

The Main Zone mineralization is a stratiform lens of Fe-Pb-Zn, minor Cu-sulphides with conspicuously altered

footwall rocks (silicified, sericitized, abundant disseminated pyrite) lacking discordant stringer mineralization. The sulphide mineralization of the Main Zone is separated into two units by up to 10m of altered (pyrite, sericite) felsic pyroclastic rocks and a discontinuous siltstone horizon. What is interpreted to be the stratigraphically lower portion consists of low grade pyrite-rich, shalerite/galena-poor mineralization disseminated in silicified felsic lapilli tuff. The upper portion is massive sphalerite with minor galena and pyrite containing significant silver. The high silver content appears to be coincident with the occurrence of carbonate-tremolite gangue towards the top of the ore body. The mineralization of the Main Zone is generally zoned from a pyrite-rich base to a sphalerite, galena and silver-rich top.

The Copper, Bog and Silver Hill Zones all lie stratigraphically below the Main Zone. Although the host rocks of the Copper Zone and Bog Zone are similar chlorite-rich intermediate to mafic tuffs the mineralization of the Copper Zone is copper rich while that of the Bog Zone is zinc-lead rich. The Silver Hill Zone is a conformable lens of spectacular carbonate-tremolite material, rich in silver with minor sphalerite and galena. It is laterally equivalent to a chlorite-rich intermediate tuff/siltstone horizon. Both the Bog Zone and Silver Hill Zone are overlain by graphitic shales.

The Road Zone, Anomaly, Bison Fault and Carrot Brook mineralization lie stratigraphically lower than the zones previously described. The mineralization of these areas is typically low grade, commonly discontinuous and associated with quartz veins in felsic to intermediate volcaniclastics or felsic flows. Sphalerite with abundant pyrite and subordinate galena, chalcopyrite and trace amounts of silver characterizes the mineralization of these zones.

The restricted occurrence of orthoclase porphyroblasts close to mineralized horizons, along with the abundance of sericite in the Main Zone area, suggests potassium enrichment of the host rocks adjacent to mineralization.

Chlorites extremely enriched in iron are found in association with the mineralization of the Bog and Road Zones while chlorites strongly enriched in magnesium are associated with the Main and Silver Hill Zones. The Mg-rich chlorites of these zones correspond to the occurrence of tremolite as a gangue mineral which suggests Mg-rich fluids were involved in the deposition of these two mineralized zones. The occurrence of Mg-rich chlorites is not however, restricted to mineralized areas and therefore cannot by itself be taken as an indicator of proximity to sulphide mineralization.

There is mineralogical evidence to suggest magnesium and potassium enrichment of the host rocks spatially associated with mineralization. The potassium enrichment is more extensive than the mineralization while mineralogical

evidence of magnesium enrichment is restricted to the ore zones.

A detailed study of the lithogeochemistry of the host rocks was conducted in an attempt to identify more extensive, possibly more subtle (i.e. not expressed mineralogically) chemical alteration patterns related to the mineralizing event.

CHAPTER 7

LITHOGEOCHEMISTRY

7.1 Sampling procedure

7.1.1 Sample distribution

Forty-nine surface rock samples were collected in an initial orientation survey which was conducted by Falconbridge personnel in the summer of 1978. These samples were taken in the area surrounding the exposed mineralization of the Copper and Main Zones. In 1979 and 1980 a larger area stretching along strike from Carrot Brook to 1000N was sampled, as well as core from six old (pre-Falconbridge) diamond drill holes and all the new (Falconbridge) holes (except holes # 16-020-1, 2, 3). A total of 411 samples were taken during their three-year sampling program; 201 surface and 210 drill core samples, representing a surface sample density of 250 samples per square kilometre.

During this study the area sampled was extended to the north, west and east in an attempt to collect samples far removed from sulphide mineralization. Fourteen drill holes, representative of the variations in lithology and mineralization along strike were also re-logged and sampled by the author (Long-Lac drill core L-1, L-10; Falconbridge drill core: 16-023-1,2,3,6,9,14,16,19,26,31 and Road Zone drill core from holes 16-023-1,2 not previously sampled). These represent a further 93 surface samples and 82 drill core samples with a surface sample density of 50 samples per

square kilometre. The surface sample locations are shown on Map No. 2 in the back pocket.

7.1.2 Sampling techniques

7.1.2.1 Surface samples

A single 2kg sample was taken at each sample location. Care was taken to collect samples as free as possible from the effects of extensive visible weathering or quartz-veining. The degree of weathering is generally a function of the degree of schistosity of the sample and often an unweathered sample was not available. Falconbridge geologists took chip samples across these weathered outcrops and retained only the freshest chips.

7.1.2.2 Drill core samples

Falconbridge geologists grouped together minor units from drill logs to form major units 5 to 25m thick in each hole. These major units were then sampled by taking small pieces of core every 30cm beginning from the midpoint of the unit and sampling for a distance of 4m on either side of the midpoint. All mineralized units were sampled as well as units above and below mineralization from a midpoint as described. Approximately five samples were taken from holes of average length (100m).

The sampling procedure followed by this author differed from that of Falconbridge geologists in that each sample was composed of a single lithology representative of the major units in the hole. Analyses of these samples then are

analyses of a single lithology. A single sample was composed of 30-40 cm of core and five to seven samples were taken from each hole sampled. Several small two or three centimetre lengths of core were also taken for thin section, polished section and polished thin section study, with no corresponding sample for geochemical analysis.

7.2 Sample Preparation

Surface samples collected by this author were trimmed of lichen and surface weathering (to an average depth of 1cm) using a diamond trim saw. Metallic stains left on the rock faces by the saw were polished off. A slab for thin sections and a representative slab for future reference were set aside from both surface and drill core samples. All samples (surface and drill core) were crushed to 1cm fragments in a chipmunk jaw crusher, then coned and quartered. One quarter of the sample was powdered to -100 mesh using a tungsten carbide swing (puck) mill. The powder was coned and quartered and one quarter (approximately 200g) was reserved for analysis.

7.3 Geochemical analysis

Rock samples collected by Falconbridge personnel were analysed by X-Ray Assay Labs in Don Mills, Ontario utilizing an X-Ray fluorescence spectrometer on fused pellets for ten major oxides, and Atomic Absorption for Cu, Pb, Zn and Ag using a warm HNO_3-HCl digestion. Loss on ignition values were also calculated by that lab.

The major elements of the samples collected by this author were analysed by Atomic Absorption (A.A.) following a warm $HF-HBO_3$ digestion. Copper was determined in a selected number of surface samples using the same method but with an increased initial sample weight. Phosphorous was determined colourimetrically. The trace elements of a selected number of samples (those analyzed for copper) were determined by X-Ray fluorescence using unfused, baked pellets. The analytical procedures used in this study are described in greater detail in Appendix B.

A batch of sixteen samples composed of one or two samples from each A.A. batch of twenty-four samples analysed by this author were run a second time. The analytical results of the single batch run compared favourably with the initial results obtained for each sample. A statistical comparison and X-Y plots of the two sets of results are contained in Appendix C. The coefficients of variation (C.V.) of the major elements range from 1.11% (FeO) to 8.88% (MnO) except for P_2O_5 which has a C.V. of 37.00%. The calculated standard deviations are well within acceptable limits, e.g. +/-0.7% SiO_2, +/-0.2% Al_2O_3. The R^2 value of the regression equations calculated for X-Y plots of the two sets of data range from .8883 (P_2O_5) to .9998 MgO).

To check the reproducibility of the geochemical analyses from X-Ray Assay Labs and the compatibility of those results with the analytical results generated by this author (M.U.N. data) 17 pulps were chosen at random from

the Falconbridge samples and analysed for major oxides using the procedure previously outlined. A statistical comparison and X-Y plots of the two sets of results are given in Appendix C. The coefficients of variation (C.V.) of the major elements range from 1.5% (SiO_2) to 7.5% (MnO) except for P_2O_5 which has a C.V. of 17.5%. The calculated standard deviations are well within acceptable limits, e.g. +/-1.036% SiO_2, +/-0.237% Al_2O_3. The R^2 value of the regression equations range from .9618 (MnO) to .9988 (CaO). While the precision estimates obtained in the comparison of these two sets of data are lower than the estimates obtained for the M.U.N. duplicates it was felt that the variation of analytical results between labs was not so great or systematic as to obscure geochemical anomalies.

The lead and zinc values of some of the samples were determined both by Atomic Absorption (X-Ray Assay Labs) and X.R.F. (M.U.N.) The X.R.F. results were generally higher than those from the A.A. analyses of X-Ray Assay Labs. The lead analyses show especially poor correlation between the two analytical methods. A statistical comparison as well as X-Y plots of the two sets of data are given in Appendix C. In the computer interpretation of the data the X-Ray Assay Lab lead and zinc results of the duplicate analyses were used because the majority of the metal analyses were performed by that lab.

7.4 Data evaluation

7.4.1 Data organization

The large numbers of samples and variables involved in this study made it necessary to use the available computer facilities to manipulate the data. The sample information and geochemical results for each rock sample were recorded on three computer cards. The first card contained information on the sample location, lithology, availability of thin or polished section, visible alteration and subordinate lithologies. Major oxide data were recorded on the second card and trace element data on the third. The sample number was recorded at the beginning of each card. Details of the codes used and a complete data list are given in Appendix D.

7.4.2 Computer methods - description

7.4.2.1 Introduction

The computer (IBM 370/158) was used for three main purposes - data organization, display and analysis. Data organization includes the classification, sorting, ranking, storage, and retrieval of data. Data display prepares simple plots (X-Y scattergrams, histograms, etc.) and data analysis involves simple univariate to complex multivariate statistical techniques. These were accomplished by using the commercially available groups of programs called statistical packages. The two packages used in this study are:

1) SAS, Statistical Analysis System, developed by SAS Institute Inc., Cary, North Carolina, U.S.A. (Helwig and Council ed., 1979).

2) BMDP, Biomedical Computer Programs, P-Series, developed at the Health Sciences Computing Facility, University of California, Los Angeles, California (Dixon and Brown ed., 1977).

7.4.2.2 Computer Programs

The SAS and BMDP programs which were used in this study are briefly described in the following section.

7.4.2.2.1 SAS/SORT

The SORT program rearranges data and can create new subsets containing the new ordered observations. SORT ranks the data so that the observation with the lowest value of a given variable is first and the observation with the next lowest value second and so on. The SORT program is generally used to sort data so that other programs can process it in subsets. In this investigation SORT was used to organize subsets based on the lithology of the sample and to order samples on the basis of a given element or residual so the data list could be subdivided into classes using the mean and standard deviation of the element or residual.

7.4.2.2.2 SAS/PRINT

The PRINT program produces a print out of any specified data set. The data set may be previously sorted by a SORT program and all the variables in that data set may be printed or just specified variables.

This program was used to generate lists of ordered data (e.g. K_2O values, K_2O residuals) which were then used in preparing maps showing the spatial distribution of the data.

7.4.2.2.3 SAS/PLOT

The PLOT program plots one variable against another, producing scattergrams (X-Y variation diagrams). PLOT automatically scales the axes of the diagram or the scales may be specified by the operator. More than one X-Y plot can be printed on a single page (within one set of axes) if required.

7.4.2.2.4 SAS/CHART

The CHART program generates histograms of a given variable, and a table giving the frequency of observations in each class, the cumulative frequency, percent of observations in each class and the cumulative percent. The width of each class may be specified otherwise it is automatically chosen by the program.

Histograms were generated in this study for each element of each lithology (e.g. K_2O in siltstone, Na_2O in siltstones; etc.). They provided visual information on the range of

values in each data set, the distribution of values and the symmetry of that distribution. This allowed comparison of the distribution of elements between groups.

7.4.2.2.5 SAS/MEANS

The MEANS program produces simple univariate statistics such as means, standard deviation, varience, skewness and kurtosis for numeric variables. MEANS will calculate statistics separately for groups of observations as specified by the operator.

The MEANS program was used to calculate the summary parameters which, along with examination of corresponding histograms, aided in the identification of lognormal populations.

7.4.2.2.6 SAS/STEPWISE, RSQUARE

These two programs are useful in exploring the relationship between a dependent variable and a number of independent variables. RSQUARE performs all possible regressions for one or more dependent variables and a collection of independent variables printing the R^2 value for each model. The R^2 value is a measure of how much variation in the dependent variable can be accounted for by the regression equation. The STEPWISE program uses a maximum R^2 improvement technique which generates the "best" one variable model (regression equation), the best two variable model and so on.

These programs were used in this study to investigate in what format would a regression equation using TiO_2, Al_2O_3 and FeO, plus the squared values of these three oxides as independent variables, best predict the behaviour of the dependent variables.

7.4.2.2.7 SAS/GLM

The GLM (General Linear Models) program is a regression procedure which measures the relationship (linear, curvilinear, etc.) between a dependent variable and a number of independent variables. The program calculates coefficients for each independent variable such that when they are combined in an equation a predicted value of the dependent variable can be calculated given the analysed values of the independent variables. The accuracy of the predicted value, i.e. with respect to the actual measured value, will depend on the strength of the relationship between the independent and dependent variables. The difference between the predicted value and the actual measured value of the independent variable is the residual value.

A complete description of regression analysis is given in Krumbein and Graybill (1965) and Koch and Link (1971) while Rose et al. (1970) and Sopuck et al. (1980) give examples of how regression analysis has been used in mineral exploration geochemistry.

The GLM program was used in this study to calculate regression equations using TiO_2, Al_2O_3, FeO and their squares

as the independent variables for the remaining major oxides as well as Cu, Pb and Zn. Residual values were calculated for these elements using the whole data set. The GLM program was also used to calculate regression equations of the major oxides and Cu, Pb and Zn against $TiO + (TiO_2)^2$ for subsets of the data and subsequently residual values.

7.4.2.2.8 BMDP/P7M - Stepwise discriminant analysis

This program performs a multiple group discriminant analysis. It generates linear classification functions by choosing variables, in a stepwise manner, which add the most to the separation of predetermined groups. The percentage of correctly classified samples of each group is calculated as are canonical variables which are plotted to give an optimal two-dimensional picture of the separation of the groups. Like stepwise multiple regression, stepwise discriminant analysis selects first those variables which contribute the most to the discrimination.

Koch and Link (1971) and Klovan and Billings (1967) describe the principles of discriminant analysis while Fox (1979), Sopuck et al. (1980) and Govett (1972) provide examples of the use of discriminant analysis in mineral exploration geochemistry.

In this study discriminant analysis was used to identify those elements which best distinguish between lithologial groups. The most significant of these elements were then used as the independent variables in regression equations.

7.4.3 Computer methods - application

7.4.3.1 Initial approach

7.4.3.1.1 Simple data description

Univariate statistics (mean, standard deviation, variance, standard error of the mean, coefficient of variation) and summary information describing the distribution of data (number of samples included in the calculations, the number of samples missing (e.g. siltstones with no recorded K_2O value), minimum value, maximum value, skewness, kurtosis) were calculated for the major oxides and trace elements of the entire set of data and separately for each lithology. Histograms were plotted for each element and examined. Those elements with strongly positively skewed distributions (lognormal distributions) were transformed to normal distributions by replacing arithmetic values with their logarithms and then the univariate statistics were recalculated. Elements with approximately lognormal distributions of the arithmetic values included all the trace elements and all the major elements except SiO_2 and Al_2O_3. The distribution of arithmetic values of Na_2O and K_2O for some lithologic groups is normal, not lognormal.

7.4.3.1.2 Single element maps

Falconbridge geologists plotted and contoured single element maps (Hinchey and Prince, 1980a) and concluded that these maps reflected the area geology - areas of high MgO values are coincident with areas of high TiO_2 and exposure of

mafic lithologies. Coincident low Na_2O values and high K_2O values correspond to areas underlain by felsic volcanics (however not all felsic rocks have associated Na_2O-K_2O anomalies). These maps are successful in highlighting the fact that much of the mineralization in the Strickland area is associated with felsic rocks, but zones of alteration more extensive than the ore itself were not delineated.

7.4.3.1.3 Multivariate statistical analysis

7.4.3.1.3.1 Previous use of multiple regression and residual techniques

Multiple regression analysis and the generation of residual values using geochemical data have been used in terrains dominated by volcanic rocks with a wide range of compositions to identify geochemical anomalies associated with volcanogenic massive sulphide deposits on both a regional and local mine scale (Lavin, 1976; McConnell,1976; Sopuck, 1977; Nichol et al., 1977).

Regression equations using TiO_2 and/or SiO_2 as independent variables were derived for various elements using data from background samples (those with no known related sulphide mineralization). These equations were then used to calculate predicted values of each element based on the samples SiO_2 and/or TiO_2 content. Residual element values were calculated by subtracting the predicted value of that element from the actual measured value. A sample enriched in an element relative to the background samples would generate

a positive residual, conversely a sample depleted in a given element would generate a negative residual.

The most important processes controlling the composition of igneous rocks are generally magmatic e.g. partial melting and/or differentiation. TiO_2 and/or SiO_2 are often used as indices of these processes and, by using these elements as independent variables in the calculation of regression equations (using background samples) the magmatic contribution to the primary chemistry of igneous rocks is accounted for. The element residuals of different lithologies (e.g. an andesite and a rhyolite) can be compared directly and used to detect enrichment or depletion patterns related to mineralization.

This approach is not directly applicable in the Strickland area where the lithologies consist of approximately 20% volcanics (predominantly felsic) ± granite, 30% volcaniclastics and 50% sedimentary rocks. The primary geochemistry (pre-mineralization) of the rocks in the Strickland area is not governed by a single process (i.e. magmatic differentiation) but by several (magmatic differentiation, weathering and erosion, deposition, etc). Thus, any regression equation used in the analysis of the Strickland data must be based on those independent variables which best characterize the geochemical variation of all the contained lithologies, not just the igneous ones.

7.4.3.1.3.2 Discriminant analysis

A discriminant analysis program (BMDP/P7M) was used to identify which variables (using major oxide data) contribute the most to the correct classification of the lithology of each rock sample. These variables are incorporated in a discriminant function for each lithology. Constraints imposed by the capacity of the program were such that discriminant functions for only seven groups could be determined at one time. Consequenty twelve of the main lithologies identified in the field, accounting for 94% of the samples collected, were grouped into seven lithological groups; MAFIC (mafic tuffs, chlorite schist), INTPX (intermediate tuffs and lapilli tuffs), FELPX (felsic tuffs, lapilli tuffs and agglomerates), FELFL (felsic flows), SSLT (siltstones), SSST (sandstones) and SHAL (shales).

The initial analysis identified in order of decreasing importance TiO_2, Al_2O_3, FeO, K_2O, Na_2O and MnO as important variables in the functions generated to discriminate between groups (see Table 7.1). The discrimination between groups, however, was not totally successful and considerable overlap between groups is evident upon examination of the classification summary (see Table 7.2): For example two samples identified as mafic rocks in the field were classified on the basis of their major oxide geochemistry and using the discriminant functions as belonging to the shale group. The erroneous classification of many of the samples presumably indicates that the lithological groups are not

Table 7.1

Discriminant classification function coefficient and constants based on all the sample data

GROUP = VARIABLE	MAFIC	INTPX	FELPX	FELFL	SSLT	SSST	SHAL
TiO_2	4.59	-2.67	-1.82	-1.26	-2.51	-2.54	-1.68
Al_2O_3	0.34	0.76	0.74	0.51	0.99	0.79	1.26
FeO	1.36	1.28	0.63	0.34	1.08	0.96	0.81
MnO	5.22	4.03	3.23	5.28	-3.91	-1.40	-6.14
Na_2O	1.79	2.22	1.88	2.88	1.90	1.77	1.27
K_2O	1.45	1.49	1.59	2.40	1.36	1.04	0.82
CONSTANT	-21.74	-15.11	-11.37	-13.14	-14.96	-10.87	-15.01

NOTE: Coefficients and constants are rounded values.

Table 7.2

A classification matrix showing the success of the discriminant functions of Table 7.1

GROUP	PERCENT CORRECT	NUMBER OF CASES CLASSIFIED INTO GROUP -						
		MAFIC	INTPX	FELFX	FELFL	SSLT	SSST	SHAL
MAFIC	83.8	31	3	1	0	0	0	2
INTPX	41.2	8	35	10	8	7	9	8
FELPX	24.0	4	12	46	50	18	37	25
FELFL	65.0	1	1	5	26	1	3	3
SSLT	24.3	1	16	8	3	28	20	39
SSST	42.9	3	3	5	2	6	18	5
SHAL	65.9	0	1	0	0	6	8	29
TOTAL	38.4	48	71	75	89	66	95	111

geochemically distinct. A small proportion of the samples may have been misclassified in the field (an intermediate tuff recorded as a siltstone). Another possible contribution to the overlap between groups may be the drill core sampling procedure followed by Falconbridge geologists where, for example, minor intercalations of shale and siltstone contained in a 25m length of core dominated by felsic tuff were included in a single sample, the lithology of which was recorded as felsic tuff.

To test this last possibility the drill core samples taken in the Falconbridge sampling program were omitted from a second discriminant analysis of the data using the same lithological groupings. The variables which contributed the most to the discrimination between groups in this analysis, listed in decreasing order of significance, include TiO_2, Al_2O_3, FeO, K_2O, Na_2O, MgO and SiO_2 (Table 7.3). An improved percentage of correct classifications using the newly generated functions was obtained for the felsic volcaniclastics, sandstone and shale groups (see Table 7.4). The percentage of intermediate volcaniclastics and siltstones correctly classified decreased and the other two lithological groups remained relatively unchanged (compare Tables 7.2 and 7.4).

Plots of the canonical variables are given for the discriminant analysis of the entire data set and the data set with the Falconbridge drill core samples omitted in Figure 7.1a,b. Canonical variables were calculated (BMDP/P7M) using

Table 7.3

Discriminant classification function coefficients and constants based on the sample data with the Falconbridge drill core samples omitted

GROUP = MAFIC VARIABLE		INTPX	FELPX	FELFL	SSLT	SSST	SHAL
SiO_2	18.65	18.66	18.61	18.92	18.57	18.65	18.16
TiO_2	64.59	56.33	56.14	57.75	55.77	56.06	56.98
Al_2O_3	12.56	12.94	12.83	13.00	13.07	13.01	13.22
FeO	25.74	25.08	24.46	24.65	24.83	24.86	23.95
MgO	26.08	26.13	25.99	26.22	25.73	25.59	24.53
Na_2O	26.71	27.65	27.06	28.27	26.92	26.76	25.42
K_2O	25.66	25.95	25.95	26.87	25.51	25.32	24.34
CONSTANT	-927.48	-917.07	-907.72	-940.20	-906.78	-910.79	-868.99

NOTE: Coefficients and constants are rounded values.

Table 7.4

A classification matrix showing the success of the discriminant functions of Table 7.3

GROUP	PERCENT CORRECT	NUMBER OF CASES CLASSIFIED INTO GROUP –						
		MAFIC	INTPX	FELPX	FELFL	SSLT	SSST	SHAL
MAFIC	81.0	17	2	0	0	0	1	1
INTPX	31.7	4	13	2	7	6	7	2
FELPX	31.3	1	8	36	30	7	23	10
FELFL	65.7	1	1	5	23	0	4	1
SSLT	17.5	0	15	4	1	11	21	11
SSST	45.5	1	3	5	1	7	15	1
SHAL	88.2	0	0	0	0	1	3	30
TOTAL	42.4	24	42	52	62	32	74	56

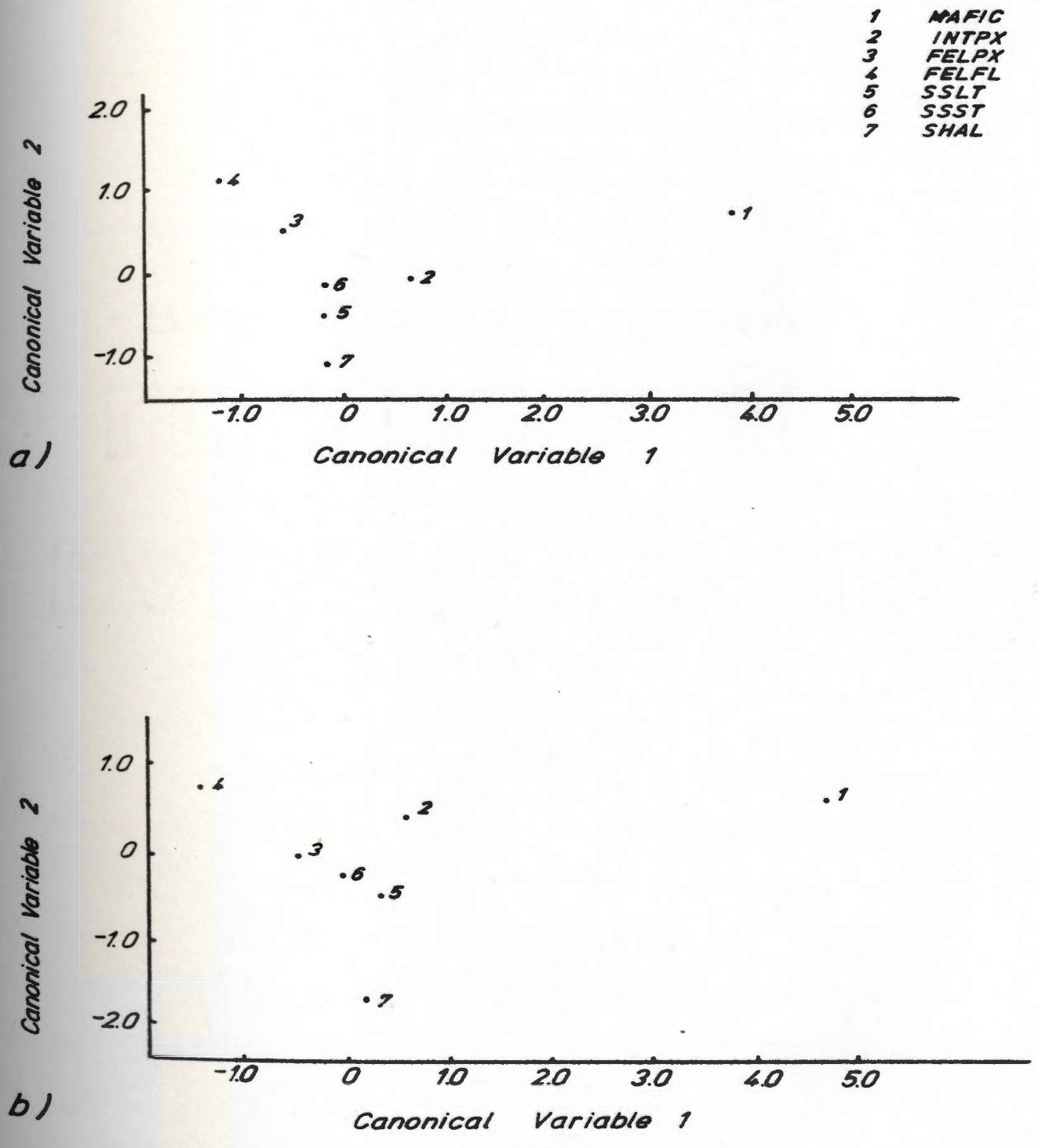

Figure 7.1. An X-Y plot of the means of the first two canonical variables for seven lithological groups (see text for the lithologies in each group) . All the data were used in a); the Falconbridge drill core data were omitted from the calculation in b).

a linear function which combined the major oxides selected as being most discriminant, (TiO_2, Al_2O_3, FeO, MnO, Na_2O, K_2O) such that the correlation between lithologies is maximized. The canonical variables are calculated in a stepwise manner whereby the first canonical variable accounts for the maximum amount of correlation between the two sets of variables (major oxides and lithological groups). The second canonical variable accounts for the maximum amount of correlation between the sets not accounted for by the first canonical variable (and so on for a total of six variables in this study). Only the averages of the first two canonical variables for each lithological group are plotted here. (See Kerlinger and Pedhazur, 1973, p. 341 and Nie et al., 1975, p. 516 for more detailed explanations of this calculation).

Inspection of the canonical variable plots and the classification tables indicates that the mafic rocks, shales and to a lesser degree the felsic flows are quite distinct, geochemically, from the other lithological groups. The clustering of the means of the felsic volcaniclastics, intermediate volcaniclastics, sandstones and siltstones is a reflection of the low percentage of correct classification of samples belonging to those groups. This overlap is not surprising considering that the provenance of the sedimentary rocks is probably proximal and largely volcanic and that during the deposition of the volcaniclastics a sedimentary component (varying in amount) was likely incorporated. The overlap suggests then that the geochemical signatures of the

felsic and intermediate volcaniclastics, sandstones and siltstones are similar.

7.4.3.1.3.3 Multiple regression analysis

Discriminant analysis of the Strickland area major oxide data for seven lithological groups indicated that these groups were best characterized using functions based on the following variables; TiO_2, Al_2O_3, FeO, K_2O, Na_2O, MgO and SiO_2. A regression equation using these oxides as independent variables would provide some means of standardizing the data in terms of lithology and allow direct comparison of the content of the remaining residual element values.

The incorporation of all seven elements as independent variables in a regression equation is unsatisfactory for at least two reasons. As no residuals are generated for any of the independent variables, observation of the behaviour of three of the most effective elements (potassium, sodium and magnesium) in identifying alteration haloes associated with volcanogenic massive sulphide deposits are precluded. Secondly, with seven of the ten major oxides included in the regression equation the value of the remaining oxides are largely constrained not by geochemical or geological processes, but by the mathematical restrictions inherent in data with a fixed and constant sum (approximately 100 in whole rock major oxide analyses).

Oxides of titanium, aluminum and iron were the first three variables selected for inclusion in the discriminant functions because they contributed the most (of the seven

variables eventually selected) to the discrimination between lithologies. This makes geological sense in that the TiO_2 contents, and to a lesser extent the FeO contents, of the rocks provide an index of the degree of differentiation of those formed by igneous processes. The Al_2O_3 content of a sedimentary rock is a discriminatory variable in distinguishing between sandstone and shale. These three elements were chosen as the most useful variables on which to base regression equations which would "see through" the geochemical behaviour of the wide range of lithologies in the Strickland area, and from which residuals of the remaining oxides could be calculated and compared. Note that by decreasing the number of variables in the discriminant function the number of samples correctly classified would also decrease. A curvilinear relationship between TiO_2, one of the three components selected as independent variables, and the other major oxides was noted in X-Y plots of TiO_2 versus the major oxides. This relationship is best approximated using a second-order regression equation.

The SAS programs STEPWISE and RSQUARE were used to compare all possible combinations of the independent variables, TiO_2, Al_2O_3, FeO and the squares of these oxides. Equations which incorporated all six variables produced the highest R^2 values, indicating that those equations best approximated the distribution of the major oxides held as dependent variables.

The SAS/GLM program was used to calculate regression equations for the various oxides using data from all the samples collected. The general form of the multiple polynomial regression equations used is

$$P = a + b_1(TiO_2) + b_2(TiO_2)^2 + b_3(Al_2O_3) + b_4(Al_2O_3)^2 + b_5(FeO) + b_6(FeO)^2$$

where P = predicted value for a given oxide

a = constant value (or intercept)

b, b_1, b_2, b_3 etc. = calculated coefficients

TiO, Al_2O_3, FeO = analysed weight % oxide.

Extreme values were omitted when the regression equations were calculated for Cu, Pb, and Zn (13 Cu analyses > 350 ppm, 11 Pb analyses > 500 ppm, 41 Zn analyses > 500 ppm). These samples are clearly anomalous and their omission resulted in an improved fit of the regression equation to the remaining data.

This approach differs from that taken in Archean terranes by Sopuck (1977), Lavin (1976) and McConnell (1976) in that the regression equations used here are based on all the data, not just on data from a background population (samples distant from mineralization). In the Strickland area a background population is difficult to define with any confidence given the widespread and sporadic occurrence of discontinuous sulphide mineralization. It was believed that any truly anomalous samples would remain distinct from the bulk of the samples and generate extremely large or small residuals.

A summary of the regression equations used is given in Table 7.5 along with the PR>F, R^2 and coefficient of variation (C.V.) statistics. If the PR>F statistic is small (.0001) it indicates that the independent variables and the regression equation accounts significantly for the variability of the dependent variable. The R^2 statistic measures how much variation in the dependent variable can be accounted for by the regression equation. An R^2 value of .776 means that the regression equation can account for 77.6% of the variance of the dependent variable by variations in the independent variables (TiO_2, Al_2O_3). The R^2 value gives an indication of how well the regression equation fits the data. The coefficient of variation describes the amount of variation of the dependent variable in the sample population. It is equal to the standard deviation of the dependent variable divided by its mean and multiplied by 100.

The regression equations were used to calculate predicted values of each oxide and three metals based on the samples TiO_2, Al_2O_3, FeO content (again using the SAS/GLM program. Residual values were then obtained by subtracting the predicted oxide or metal value from the analysed oxide or metal value of each sample.

Univariate statistics and histograms of the residuals for each element were generated and examined. The residuals of several elements showed a lognormal distribution (MnO, MgO, CaO, Na_2O, K_2O, Cu, Pb, Zn). The residuals of these

Table 7.5

A summary of regression equations and regression statistics using all the geochemical data

Dependent variable	intercept	Independent variable coefficients						PR>F	R^2	C.V.*
		TiO_2	$(TiO_2)^2$	Al_2O_3	$(Al_2O_3)^2$	FeO	$(FeO)^2$			
SiO_2	91.935	-4.774	0.168	-0.821	-0.004	-1.873	0.027	0.0001	0.777	7.158
MnO	0.013	0.016	-0.002	0.002	-0.000	0.018	0.001	0.0001	0.653	60.473
MgO	0.511	1.138	0.050	-0.077	0.001	0.350	-0.005	0.0001	0.464	78.368
CaO	1.874	2.139	-0.149	-0.276	0.005	0.163	-0.009	0.0001	0.295	155.615
Na_2O	-1.324	1.134	-0.172	0.562	-0.019	-0.349	0.015	0.0001	0.128	70.580
K_2O	1.246	-2.401	0.314	0.270	0.000	-0.105	0.007	0.0001	0.293	52.690
Cu	-10.662	-16.307	0.478	1.517	-0.095	13.323	-0.549	0.0001	0.131	113.157
Pb	1.881	-1.184	-3.578	0.320	-0.094	9.801	-0.211	0.0001	0.066	212.934
Zn	-48.504	12.793	-8.244	6.120	-0.239	19.657	-0.314	0.0001	0.300	89.074

* Coefficient of Variation

elements were transformed into logarithmic values by adding a constant to generate all positive values and then taking the common logarithm of these values. Univariate statistics of the log-residuals were then calculated and the residuals of each element ranked (from lowest to highest value) and subdivided into five classes using the mean plus or minus one and two standard deviations. (It is common practice in geochemical exploration when dealing with a normal distribution to consider the mean plus or minus two standard deviations as the threshold between anomalous and background geochemical values (Hawkes and Webb, 1962)). Maps and cross sections showing the distributions of these five classes of residuals were prepared for each element, showing the spatial relation of rock chemistry to areas of known mineralization. Representative examples of these maps and cross sections and a discussion of the results are given in Chapter 8.

7.4.3.2 The second approach

A second approach was also taken in this study to try and define meaningful lithogeochemical anomalies in the Strickland area sample group. The samples were divided according to lithology into one of three groups, igneous, mixed or sedimentary. The igneous groups included all those samples identified in the field as flows, dykes or granites. The mixed group contained all the volcaniclastics and tuffaceous sediments - those rocks dominantly igneous in origin with some sedimentary component. The sedimentary

group contains the siltstone, sandstone and shale samples as well as samples specified only as sedimentary by Falconbridge geologists.

7.4.3.2.1 Regression Analysis of the Igneous and Mixed Groups

The main process governing variation in the geochemistry of the igneous group, and to a lesser extent the mixed group, is probably magmatic. With these groups the use of TiO_2 as the sole independent variable in a regression equation is therefore justified. Examination of X-Y plots where the major oxides are plotted against TiO_2 show curvilinear trends with both lithological groups. Plots using the mixed group data show a greater scatter than the igneous group plots, but the change in major oxide content of the majority of the mixed group sample does appear to be linked to the TiO_2 content of that sample (Figures 7.2a,b). Curvilinear regression equations of the form $P = a+b_1(TiO_2) + b_2(TiO_2)^2$ were generated for each oxide (except P_2O_5) and the metals Cu, Pb and Zn of the two groups. The regression equations and regression analysis statistics are summarized in Tables 7.6 and 7.7. Note that the PR>F statistic indicates that the regression equations in the igneous group do not account significantly for the variation of Na_2O, Cu and Pb. Residual oxide values were then calculated for each element of the two groups.

These residuals were standardized by multiplying each by the R^2 value of the regression equation which generated the residual. This step was thought to be necessary if residuals from the igneous group were to be directly comparable to

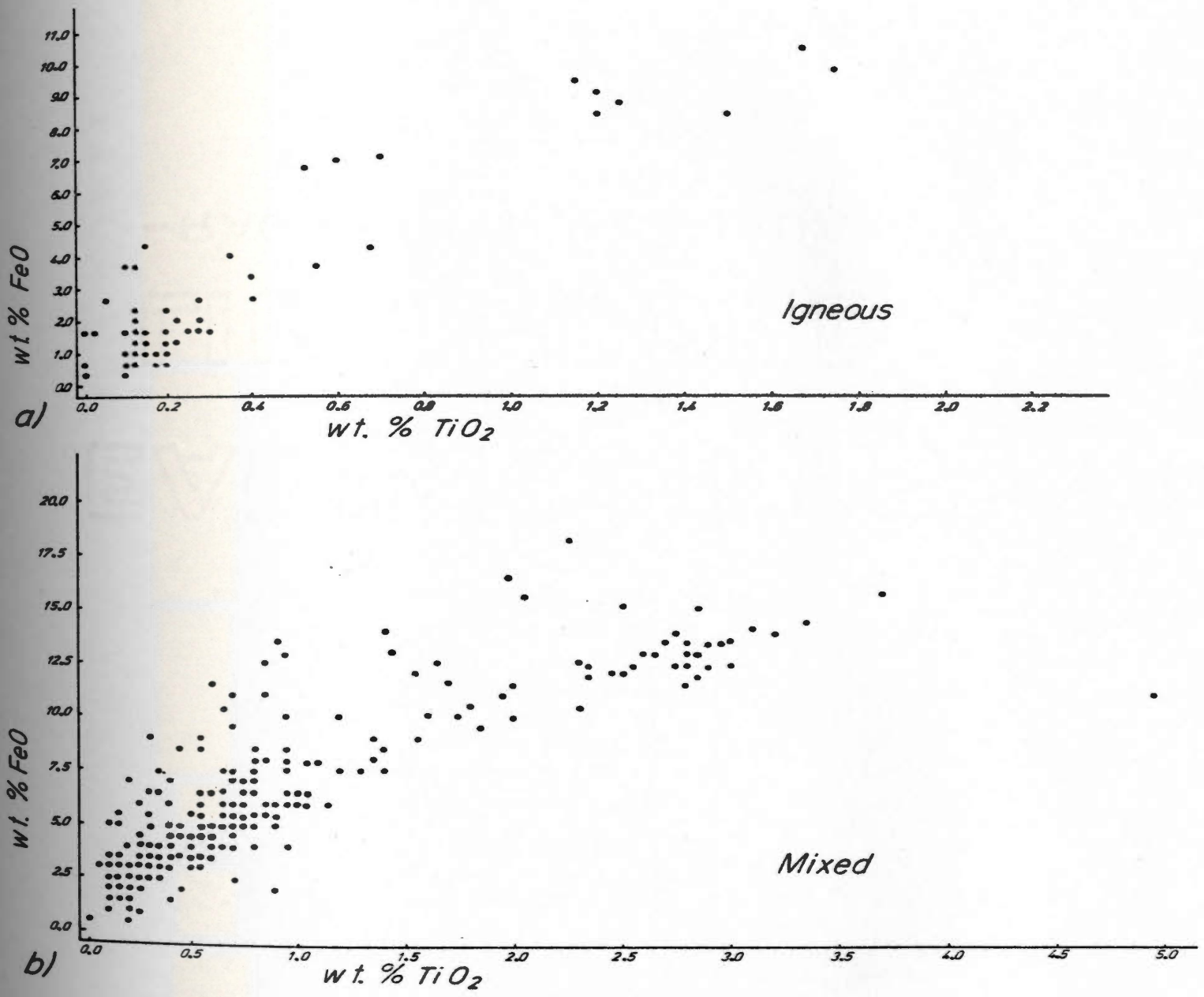

Figure 7.2. Plots of FeO versus TiO_2 for the samples in the a) igneous group and b) the mixed group of samples in the second pass analysis of the Strickland data.

Table 7.6

A summary of regression equations and regression statistics based on data from the Igneous group of lithologies

Dependent variable	Intercept	Independent variable coefficients TiO_2	$(TiO_2)^2$	PR>F	R^2	C.V.
SiO_2	83.996	-32.783	7.284	0.0001	0.834	5.753
Al_2O_3	10.355	4.770	-1.065	0.0021	0.188	24.705
FeO	0.424	8.441	-1.567	0.0001	0.889	-32.957
MnO	0.011	0.169	-0.020	0.0001	0.729	62.055
MgO	-1.065	9.251	-2.297	0.0001	0.809	81.303
CaO	-1.237	9.393	-2.446	0.0001	0.790	95.949
Na_2O	2.357	1.264	-0.426	0.5482	0.020	70.967
K_2O	4.653	-4.207	0.928	0.0036	0.174	78.777
Cu	11.505	1.083	-2.867	0.8407	0.013	129.690
Pb	27.081	0.051	-8.441	0.7835	0.018	186.280
Zn	15.888	159.677	-69.807	0.0547	0.194	107.881

Table 7.7

A summary of regression equations and regression statistics based on data from the Mixed group of lithologies

Dependent Variable	Intercept	Independent variable coefficients TiO_2	$(TiO_2)^2$	PR>F	R^2	C.V.
SiO_2	81.352	-23.395	4.142	0.0001	0.753	7.994
Al_2O_3	9.124	7.219	-2.076	0.0001	0.294	20.945
FeO	1.371	7.253	-1.053	0.0001	0.805	29.356
MnO	0.013	0.219	-0.032	0.0001	0.566	62.351
MgO	0.707	2.789	-0.181	0.0001	0.500	68.197
CaO	-0.263	2.021	-0.116	0.0001	0.058	97.168
Na_2O	1.201	1.099	-0.255	0.0002	0.053	79.747
K_2O	3.875	-1.206	0.019	0.0001	0.235	56.970
Cu	13.309	50.740	-15.819	0.0002	0.073	121.723
Pb	3.477	80.778	-23.139	0.0007	0.063	193.222
Zn	2.112	191.527	-48.889	0.0001	0.257	96.590

residuals from the mixed group. For example, an anomalous K20 residual derived from a regression equation with an R^2 value of .889 is more significant (or should carry more weight) than a K_2O residual of similar magnitude derived from a regression equation with an R^2 value of .805 (the lower R^2 value indicates a greater scatter of points about the calculated regression line).

The residuals are weighted by the multiplication, and the two data sets (K_2O residuals from the igneous group and K_2O residuals from the mixed group) can be combined and treated as a single group.

Residuals with lognormal distributions must first be transformed (by adding a constant to each residual to generate positive numbers and taking the common logarithm of those values). Univariate statistics were calculated for the residuals or log-residuals of all the elements. The residuals of each element were then ranked and divided into five classes using the calculated means and standard deviations. Representative maps and cross sections showing the distribution of these classes with respect to known mineralization are presented and the results discussed in Chapter 8.

The sequence of steps from the transformation of lognormally distributed residuals to the subdivision into five classes of residuals was conducted for the standardized residuals of the igneous group and the standardized residuals

of the mixed group as well as for the standardized residuals of the two groups after they were combined.

It was discovered that those samples identified as having anomalous residuals in a given oxide before standardization were, for every oxide except Na_2O, identical to those identified as having anomalous residuals after standardization. Standardization was therefore ineffective, but it did reduce the number of data lists (from two to one) which had to be referred to during plotting. The standardization procedure eliminated all the samples from the igneous group which were previously identified as positive Na_2O residual anomalies. The second pass plots for Na_2O therefore are the anomalous residuals from the igneous and mixed groups not the anomalous standardized residuals from the combined groups.

7.4.3.2.2 Anomaly definition in the sedimentary group

The regression analysis techniques used in previous portions of this study are not applicable to the sedimentary group of rocks because the chemical variation of these rocks is not a function of a single predictable process, but the product of several. Patterns in the chemical signatures of different sedimentary lithologies which have been noted by previous authors include the concentration of calcium and sodium (plagioclase detritus) in lithic sandstones (which like many arenites tend to be low in Al_2O_3) and the

concentration of Al_2O_3 and K_2O in shales (as clay minerals). The detrital accumulation of heavy minerals such as ilmenite is less predictable. Plots of the major oxides, first against TiO_2 and then against Al_2O_3 showed no systematic variation except in the following cases; SiO_2 showed a negative correlation with both TiO_2 and Al_2O_3 (possibly a forced correlation produced by plots of variables with a constant sum or relicts of an igneous provenance). FeO showed a positive correlation with both TiO_2 and Al_2O_3 (possibly Fe/Ti tied up in oxide minerals and Fe/Al in epidote and chlorite). The MgO versus TiO_2 and FeO versus TiO_2 plots are shown in Figure 7.3a,b, as examples of the random and systematic variation respectively of oxides with respect to TiO_2 in the sedimentary rock group.

Anomalies in the sedimentary group were defined by using the mean plus or minus one and two standard deviations to divide analyses of each oxide or element into five classes. These were plotted on maps and cross sections along with the five residual classes generated for the igneous and mixed groups to see how the anomalous samples related to the areas of known mineralization. Representative examples of these plots and a discussion of the results are presented in Chapter 8.

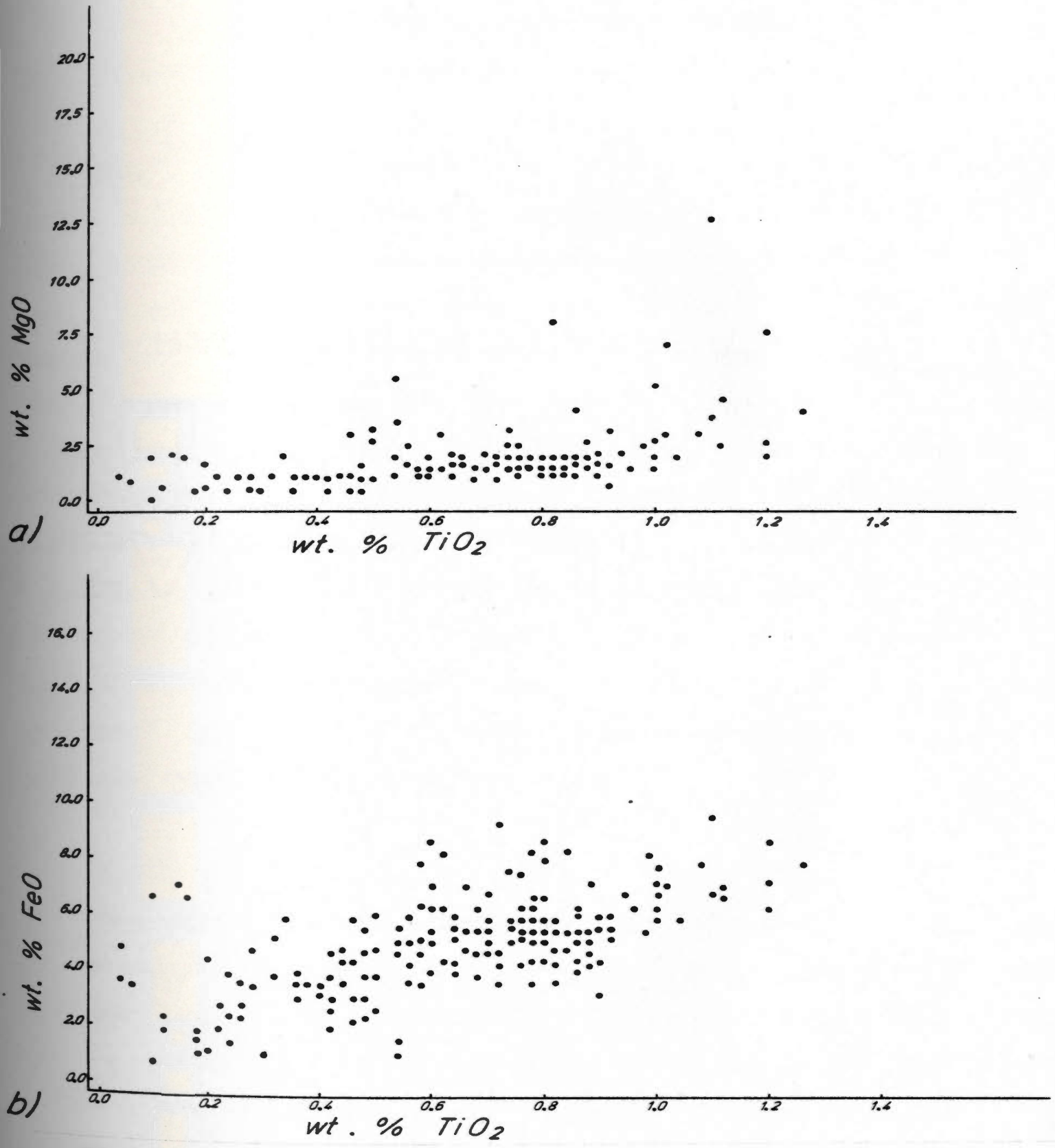

Figure 7.3. Plots of a) MgO and b) FeO versus TiO_2 of samples in the sedimentary group of samples in the second pass analysis of the Strickland data.

CHAPTER 8

DISCUSSION OF LITHOGEOCHEMISTRY

8.1 Compositional averages

8.1.1 Introduction

The average compositions of the major lithologies (those with greater than six samples) of the Strickland area were calculated with widely anomalous values deleted (e.g. SiO_2 > 90%). These average compositions are recorded in Tables 8.1, 8.2 and 8.3 along with average compositions of other rocks from around the world. Because all oxides except SiO_2 and Al_2O_3 have a lognormal distribution, the average value recorded is the antilog of the lognormal average (or the geometric mean). Histograms of the lognormal values of Na_2O and K_2O of some lithologies proved to be strongly negatively skewed. The average Na_2O or K_2O value recorded for these lithologies is that of the unlogged (or normal) values which have only a slight positive skew to the distribution.

8.1.2 Mafic lithologies

The mafic dykes of the Strickland property are similar in chemistry to other mafic igneous rocks except for the MgO/CaO ratio (see Table 8.1). The Strickland mafic dykes have a ratio approximately equal to 1 whereas with other mafic igneous rocks it is typically less than 0.8. The mafic tuffs, combined with the chlorite schist samples, have an average composition which is rich in TiO_2, Fe_2O_3 and has a high MgO/CaO ratio (2) relative to the mafic dykes. The

Table 8.1

The average composition of Strickland mafic and intermediate lithologies compared with those from other areas

	D/M:[d]	Calc-Alk Basalt	Low Ti-Basalt	C#SC + M:TF	Footwall Basalt	I:TF	I:LT	Calc-Alk Andesite	Dacite
Reference		1	2		3			4	5
No.[a]	6	180	8	33	1	67	18	15	1
SiO_2	50.0	50.0	47.4	51.5	47.9	68.3	66.0	56.2	65.6
TiO_2	1.41	0.99	0.83	2.95	0.74	0.72	0.78	0.93	0.46
Al_2O_3	15.3	16.7	15.82	13.3	16.1	14.0	14.2	16.1	15.8
Fe_2O_3[b] (Fe_2O_3)[c] (FeO)	9.12	2.10 7.44	10.49	14.48	3.59 7.03	7.52	6.97	10.16	3.44 1.08
MnO	0.19	0.18	0.18	0.36	0.11	0.15	0.18	0.11	0.09
MgO	8.68	5.80	7.28	6.44	8.26	2.43	3.45	4.18	2.24
CaO	8.89	8.16	8.73	3.30	4.48	0.70	1.13	6.48	3.22
Na_2O	2.80	2.86	2.35	1.81	1.98	1.58	1.90	4.10	5.36
K_2O	0.57	0.54	0.91	0.63	1.02	2.24	2.43	0.82	0.30
P_2O_5	0.16	0.19	0.23	0.57	0.00	0.14	0.16	NA[f]	0.06
LOI	1.77	5.01[e]	5.87	4.66	5.29	2.27	2.76	NA	2.21[g]

Table 8.1 continued.

Footnotes

a - No. represents the number of analyses included in each average.
b - Total iron reported as Fe_2O_3, unless both species were analysed in which case Fe_2O_3 is reported above FeO.
c - Both species of iron are reported where possible.
d - D/M:, mafic dyke; C#SC, chlorite schist; M:TF, mafic tuff; I:TF, intermediate tuff; I:LT, intermediate lapilli tuff.
e - LOI = CO_2 + H_2O.
f - NA = not analysed.
g - LOI = H_2O^+ + H_2O^-

References

1. Goodwin (1977), Table V, Archean Superior Province.
2. Thurlow (1980), Table 7, Buchans Nfld.
3. Henley and Thornley (1981), Appendix, Buchans Nfld.
4. Jolly (1979), Table 6, Abitibi area.
5. Ewart and Bryan (1972), Table 3, E8, Eua, Tongan Islands.

MgO/CaO ratio of the Strickland mafic tuffs is similar to that of the Buchans footwall basalt, both of which are unusually high compared to other mafic igneous rocks. The average Na_2O values of the Strickland mafic tuffs and the Buchans basalt are also somewhat low when compared to other mafic rocks.

8.1.3 Intermediate lithologies

The average composition of the Strickland intermediate tuff and intermediate lapilli tuff are quite similar except that the lapilli tuff is slightly richer in MgO (see Table 8.1). They contain SiO_2 and TiO_2 averages intermediate between an andesite and a dacite and are noticably depleted in CaO and Na_2O. The MgO/CaO ratio of 3 in the Strickland intermediate volcaniclastics is unusually high.

8.1.4 Felsic lithologies

The felsic flows are silicified, being extremely high in SiO_2, low in TiO_2 and total alkalis (wt. % $Na_2O + K_2O$ = 5.3%) in comparison to other felsic flow material (see Table 8.2). It is especially interesting to compare the Strickland average with the average of twelve samples of the correlative Bay du Nord felsite bands collected by Chorlton (1980, Table XI). The ratio of Na_2O/K_2O for the Strickland felsic flows is 0.27 and for the felsite bands is 1.5, suggesting that sodium has been stripped from the Strickland flows and partially replaced by K_2O. A

Table 8.2

The average composition of Strickland felsic lithologies compared with those from other areas

	F:FL[a]	Felsite bands	Rhyolite	Calc-Alk Rhyolite	F:TF	F:LT	Ignim-brite	D/F:	Baggs Hill Granite	Quartz Mon-zonite
Reference		1	2	3			4			5
No.	40	12	1	4	136	53	17	3	11	25
SiO_2	79.7	76.0	71.45	71.4	76.5	70.4	73.85	78.6	77.7	75.4
TiO_2	0.15	0.24	0.13	0.50	0.31	0.43	0.23	0.22	0.18	0.1
Al_2O_3	11.3	13.0	14.42	13.2	11.8	12.9	13.55	11.0	11.8	13.3
Fe_2O_3[b]	1.79	0.48 1.28	0.87 2.27	4.35	3.64	4.11	1.25 0.60	2.37	1.78	0.3 0.74
MnO	0.03	0.04	0.16	0.03	0.06	0.08	0.05	0.03	0.03	0.08
MgO	0.41	0.33	0.10	0.82	0.95	1.72	0.30	0.49	0.12	0.12
CaO	0.25	0.48	0.40	2.03	0.32	0.38	1.53	0.27	0.22	0.48
Na_2O	1.14	4.17	5.35	4.07	0.83	1.58	3.71	3.77	4.33	4.1
K_2O	4.19	2.72	4.70	1.60	3.66	3.49	3.60	2.48	3.00	4.5
P_2O_5	0.05	0.02	0.05	NA[d]	0.05	0.06	0.05	0.03	0.02	0.01
LOI	0.99	0.85	0.13[c]	NA	1.86	2.15	0.97[c]	0.60	0.50	.46[e]

Table 8.2 continued

Footnotes

a - F:FL, felsic flows; F:TF, felsic tuff; F:LT, felsic lapilli tuff; D/F:, felsic dyke.
b - Total iron reported as Fe_2O_3 unless both species were analysed in which case Fe_2O_3 is reported above FeO.
c - LOI = H_2O
d - NA, not analysed.
e - LOI = (H_2O^+) + (H_2O^-) + (CO_2) + (Cl)

References

1. Chorlton (1980), Table XI, Bay du Nord Group, Nfld.
2. Oskarsson et al. (1982), Table 1, sample 26 (SNS32), Iceland.
3. Jolly (1980), Table 6, Abitibi area.
4. Ewart and Stipp (1968), New Zealand.
5. Bateman et al. (1963), p. 29, Sierra Nevada.

negative relationship between Na_2O and K_2O is evident in Figures 8.1a,b,c which shows all the Strickland rocks divided into three groups, sedimentary, igneous and mixed. Yet a plot of the felsic flows and felsite bands (Figure 8.2) shows a different pattern with only a handful of Strickland flows depleted in K_2O (K_2O < 1%) while most show strong depletion in Na_2O (Na_2O < 1.5%) and corresponding high K_2O values (K_2O > 1.5%). In thin section the low-K_2O flows appear to have been mylonitized and contain calcite, epidote and numerous quartz veins. When phenocrysts are present, they are broken, abraded and resorbed plagioclase phenocrysts. The low-Na_2O flows display delicate quench and devitrification textures. Phenocrysts are rare and are dominantly quartz. Secondary biotite and sericite is common in the matrix and are concentrated along fractures.

If the felsite samples are taken as background or normal and unaltered samples then the felsic flows of the Strickland property have been exposed to a unique process unrelated to regional metamorphism, a process which resulted in Na_2O depletion and K_2O enrichment. One felsite sample collected from a sulphide-mineralized outcrop not included in the calculated average has an Na_2O content of 0.25% and a K_2O content of 8%. The average total alkali content of the Strickland felsic flows is less than that of the felsite bands (5.33 wt.% and 6.89 wt.% respectively).

The felsic tuffs and felsic lapilli tuffs of the Strickland property are titanium-, iron-, and magnesium-rich

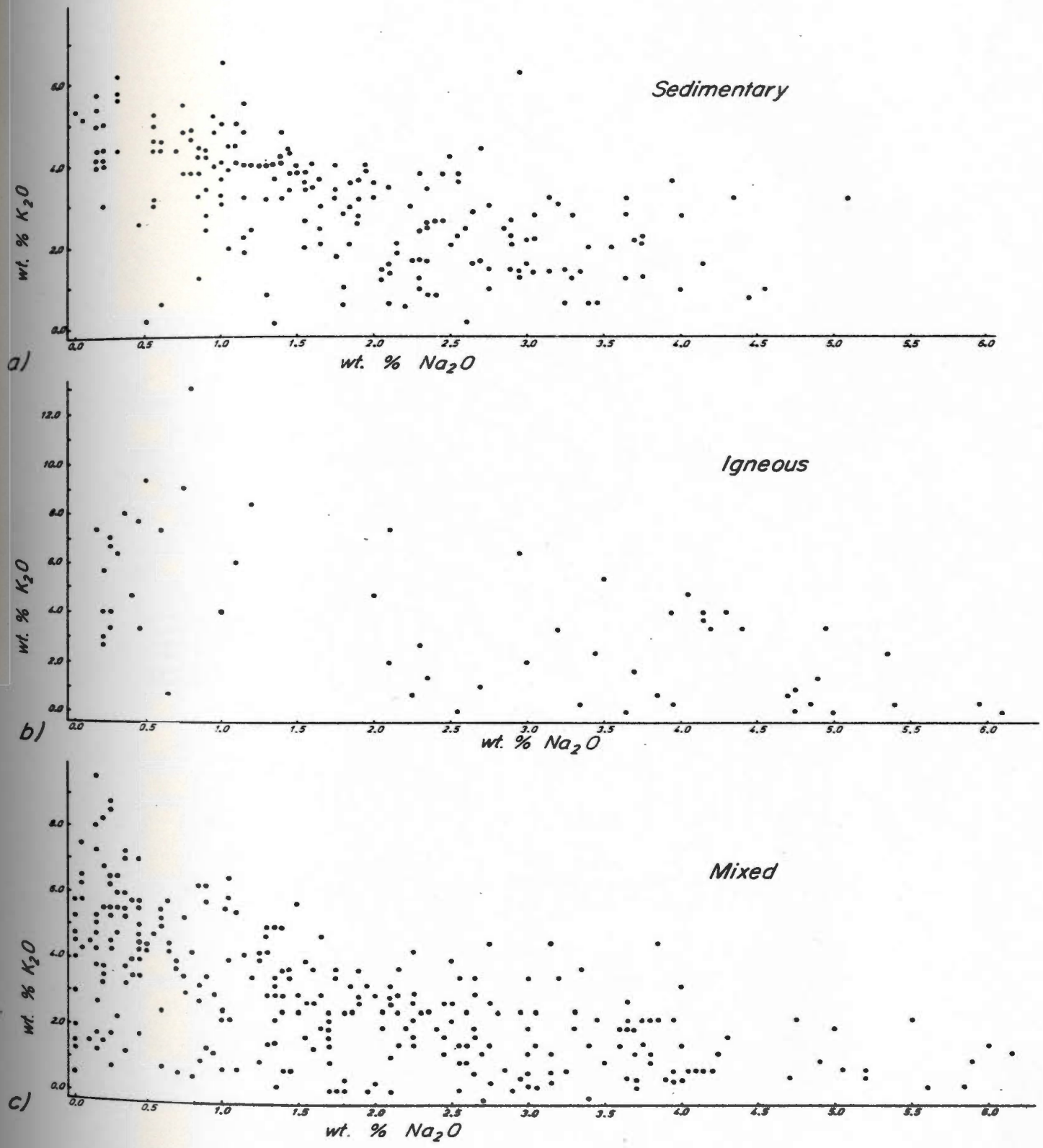

Figure 8.1. K_2O versus Na_2O plots for the a) sedimentary, b) igneous and c) mixed groups of samples.

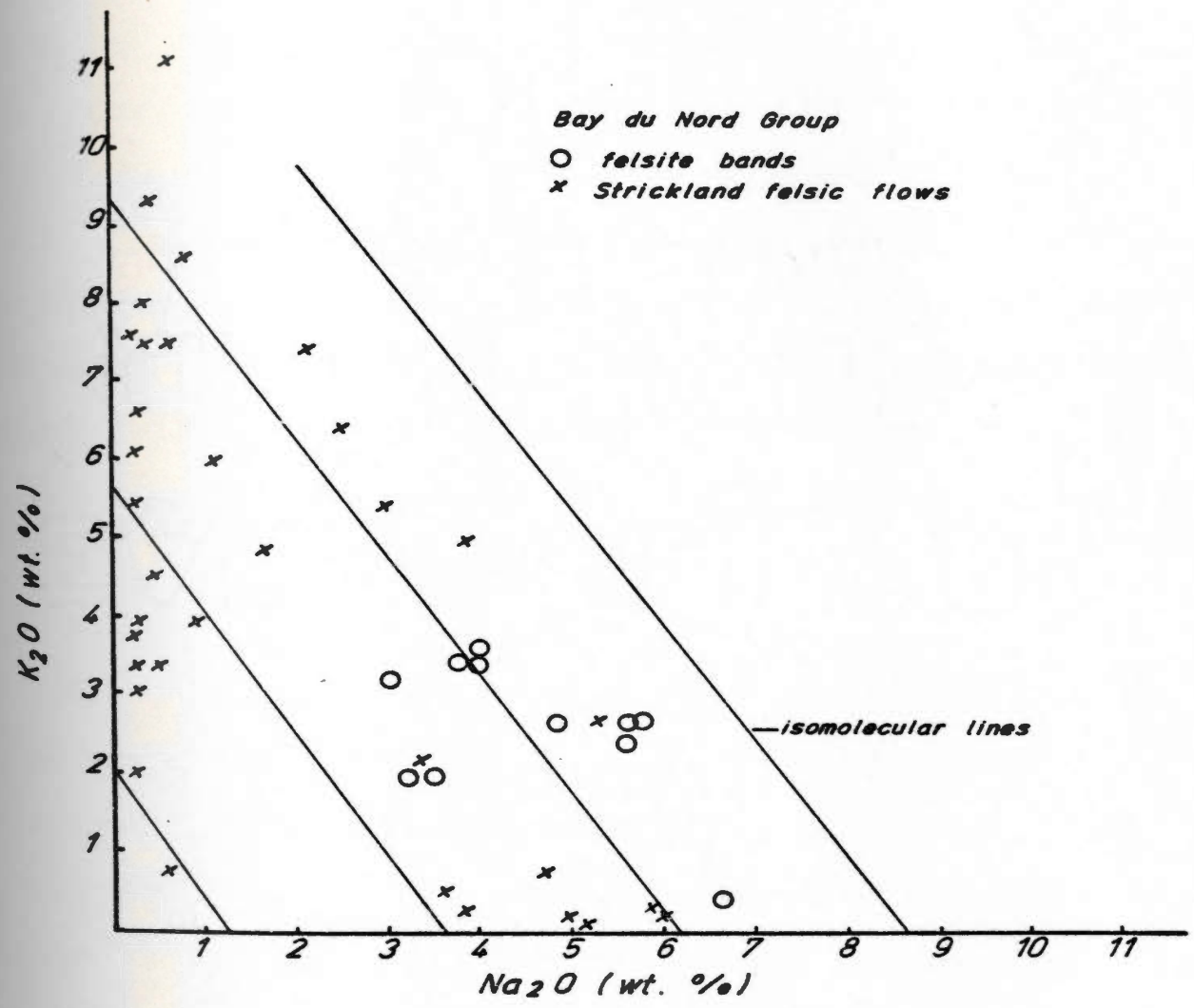

Figure 8.2. Na_2O and K_2O for Bay du Nord felsite bands (Chorlton, 1980) and the Strickland felsic flows plotted on a diagram contoured for molar equivalents.

and sodium-depleted compared to analyses reported by other authors (see Table 8.2). They are slightly enriched in MgO and FeO and depleted in total alkalis relative to the felsic flows.

The sample population of felsic dykes is very small (3) reducing the significance of the compositional average, but it is included in Table 8.2 because of its similarity with the average composition of the Baggs Hill Granite. Both are sodic, in contrast to the potassic chemistry of the felsic flows and volcaniclastics. On the basis of petrographic observations and geochemical trends Chorlton (1980) has suggested that the Baggs Hill Granite underwent early metasomatic or hydrothermal sodium enrichment. Note that it is the most sodic lithology in Table 8.2.

8.1.5 Sedimentary lithologies

The average composition of the Strickland sandstone compares most closely to that of greywackes but it is relatively depleted in calcium (Table 8.3). The average Strickland siltstone is rich in iron and potassium relative to the sandstone. It has an alkali content comparable to the Buchans cycle 2 and 3 siltstones, but is poorer in MgO and CaO. The Strickland shale is rich in SiO_2 (possibly the result of volcanic ash input) and poor in CaO.

8.1.6 Diagramatic comparisons

The Strickland data are plotted in Figure 8.3 on a

Table 8.3

The average composition of Strickland sedimentary lithologies compared with those from other areas

	SSST[a]	Greywacke	Arkose	SSLT	Siltstone	SHAL	Shales
Reference		1	1		2		3
No.	42	61	32	115	11	43	277
SiO_2	73.7	66.7	77.1	67.6	67.1	68.0	58.9
TiO_2	0.43	0.6	0.3	0.6	0.35	0.67	0.78
Al_2O_3	11.5	13.5	8.7	14.2	13.25	15.5	16.7
Fe_2O_3[b]	4.60	1.6 3.5	1.5 0.7	5.57	4.83	5.64	2.8 3.7
MnO	0.07	0.1	0.2	0.07	0.17	0.05	0.09
MgO	1.21	2.1	0.5	1.58	2.46	1.50	2.6
CaO	0.52	2.5	2.7	0.56	2.39	0.50	2.2
Na_2O	1.96	2.9	1.5	1.83	2.16	1.72	1.6
K_2O	2.18	2.9	2.8	3.35	3.34	3.14	3.6
P_2O_5	0.10	0.2	0.1	0.12	0.09	0.10	0.16
LOI	2.08	4.2[c]	3.9[c]	2.08	3.18	3.15	5.6[c]

Footnotes

a – SSST, sandstone; SSLT, siltstone; SHAL, shale.
b – Total iron reported as Fe_2O_3 unless both species were analysed, in which case Fe_2O_3 is reported above FeO.
c – LOI = (H_2O+) + (H_2O-) + (CO_2).

References

1. Pettijohn (1963), p. 15.
2. Thurlow (1980), Table 8, Buchans Nfld., cycle 2 and 3 siltstone.
3. Clark (1924), Goldschmidt (1933), Minami (1935), Shaw (1956), geosynclinal shales — taken from Wedepohl (1969).

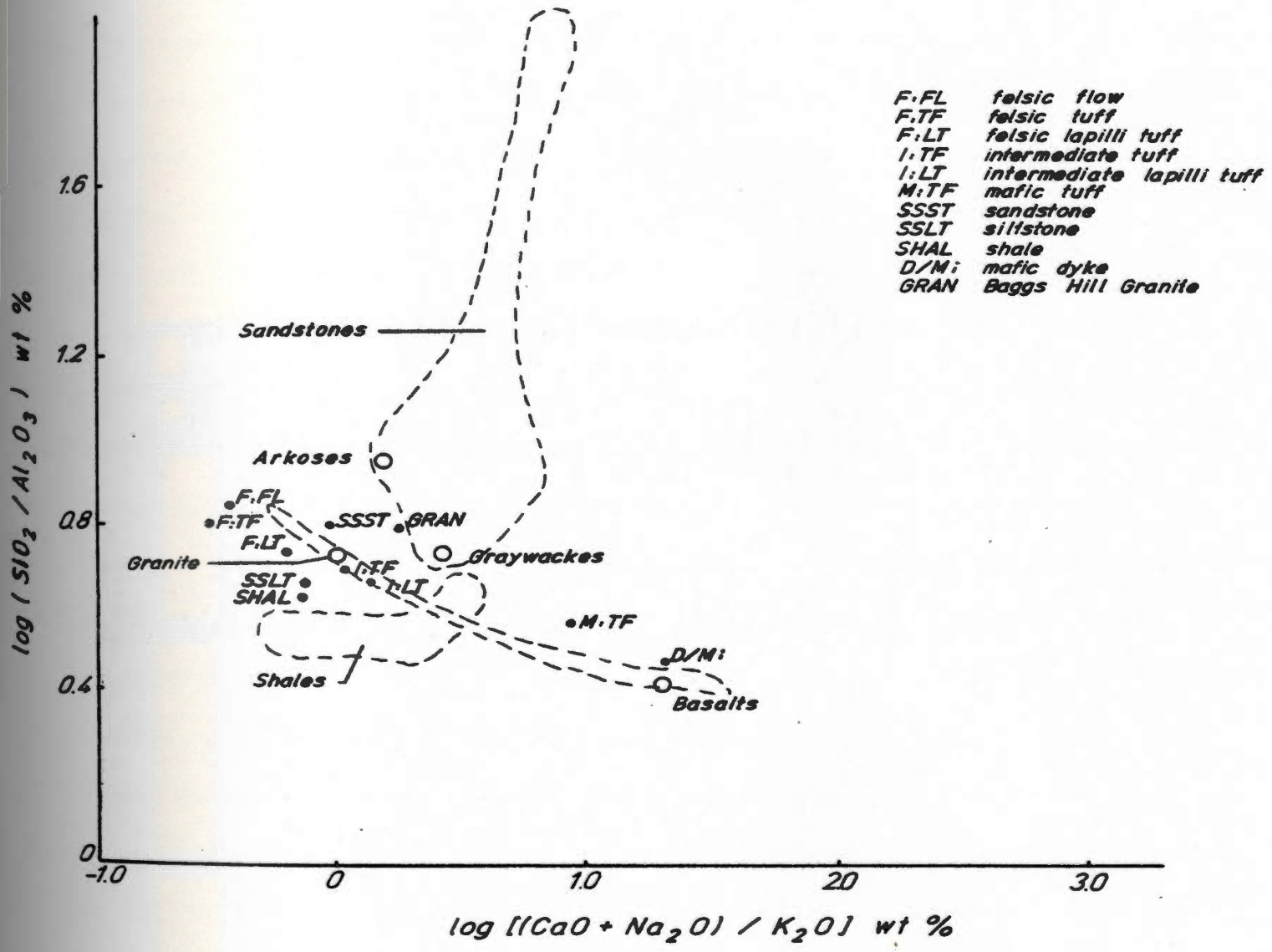

Figure 8.3. Composition of the Strickland rocks compared to typical igneous and sedimentary rocks (from Garrels and MacKenzie, 1971).

logarithmic plot along with a variety of typical igneous and sedimentary rocks (from Garrels and MacKenzie, 1971). The axes effectively separate argillaceous and arenaceous sediments and show igneous rocks on a smooth tight trend. The Strickland mafic dykes plot close to the mafic end of the well-defined igneous curve. The shale plots slightly above (on the siliceous side) the typical shale field. The Baggs Hill Granite is displaced from the igneous curve as a result of its silica and slightly sodium-rich chemistry. The felsic flow average plots off the high-silica, high-potassium end of the igneous curve. The intermediate volcaniclastics plot on the igenous curve between the typical granite and granodiorite. The composition of the Strickland sandstone shows more affinity with the typical granite composition than either greywacke or arkose.

In terms of the ratios Na_2O/Al_2O_3 and K_2O/Al_2O_3 (Figure 8.4) the Strickland mafic dykes plot in the field of mafic igneous rocks. The felsic flow and felsic tuff averages plot in a sodium-depleted field well below the igneous boundary. The Baggs Hill Granite plots in the sodium-rich area of the diagram, but its K_2O/Al_2O_3 ratio is not unusual compared to other granites. The Strickland shale plots within the typical shale field between low and high-grade pelites.

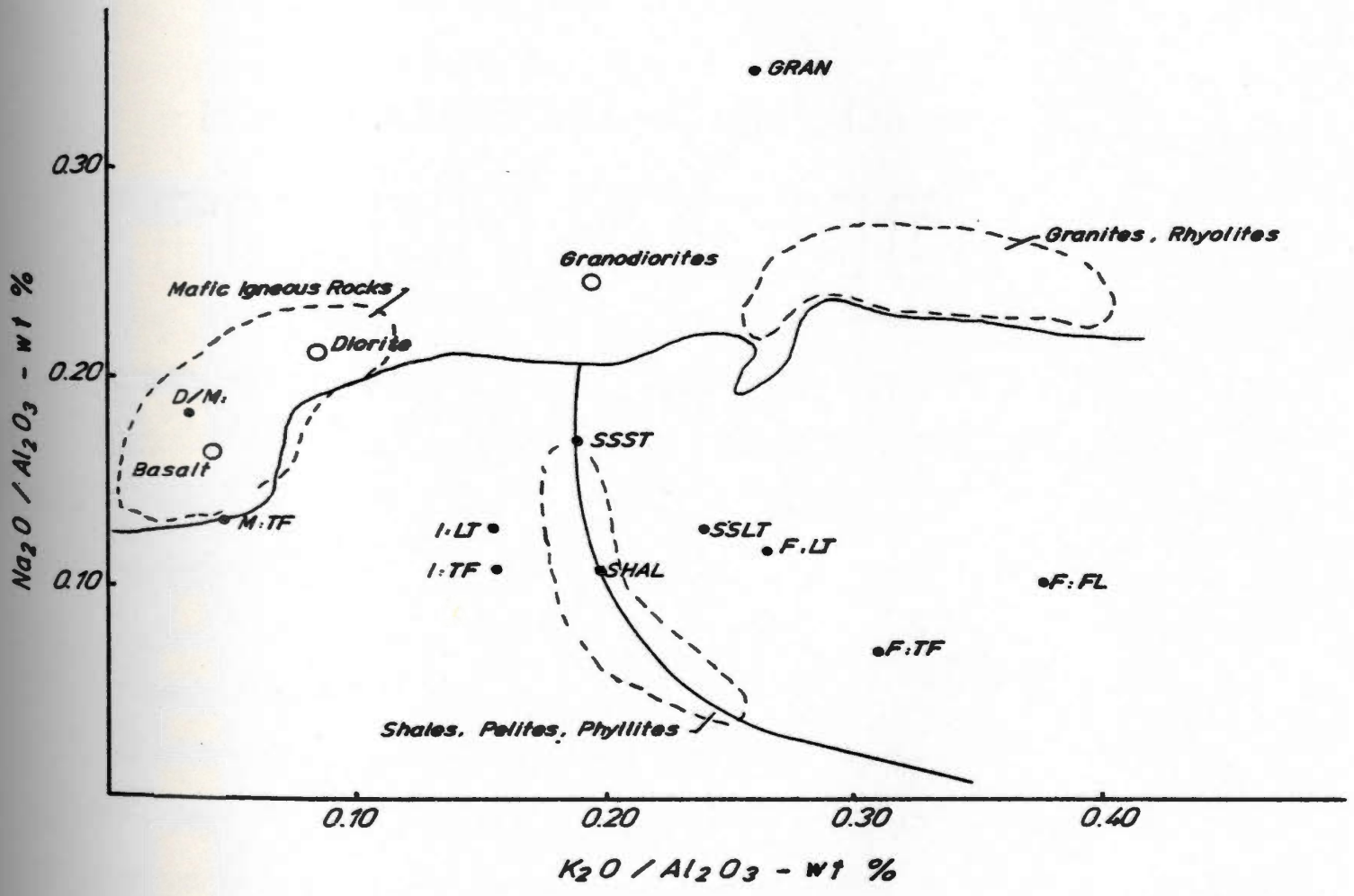

Figure 8.4. Composition of the Strickland rocks compared with lutites and igneous rocks in terms of their Na_2O and K_2O content (from Garrels and MacKenzie, 1971). For a key to the lithologies see Figure 8.3. .

8.1.7 Summary

Table 8.4 summarizes the observed oxide enrichments and depletions noted in the Strickland rocks relative to other similar lithologies. MgO and Na_2O depletion is persistent in several of the Strickland lithologies. The Baggs Hill Granite is noticeably enriched in Na_2O. Comparison of the average compositions of the Strickland felsic flows with their regional equivalents (the Bay du Nord felsite bands) shows the flows to be more silicic and more depleted in sodium as well as total alkalis relative to the felsite bands.

The spatial variation of these broad enrichment and depletion patterns are investigated in greater detail in the following section where the raw geochemical data and residuals are plotted with reference to sulphide mineralization.

8.2 Trace elements

A total of 128 surface samples were analyzed for Zr, Sr, Rb, U, Th, Ga, Ni, Y, Pb and Zn. These data are listed in Appendix D. In Figure 8.5 zirconium is plotted against titanium. The mafic rocks show a strong positive correlation between titanium and zirconium. The felsic rocks form another prominent group with consistently low Ti values and a corresponding wide range of Zr values. Most of the shale samples lie in a tight cluster between the mafic and felsic

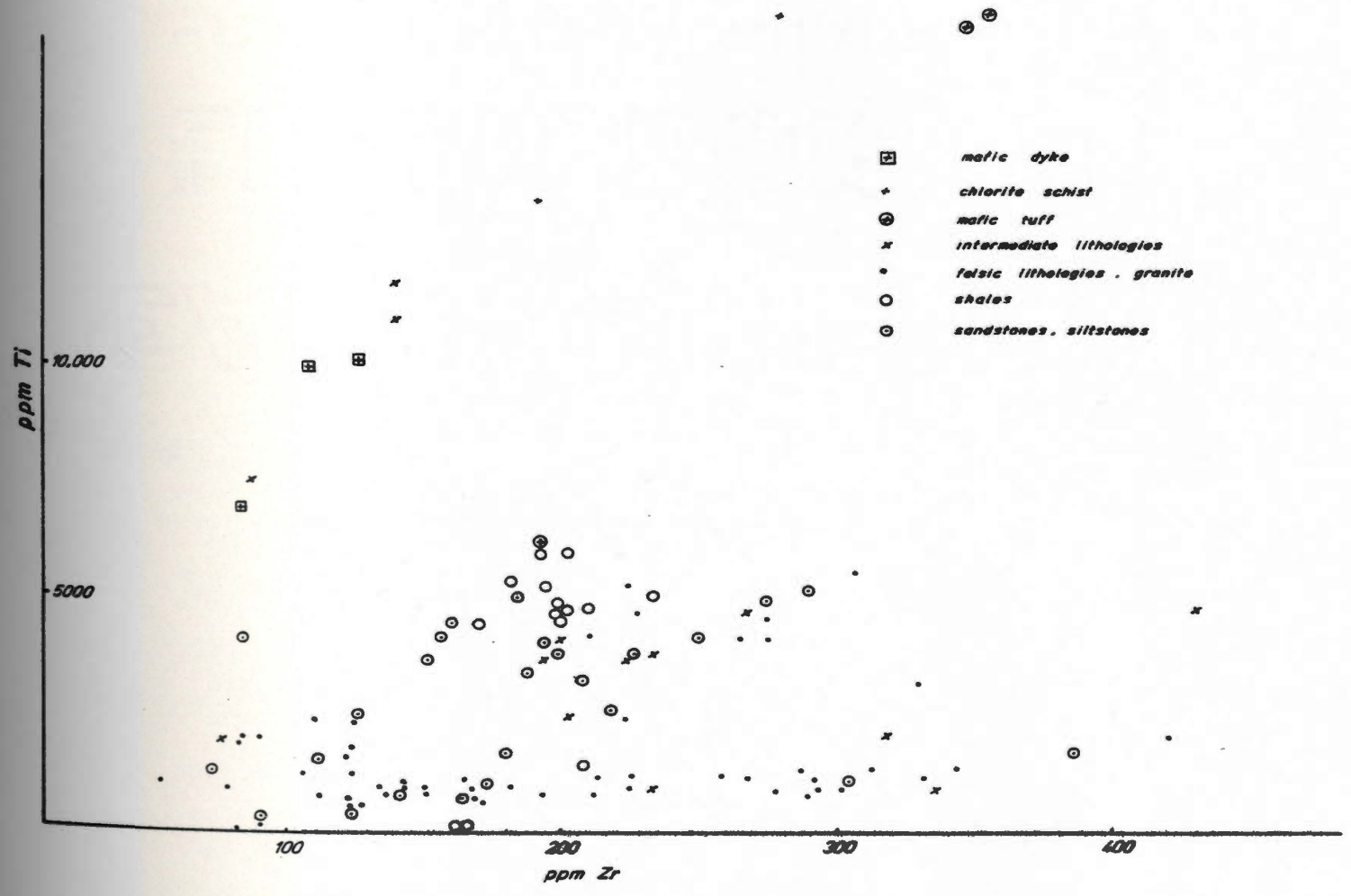

Figure 8.5. ppmZr vs. ppmTi plot for a selected number of Strickland surface samples.

Table 8.4

Summary of the average enrichments or depletions of the Strickland rocks relative to other similar lithologies (see Tables 8.1,8.2,8.3)

	D/M:	M:TF	I:TF/I:LT	F:FL	F:TF	F:LT	GRAN	SSST	SSLT	SHAL
SiO_2				+						+
TiO_2		+		(-)	(+)	+				
Al_2O_3										
Fe_2O_3					+	+			(+)	
MgO	(+)	+	+		+	+				
CaO	(-)	-	-					(-)		-
Na_2O		-	-	-	-	-	+			
K_2O				+(-)					+	

NOTES: + enriched
- depleted
() weakly enriched or depleted

trends. The anticipated dispersal effects of sedimentary processes on the shale composition is not observed and the Strickland shales are similar in composition (with respect to Ti and Zr) to many shales world wide (Erlank et al. 1978, Correns, 1978). The majority of the intermediate samples and sandstones also plot between the felsic and mafic trends. The overlap of intermediate samples into the mafic and felsic trends (siltstones, intermediate tuffs) is probably due in part to the misclassification of samples.

Figure 8.6 shows the Rb (ppm) values plotted on a logarithmic scale against the log K (ppm) values. It is evident from this plot that the behaviour of the trace element (Rb) is overall closely analogous to that of the major element (K), i.e. with a relatively constant K/Rb ratio of 85:1. It was felt therefore that a detailed examination of the distribution of major element anomalies alone would identify any alteration patterns related to mineralization. In the discussion which follows the distribution of anomalous values of the major elements and metals (Cu, Pb, Zn) are described.

8.3 Comparison of raw and residual data plots

8.3.1 Introduction

The three sets of data discussed in this section include the concentrations of major oxides and metals in what is termed the raw data set and two data sets (the first pass and second pass data sets) generated using a

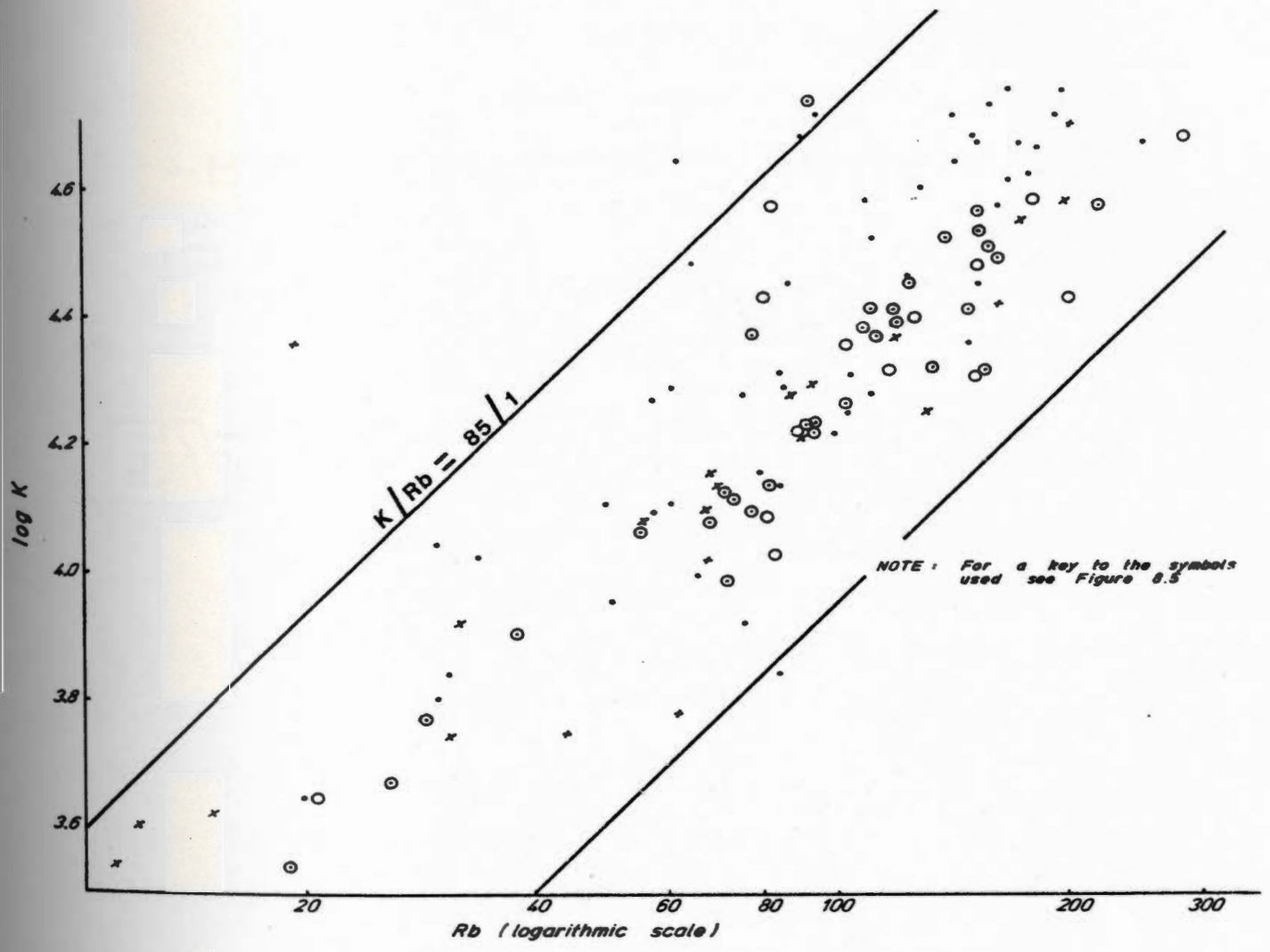

Figure 8.6. Rb(ppm) vs. log K (ppm) for a selected number of Strickland surface samples.

modification of the residual techniques used by Lavin (1976), McConnell (1976) and Sopuck (1977). The first pass data set contained residual values generated from the entire raw data set using regression equations with TiO_2, Al_2O_3, FeO and their squares as independent variables. The second pass data set included residuals generated from two groups of rocks - those igneous in origin and those from a mixed igneous and sedimentary origin using regression equations with TiO_2 and $(TiO_2)^2$ as independent variables. Also in the second pass data sets are the anomalous oxide/metal analyses of rocks with a dominantly sedimentary source.

The raw data (major oxides, metals) are listed in Appendix D. The first and second pass residual data lists are too voluminous to be included within this thesis and are, therefore, on file along with the preliminary data plots at the Department of Earth Sciences of Memorial University of Newfoundland.

The concentrations of MnO, P_2O_5 and Ag in the Strickland rocks are generally close to, or below, the detection limit of the analytical methods used. Consequently, they were not included in the data plots or interpretation and will not be considered further.

8.3.2 Comparison

The anomalous samples (strongly anomalous = mean +/- two standard deviations, weakly anomalous = mean +/- one standard deviation) of each of the three sets of data were plotted on plan maps (the surface samples) and

cross-sections (the diamond drill core samples). Figures 8.7 through 8.12 show the relationship between the lithologies and the K_2O and CaO anomalies as defined in each of the three data sets for drill holes #16-023-4, 16-023-8, 16-023-19 through the Copper, Main and Silver Hill Zones respectively.

The anomalous samples in the raw data plots are commonly just reflections of the sample lithology - mafic tuffs are represented by negative K_2O anomalies (Figure 8.7), felsic tuffs by positive K_2O anomalies (Figure 8.9). Many of these anomalies disappear or are reduced (from plus two standard deviations to plus one standard deviations) when anomalous residual values are plotted. For example a CaO value of 4.09% is not anomalous in a mafic tuff with a TiO_2 content of 3.18% (Figure 8.10, DDH# 16-023-8, sample A7174). Examination of the first-pass plots shows that the variation of the oxide content of a sample relative to its TiO_2 content (not FeO or Al_2O_3) determines whether it is defined as anomalous or not. The controlling effect of FeO or Al_2O_3 in the regression equation then is negligible. The samples defined as anomalous in the first-pass treatment of the raw data are, overall, similar to those defined as anomalous in the second pass, with the exception of the sedimentary samples. Several of the anomalous sedimentary samples from the second pass were not defined as anomalous in the first pass. In many cases the TiO_2 content of these samples is matched by an oxide

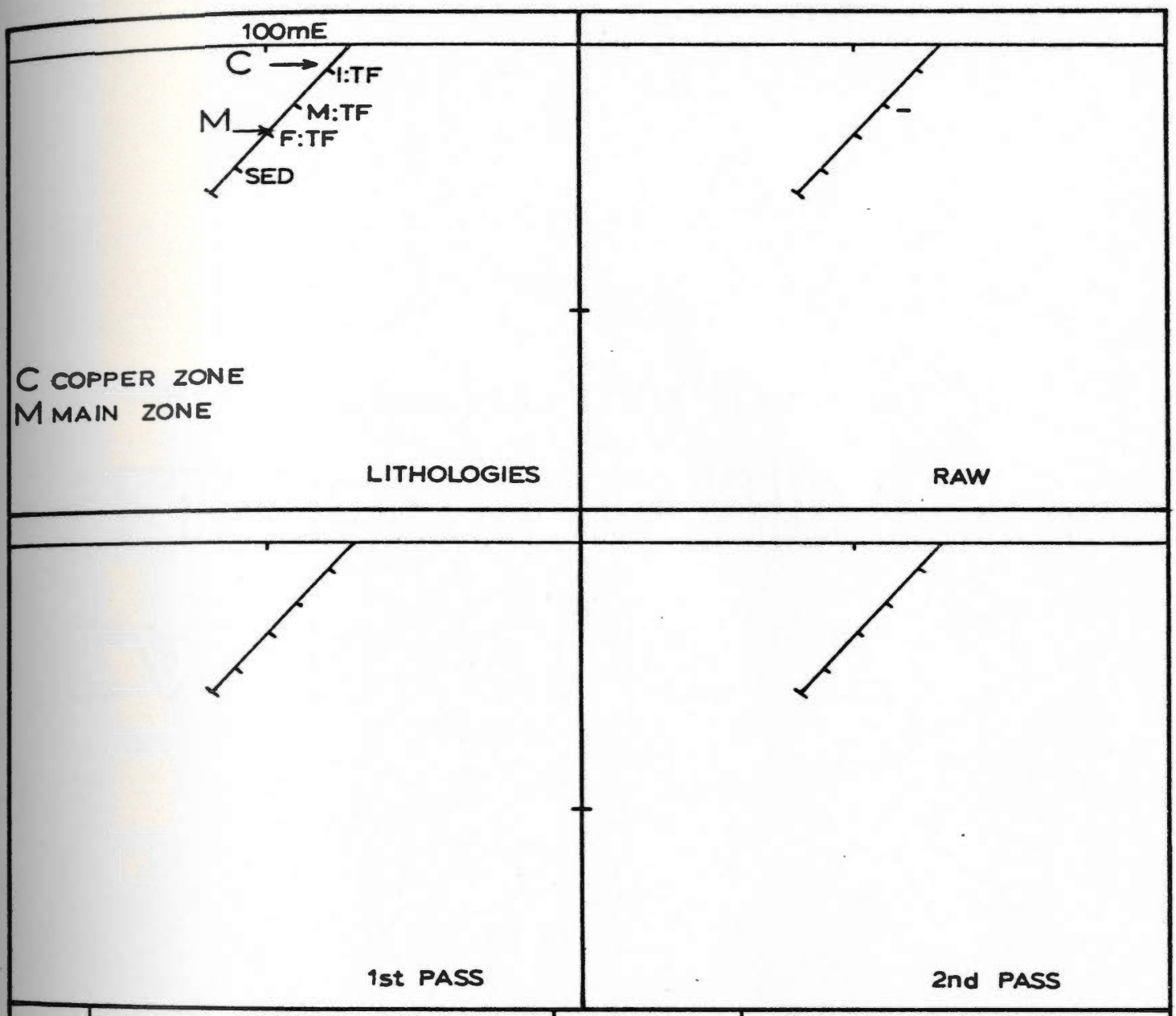

sample no.	%										ppm			
	SiO_2	Al_2O_3	CaO	MgO	Na_2O	K_2O	FeO	MnO	TiO_2	P_2O_5	Cu	Pb	Zn	Ag
A7192	61.6	12.1	0.92	4.10	1.34	2.29	11.60	0.43	0.61	0.17	860	81	310	2
7193	45.6	12.6	6.08	7.83	1.24	0.96	11.5	0.37	2.78	0.66	24	2	100	<1
7194	73.7	11.1	0.26	3.49	1.49	2.44	2.16	0.05	0.19	0.02	13	260	1080	<1
7195	67.3	13.9	0.62	1.41	1.14	3.30	6.16	004	0.70	0.12	24	4	48	<1

+,++ mean plus one, two standard deviation(s)

−,= mean minus one, two standard deviation(s)

Samples collected by:

/ Falconbridge personnel

LOOKING SW ON LINE 500S.

SCALE 1:2500

FIGURE 8.7: K_2O Anomalies, DDH 16-023-4, Copper Zone.

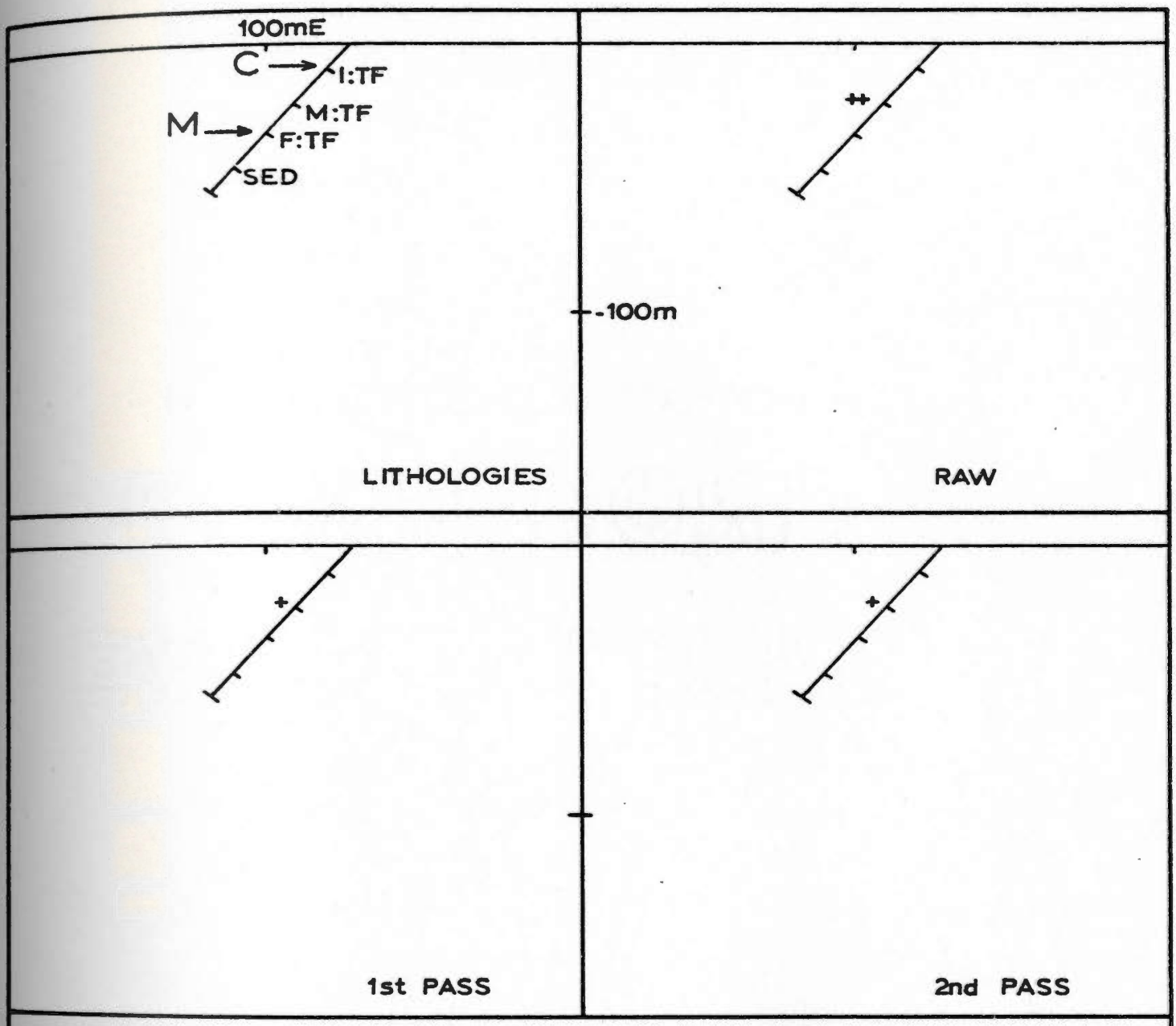

(see figure 8.7 for geochemistry)

Samples collected by:

Falconbridge personnel

LOOKING SW ON LINE 500S.
SCALE 1:2,500

FIGURE 8.8: CaO Anomalies, DDH 16-023-4, Copper Zone.

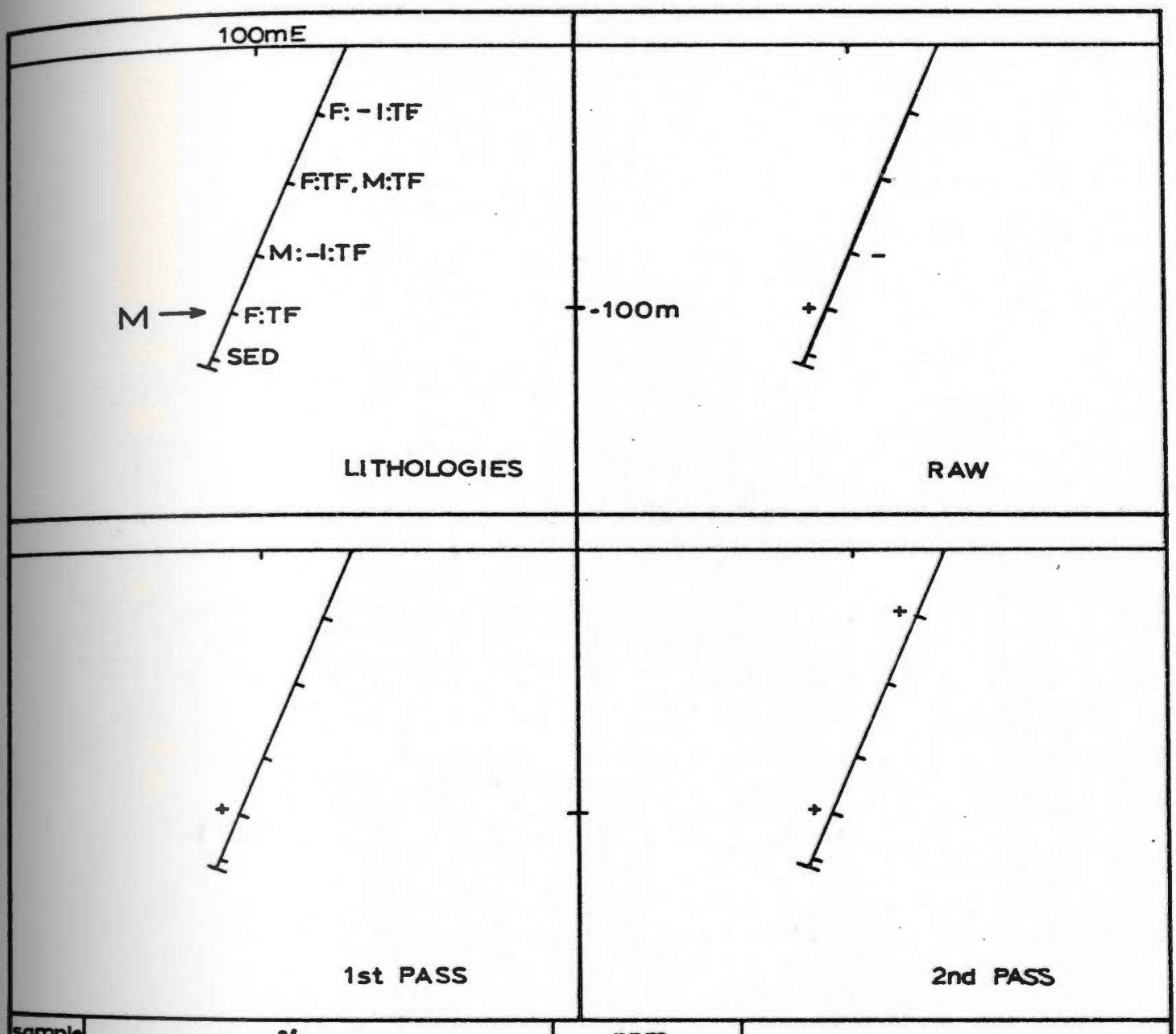

sample no.	%										ppm			
	SiO_2	Al_2O_3	CaO	MgO	Na_2O	K_2O	FeO	MnO	TiO_2	P_2O_5	Cu	Pb	Zn	Ag
A7172	66.2	15.6	0.38	2.00	0.47	4.76	6.76	0.15	0.71	0.09	33	22	110	<1
7173	73.8	11.8	0.42	1.18	0.47	3.98	4.22	0.08	0.38	0.06	38	25	110	<1
7174	47.3	13.7	4.09	9.50	1.76	0.19	14.1	0.28	3.18	0.77	23	<2	96	<1
7175	65.9	16.3	0.35	2.16	0.45	4.95	5.96	0.05	0.96	0.11	26	39	34	1
7176	66.0	16.3	0.43	1.61	1.47	4.20	5.49	0.04	0.74	0.12	34	3	66	<1

Samples collected by;

/ Falconbridge personnel

LOOKING SW ON LINE 015N

SCALE 1:2,500

FIGURE 8.9: K_2O Anomalies, DDH 16-023-8, Main Zone.

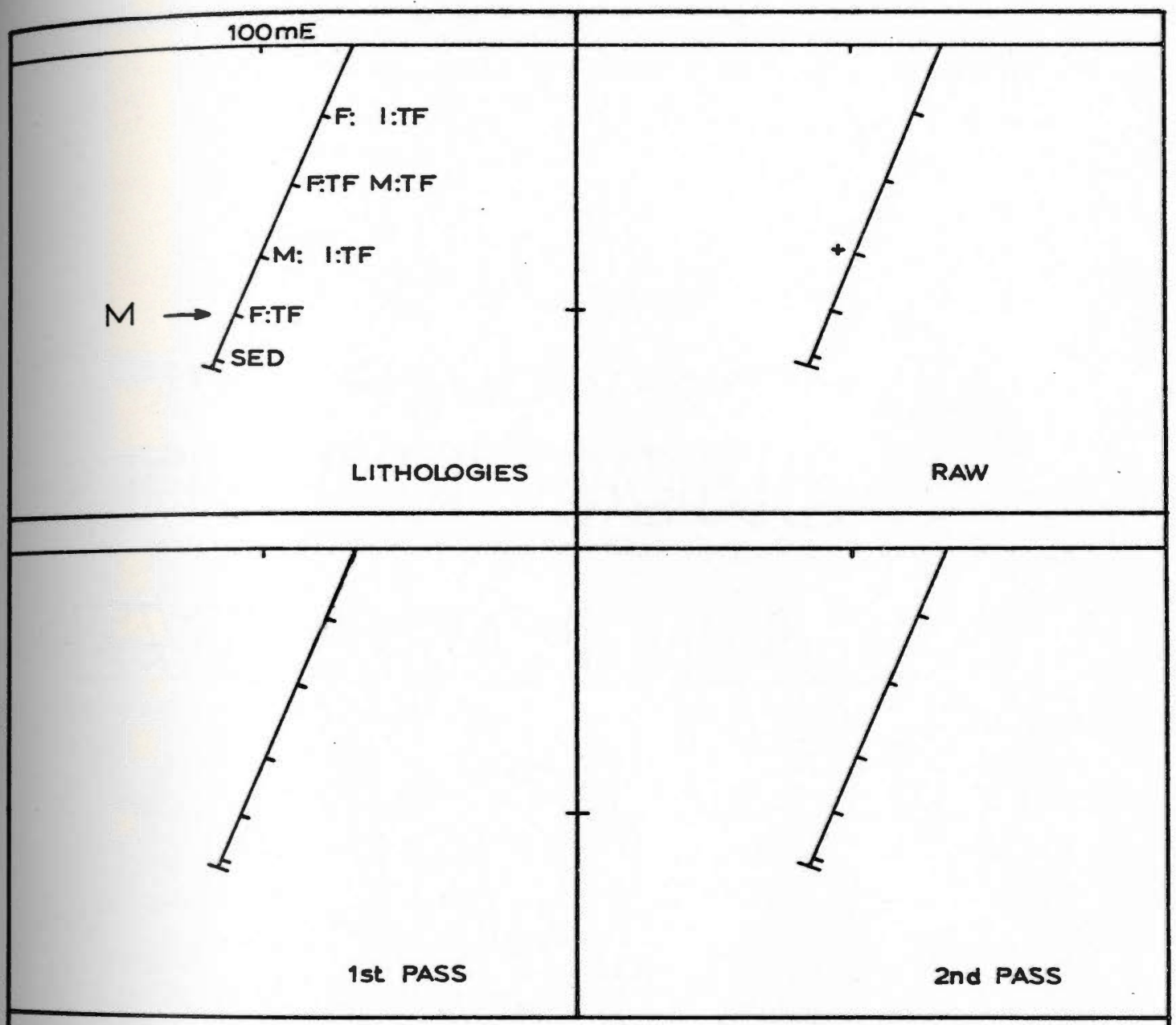

(see figure 8.9 for geochemistry)

Samples collected by;

/ Falconbridge personnel

LOOKING SW ON LINE 015N.
SCALE 1:2,500

FIGURE 8.10: CaO Anomalies, DDH 16-023-8, Main Zone.

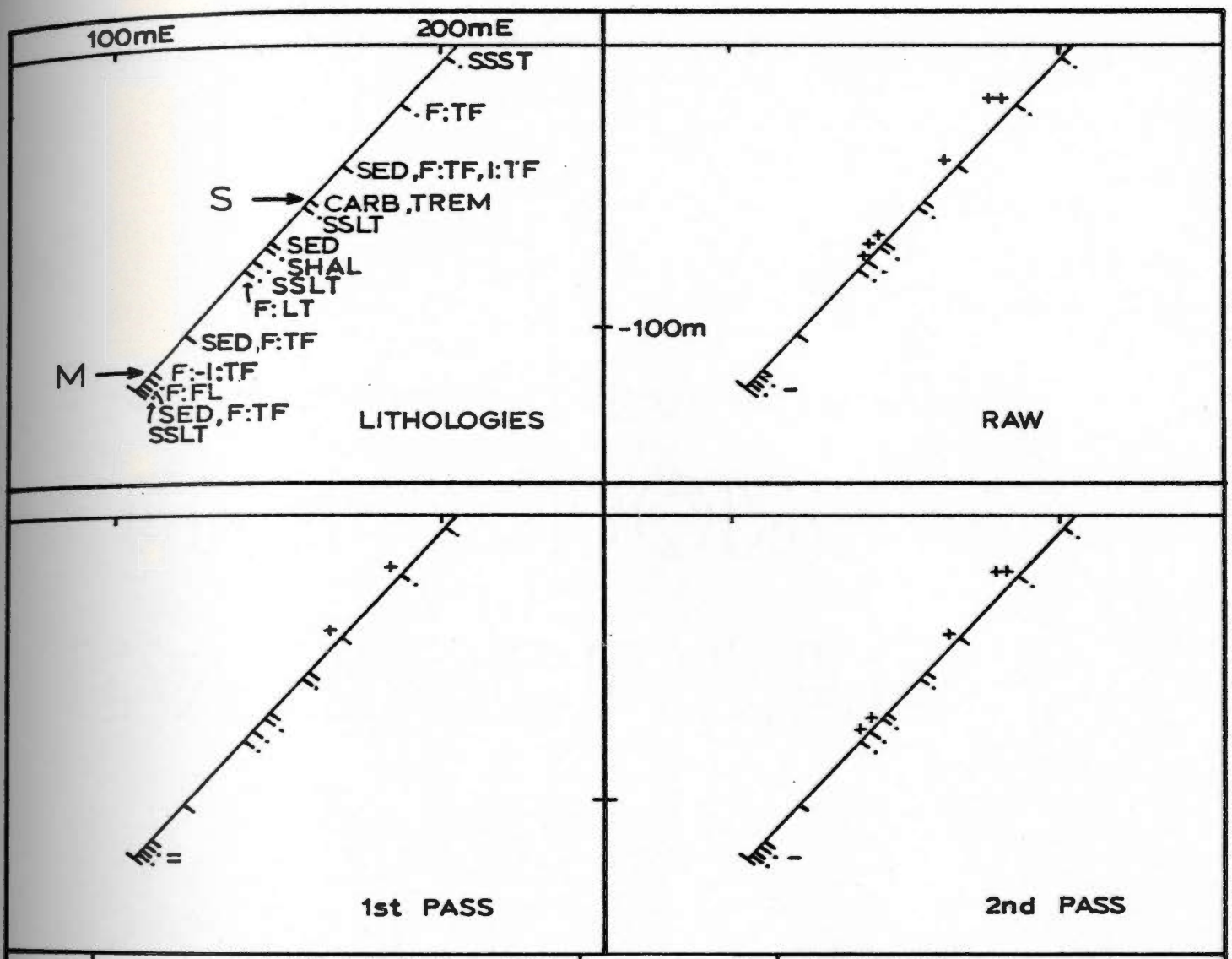

sample no.	%										ppm			
	SiO_2	Al_2O_3	CaO	MgO	Na_2O	K_2O	FeO	MnO	TiO_2	P_2O_5	Cu	Pb	Zn	Ag
A7118	66.9	13.3	0.55	1.75	0.20	5.05	6.92	0.14	0.70	0.14	430	5	97	<1
7119	50.1	10.1	10.1	6.37	0.30	3.53	4.16	0.36	0.26	0.13	140	5600	1600	78
7120	58.1	20.4	0.49	2.00	1.38	4.90	6.07	0.06	1.05	0.10	45	10	72	<1
7121	65.4	16.0	0.73	2.07	1.75	3.92	4.86	0.08	0.69	0.11	33	18	120	1
7122	71.4	10.2	1.22	2.74	2.45	1.87	3.00	0.13	0.30	0.04	39	900	6000	<1
7123	65.5	15.7	1.44	1.58	1.57	3.57	5.39	0.00	0.79	0.11	34	10	110	<1
W6219	73.0	12.7	0.37	1.20	2.64	3.04	5.07	0.10	0.46	0.01				
6220	49.8	26.3	0.11	1.49	0.17	9.52	6.52	0.06	0.37	0.01				
6224	64.9	13.4	1.33	5.68	0.92	2.77	4.89	0.10	0.53	0.05				
6225	60.8	19.2	0.18	1.46	1.17	5.34	5.94	0.04	0.76	0.05				
6226	62.9	17.7	0.13	1.91	0.23	5.38	6.08	0.07	0.65	0.06				
6233	67.3	12.4	1.74	5.75	3.00	3.39	3.43	0.22	0.28	0.02				
6234	79.3	19.7	0.30	0.93	4.75	0.16	1.50	0.03	0.01	0.05				
6236	67.7	15.5	0.54	1.71	1.29	4.09	5.23	0.05	0.70	0.13				

Samples collected by;

Falconbridge personnel

P.J.Wynne

LOOKING SW ON LINE 594N

SCALE 1:2,500

FIGURE 8.11: K_2O Anomalies, DDH 16-023-19, Silver Hill Zone.

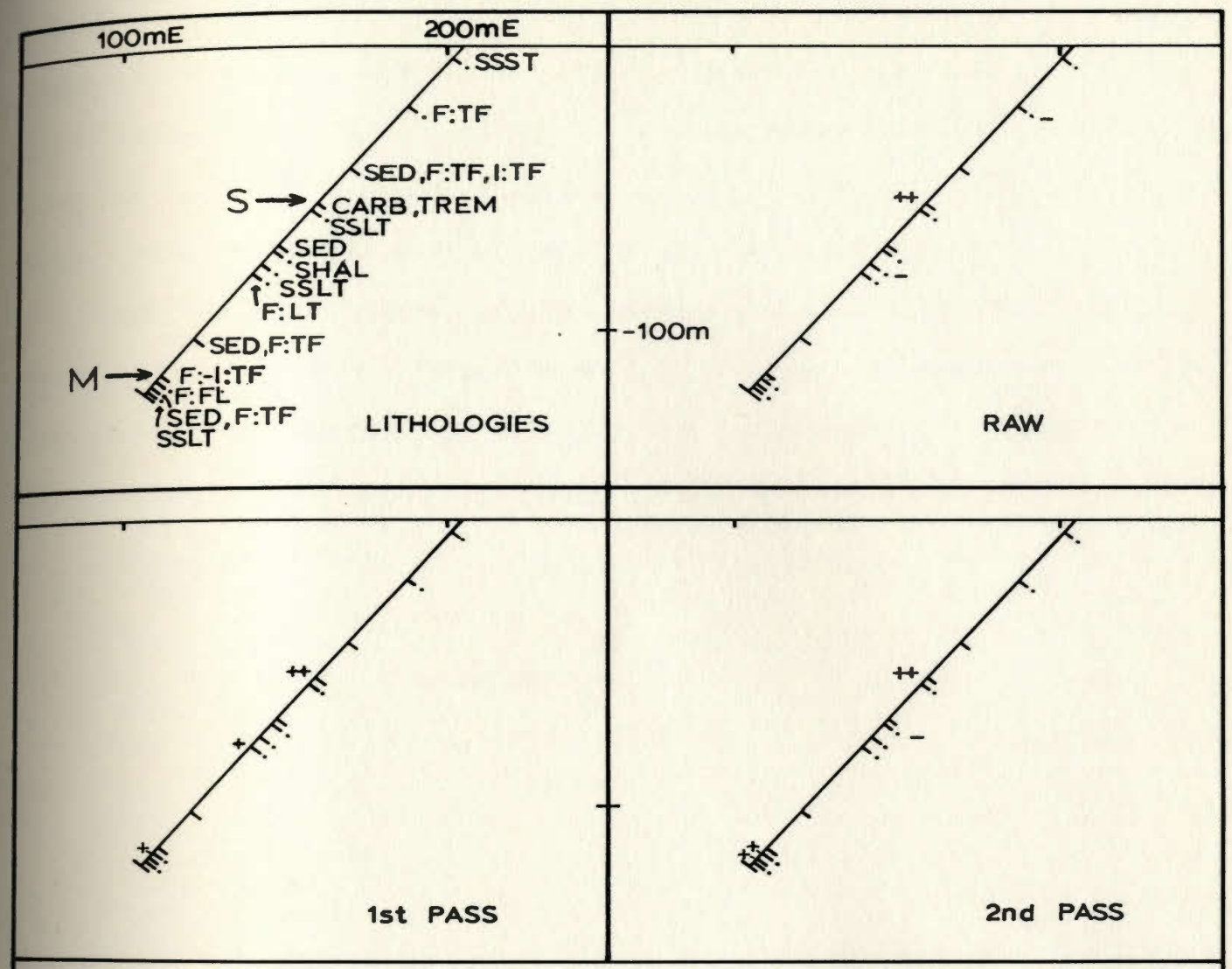

(see figure 8.11 for geochemistry)

Samples collected by;

Falconbridge personnel

P.J.Wynne

LOOKING SW ON LINE 594N

SCALE 1:2,500

FIGURE 8.12: CaO Anomalies, DDH 16-023-19, Silver Hill Zone.

content which is not unusual for an igneous rock but is unusual when compared to other sedimentary rocks (Figure 8.12, samples W6225, A7123). Note that strongly anomalous samples persist as anomalies in all three plots (Figure 8.11, sample W6220 and Figure 8.12, sample A7119).

The second pass plots thus appear to be the most sensitive to the detection of truly anomalous samples regardless of lithology and in the discussion that follows only second pass anomaly plots will be referred to.

8.4 Second pass plots

8.4.1 Introduction

Plan maps (for surface sample anomalies), cross sections and dip surface plots were prepared for each oxide and the metals (Cu, Pb, Zn). Dip-surface plots were drawn for the hanging wall sediments, for the main horizon of mineralization of the Main, Copper, Bog and Silver Hill Zones and also for a horizon 25m stratigraphically below (this is referred to as the underlying horizon). Figure 8.13 is a key to the drill hole intersections shown in the dip surface plots. Only those plan maps and dip-surface plots with interesting anomaly patterns are presented here, and a complete set is on file at Memorial University. Included here are cross sections of seven diamond drill holes which intersect lithologies and mineralization typical of each of the four principal mineralized zones. These holes and the mineral zones they penetrate are listed in Table 8.5, and the geochemical results from these holes in Tables 8.6 and 8.7. The plots are organized and discussed by oxide, dealing first with the surface sample and then drill core sample data. The metals (Cu, Pb, Zn) are plotted and described together.

8.4.2 Metals

The surface plot and the complete set of down-dip plots are included in Figures 8.14 to 8.16. The positive Cu,Pb,Zn second pass anomalies are included in each plot. Not many of the surface samples collected for lithogeochemistry were

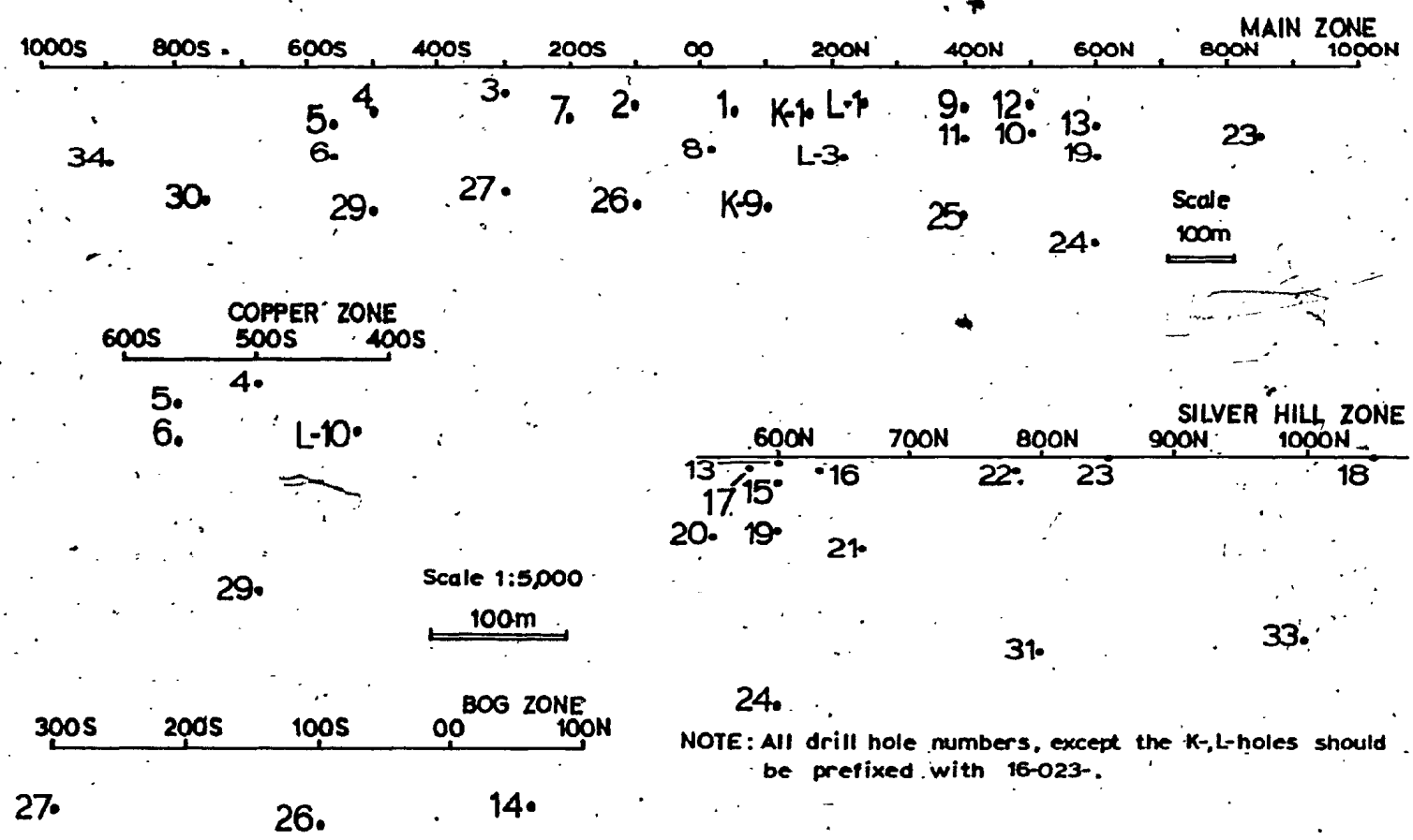

NOTE: All drill hole numbers, except the K-, L-holes should be prefixed with 16-023-.

FIGURE 8.13: A key to the drill hole intersections shown in the dip surface plots of this chapter. (FIGURES 8.15 - 8.46)

Table 8.5

A summary of the drill holes presented as representative of the four principal mineralized zones

Drill Hole Number	Mineralized Zone(s) Intersected
16-023-1	Main
16-023-4	Copper, Main (south extension)
16-023-5	Copper, Main (south extension)
16-023-6	Copper, Main (south extension)
16-023-26	Bog, Main
16-023-19	Silver Hill, Main (north extension)
16-023-21	Silver Hill

Table 8.6

A list of the geochemistry of samples from drill holes 16-023-1, -4, -5, -6. The samples are listed in the order in which they appear from the top of the hole to the bottom of the hole in the cross-sectional diagrams which follow (Note, in the diagrams the straight "ticks" represent samples collected by Falconbridge personnel and the dotted "ticks" those collected by this author).

DDH no.	Sample no.	Weight %										(ppm)			
		SiO_2	Al_2O_3	CaO	MgO	Na_2O	K_2O	FeO	MnO	TiO_2	P_2O_5	Cu	Pb	Zn	Ag
16-023-1	A3639	65.9	14.6	0.49	2.26	1.48	3.05	5.40	0.08	0.85	0.09	28	18	88	<1
	A3640	48.2	13.1	3.60	8.92	1.94	0.27	13.3	0.27	2.95	0.70	22	<2	110	<1
	A3641	68.8	12.4	0.84	3.68	0.52	4.32	3.74	0.09	0.50	0.06	67	820	1480	3
	A3642	21.1	5.59	26.4	6.00	0.27	1.18	4.08	0.50	0.27	0.09	88	3000	1280	44
	A3643	69.2	13.5	1.28	0.93	1.58	3.37	4.18	0.03	0.59	0.20	23	22	84	1
	W5052	64.3	16.0	0.54	2.90	2.54	3.71	5.80	0.07	0.45	0.94				
	W5053	48.4	13.1	3.22	9.57	2.68	0.06	13.23	0.19	2.79	1.78				
	W5055	76.9	9.6	0.15	1.81	0.68	3.74	3.55	0.08	0.35	0.08				
	W5056	76.7	6.5	3.19	2.91	0.47	1.66	2.26	0.13	0.26	0.02				
	W5061	67.8	15.0	0.56	1.29	2.48	4.14	4.84	0.02	0.58	1.13				
16-023-4	A7192	61.6	12.1	0.92	4.10	1.34	2.29	11.6	0.43	0.61	0.17	860	81	310	2
	A7193	45.6	12.6	6.03	7.83	1.24	0.96	11.5	0.37	2.78	0.66	24	2	100	<1
	A7194	73.7	11.1	0.26	3.49	1.49	2.44	2.16	0.05	0.19	0.02	17	260	1080	<1
	A7195	67.3	13.9	0.62	1.41	1.14	3.30	6.16	0.04	0.70	0.12	24	4	48	<1
16-023-5	A7187	63.5	14.9	0.74	2.73	2.61	2.39	7.52	0.25	0.79	0.17	39	180	310	<1
	A7188	53.7	11.4	1.47	5.62	0.86	1.04	15.7	0.44	2.04	0.52	990	20	280	<1
	A7189	57.1	11.2	5.10	4.45	1.03	2.31	7.66	0.37	1.21	0.27	67	260	440	1
	A7190	75.2	11.0	0.33	2.56	1.47	3.41	2.47	0.05	0.19	0.02	17	11	110	<1
	A7191	70.3	12.9	0.55	1.04	0.87	3.25	6.28	0.03	0.58	0.13	20	<2	42	<1
	A7182	62.3	15.1	1.06	2.78	0.38	3.53	8.02	0.26	0.95	0.18	45	210	940	2
	A7183	44.5	14.7	2.37	8.01	1.35	1.51	15.2	0.72	2.50	0.68	580	370	3220	<1
	A7184	52.4	17.5	1.32	4.99	0.51	4.48	9.78	0.27	1.28	0.24	400	100	350	2

Table 8.6 continued.

DDH no.	Sample no.	Weight %										(ppm)			
		SiO_2	Al_2O_3	CaO	MgO	Na_2O	K_2O	FeO	MnO	TiO_2	P_2O_5	Cu	Pb	Zn	Ag
	A7185	71.7	11.1	0.64	2.45	0.17	4.87	3.55	0.10	0.29	0.05	25	630	1720	1
	A7186	66.0	16.1	0.68	1.73	1.07	3.77	4.91	0.04	0.66	0.10	33	9	71	<1
16-023-6	W5030	61.8	17.7	0.49	1.84	1.10	4.92	6.13	0.07	0.70	0.58				
	W5031	49.6	10.8	1.90	7.04	0.70	0.75	17.98	0.65	2.24	0.56				
	W5033	57.8	19.3	0.31	4.42	0.19	5.62	6.52	0.16	0.63	0.05				
	W5035	77.9	10.4	0.10	1.58	2.17	2.47	2.66	0.09	0.14	0.00				
	W5036	71.1	12.7	0.17	3.15	3.20	3.54	3.19	0.14	0.30	0.56				
	W5037	62.1	17.7	0.43	2.07	0.89	6.32	5.47	0.05	0.88	0.60				
	W5038	63.0	16.9	0.24	1.78	2.44	3.72	5.68	0.04	0.53	0.50				

Table 8.7

A list of the geochemistry of samples from drill holes 16-023-26, -19, -21. As in Table 8.6 the samples are listed in the order in which they appear from the top of the hole to the bottom of the hole in the cross-sectional diagrams which follow.

DDH no.	Sample no.	Weight %										(ppm)			
		SiO_2	Al_2O_3	CaO	MgO	Na_2O	K_2O	FeO	MnO	TiO_2	P_2O_5	Cu	Pb	Zn	Ag
16-023-26	A7619	69.1	13.5	0.48	1.35	1.45	3.74	5.53	0.08	0.59	0.09	39	8	38	<1
	A7620	64.7	13.9	1.14	1.48	3.67	1.97	7.16	0.20	0.77	0.16	26	28	160	<1
	A7621	71.9	11.1	0.19	5.04	1.54	1.70	3.02	0.11	0.35	0.04	17	48	110	<1
	A7622	55.1	15.5	2.56	4.05	1.86	2.53	10.1	0.29	2.02	0.49	54	120	710	<1
	A7623	54.2	15.2	2.52	3.91	1.88	2.62	9.99	0.29	1.99	0.51	27	130	410	1
	A7624	66.5	14.6	0.28	1.95	1.35	3.22	5.78	0.10	0.70	0.07	130	40	110	<1
	A7625	55.4	13.0	1.20	6.70	3.08	0.92	11.4	0.32	1.72	0.54	26	80	400	<1
	A7626	65.3	15.3	0.56	1.66	1.87	3.06	5.94	0.04	0.76	0.14	1	20	59	<1
	W5077	76.9	10.7	0.43	0.93	2.43	2.82	3.58	0.50	0.31	0.11				
	W5078	71.8	10.9	0.23	1.37	1.71	1.96	7.60	0.12	0.36	0.11				
	W5080	67.3	11.8	1.08	1.97	3.35	0.47	4.43	0.12	0.61	0.16				
	W5081	75.1	10.8	0.12	4.53	3.51	0.96	2.06	0.09	0.16	0.69				
	W5082	48.6	12.7	4.22	6.24	3.97	0.38	13.40	0.35	2.78	0.79				
	W5085	73.1	10.8	0.21	2.36	2.42	1.95	6.76	0.18	0.20	0.70				
	W5086	49.1	11.8	8.36	7.52	2.98	0.22	12.04	0.50	2.84	1.03				
	W5087	35.2	4.1	17.55	20.30	0.51	0.23	1.48	0.55	0.17	0.48				
	W5088	65.7	17.0	0.16	1.64	1.94	3.95	5.47	0.03	0.80	0.32				
16-023-19	A7118	66.9	13.4	0.55	1.75	0.20	5.05	6.92	0.14	0.70	0.14	430	5	97	<1
	A7119	50.1	10.1	10.1	6.37	0.30	3.53	4.16	0.36	0.26	0.13	146	5600	16100	78
	A7120	58.1	20.4	0.49	2.00	1.38	4.90	6.07	0.06	1.05	0.10	45	10	72	<1
	A7121	65.4	16.0	0.73	2.07	1.75	3.92	4.86	0.08	0.69	0.11	33	18	120	1
	A7122	71.4	10.2	1.22	2.76	2.45	1.87	3.00	0.13	0.30	0.04	39	900	6000	<1
	A7123	65.5	15.7	1.44	1.58	1.57	3.57	5.39	0.07	0.79	0.11	34	10	110	<1
	W6219	73.0	12.7	0.37	1.20	2.67	3.04	5.07	0.10	0.40	0.01				
	W6220	49.8	26.3	0.11	1.49	0.17	9.52	6.52	0.06	0.37	0.01				

Table 8.7 continued.

DDH no.	Sample no.	Weight %										(ppm)			
		SiO_2	Al_2O_3	CaO	MgO	Na_2O	K_2O	FeO	MnO	TiO_2	P_2O_5	Cu	Pb	Zn	Ag
16-023-19	W6224	64.9	13.4	1.33	5.68	0.92	2.77	4.89	0.10	0.53	0.05				
	W6225	60.8	19.2	0.18	1.46	1.17	5.34	5.94	0.04	0.76	0.05				
	W6226	62.9	17.7	0.13	1.91	0.23	5.38	6.08	0.07	0.65	0.06				
	W6233	67.3	12.4	1.74	5.75	3.00	3.39	3.43	0.22	0.28	0.02				
	W6234	79.3	19.7	0.30	0.93	4.75	0.16	1.50	0.03	0.01	0.05				
	W6236	67.7	15.5	0.54	1.71	1.29	4.09	5.23	0.05	0.70	0.13				
16-023-21	A7107	66.2	15.6	0.42	1.55	0.96	4.04	6.12	0.09	0.69	0.08	7	<2	64	<1
	A7108	72.4	12.7	0.30	0.98	0.27	6.55	4.31	0.08	0.39	0.03	65	8	52	<1
	A7109	70.8	12.4	0.44	1.59	0.15	4.28	6.37	0.13	0.67	0.17	57	<2	150	<1
	A7110	68.2	12.3	0.54	2.00	0.15	4.90	8.02	0.15	0.80	0.27	76	4	91	<1
	A7111	39.5	11.1	3.73	16.2	0.30	1.51	8.72	0.39	0.45	0.17	160	190	650	2

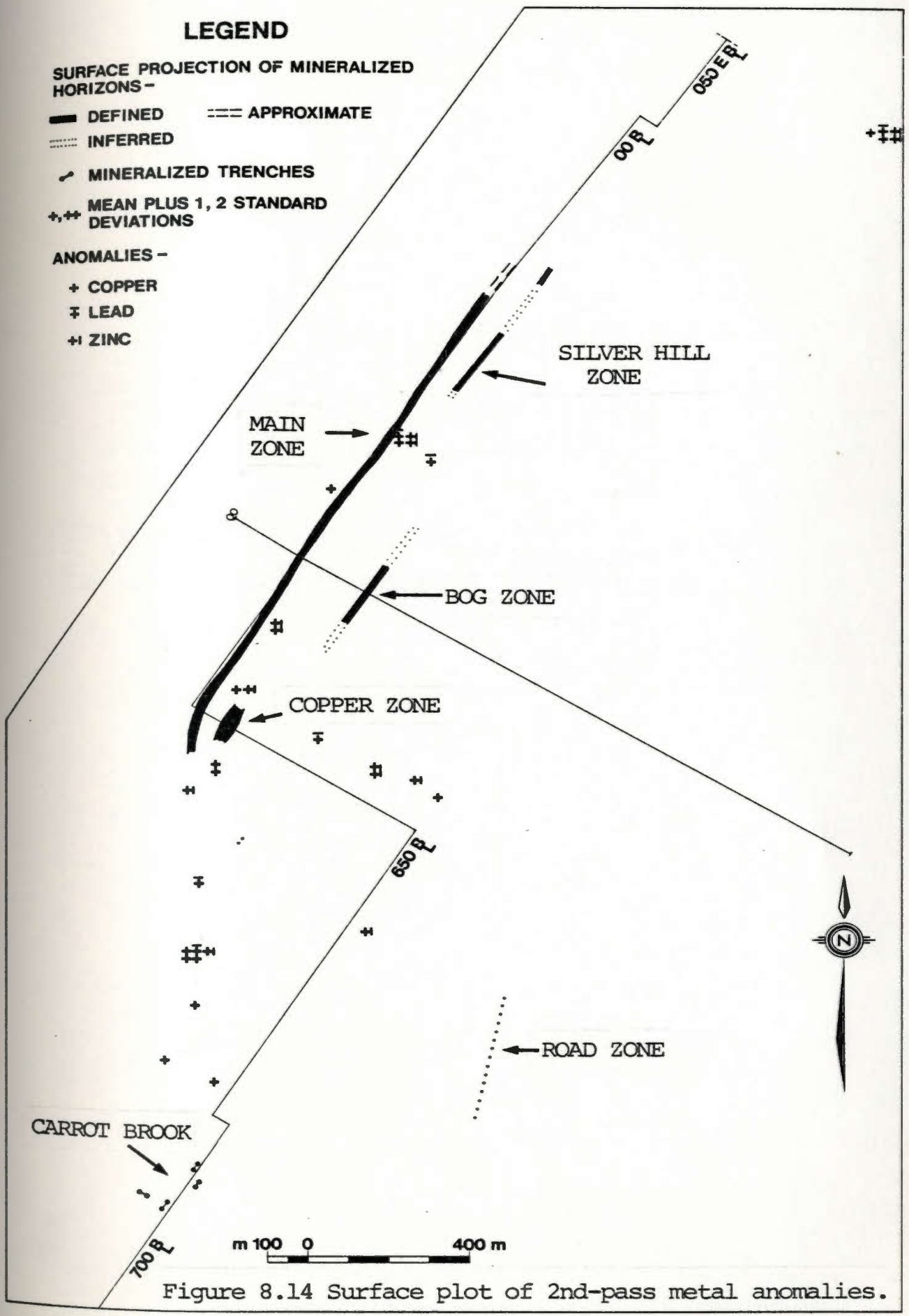

Figure 8.14 Surface plot of 2nd-pass metal anomalies.

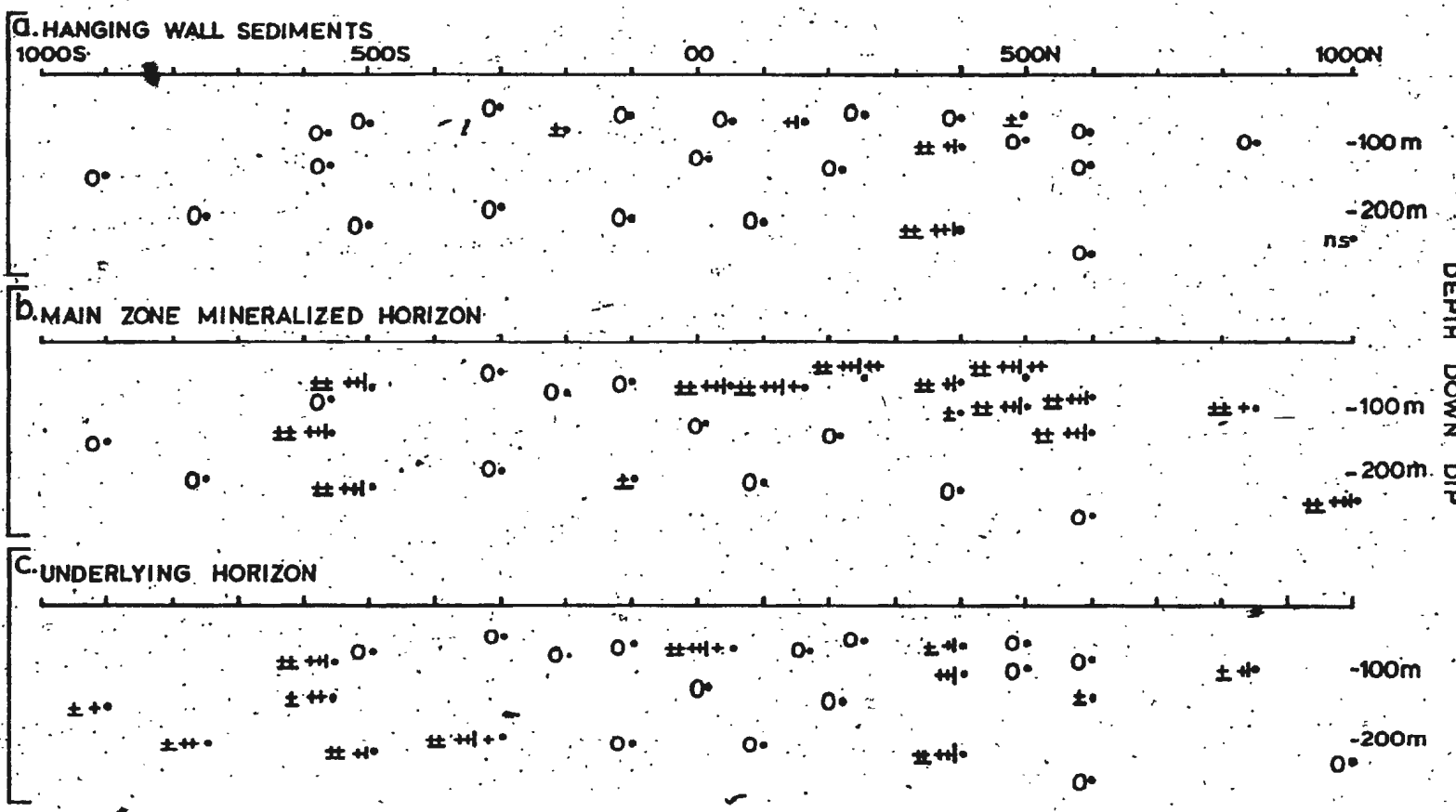

Copper + ++ ,Lead + ++ ,Zinc ± ±± ;No positive anomaly,O;no sample,ns. Scale 1:10,000
+ mean plus one standard deviation, ++mean plus two standard deviations.

Figure 8.15 Dip surface plots of 2nd pass metal anomalies in a) the hanging wall sediments, b) the Main Zone mineralized horizon and c) the underlying horizon (25 m stratigraphically below the mineralized horizon).

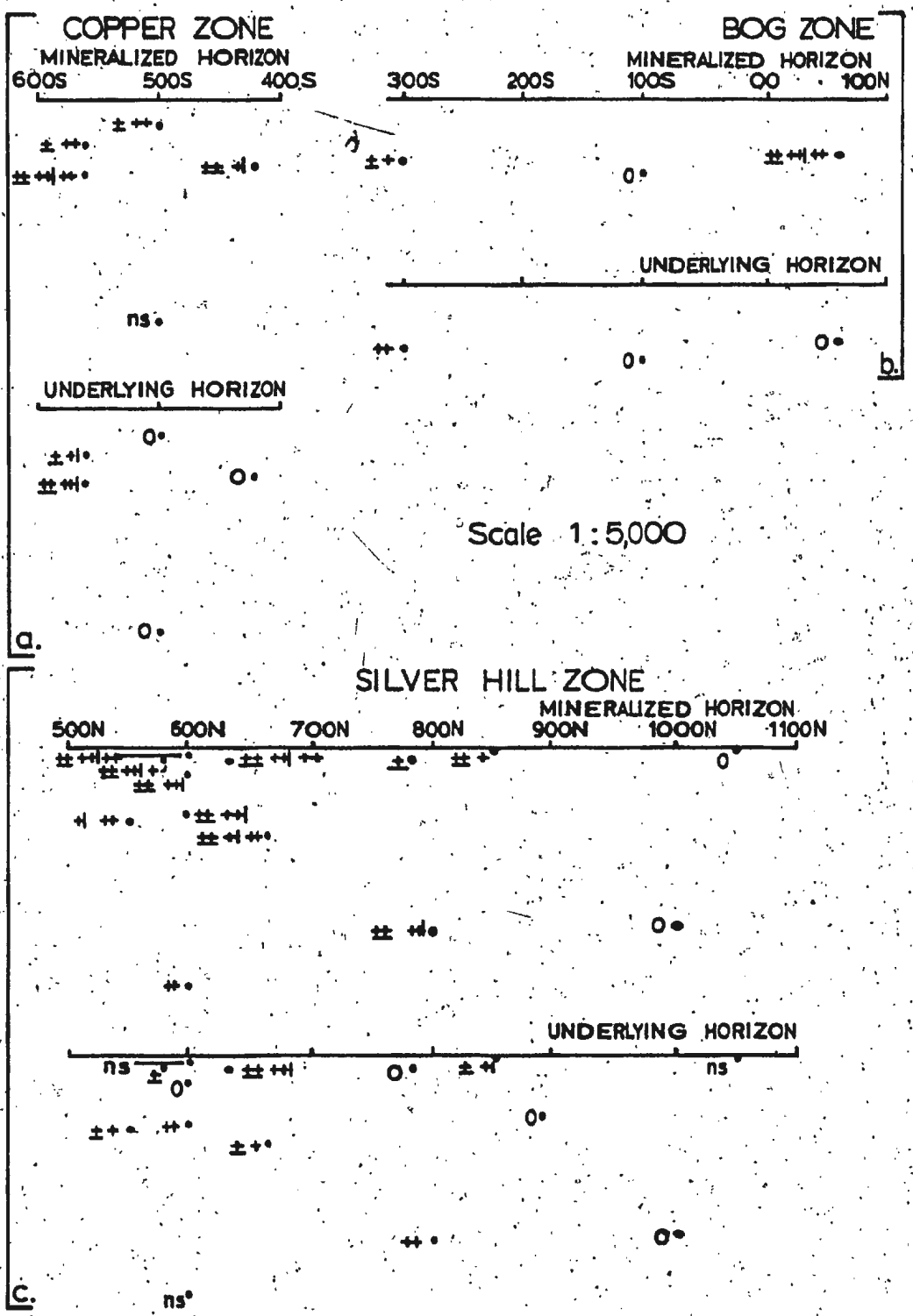

Figure 8.16. Dip surface plots of 2nd pass metal anomalies in the a) Copper, b) Bog and c) Silver Hill Zones and horizons 25m stratigraphically below these zones. See Figure 8.15 for a key to the symbols used.

mineralized and this is reflected in the spotty distribution of anomalies (Figure 8.14). The most significant observation of the dip surface plots is that while the richest mineralization occurs in the mineralized horizons it is not confined to these horizons. Weaker and more scattered mineralization occurs in the underlying horizons of all the ore zones and in the hanging wall sediments of the Main Zone. This is evident in the cross sections as well.

8.4.3 MgO

The distribution of second pass MgO anomalies on surface is patchy, with elongate clusters of anomalous samples trending parallel to the strike (Figure 8.17). A single group of five negative MgO anomalies on line 800S from 250E to 700E lies at right angles to the strike. Similar clusters at that location were not noted in the plots of the other oxide anomalies. The Main Zone, north extension is marked by a narrow cluster of samples trending parallel to the strike which are weak positive MgO anomalies. These are stratigraphically underlain by a cloud of weak negative MgO anomalies which extends south to the Bog Zone. Anomalous samples in the hangingwall sediments on surface are generally negative.

The drill hole cross sections (Figures 8.18 and 8.19) show a weak correlation between positive MgO anomalies and mineralization especially associated with the Main and Silver Hill Zones (diamond drill holes (D.D.H.) #16-023-1,

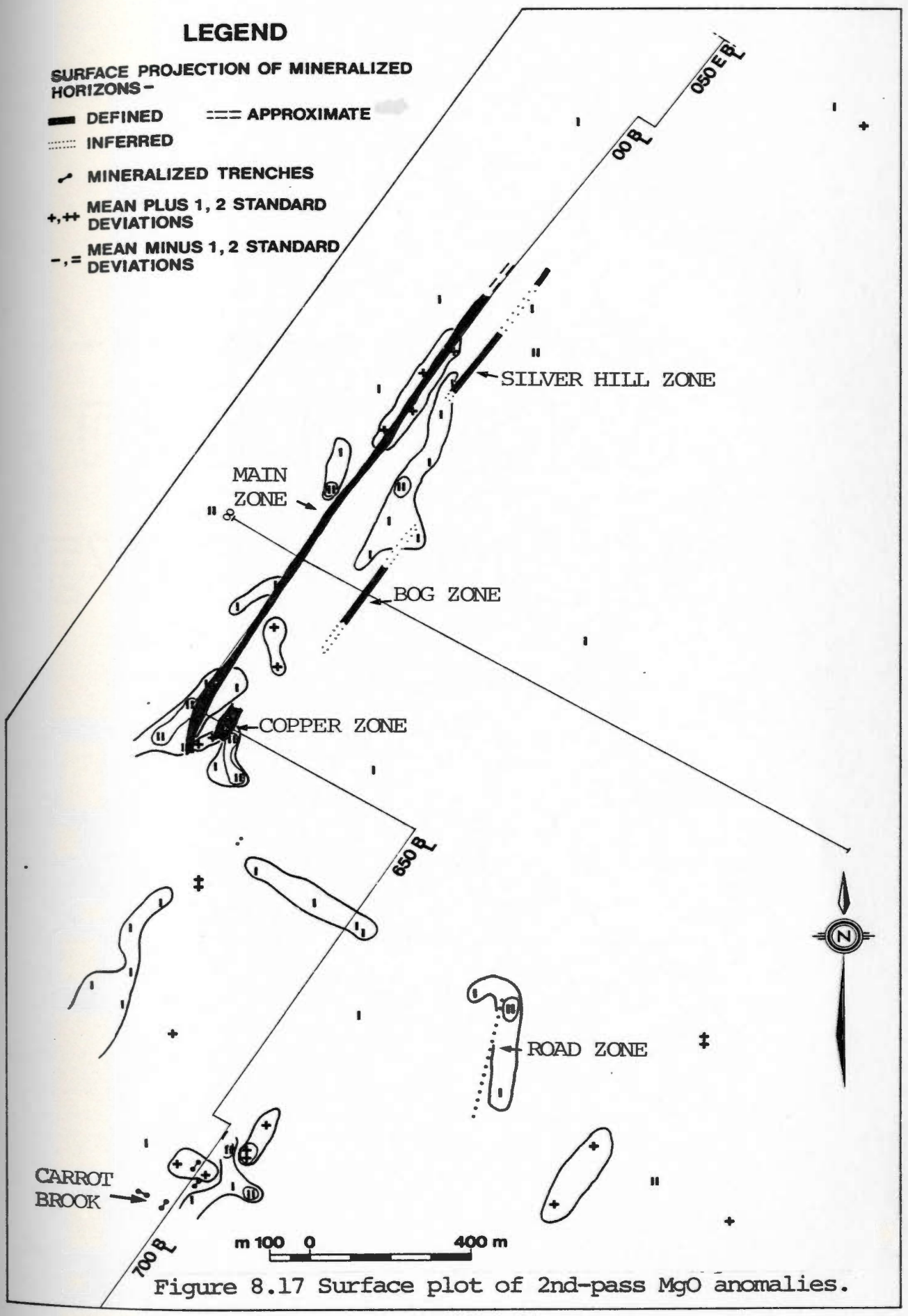

Figure 8.17 Surface plot of 2nd-pass MgO anomalies.

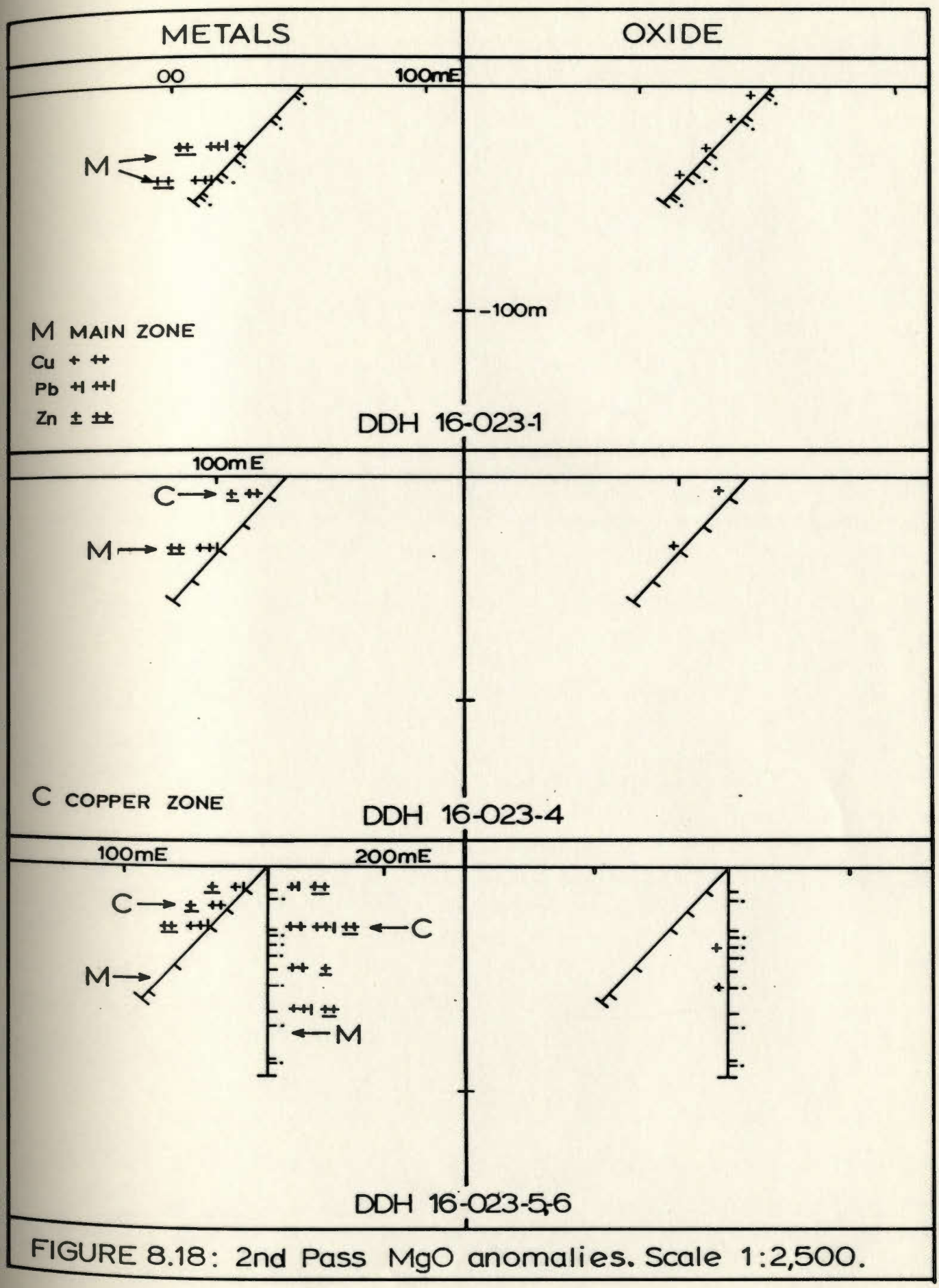

FIGURE 8.18: 2nd Pass MgO anomalies. Scale 1:2,500.

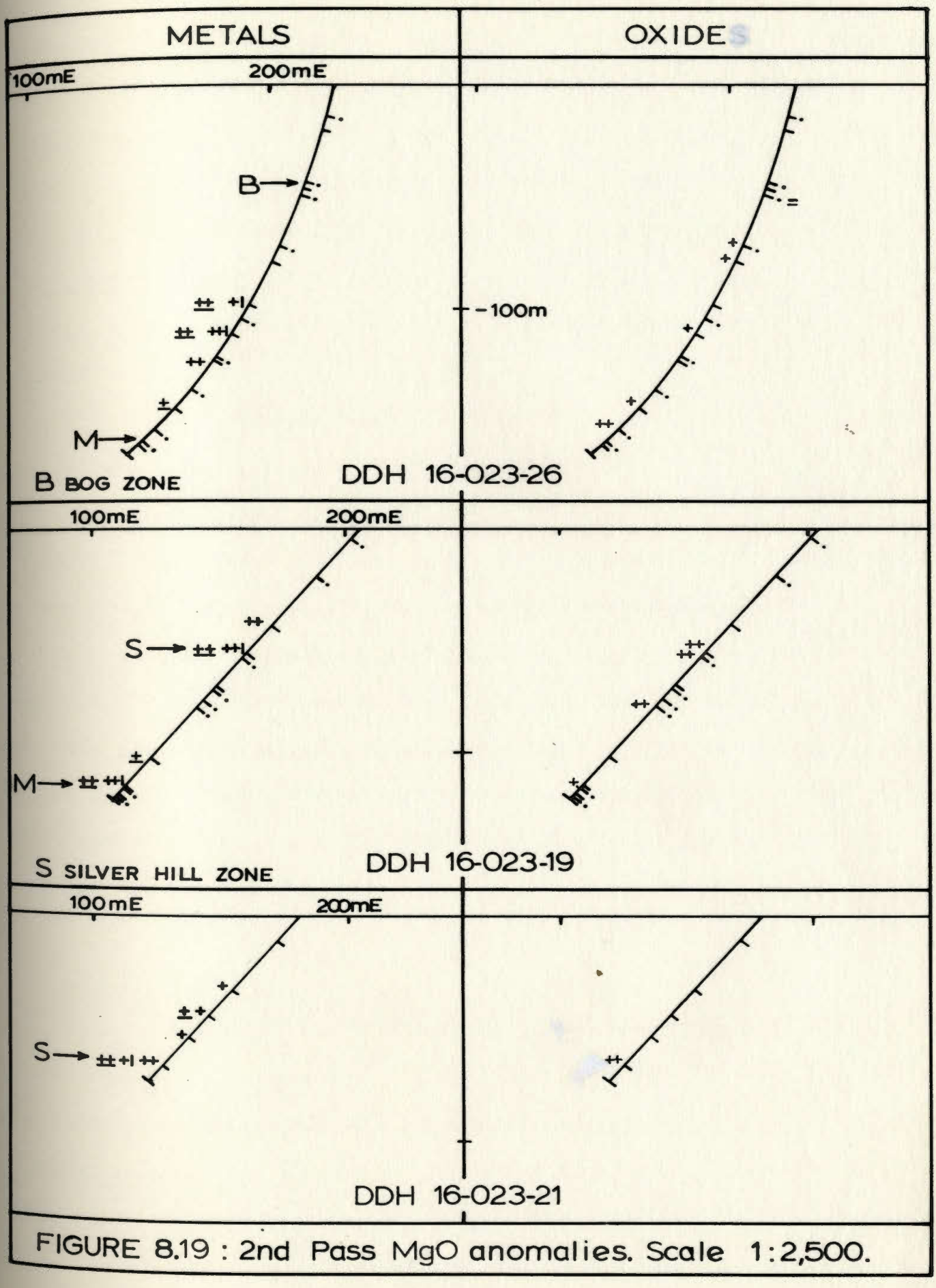

FIGURE 8.19 : 2nd Pass MgO anomalies. Scale 1:2,500.

16-023-14 and 16-023-19, 16-023-21 respectively). Weak to strong positive anomalies are clearly evident in the dip-surface plot of the Silver Hill Zone mineralized horizon (Figure 8.20a). These reflect the magnesium-rich chemistry of the carbonate-tremolite gangue of the Silver Hill Zone mineralization. This pattern does not extend into the horizon 25m stratigraphically below the Silver Hill Zone (Figure 8.20b).

The distribution of positive MgO anomalies in the Main Zone mineralized horizon is more irregular than in the Silver Hill Zone, as is the distribution of carbonate-tremolite gangue. More sporadic positive magnesium anomalies persist in the rock 25m below the Main Zone mineralization.

The mineralized horizon of the Copper Zone contains two weak positive MgO anomalies and the Bog Zone is a confused mix of anomalies (one positive, one negative) as well as a single normal (not anomalous) sample. Stratigraphically below the Copper Zone a single strongly negative MgO anomaly is present and below the Bog Zone there are none.

8.4.4 CaO

The surface distribution of the second pass CaO anomalies is in patchy, two- to four-sample clusters which are elongate parallel to the strike (Figure 8.21). A cluster of four weakly to strongly negative CaO anomalies lies between 100S and 100N within and just stratigraphically below the Main Zone horizon. The Copper Zone is marked by a 3-sample

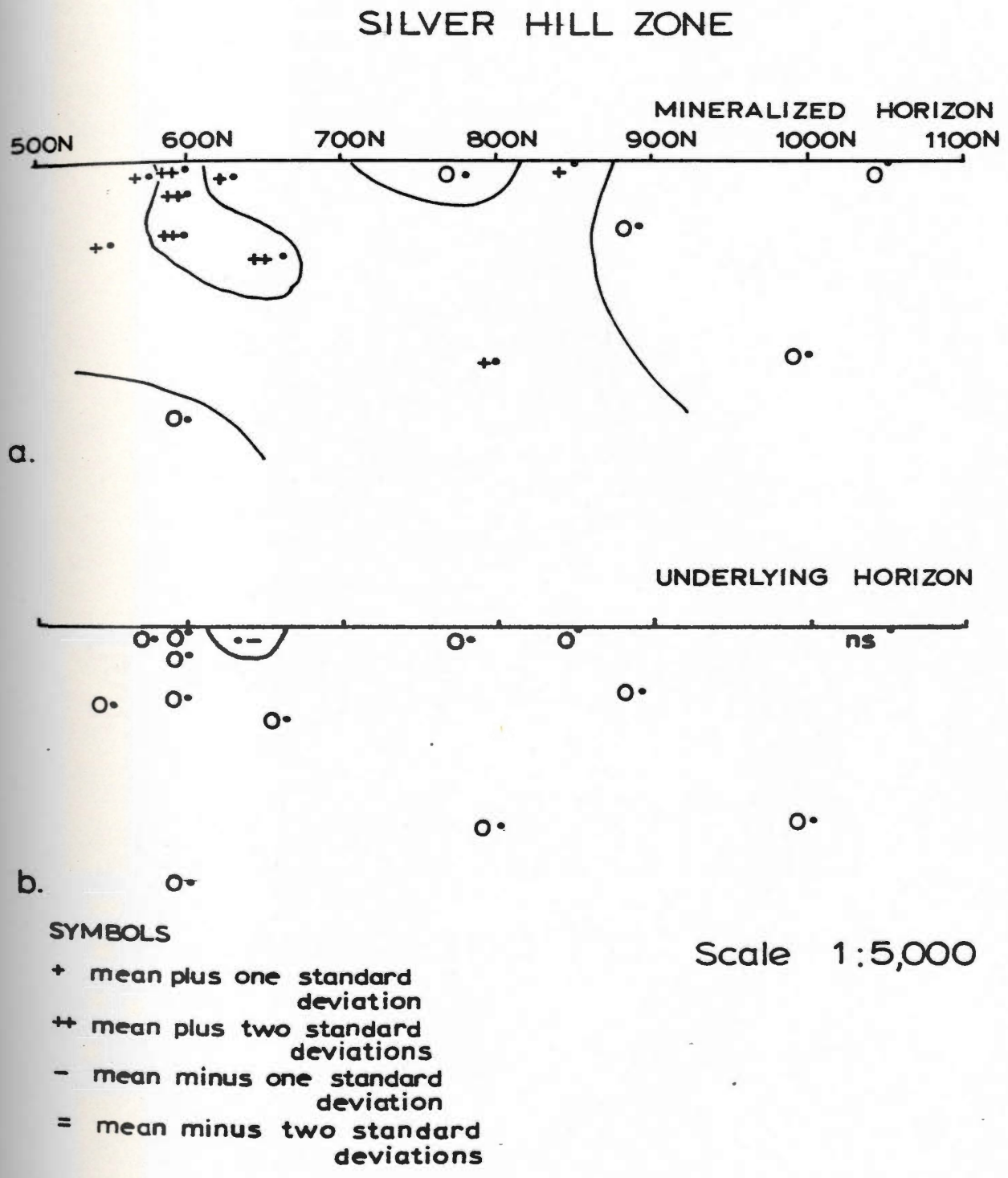

Figure 8.20. A dip surface plot of 2nd pass MgO anomalies in the Silver Hill Zone a)mineralized horizon and b) underlying horizon.

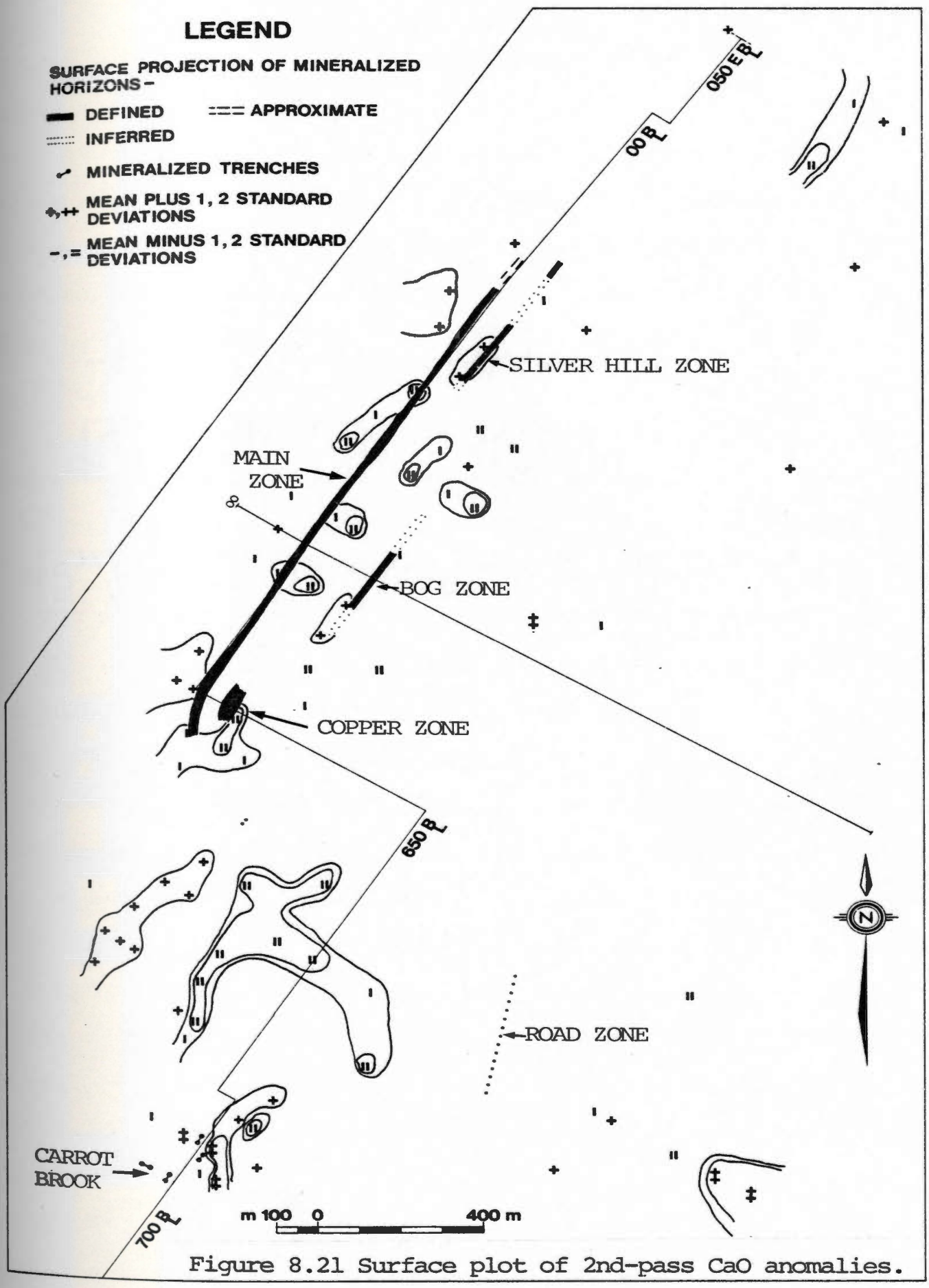

Figure 8.21 Surface plot of 2nd-pass CaO anomalies.

cluster of negative CaO anomalies. The most significant concentration of negative CaO anomalies in the Strickland area lies 300m to the southeast of the Copper Zone (see Figure 8.21). The cluster includes ten samples (sandstone, felsic tuffs and flows) and is both conformable to and cross-cuts the regional strike. Any anomalous samples in the hangingwall sediments are positive anomalies.

In the drill sections (Figures 8.22 and 8.23) positive CaO anomalies are often but not invariably associated with mineralization. Negative anomalies associated with mineralization in the Copper Zone mafic tuffs represent samples with low CaO values relative to high TiO_2 contents (Figure 8.22, DDH #16-023-6, Sample #A7183; 2.37 wt% CaO with 2.5 wt% TiO_2). The dip surface plots of the Main Zone show a scattered combination of positive and negative CaO anomalies. Five of the seven anomalies are positive and the two strongest positive anomalies are samples with carbonate-tremolite gangue associated with mineralization. The significance of the two negative anomalies is unknown. Isolated positive anomalies also occur in the horizon underlying the Main Zone. The mineralized horizon of the Silver Hill Zone is characterized by strong positive CaO anomalies (Figure 8.24) which correspond to the positive MgO anomalies. Not every MgO anomaly is matched by a CaO anomaly. This pattern is a reflection of the carbonate-tremolite gangue of the Silver Hill Zone mineralization. In the underlying horizon of the Silver Hill

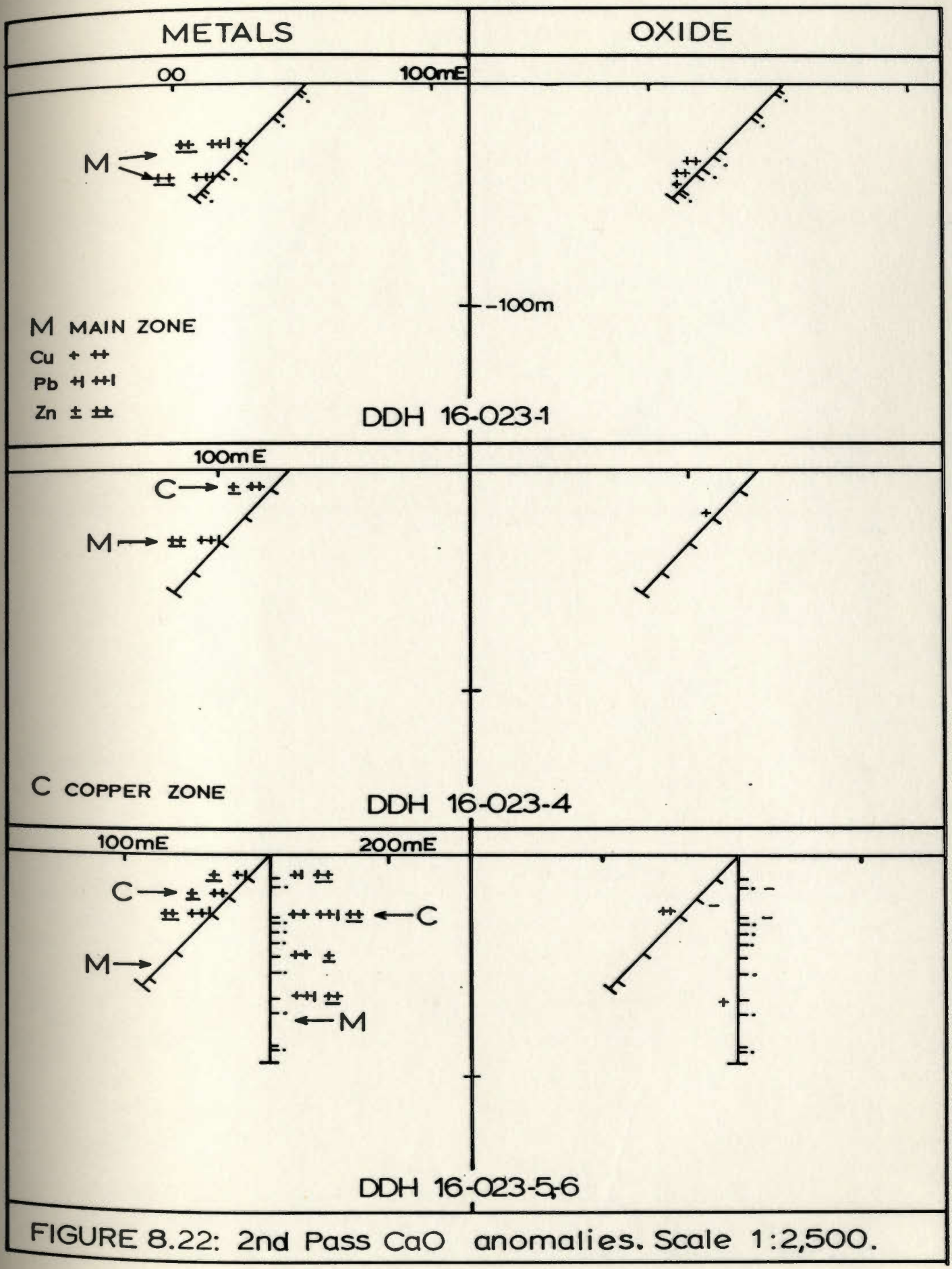

FIGURE 8.22: 2nd Pass CaO anomalies. Scale 1:2,500.

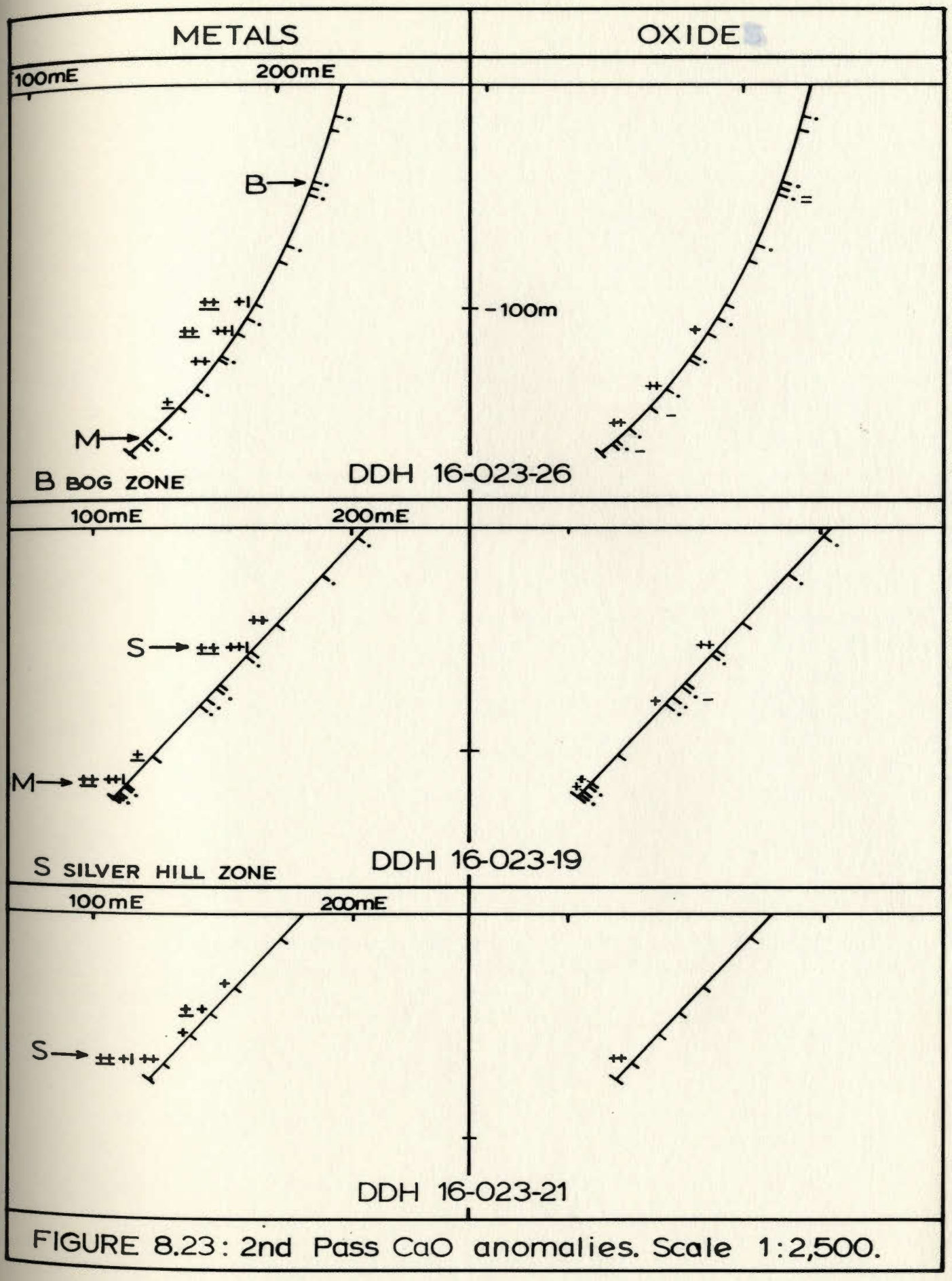

FIGURE 8.23: 2nd Pass CaO anomalies. Scale 1:2,500.

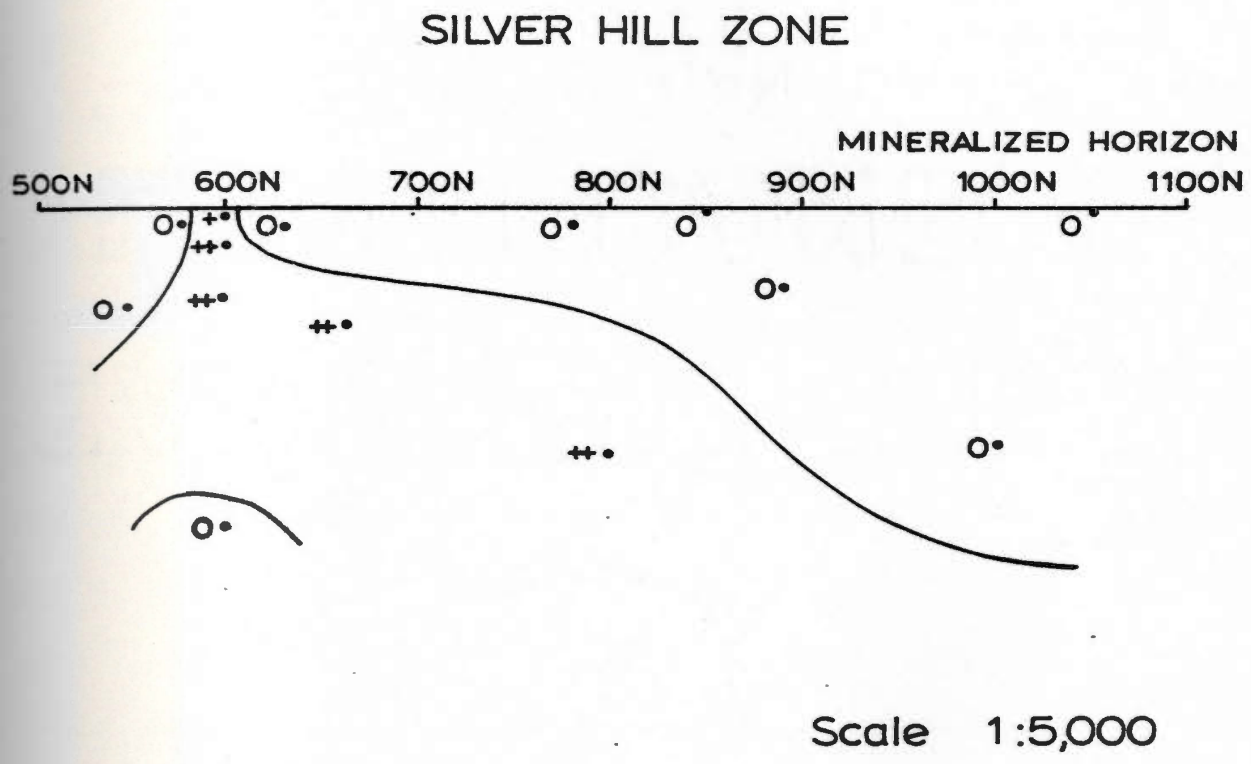

Figure 8.24. A dip surface plot of the 2nd pass CaO anomalies in the Silver Hill Zone mineralized horizon. See Figure 8.20 for a key to the symbols used.

Zone two samples are weakly anomalous ; one positively,the other negatively.

8.4.5 Na_2O

As with CaO and MgO, scattered clusters of conformably elongate anomalies characterize the surface distribution of the second pass Na_2O anomalies (Figure 8.25). The majority of the anomalies on surface are positive anomalies. Silver Hill is marked by a cluster of weak negative Na_2O anomalies which extends to the southwest towards the Bog Zone. A significant cluster of eight weak to strongly negative Na_2O anomalies lies to the southeast of the Copper Zone. This cluster cross-cuts the regional strike and is roughly coincident with a similarly shaped cluster of negative CaO anomalies described earlier (see Figure 8.25, compare with Figure 8.21).

An arc of weak and strong positive anomalies lies below the Main Zone and above and within the Bog Zone. A broad area in the center of the property contains samples with weak to strong Na_2O anomalies. The Carrot Brook area is marked by an eight sample cluster of positive Na_2O anomalies. The anomalies in the hangingwall sediments are generally positive. Rocks on the north flank of Baggs Hill, including only one granite sample, are identified as positive Na_2O anomalies.

Examination of the drill hole cross-sections (Figures 8.26 and 8.27) indicates the common association of negative

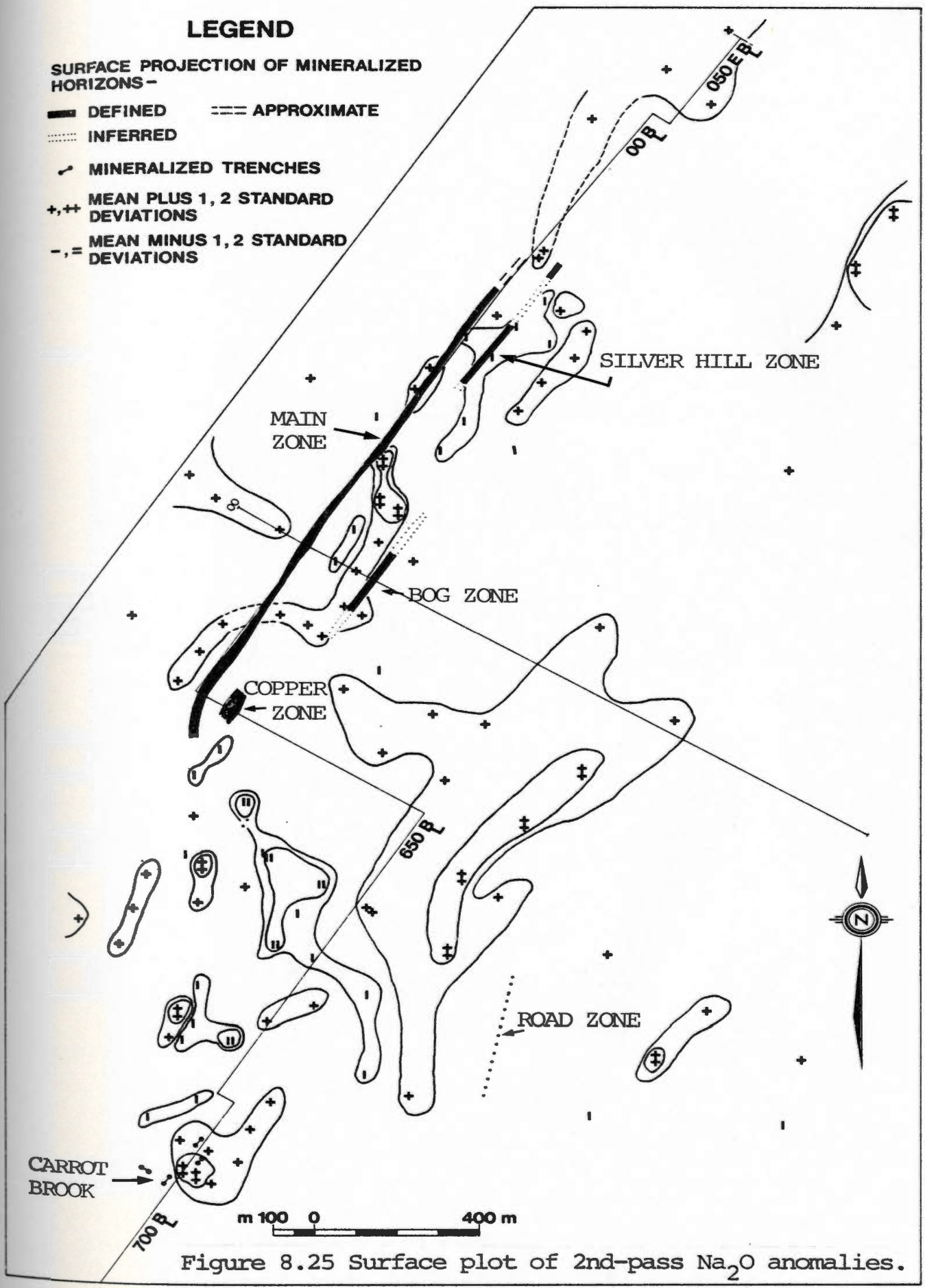

Figure 8.25 Surface plot of 2nd-pass Na_2O anomalies.

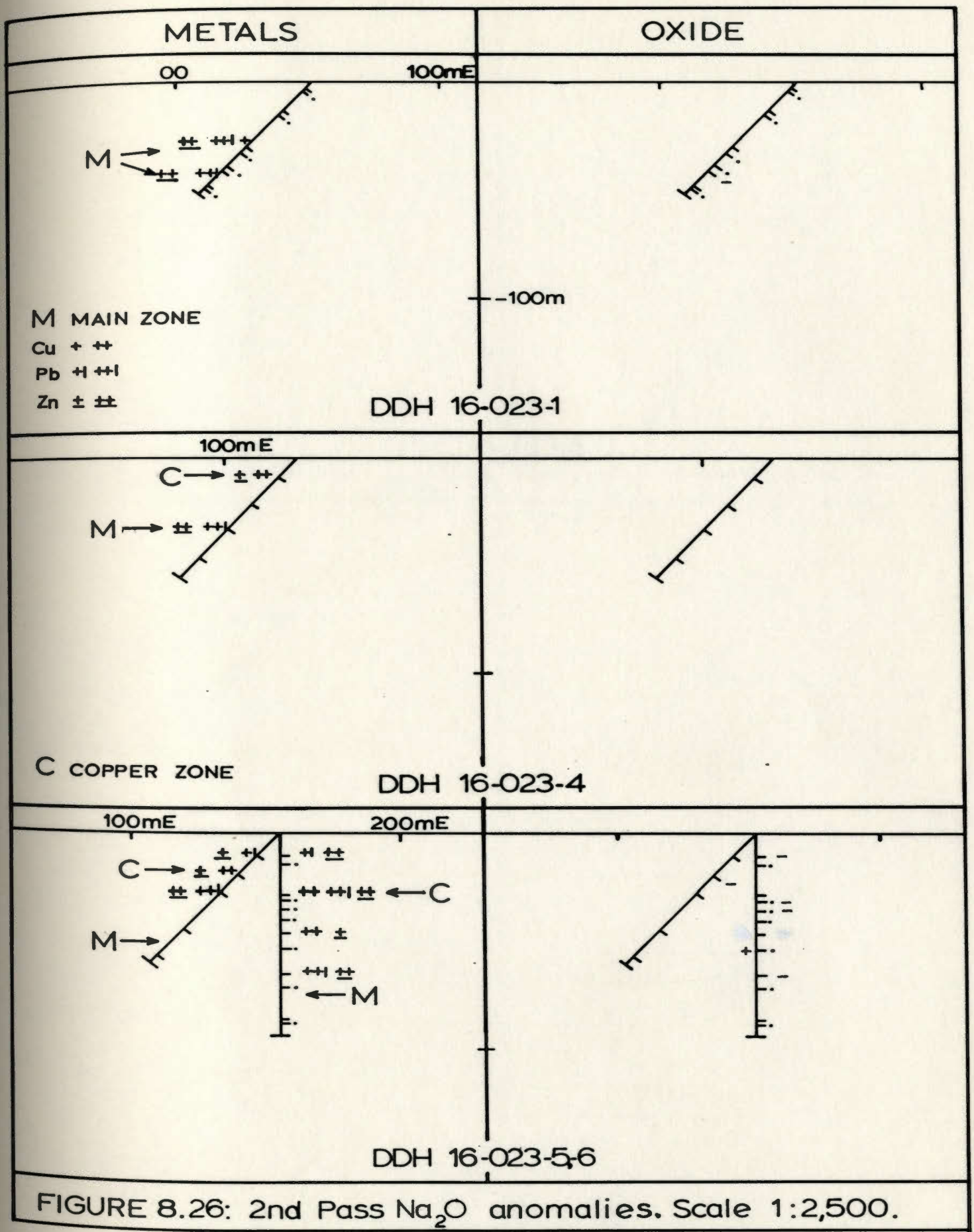

FIGURE 8.26: 2nd Pass Na_2O anomalies. Scale 1:2,500.

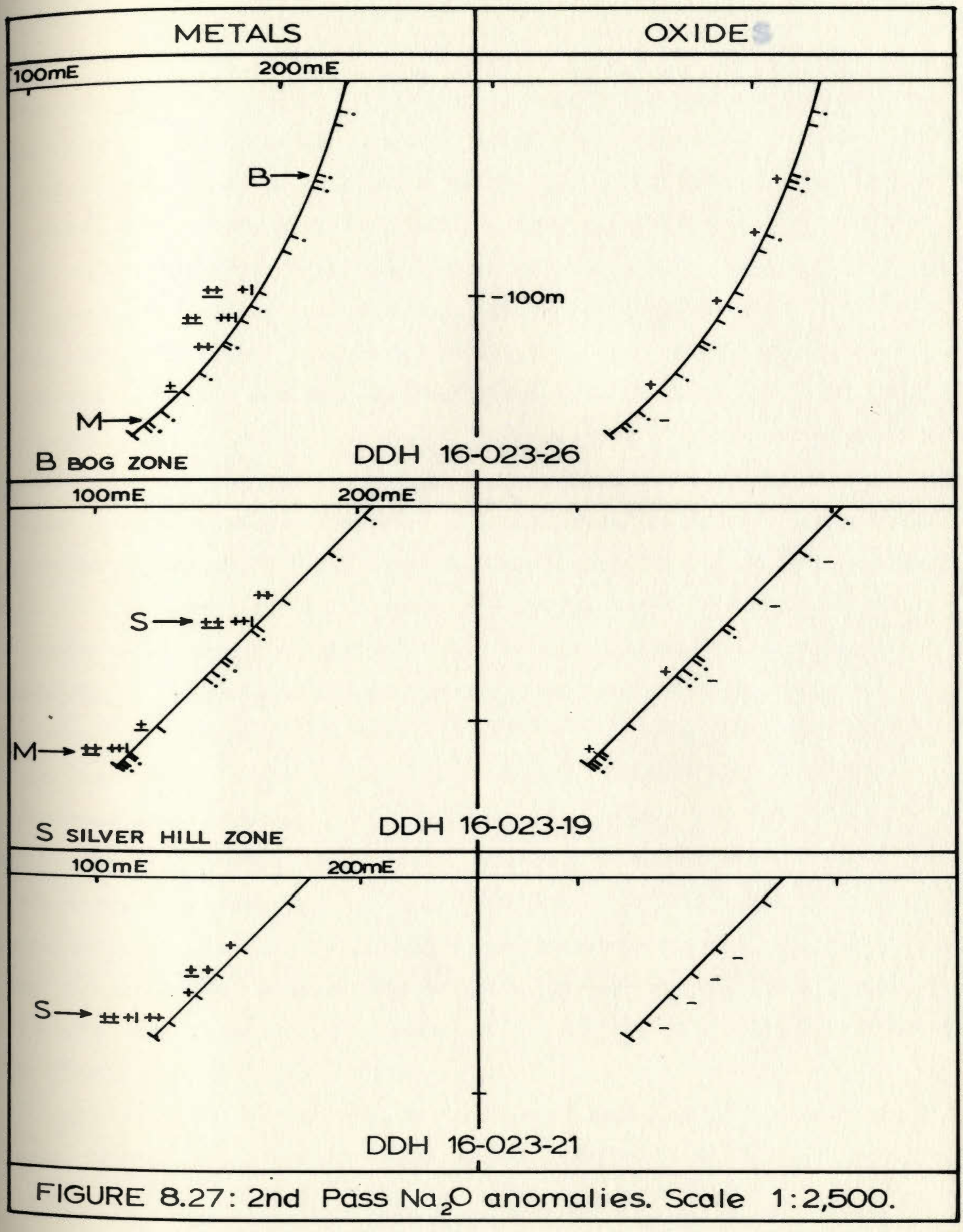

FIGURE 8.27: 2nd Pass Na_2O anomalies. Scale 1:2,500.

second pass Na_2O anomalies with mineralization. (Note that 60% of the anomalous samples in the drill holes are negative anomalies). However, not all the negative Na_2O anomalies are mineralized samples and at least one mineralized sample is marked by a positive Na_2O anomaly (Figure 8.27, DDH #16-023-26). The association of negative Na_2O anomalies with mineralization is again evident in the dip surface plots of the mineralized horizons. The Main Zone mineralized horizon contains a discrete knot of negative Na_2O anomalies (Figure 8.28b). This tight cluster does not persist stratigraphically below the mineralized horizon (Figure 8.28c). Negative Na_2O anomalies are also present in the Silver Hill mineralized horizon (Figure 8.29c) these Na_2O anomalies (and at least two in the main zone) again reflecting the chemistry of the carbonate-tremolite gangue in which no sodic minerals are present. Negative Na_2O anomalies are ubiquitous in the underlying horizon of the Silver Hill Zone (Figure 8.29c). Thin sections show that the rocks from this horizon are intermediate tuffs and siltstones with 20-30% secondary sericite and brown biotite. Broken and augened quartz and K-feldspar phenocrysts are common in the tuffs whereas plagioclase phenocrysts were not observed. It appears that the primary low sodium chemistry of these rocks was further reduced by subsequent potassic alteration which produced sericite and biotite.

In the Copper Zone mineralized section two samples show weak negative Na_2O anomalies which do not persist

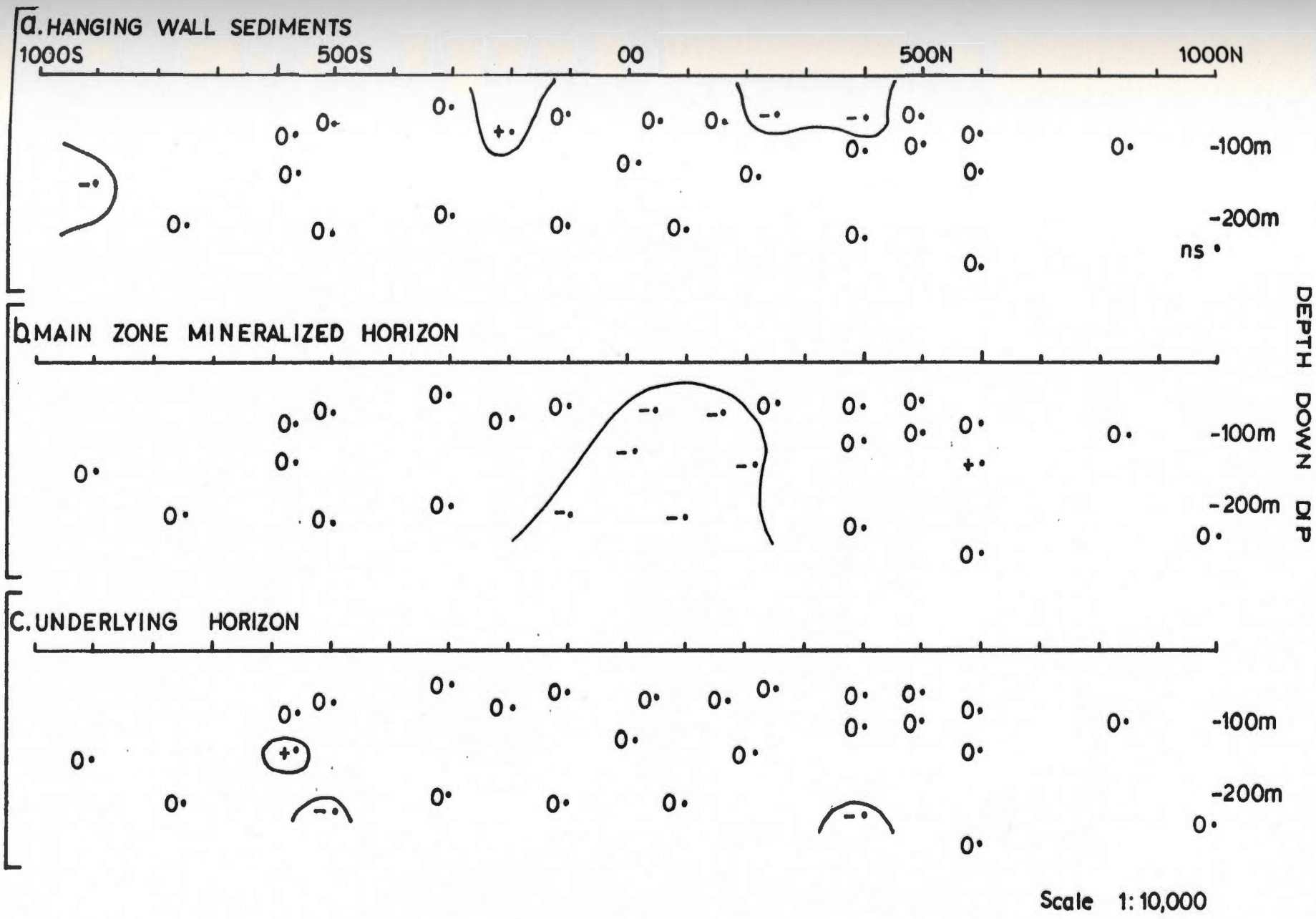

Figure 8.28 A dip surface plot of 2nd pass Na_2O anomalies in A) the hanging wall sediments, b) Main Zone mineralized horizon and c) underlying horizon. See Figure 8.20 for a key to the symbols used.

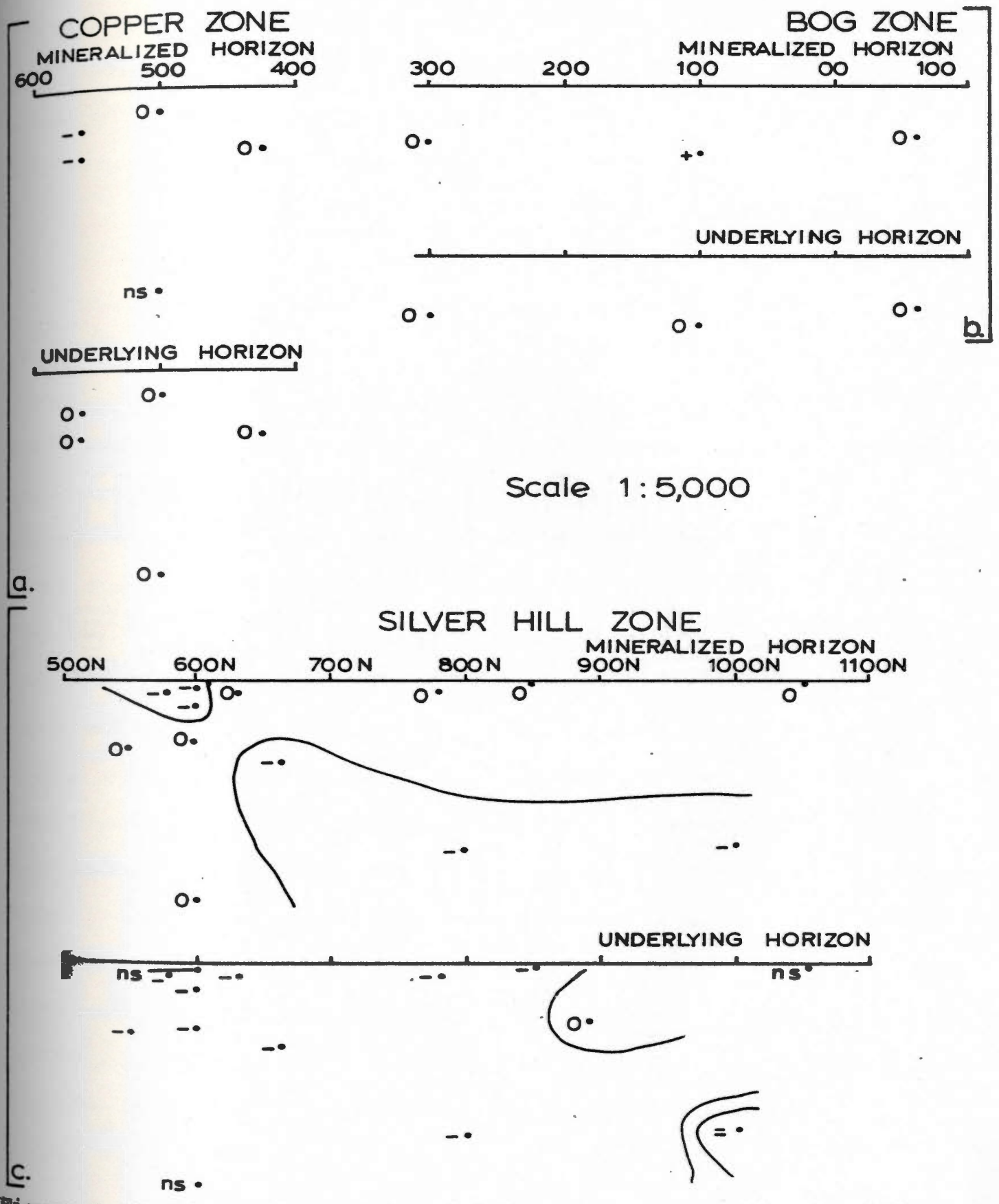

Figure 8.29. Dip surface plots of 2nd pass Na_2O anomalies in a) the Copper , b) Bog and c) Silver Hill Zones and underlying horizons. See Figure 8.20 for a key to the symbols used.

stratigraphically below (Figures 8.29a). One bog sample in the mineralized horizon is marked by a weak positive Na_2O anomaly. There are no Na_2O anomalies in the underlying horizon of the Bog Zone (Figures 8.29b).

8.4.6 K_2O

The surface plot of K_2O anomalies shows a string of unconnected clusters of negative K_2O anomalies stratigraphically below the Main Zone and through the Bog Zone (Figure 8.30). These correlate loosely with a band of positive Na_2O anomalies. A narrow and elongate band of seven positive K_2O anomalies extend over a distance of 700m from immediately southeast of Silver Hill to east of the Bog Zone. These correspond to positive K_2O anomalies present 25m stratigraphically below the Silver Hill Zone (dip surface plot Figure 8.33) and identified previously as rocks with abundant secondary biotite and sericite. The hangingwall sediments on surface are marked by negative K_2O anomalies as are the rocks on the east flank of Baggs Hill. There is a spindly Y-shaped cluster of positive K_2O anomalies east of the Copper Zone on the plan map which is repeated in the cross section plot of DDH #16-023-6 (Figure 8.31). There is no cluster of K_2O anomalies corresponding to the previously described Na_2O and CaO anomaly clusters along line 900S, southeast of the Copper Zone.

A loose negative correlation between Na_2O and K_2O anomalies is evident from the surface plots and in the drill

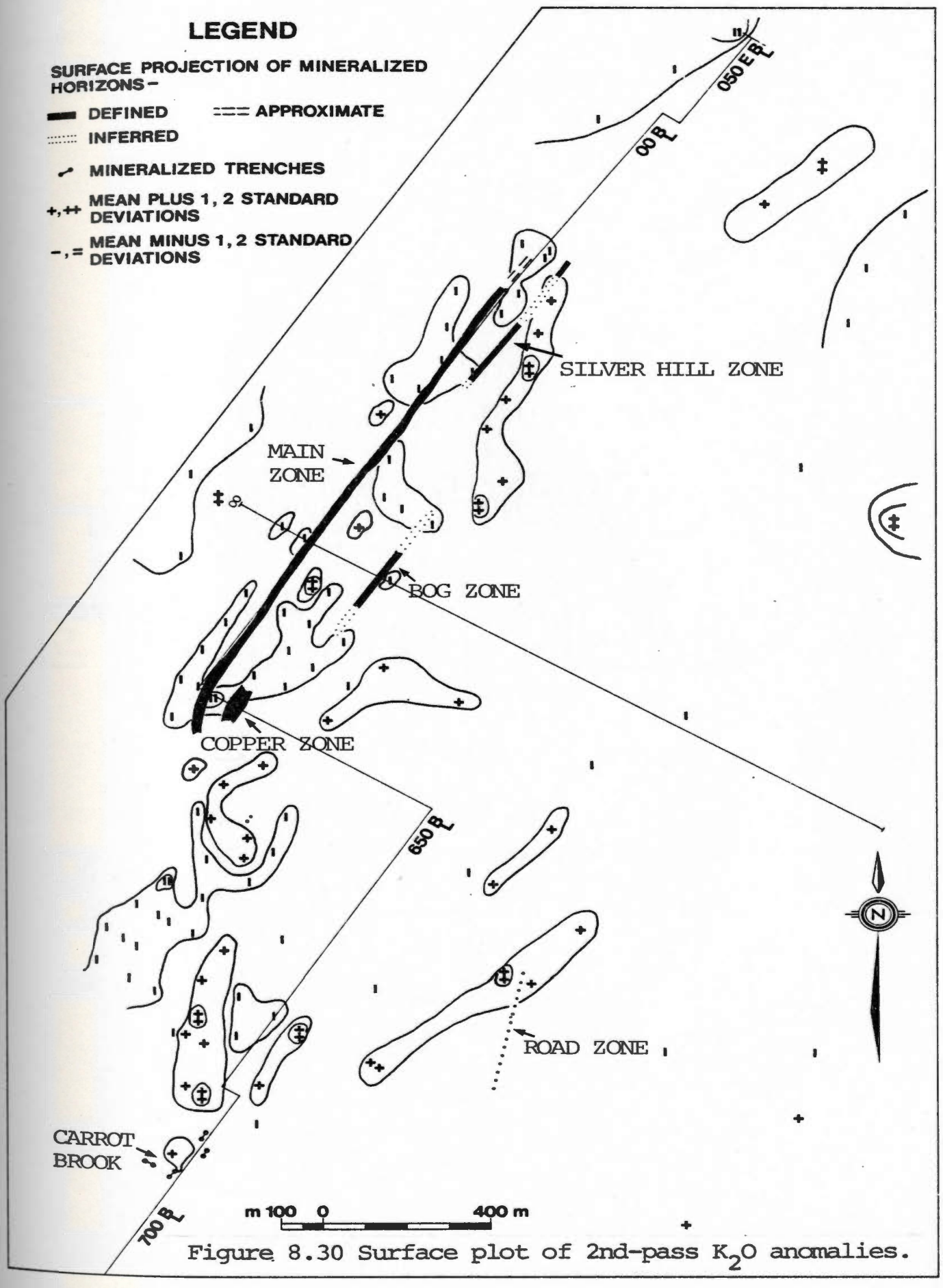

Figure 8.30 Surface plot of 2nd-pass K_2O anomalies.

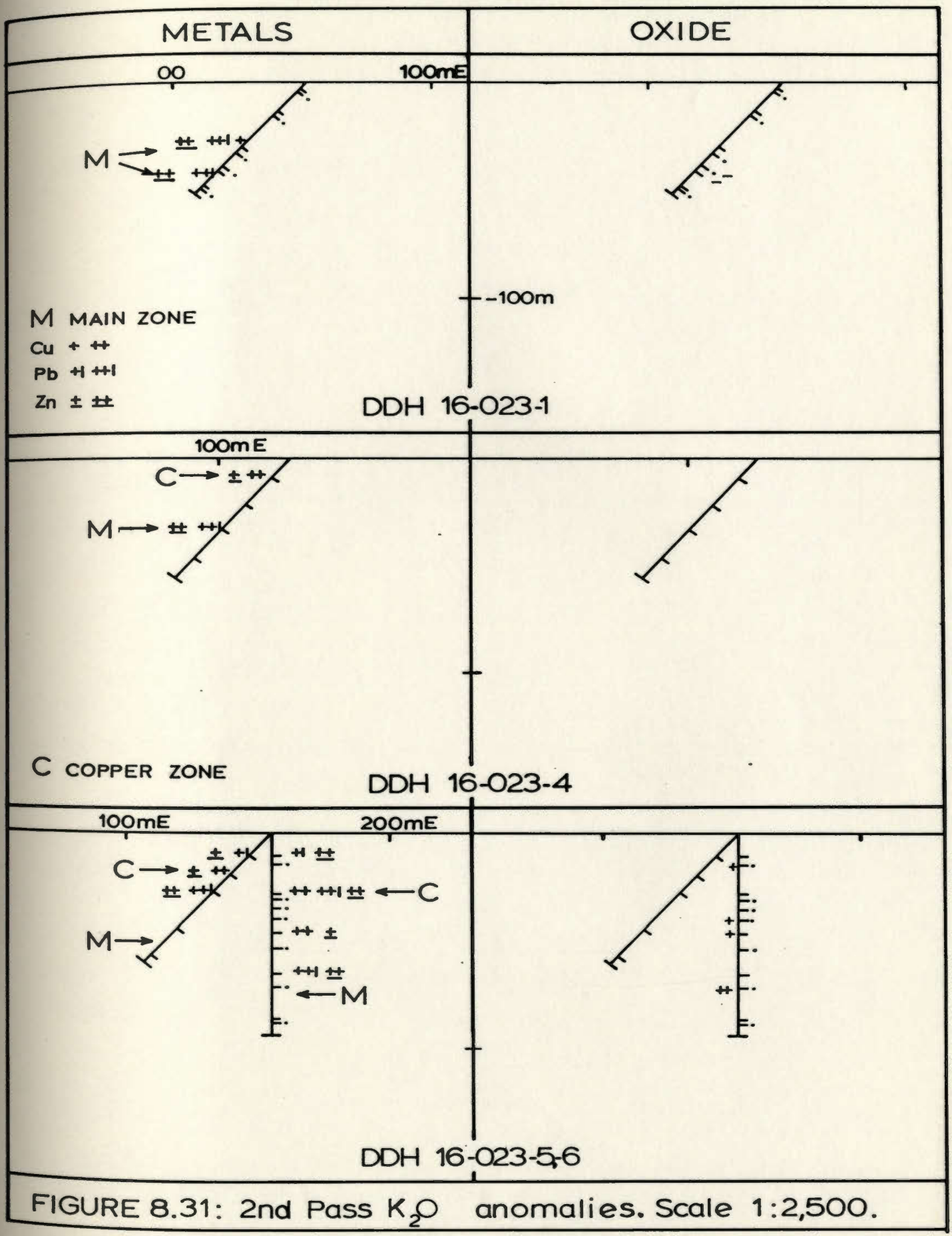

FIGURE 8.31: 2nd Pass K_2O anomalies. Scale 1:2,500.

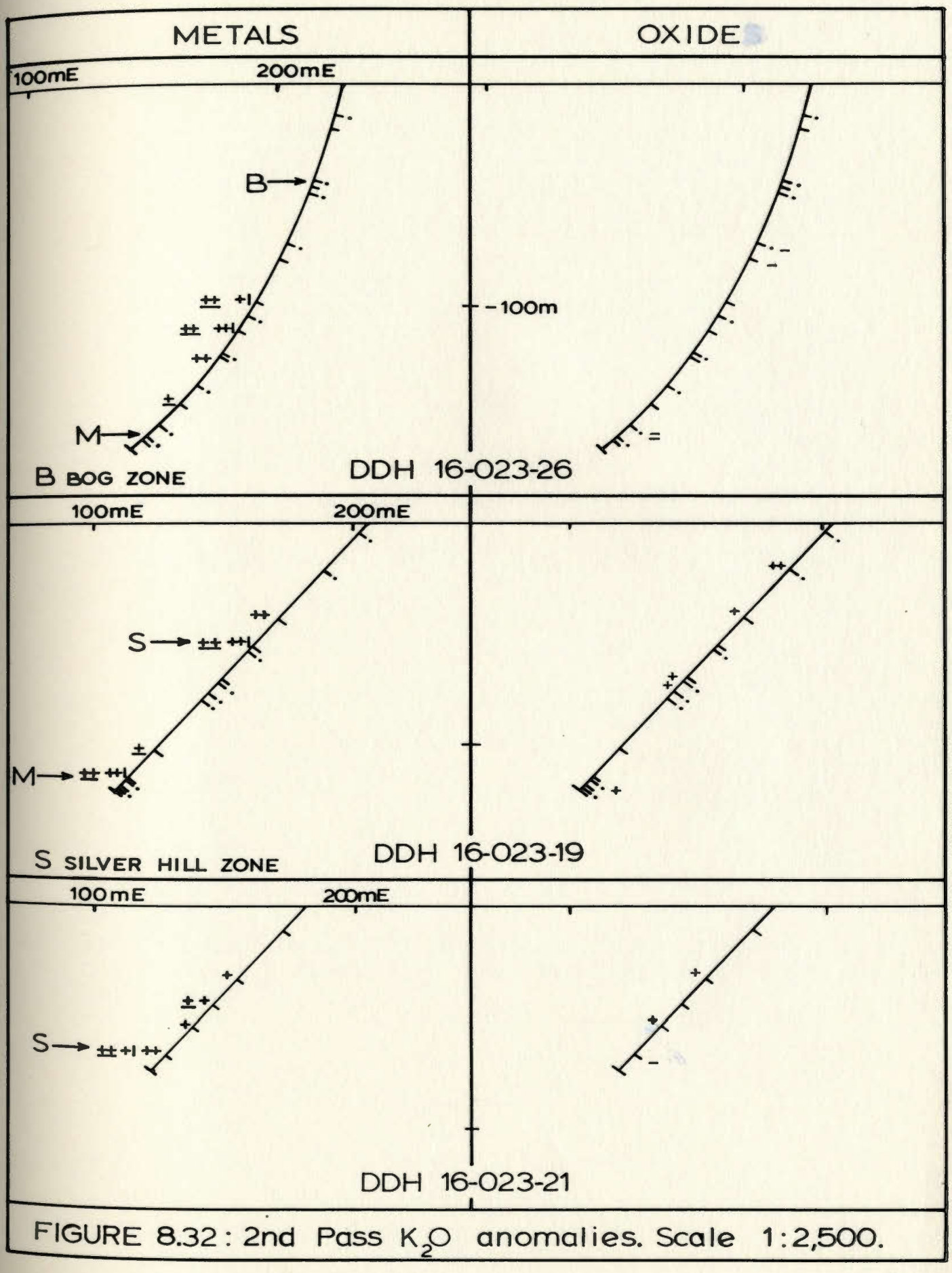

FIGURE 8.32 : 2nd Pass K_2O anomalies. Scale 1:2,500.

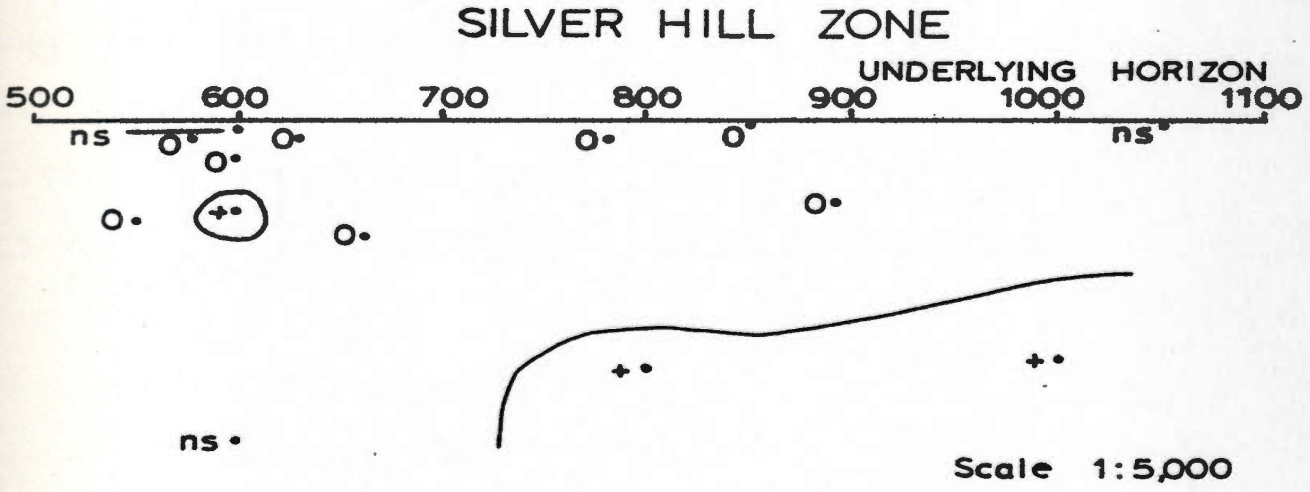

Figure 8.33. Dip surface plot of the 2nd pass K_2O anomalies in the horizon underlying the Silver Hill Zone. See Figure 8.20 for a key to the symbols used.

sections (compare Figure 8.27 and 8.32, DDH # 16-023-19) except where mineralized samples with carbonate-tremolite gangue are present. These samples show negative anomalies for both Na_2O and K_2O (Figures 8.26 and 8.31 DDH #16-023-1 and Figures 8.27 and 8.32 DDH #16-023-21). Besides these carbonate-tremolite mineralized samples there is a weak association of positive K_2O anomalies with mineralization (Figures 8.31 and 8.32).

The K_2O anomalies on the dip surface plots of the mineralized horizons are scattered.

There are three samples besides the two carbonate-tremolite samples which have negative K_2O anomalies in the Main Zone mineralized horizon (Figure 8.34). These correspond to positive Na_2O anomalies and lie in the Main Zone north extension. There are two clusters (one and two samples each) of positive anomalies which lie near 00N and in the south extension of the Main Zone mineralized horizon. The Copper Zone dip surface plot shows no K_2O anomalies in the mineralized zone and the Bog Zone contains a single negative anomaly. A single negative K_2O anomaly (a carbonate-tremolite sample) and a single positive anomaly is present in the Silver Hill mineralized horizon. A thin section from close to the positive anomaly sample shows pyrrhotite flakes surrounded by biotite haloes and small porphyroblasts(?) of orthoclase in a matrix of sericite-rich siltstone.

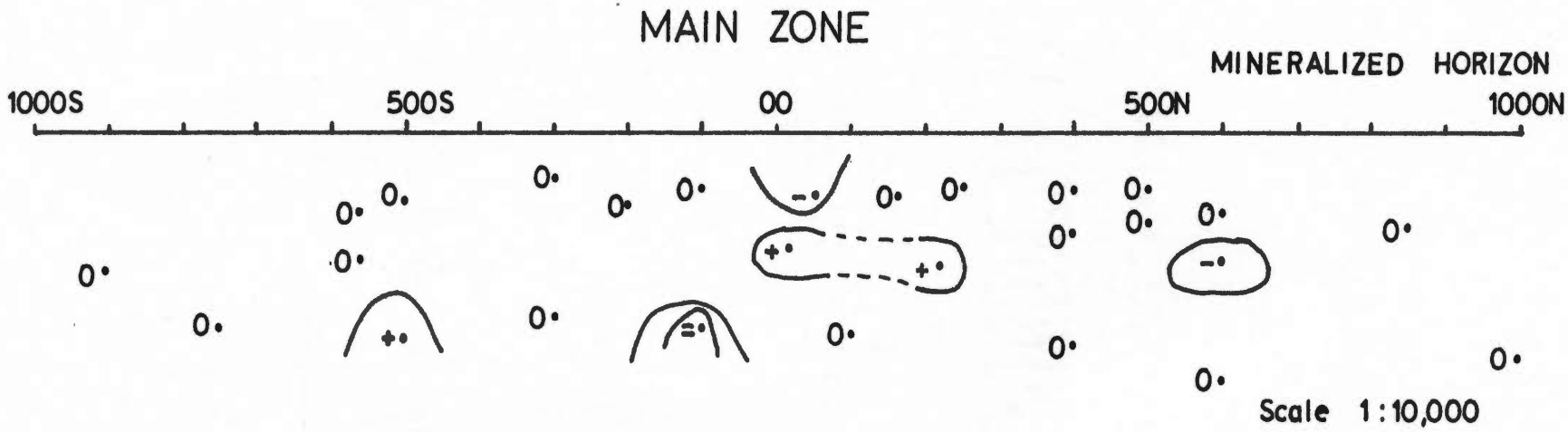

Figure 8.34 A dip surface plot of 2nd pass K_2O anomalies in the Main Zone mineralized horizon. See Figure 8.20 for a key to the symbols used.

8.4.7 FeO

On surface the Bog Zone is marked by two narrow clusters of positive FeO anomalies, one of which extends to the northeast, stratigraphically below the Silver Hill Zone (Figure 8.35). Anomalies in the hangingwall sediments are predominantly negative. In the drill hole cross sections (Figures 8.36 and 8.37) those FeO anomalies corresponding to mineralization are positive. This is especially evident in the dip surface plots of the mineralized horizons of the Copper and Silver Hill Zones (Figures 8.38 and 8.39). In the Copper Zone the analyses are very iron-rich even for such mafic rocks (15.2% FeO with 2.50% TiO_2). In the Silver Hill mineralized horizon the iron probably occurs in solid-solution with magnesium in the tremolite. The Main Zone mineralized interval contains weak negative FeO anomalies (4.47% FeO with 1.11% TiO_2) which are not considered significant. A single positive anomaly is present in the mineralized horizon of the Bog Zone and the horizon 25m stratigraphically below. Iron-rich chlorites were found associated with the Bog Zone mineralization (Section 5.1.1, page 94).

8.4.8 Al_2O_3

The single most interesting area of Al_2O_3 anomalies on the surface plot extends southeast from the Copper Zone and consists of two clusters (three and eight samples each) of strongly negative anomalies (Figure 8.40). These correspond

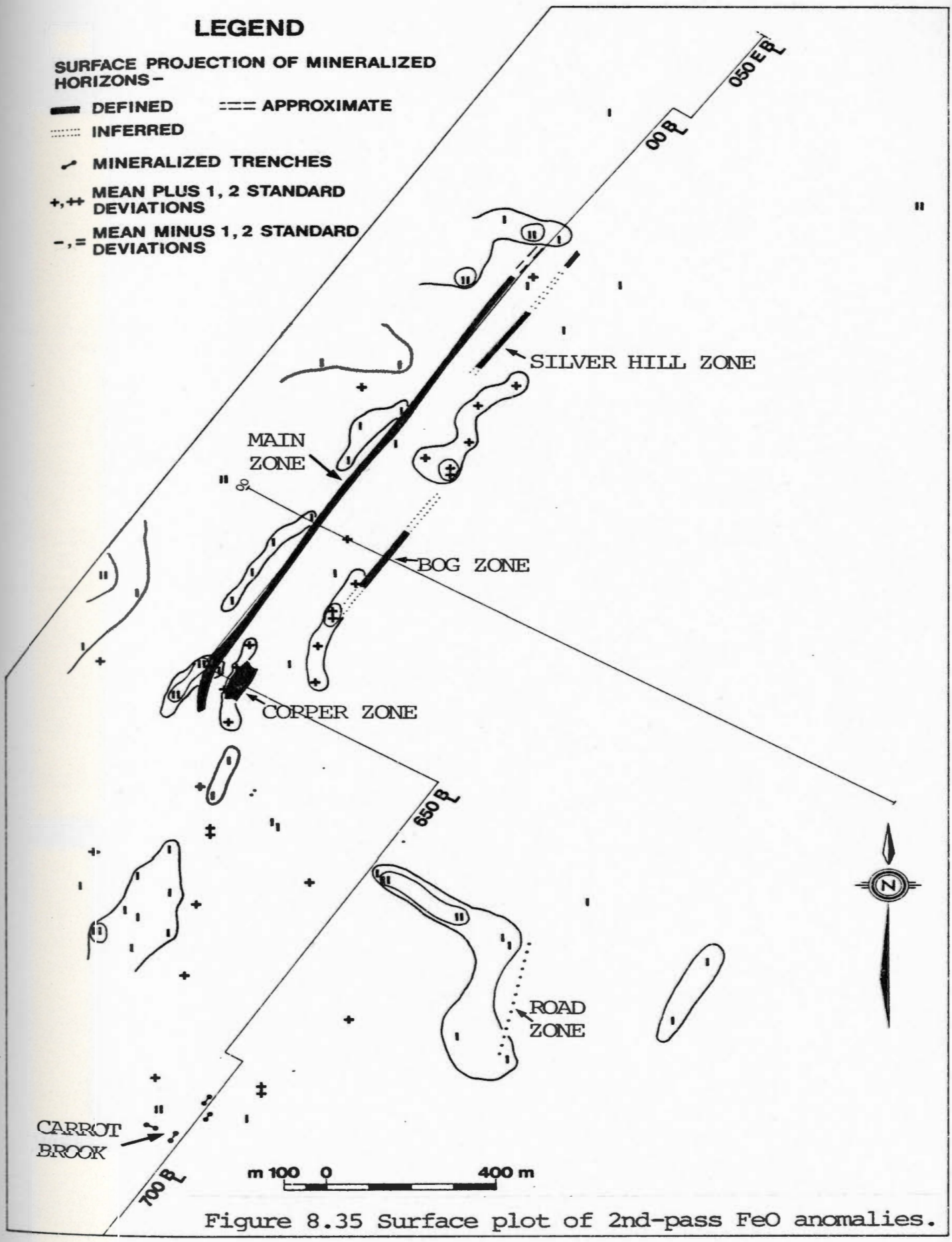

Figure 8.35 Surface plot of 2nd-pass FeO anomalies.

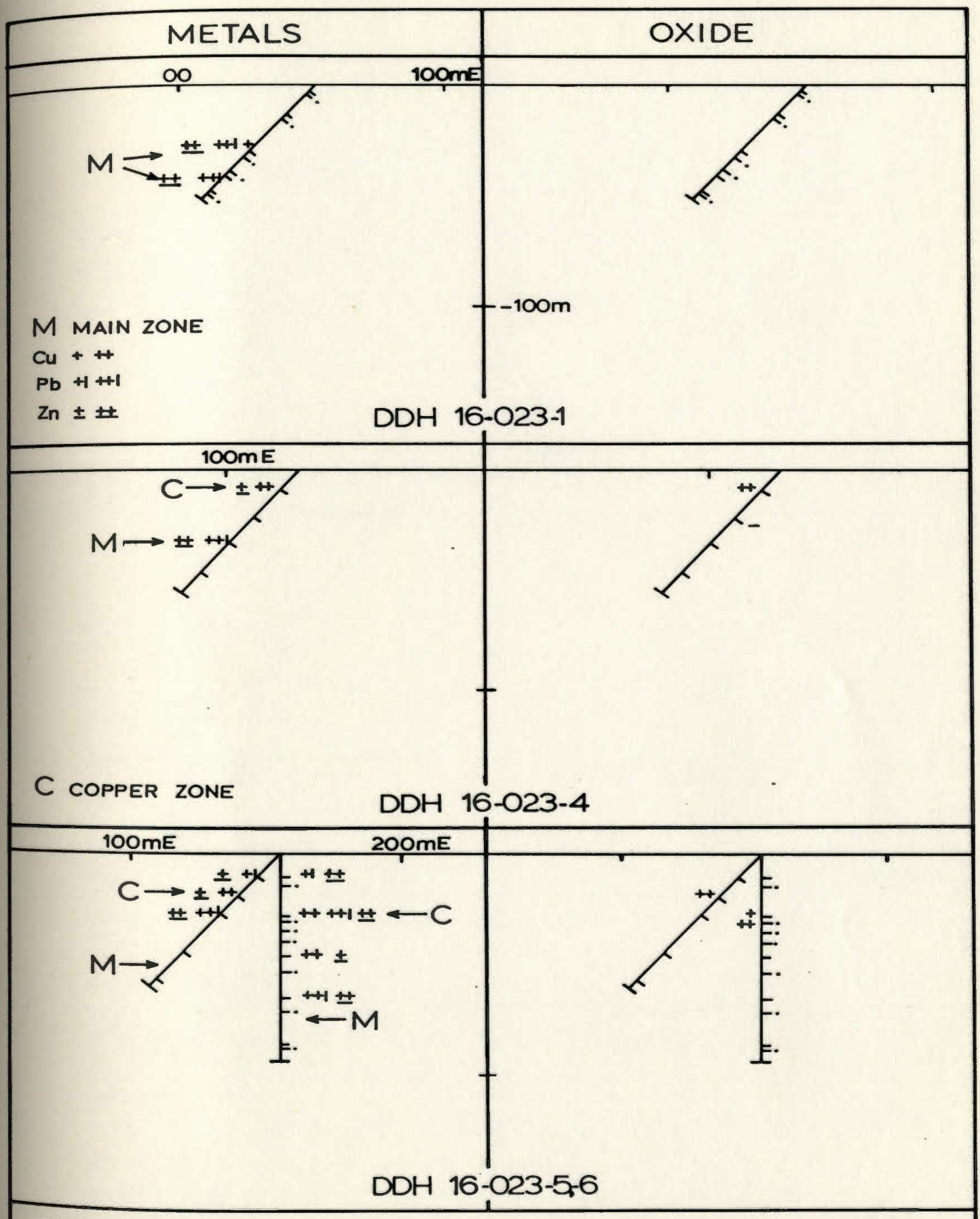

FIGURE 8.36: 2nd Pass FeO anomalies. Scale 1:2,500.

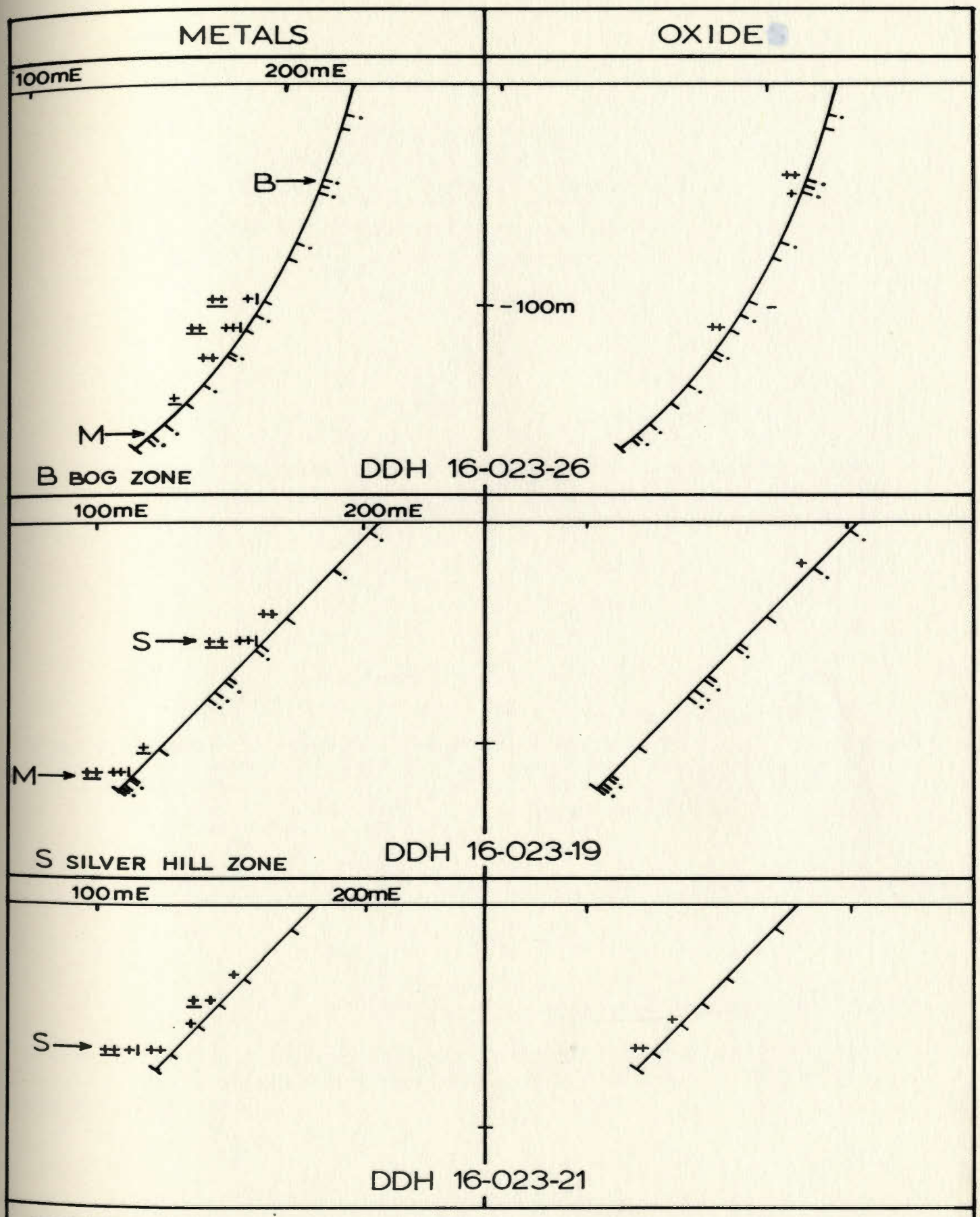

FIGURE 8.37: 2nd Pass FeO anomalies. Scale 1:2,500.

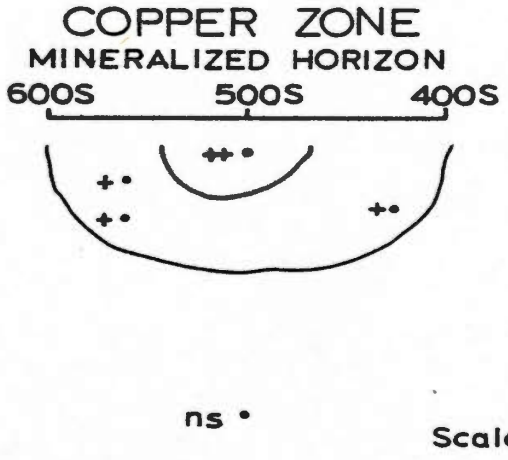

Figure 8.38. A dip surface plot of 2nd pass FeO anomalies in the Copper Zone mineralized horizon. See Figure 8.20 for a key to the symbols used.

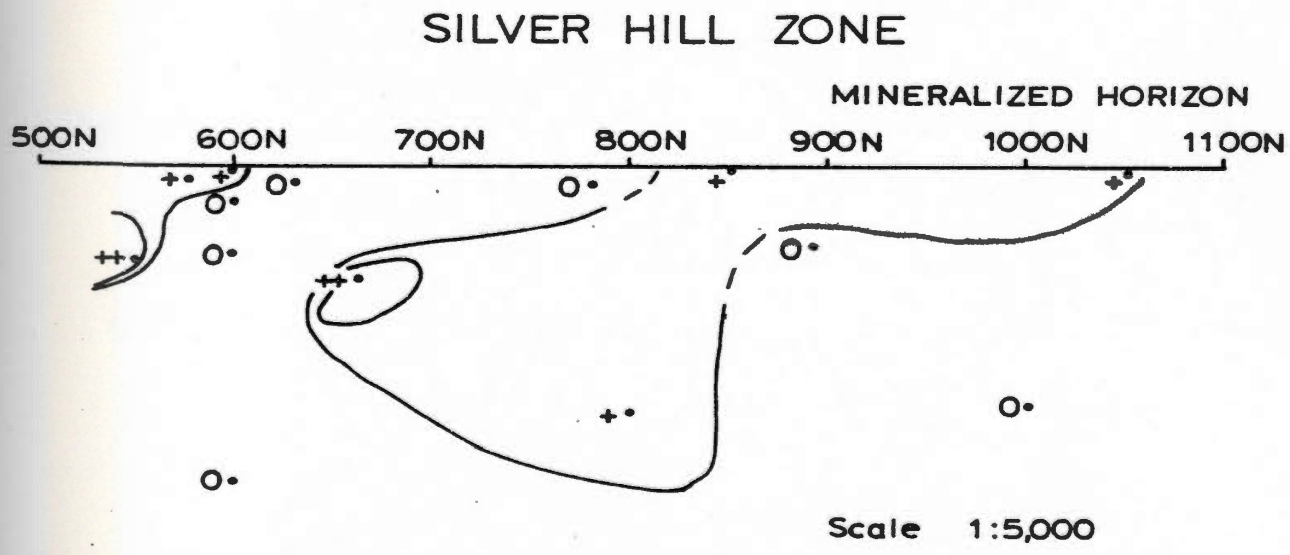

Figure 8.39. A dip surface plot of 2nd pass FeO anomalies in the Silver Hill Zone mineralized horizon. See Figure 8.20 for a key to the symbols used.

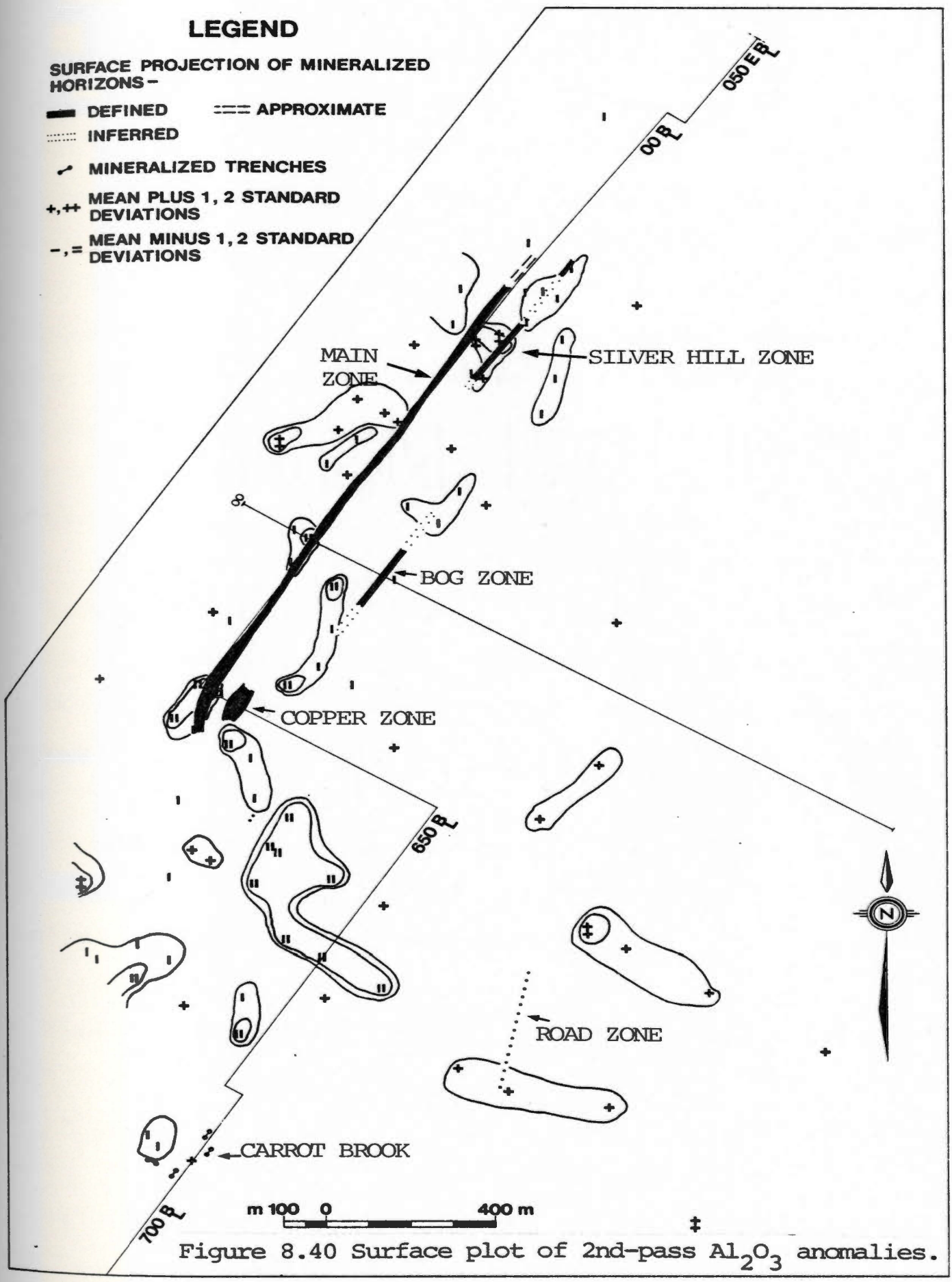

Figure 8.40 Surface plot of 2nd-pass Al_2O_3 anomalies.

to similarly shaped negative CaO and Na_2O clusters. There is no apparent correlation between mineralization and Al_2O_3 anomalies evident in the drill sections presented here (Figures 8.41 and 8.42). The dip surface plot of the Main Zone mineralized horizon is characterized by a few scattered weak positive Al_2O_3 anomalies (and two negative anomalies corresponding to the carbonate-tremolite samples). The mineralized horizons of the Copper, Bog and Silver Hill Zones show scattered weak negative anomalies. No interesting patterns are evident in the dip surface plots of intervals stratigraphically below the mineralized horizons.

8.4.9 SiO2

The majority of the SiO_2 anomalies on the surface plot are positive. The Main Zone is surrounded by isolated clusters of positive anomalies and interestingly two clusters extend across strike southeast of the Copper Zone (Figure 8.43). These correspond to previously described negative CaO, Na_2O, and Al_2O_3 clusters. The abundance of positive anomalies might be the result of preferential sampling of resistant (siliceous) outcrops.

Examination of the drill sections (Figures 8.44 and 8.45) indicates an association of negative SiO_2 anomalies with mineralization which is repeated in the dip surface plots. Two of the negative anomalies in the Main Zone mineralized interval and the eight strongly negative anomalies of the Silver Hill Zone (Figure 8.46) again reflect

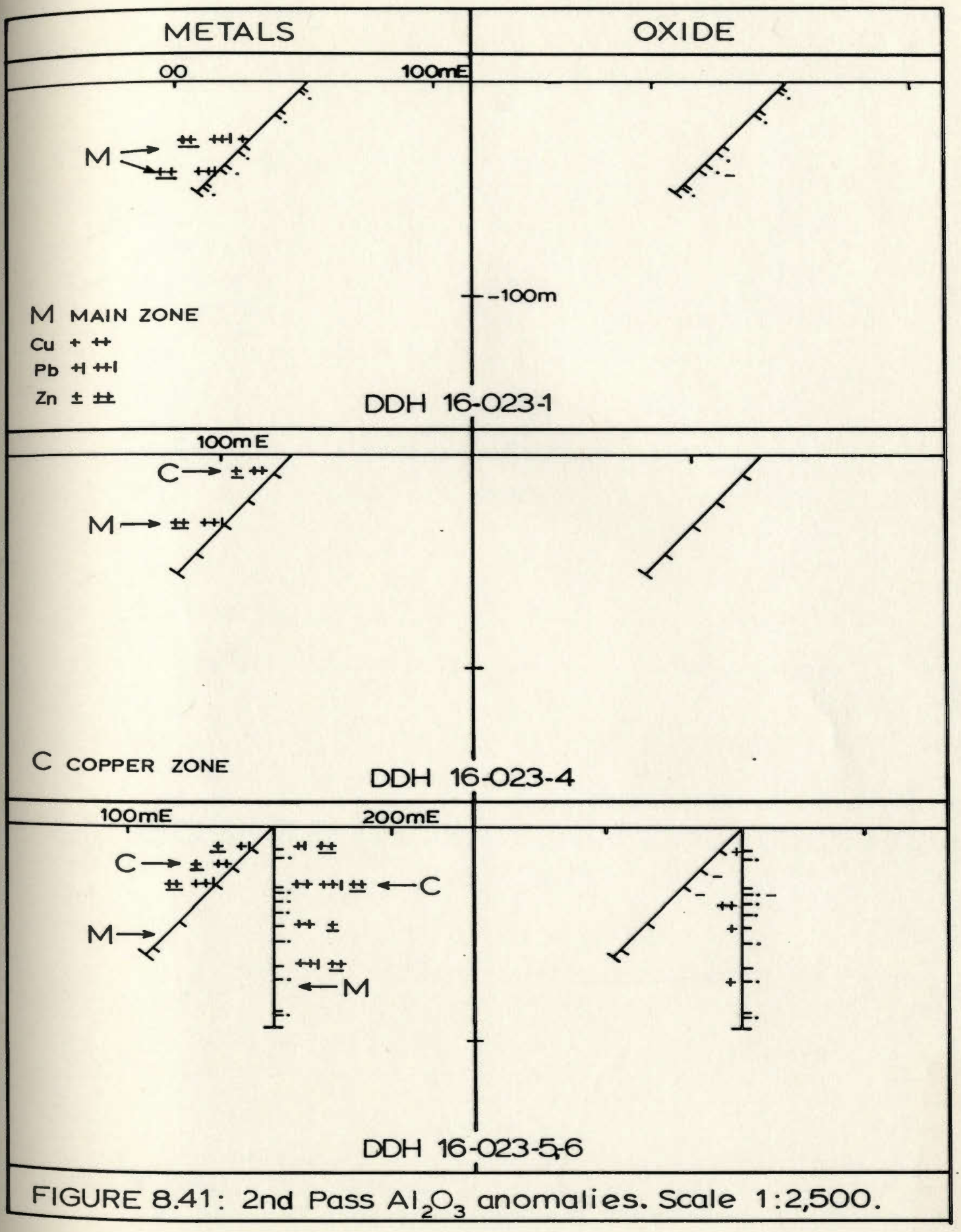

FIGURE 8.41: 2nd Pass Al_2O_3 anomalies. Scale 1:2,500.

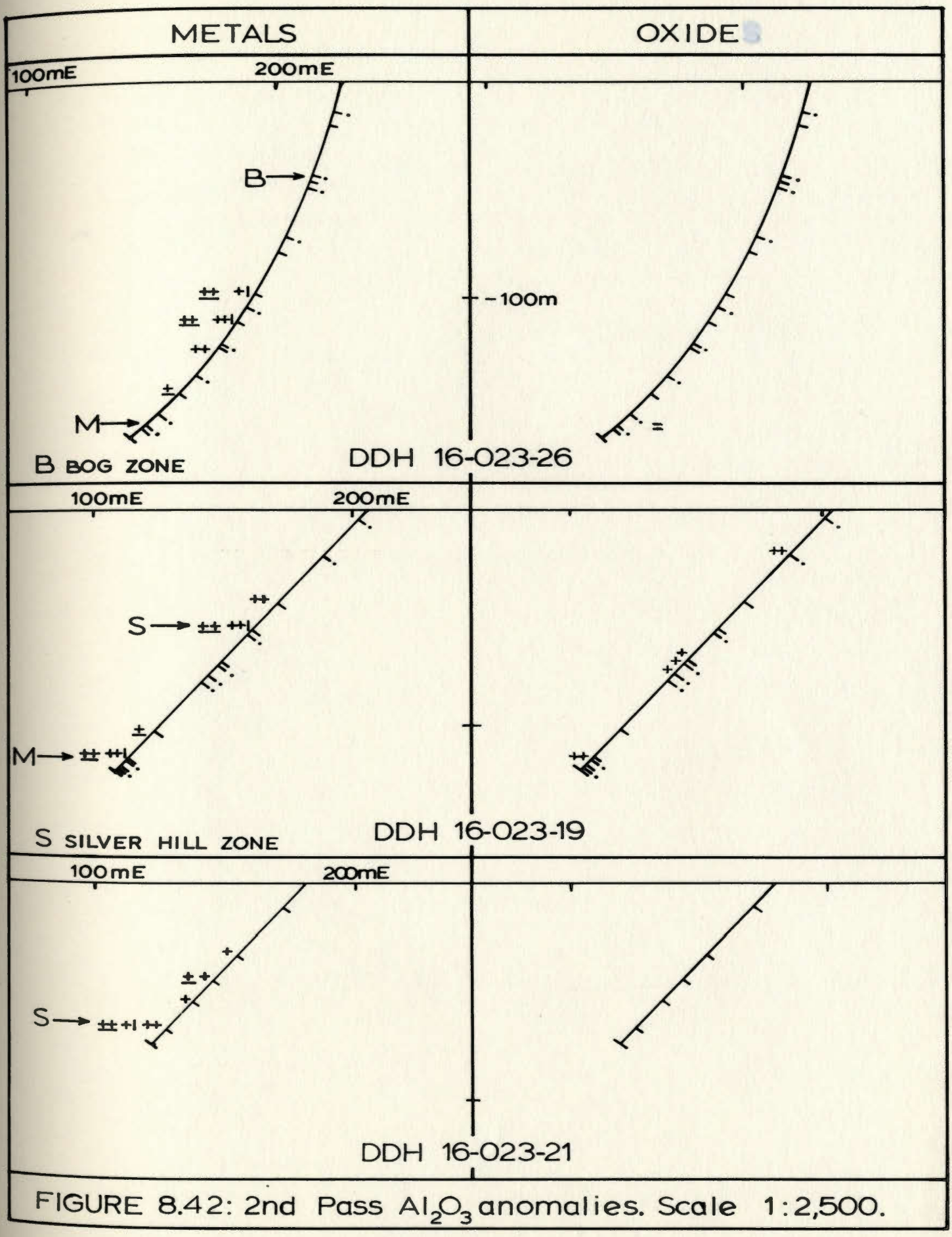

FIGURE 8.42: 2nd Pass Al_2O_3 anomalies. Scale 1:2,500.

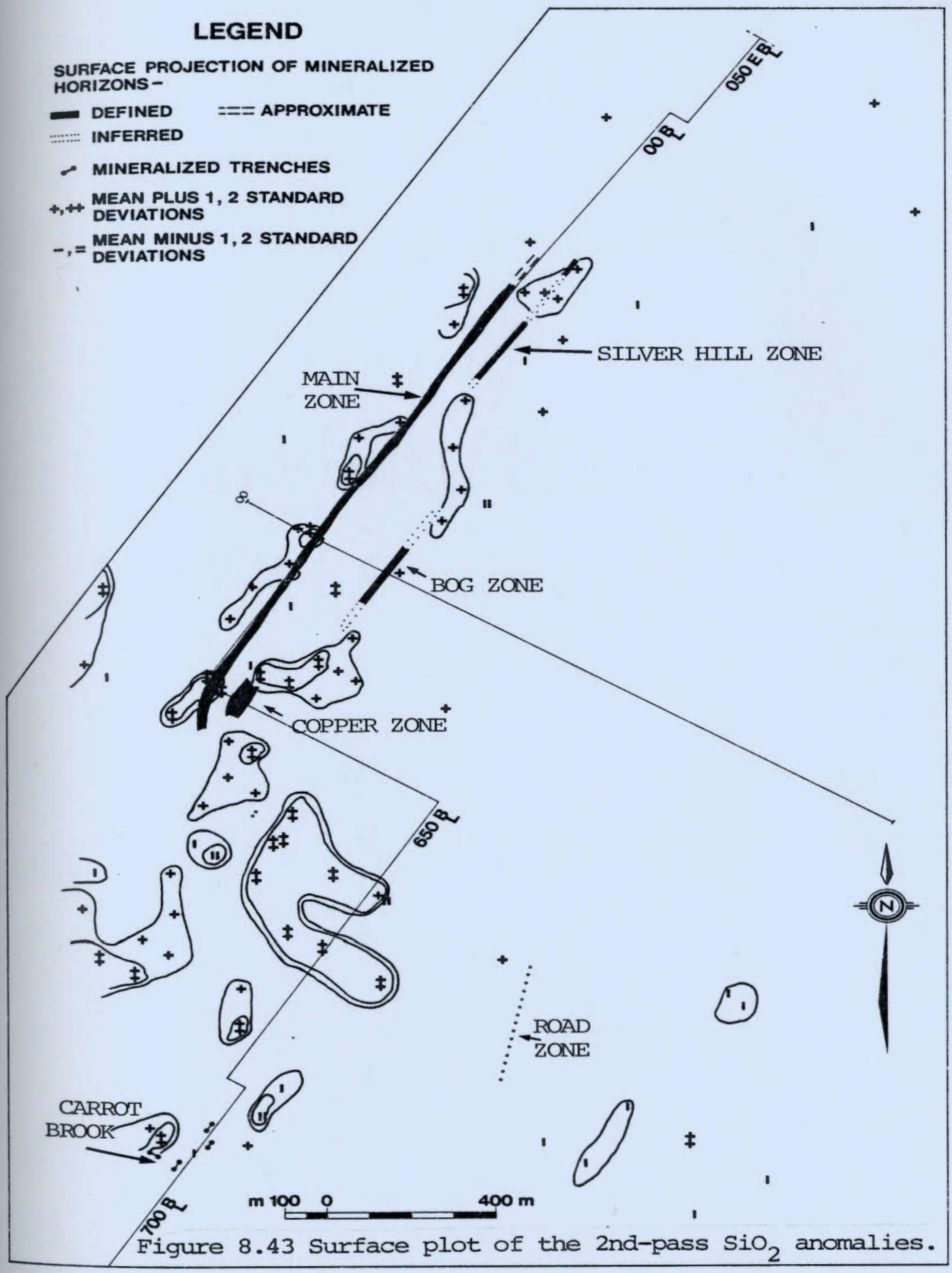

Figure 8.43 Surface plot of the 2nd-pass SiO_2 anomalies.

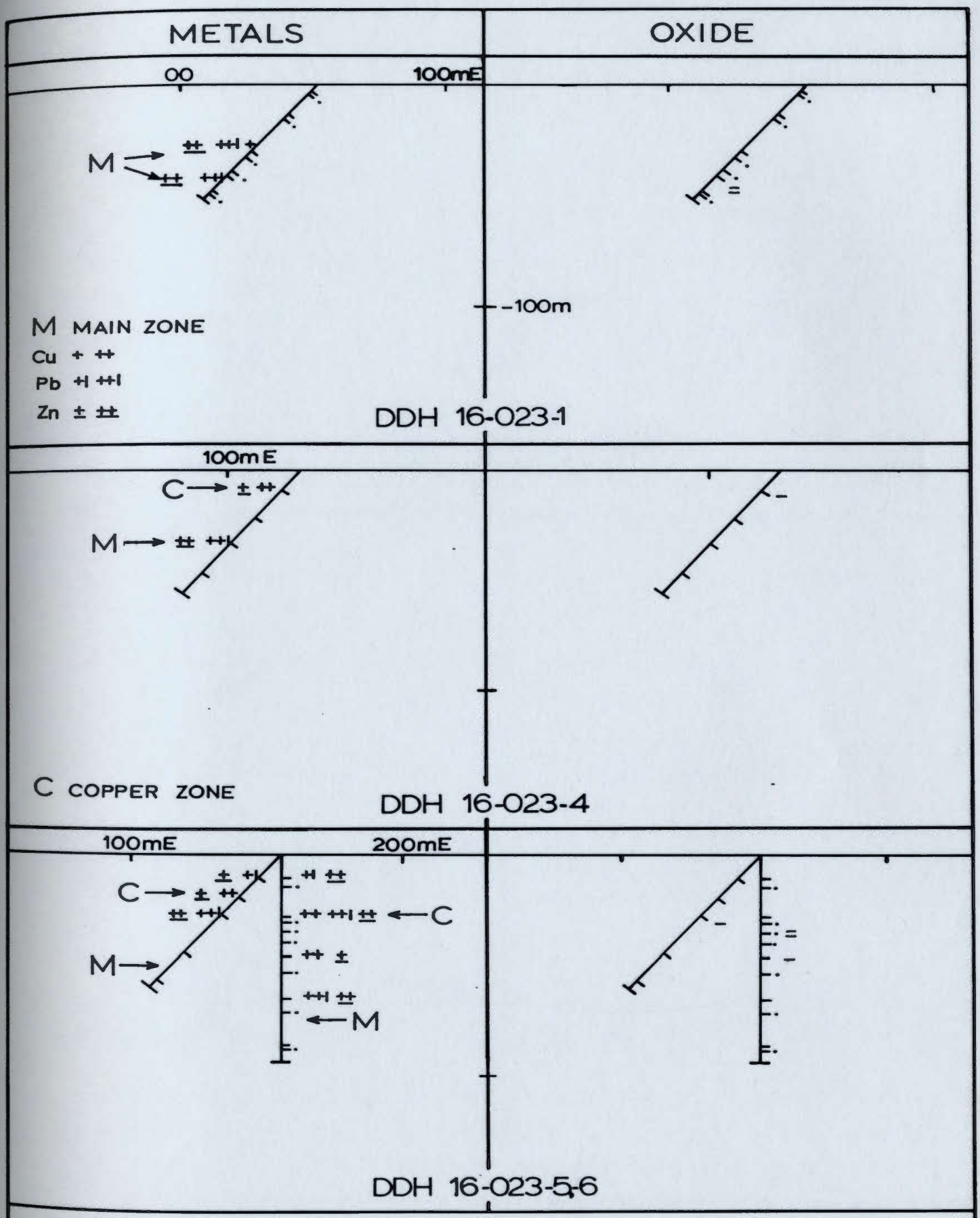

FIGURE 8.44: 2nd Pass SiO_2 anomalies. Scale 1:2,500.

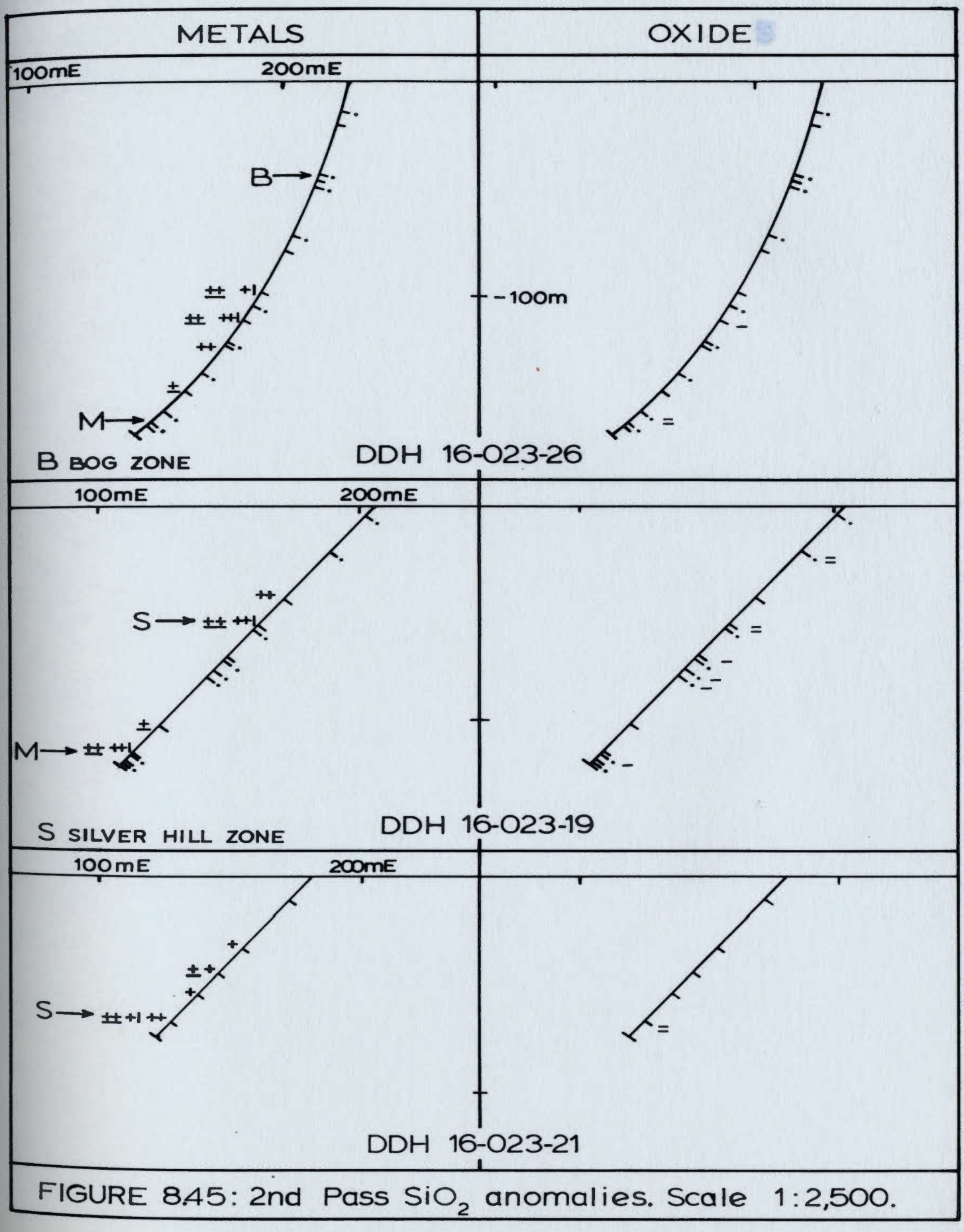

FIGURE 8.45: 2nd Pass SiO_2 anomalies. Scale 1:2,500.

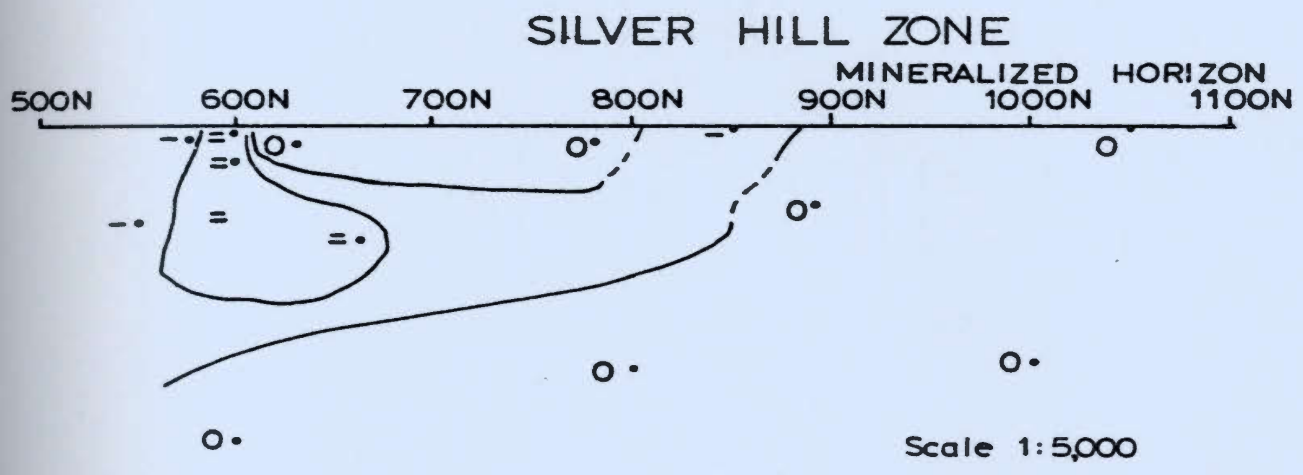

Figure 8.46. A dip surface plot of the 2nd pass SiO_2 anomalies in the Silver Hill Zone mineralized horizon. See Figure 8.20 for a key to the symbols used.

the carbonate and tremolite mineralogy which dominates these samples. Stratigraphically below the Main Zone negative SiO_2 anomalies persist (4 samples in 2 clusters of three and one sample each). A single negative anomaly is present in the Copper Zone mineralized horizon and in the underlying horizon. There are no SiO_2 anomalies on the Bog Zone plots.

8.3.10 Summary

The anomaly patterns of all the oxides are generally scattered, sporadic and elongate parallel to the regional strike. Those samples with carbonate-tremolite gangue in the Main Zone and Silver Hill Zones are repeatedly identified as anomalous ($-Na_2O$, $+MgO$, $+CaO$, $+FeO$, $-SiO_2$). Negative Na_2O anomalies are prevalent in the drill core samples. This, in conjunction with the average low sodium chemistry of the Strickland felsic flows relative to regionally collected felsite bands suggests that the Strickland property felsic volcanics have been largely stripped of sodium. The coincident clusters of negative Na_2O, CaO and Al_2O_3 anomalies with positive SiO_2 anomalies which extend southwest of the Copper Zone comprise the most coherent lithogeochemical pattern of the Strickland property. These clusters cut across the strike and the rocks are highly siliceous (most are between 78 and 92% SiO_2). The horizon 25m below the Silver Hill Zone is marked by strong positive K_2O anomalies and corresponding negative Na_2O anomalies. These rocks are rich in secondary biotite, sericite and occasionally K-feldspar porphyroblasts - an assemblage also noted in rocks from the Copper Zone. There is thus evidence of largely conformable secondary potassium enrichment highlighted by positive K_2O anomalies, visible in thin section and in outcrop.

CHAPTER 9

INTERPRETATION OF THE LITHOGEOCHEMICAL PATTERNS

9.1 General

The mineralized zones of the Strickland area are contained in a sequence of felsic volcanics, minor mafic tuffs and intercalated clastic sediments which are conformably overlain by a sequence of sedimentary rocks. The Main Zone mineralization lies at the contact between the two sequences which is also locally marked by discontinuous outcrops of quartz-graphite rock. The pyritic Carrot Brook Zone lies at the same horizon 1.5 km southwest along strike from the Main Zone. The Copper, Bog, Silver, Road, and Bison Fault Zones lie stratigraphically below the Main Zone. All the zones are stratiform. The Baggs Hill Granite is exposed in the northeast corner of the property. Mafic dykes (usually almost conformable with the regional northeast strike) and sills outcrop in the southern portion of the map area.

All of these rocks have been subjected to intense deformation and upper greenschist facies metamorphism. Boudinage structures are evident in thin section and in outcrop. In thin section zones of strongly mylonitized material occur next to coarsely recrystallized domains which are evidence of inhomogeneous cataclastic deformation. Phenocrysts are commonly fractured, pulled apart, rotated or augened. In other thin sections delicate primary igneous and

devitrification textures are preserved (microlites, skeletal plagioclase, spherulites, etc). Contorted folding of muscovite flakes contained in the sulphides of the Main Zone, and the occurrence of euhedral and broken pyrite porphyroblasts, provide evidence that the sulphide mineralization has undergone the same deformational and metamorphic history as the host rocks.

The association of stratiform Fe-Pb-Zn-Cu-Ag mineralization with footwall rocks dominated by felsic pyroclastics and overlain by sediments, as observed in the Strickland Main Zone, is characteristic of the Miocene Kuroko V.M.S. deposits (Lambert and Sato, 1974, Sato, 1977). The mineralization found in the Strickland area is therefore interpreted as having been deposited synvolcanically from metal bearing hydrothermal solutions. The Kuroko deposits are typically underlain by feeder pipes with stockwork mineralization. These pipes are not vertically extensive, but alteration associated with the pipes is mineralogically well defined with a quartz-sericite core and Mg-rich chlorite halo (Franklin, et al. 1981). Such a pipe, transecting the footwall rocks, was not recognized below any of the zones of mineralization on the Strickland property. The Kuroko alteration pipes are chemically characterized by an enrichment of potassium and silica in the core and iron and magnesium in the surrounding halo with an overall depletion in Na_2O and CaO (Izawa et al., 1978; Izawa, 1980; Franklin, et al., 1981).

It was hoped that chemical patterns such as those recognized below the Kuroko deposits, not expressed mineralogically in the Strickland area might be highlighted by a study of the lithogeochemistry of the host rocks. Thus, it is essential that any lithogeochemical anomalies produced during the synvolcanic emplacement of the sulphides survive the effects of subsequent metamorphism and deformation, if they are to be recognized. Work done on other metamorphosed V.M.S. deposits has shown that metamorphism does not significantly affect the bulk composition of the rocks (Riverin and Hodgson, 1980; McConnell, 1976). Synvolcanic alteration mineral assemblages will be replaced by metamorphic assemblages, but the chemistry of the rock remains largely constant.

There is abundant evidence in the Strickland rocks that they have been subjected to complex deformation with both pure shear (producing flattened clasts and boudinage structures) and simple shear components (producing cataclastic structures). Sangster (1972) and Sundblad (1980) have pointed out that progressive deformation of this type would flatten a V.M.S. ore zone and the underlying pipe, as well as attenuate and transpose the pipe into a position close to parallel, and almost adjacent to the overlying lense of massive sulphides. Extreme deformation of this type could conceivably obliterate any evidence of an alteration pipe. Such deformation may be responsible for the observed patchy and discontinuous distribution and the clusters of

lithogeochemical anomalies which are commonly elongate parallel to the strike in the Strickland area.

The evidence of extensive deformation in the Strickland area, coupled with the absence of mineralogical evidence of cross-cutting pipes, might lead to the conclusion that either no alteration pipes existed below the mineralized zones or that those originally present have been destroyed (or at least obscured) by the deformation. A group of samples which stretch across strike for 700m southeast from the Copper Zone are marked by multi-element anomalies ($+SiO_2$, $-Al_2O_3$, $-Na_2O$, $-CaO$). The observed enrichments and depletions are similar to those reported in the alteration pipes of Kuroko deposits (Lambert and Sato, 1974; Izawa, 1980) as is the discordant shape. In this area a drill hole (16-023-30) intersected almost 2m of silicate breccia with a chalcopyrite and sphalerite matrix (the Bison Fault mineralization). The copper-rich nature of this mineralization is consistent with that characteristic of stockwork zones. If this cluster is interpreted as an irregularly-shaped alteration pipe, one might conclude that primary (synvolcanic) alteration pipes have survived the deformation processes which affected the Strickland area, and that the absence of pipes below the other zones of mineralization must be explained in some other manner (besides being structurally obscured). On the basis of this premise then the Copper Zone with its veined and disseminated chalcopyrite-pyrite-sphalerite mineralization in a chloritic host rock lies at the stratigraphic top of

what is interpreted here as a hydrothermal feeder pipe (identified on the basis of multi-element lithogeochemical anomalies). The mineralizing processes centered there were terminated by renewed felsic volcanism, and the conduit was overlain by the felsic pyroclastics which host the Main Zone. This pipe does not appear to be related to the Main Zone mineralization.

The Main Zone mineralization is a 10m thick sequence of massive sulphides intercalated with felsic volcaniclastics and sediments. It grades upwards from a low grade pyritic base (with minor chalcopyrite and sphalerite) through volcaniclastics and a thin lens of siltstone into a sphalerite-rich (minor galena and pyrite) massive sulphide layer, locally with 2-5 cm silicate clasts in a (dominantly sphalerite) sulphide matrix. Argentiferous pods with carbonate-tremolite gangue and weak sphalerite-galena mineralization occur near the top of the massive sulphide ore. The quartz-graphite rock, which outcrops discontinuously between the sulphides and the hangingwall sediments, is interpreted to be a boudinaged chert horizon (a megascopic pinch and swell structure) which once continuously overlay the sulphides. The immediate footwall rocks of the Main Zone are intensely sericitized and silicified.

The features of the Main Zone can be explained in a number of ways: 1) it may represent a flank portion of an "insitu" ore body with a deeply buried pipe or a pipe which has been eroded away; 2) it may be a transported ore body,

slumped in a semi-consolidated state, from an unstable site of deposition close to the feeder pipe or 3) it may represent an example of one of Sato's (1972) Type I or Type II orebodies which precipitated in a basin downslope from the feeder vent. The preservation of a metal zonation pattern (pyritic base to sphalerite/silver-rich top) common in undisturbed deposits (Sato, 1977; Large, 1977; Sangster and Scott, 1976) argues against the second (transported) interpretation. Therefore, the third suggestion will be used as the basis for reconstruction of the environment of deposition of the Main Zone. It has been suggested (Hodgson & Lydon, 1977) that the hydrothermal solutions responsible for the transport of Zn-Pb rich mineralization (like that of the Main Zone) are highly saline, acidic and of relatively low temperature and would tend to pond and deposit sulphides in basins downslope from the feeder pipe. An isopach map of the felsic volcaniclastics which host the Main Zone mineralization (Figure 9.1) shows abrupt changes in thickness of the unit. These might be a reflection of an irregular paleotopography and indicate the presence of suitable trap basins.

The mineral zonation may reflect a change in the chemistry (pH, sulphur activity) or the physical properties (density, temperature) of the mineralizing solutions introduced to the basin (Large, 1977). Reaction of the footwall rocks with the metal-bearing brines may have produced the intense sericitization and silicification beneath the Main Zone ("auto-alteration" of Sangster and Scott, 1976). The

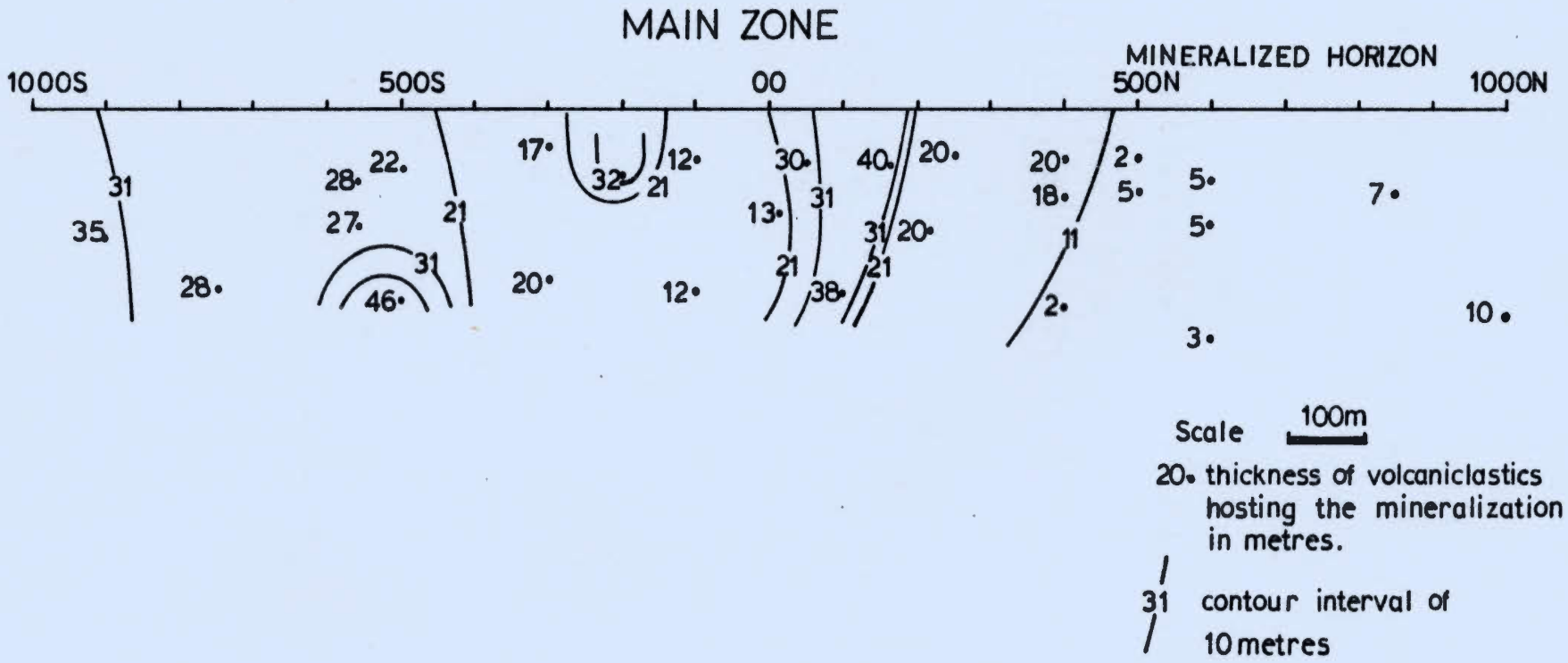

Figure 9.1 A dip surface plot of the Main Zone mineralized horizon showing the thickness of the felsic volcaniclastics which host the sulphides.

intercalated volcaniclastics and sediments may have been introduced to the basin from another source area, possibly as slump deposits, only temporarily interupting deposition of the sulphides. The silicate clasts contained in a matrix of massive sphalerite (Figure 6.6b, page 116) high up in the Main Zone may have been transported down slope with the mineralizing brine and settled into the already precipitated sulphides. Swinden (1981) pointed to these clasts as possible evidence that the entire ore body may have been transported. Alternatively they may have been clasts borne explosively into the basin by some nearby phreatic or other explosion.

The silver-rich zones of mineralization in the Strickland area are invariably associated with carbonate-tremolite gangue and weak sphalerite-galena mineralization. Lenses of this material occur at stratigraphically high levels in the Main Zone and comprise the sole type of mineralization in the Silver Hill Zone. The conformable nature of the carbonate-tremolite mineralization and the intimate association of it with the massive sulphides of the Main Zone suggest that it is a metamorphosed product of the synvolcanic mineralizing event. The stratigraphic position of the argentiferous-carbonate-tremolite pockets in the Main Zone may indicate that the slightly alkaline solutions capable of producing carbonate (Sato, 1977) came late in the Main Zone mineralizing event. The association of silver with a carbonate gangue implies that CO_2^{-3} might be an important metal-complexing

agent in the mineralizing solutions (Kerrich and Fryer, 1981). The Silver Hill Zone is a conformable lens of argentiferous carbonate-tremolite mineralization which grades laterally into tuffaceous siltstone and is underlain by a massive felsic flow/ volcaniclastic unit. This carbonate-tremolite assemblage has been previously interpreted as the metamorphosed equivalent of chemical sediments (chert, calcite, dolomite) precipitated with the sulphides on the sea floor (Silver Hill zinc deposit, North Carolina, Indorf, 1981). Dolomite occurs in significant quantities as a gangue mineral in the dominantly sediment hosted McArthur Zn-Pb-Ag deposit (where Lambert (1976) considers it to be syngenetic or an early diagenetic alteration of calcite) and the Heath Steele deposit of the Bathurst camp (Chen and Petruck, 1980). On the basis of this evidence, the mineralization of the Silver Hill Zone is interpreted to be a pocket of distally precipitated chemical sediment, rich in magnesium and silver, relatively poor in lead and zinc, which acted as a cement to previously deposited tuffaceous sediments. The presence of some aluminous contamination of the chemical sediments (calcite, dolomite) is necessary to produce by metamorphic reactions the tremolite, characteristic of the high-silver zones. The Silver Hill Zone may have been produced by an earlier mineralizing pulse from the Main Zone hydrothermal feeder or as distal mineralization originating from a separate source.

A thick layer (20-30m) of mixed felsic flows and volcaniclastics separates the Silver Hill Zone from an

underlying horizon of tuffs and siltstone characterized by ubiquitous negative sodium anomalies (Figure 8.21, page 212) and more scattered positive potassium anomalies. These anomalies reflect the presence of abundant secondary sericite and biotite and rare orthoclase porphyroblasts which may have been produced by hydrothermal solutions similar to those responsible for the alteration of the footwall rocks of the Main Zone. This horizon may have served as an aquifer for the movement of hydrothermal solutions with the overlying felsic flow/ volcaniclastic acting as an impermeable cap. Such conformable and altered horizons have been noted elsewhere (Hodgson and Lydon, 1977; Walford and Franklin, 1982, taken from Franklin et al., 1981). Because the sericitization of these rocks is less intense than that of the Main Zone footwall rocks, it is speculated that the transport of hydrothermal solutions through the horizon was relatively short-lived.

The Carrot Brook Zone (Fe-Pb-Zn-Cu) is exposed at the same stratigraphic horizon as the Main Zone. It may represent a transported or distally precipitated ore body originating from the same hydrothermal source as the Main Zone.

The Bog and Road Zones lie stratigraphically below the Main Zone (100m and 850m respectively). Both zones of mineralization are apparently conformable and similar in composition to that of the Main Zone (dominantly sphalerite, pyrite, + galena with minor chalcopyrite). The host rocks of

the Bog Zone are mafic to intermediate tuffs. The Road Zone is contained in silicified and sericitized intermediate lapilli tuffs. These zones are also interpreted to have been formed synvolcanically and therefore represent earlier examples of the mineralizing processes which culminated in the Main Zone sulphides.

Comparison of the average chemistry of the Strickland felsic flows with regionally sampled felsite bands indicates that the Strickland samples are conspicuously low in Na_2O and (less conspicuously) rich in K_2O and SiO_2. The rocks of the Strickland area therefore have been subjected to metasomatic processes which removed sodium and added potassium and silica. This process cannot be related to the effects of regional metamorphism since only the rocks of the Strickland area have been affected (plus a mineralized outcrop just south of Carrot Brook - Sample #78LC442, Chorlton, 1980). It is therefore suggested that the association of sodium-depleted rocks with the volcanogenic mineralization in the Strickland area is not fortuitous, but probably genetic. It is probable that the hydrothermal processes responsible for the concentration of sulphides have significantly depleted the host rocks in sodium. As reviewed in Table 1.1 sodium depletion has been recognized on a similar scale (5-10 square kilometres) in productive cycles of volcanism in Archean greenstone belts (Sopuck et al., 1980). There it was interpreted to have been produced by subaqueous metasomatic processes accompanying devitrification

synchronous with the deposition of sulphides.

If some of the many faults of the Strickland area are indeed synvolcanic, as suggested by Prince and Briggs (1978), they may have played a significant role in focusing and channelling the mineralizing hydrothermal fluids to the seafloor. Numerous authors (e.g. Hodgson and Lydon, 1977 and Scott, 1978) have emphasized the importance of such structures in the formation of V.M.S. deposits.

The part played by the Baggs Hill Granite in the history of the Strickland area is unclear. It is an equigranular, leucocratic granite enriched in sodium, possibly as the result of subsolidus hydrothermal alteration by a sodium-enriched fluid phase, as suggested by Chorlton (1980). No prominent contact aureole was observed. The effects of cataclastic deformation so evident in the rest of the Strickland rocks has also affected the margins and apophyses of the Baggs Hill Granite. It has ben suggested that the granite was a hypabyssal volcanic feeder (Briggs and Prince, 1979) yet no chemical affinity between it and the felsic volcanics could be proven, possibly because of the suggested metasomatic alteration of both lithologies. If, however, the two are genetically linked, it is possible that the fluids responsible for stripping the volcanic rocks of sodium and depositing sulphides were the same ones which, upon recirculation, to some depth, enriched the granite in sodium (in an alkali exchange process). The granite pluton and sills (dykes) would provide the heat source to

circulate the hydrothermal fluids which may have deposited the sulphides.

The interpretation of the zones of mineralization described above is summarized in Figure 9.2

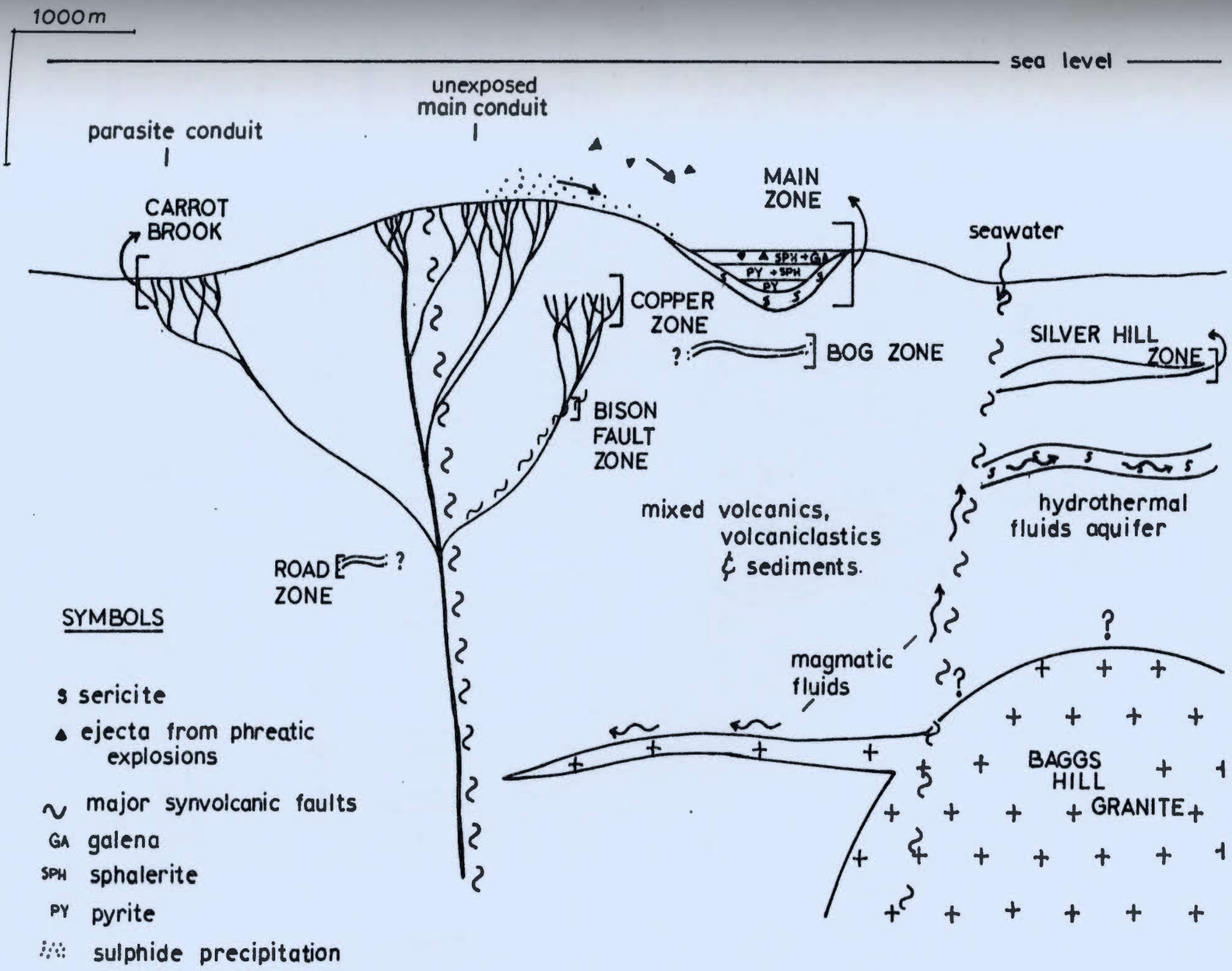

Figure 9.2. A schematic cross section of the Strickland area illustrating the possible relationships between the synvolcanic hydrothermal activity , fault zones and sulphide mineralization.

CHAPTER 10

SUMMARY AND CONCLUSIONS

10.1 Summary

In this study a total of 294 surface samples and 292 diamond drill core samples were analysed for eight major oxides and volatiles (loss on ignition). Four-hundred and eleven of these were analysed for the metals Cu, Pb, Zn and Ag, and a total of 128 surface samples were analysed for the trace elements (Zr, Sr, Rb, U, Th, Ga, Ni, Y). Seventy percent of these samples were collected by Falconbridge personnel and analysed commercially. The remaining 30% of the samples were collected and analysed by the author. The host rocks were examined and described in detail both in surface exposures and drill core. Thin sections of the host rocks, polished thin sections and polished sections of the sulphides were prepared and examined. Minerals intimately associated with sulphide ore (chlorite, carbonate, tremolite) and others found in the host rocks (actinolite and tourmaline) were analysed. The applicability of the sphalerite geobarometer to the Main Zone mineralization was tested and found wanting.

Plots of Ti vs Zn and Rb vs K indicate that the trace elements show no enrichment or depletion patterns not expressed by the major elements. Computer facilities were used to calculate descriptive statistics and plot histograms for each element and oxide of each lithology. It was shown

that in order to recognize geochemical anomalies the effects of the primary chemistry of the rocks must first be compensated for. To accomplish this, discriminant analysis was used to identify which oxides contributed the most to distinguishing between the principal lithologies using their major oxide chemistry. The three oxides which contributed most to the discrimination between lithologies (TiO_2, Al_2O_3, FeO) were then used as the independent variables in curvilinear regression equations with which residual values for the other oxides and metals were calculated. These residuals constitute the first-pass data set. In order to further refine the recognition of anomalous samples, irrespective of lithology, the samples were divided into three lithological groups based on origin; igneous, sedimentary and mixed (samples with combined sedimentary and igneous input) groups. Residuals were generated for the oxides and metals of the igneous and mixed groups using simplified curvilinear regression equations with TiO_2 and $(TiO_2)^2$ as the independent variables. These residuals, combined with "raw" geochemical analyses of the sedimentary group, constitute the second-pass data set.

Surface plots and drill hole cross sections were prepared for the anomalous (mean +/- one and two standard deviations) geochemical values of the raw data set and the anomalous residual values of the first and second pass data sets for the metals (Cu, Pb, Zn) and major oxides. Dip surface plots of the second pass data were prepared for each oxide and the metals for the mineralized horizons, a horizon

25m stratigraphically below each mineralized horizon and the hanging wall sediments.

10.2 Conclusions

On the basis of this study the following conclusions are possible:

1) The zones of mineralization exposed in the Strickland area are interpreted to represent portions of one or more volcanogenic massive sulphide deposits which have been subjected to cataclastic deformation and upper greenschist facies metamorphism.

2) The application of the sphalerite geobarometer to estimate the peak metamorphic pressures using the Main Zone ores was not successful. Possibly the peak metamorphic temperatures were out of the range where the geobarometer is effective or the sphalerite has undergone a low temperature re-equilibration process.

3) The plots of anomalous "raw" geochemical analyses reflect the primary chemistry of the rocks.

4) The regression analyses employed successfully compensated for the primary chemistry, except when dealing with extreme variations of rock type (e.g. the carbonate-tremolite rocks) and the anomalous residual plots for the most part represent samples which can be recognized as anomalous irrespective of lithology.

5) The method used to generate the second-pass data set is the most sensitive in accounting for the primary chemistry of the rocks.

6) The felsic flows of the Strickland area are anomalously low in Na_2O when compared to equivalent

lithologies sampled regionally (1.14% Na_2O vs 4.17% Na_2O). The low Na_2O signature evident in these Strickland volcanics may provide an exploration tool useful in distinguishing potentially mineralized areas (low-Na_2O) from barren areas on a regional basis, although patterns are more complex on a local scale. Lithogeochemical anomalies in the Strickland property generally occur in sporadic clusters conformable with the strike.

7) A concentration of multi-oxide anomalies ($-Al_2O_3$, $-Na_2O$, $-CaO$, $+SiO_2$) which terminate in the Copper Zone may indicate the presence of a hydrothermal conduit responsible for the Copper Zone mineralization, but appears to be unrelated to the Main Zone.

8) The Main Zone is interpreted to be a sulphide body precipitated in a basin removed from the hydrothermal feeder conduit.

9) The intense silicification and sericitization of the Main Zone footwall rocks are interpreted to be the result of autometasomatic processes.

10) The Silver Hill Zone is interpreted to be a distal magnesium- and silver-rich carbonate precipitate which formed the cement for previously deposited tuffaceous sediments. The persistent lithogeochemical anomalies associated with the Silver Hill Zone ($-Na_2O$, $-SiO_2$, $+MgO$, $+CaO$, $+FeO$) reflect this unique primary chemistry.

11) A horizon of mixed volcaniclastics and tuffs which

occurs 25m stratigraphically below the Silver Hill Zone, characterized by negative Na_2O and positive K_2O anomalies, with abundant secondary biotite and sericite and occasional orthoclase porphyroblasts is interpreted to have been a short lived aquifer (a stratiform conduit for hydrothermal solutions). Its relationship to known mineralization is unclear.

12) The Baggs Hill Granite was emplaced before the cataclastic deformation of the rocks in the Strickland area. Its relation to the felsic volcanics is unknown, but there is a close spatial relationship between the two and they are characterized by reciprocal Na_2O anomalies (the granite is Na_2O-rich, the volcanics Na_2O-poor). It has been suggested that the volcanics and the granite are genetically linked - if so, the Na_2O anomalies may represent relicts of an alkali exchange process produced by circulating hydrothermal fluids - possibly those responsible for the deposition of the sulphide mineralization.

13) The Pb-isotope signatures of galena from the Strickland showings are very similar to those of the Bathurst, N.B. camp. Both deposits have been interpreted to have been deposited in a back-arc basin. The isotopic ratios of the Bathurst Pb-isotopes has been interpreted to indicate that the arc system was emplaced through continental crust (ensialicly). The similarities between the Bathurst camp (which includes deposits like Brunswick 12 with ore reserves of 109.2 million metric tons) and the

Strickland area (age, host lithologies, ore mineralogy, Pb-isotope signature) and the tendency of these deposits to cluster (there are 30 deposits in the Bathurst camp) might indicate that the sequence of rocks which host the Strickland mineralization has potential for hosting other significant deposits which are as yet undiscovered.

REFERENCES

Abbey, S., 1968. Analysis of rocks and minerals by atomic absorption spectroscopy, Part 2. Determination of total iron, magnesium, calcium, sodium and potassium. Geol. Surv. of Can., Paper 68-20, 21 pp.

Bateman, P.C., Clark, L.D., Huber, N.K., Moore, J.G., and Pinehart, C.D., 1963. The Sierra Nevada Batholith, U.S.G.S. Prof. Paper, 414-D

Bell, K. and Blenkinsop, J., 1981. A geochronological study of the Buchans area, Newfoundland. In: The Buchans orebodies; fifty years of geology and mining, Swanson, E.A., Strong, D.F. and Thurlow, J.G. (eds.), Geol. Assoc. of Can., Spec. Paper No. 22, pp. 91-111.

Briggs, D.N. and Prince, D.R., 1979. Summary report on the 1979 Hermitage Joint Venture, Nfld. Program and proposals for 1980 program. Unpubl. co. report, Falconbridge Nickel Mines Ltd., 32 pp.

Brown, P.A., 1972. Structural and metamorphic history of the gneisses of the Port aux Basques region, Newfoundland. Unpubl. M.Sc. Thesis, Memorial University of Newfoundland, 113 pp.

Chen, T.T., and Petruck, W., 1980. Mineralogy and characteristics that affect recoveries of metals and trace elements from the ore at Heath Steele Mines, New Brunswick. Can. Min. Metall. Bull., v. 73, No. 823, pp. 167-179.

Chorlton, L.B., 1978a. The geology of the La Poile map area (110/9), Newfoundland. Newfoundland Dept. of Mines and Energy, Minerals Development Division, Report 78-5, 14 pp.

Chorlton, L.B., 1978b. La Poile River map area (110/16), Newfoundland. Newfoundland Dept. of Mines and Energy, Mineral Development Division, Map 78168, with marginal notes.

Chorlton, L.B., 1979a. La Poile River map area (110/16), Newfondland. In: Report of Activities for 1978. Gibbons, R.V. (ed.), Newfoundland Dept. of Mines and Energy, Mineral Development Division, Report 79-1, pp. 45-53.

Chorlton, L.B., 1979b. La Poile River. Newfoundland Dept. of Mines and Energy, Mineral Development Division, Map 79-124.

Chorlton, L.B., 1980. Geology of the La Poile River area (110/16), Newfoundland. Newfoundland Dept. of Mines and Energy, Mineral Development Division, Report 80-3, 86 pp.

Church, W.R., and Stevens, R.K., 1971. Early Paleozoic ophiolite complexes of the Newfoundland Appalachians as mantle-ocean crust sequences, Geophys. Res., V. 76, No. 5, pp. 1460-1466.

Colman-Sadd, S.P., 1980. Geology of south-central Newfoundland and evolution of the eastern margin of Iapetus. Am. J. of Sci., v. 280, pp. 991-1017.

Colman-Sadd, S.P., and Swinden, H.S., 1980. Geology and mineral potential of south-central Newfoundland. Newfoundland Dept. of Mines and Energy, Mineral Development Division, Report 81-5, 84 pp.

Cooper, J.R., 1954. The La Poile - Cinq Cerf map area, Newfoundland. Geol. Surv. of Can., Memoir 256, 62 pp.

Correns, C.W., 1978. Titanium, 22-K. Abundance in common sediments and sedimentary rocks. In: Wedepohl, K.H., (ed.), Handbook of Geochemistry, Springer-Verlag, New York, pp. 22-K-1 to 22-K-7.

Davies, J.L., and McAllister, A.L., 1980. Geology of the Bathurst-Newcastle area. Geol. Assoc. Canada, Ann. Mtg., Halifax, May 1980, Field Trip Guidebook #16, 56 pp.

Descarreaux, J., 1973. A petrochemical study of the Abitibi volcanic belt and its bearing on the occurrence of massive sulphides ores. Can. Min. Metall. Bull., v. 66, no. 730, pp. 61-69.

Dixon, W.I., and Brown, M.B., 1977. BMDP, Biomedical Computer Programs, P-Series, devloped at the Health Sciences computing facility, University of California, Los Angeles, California.

Doe, B.R., and Zartman, R.E., 1979. Plumbotectonics Phanerozoic. In: Geochemistry of hydrothermal ore deposits, Barnes, H.L. (ed.), pp. 22-70.

Dorf, F., and Cooper, J.R., 1943. Early Devonian plants from Newfoundland. Paleontol., v. 17, pp. 264-270.

Erlank, A.J., Smith, H.S., Cardoso, M.P., Ahrens, L.H., 1978. Zirconium, 40-K. Abundance in common sediments and sedimentary rocks. In: Wedepohl, K.H., (ed.), Handbook of Geochemistry, Springer-Verlag, New York, pp. 40-K-1 to 40-K-8.

Ewart, A., and Bryan, W.B., 1972. Petrography and geochemistry of the igneous rocks from Eua, Tongan Islands. Geo. Soc. Am. Bull., v. 83, pp. 3281-3298.

Ewart, A., and Stipp, J.J., 1968. Petrogenesis of the volcanic rocks of the Central North Island, New Zealand, as indicated by a study of Sr^{87}/Sr^{86} ratios and Sr, Rb, K, U and Th abundances. Geochem. Cosmochim. Acta, v. 32, pp. 699-735.

Franklin, J.M., Kasarda, J., and Poulsen, K.H., 1975. Petrology and chemistry of the alteration zone of the Mattabi massive sulphide deposit. Econ. Geol., v. 70, pp. 63-79.

Franklin, J.M., Gibb, W., Poulsen, K.H. and Severin, P., 1977. Archean metallogeny and stratigraphy of the south Sturgeon Lake area. Inst. on Lake Superior Geology, 23rd Ann. Mtg., Thunder Bay, Ont., Guidebook, 73 pp.

Franklin, J.M., Lydon, J.W. and Sangster, D.F., 1981. Volcanic-associated massive sulphide deposits. Econ. Geol., 75th Anniversary volume, pp. 485-627.

Garrels, R.M., and Mackenzie, F.T., 1971. Evolution of sedimentary rocks. W.W. Norton & Company, Inc., N.Y., 397 pp.

Gillis, J.W., 1972. Geology of the Port aux Basques map area, Newfoundland. Geol. Surv. of Can., Paper 71-42, 6 pp., plus 1:250,000 map.

Gjelsvik, I., 1968. Distribution of major elements in the wall rocks and silicate fraction of the Skorovass pyrite deposit, Grong area, Norway. Econ. Geol., v. 63, pp. 217-231.

Goodfellow, W.D., 1975. Major and minor element halos in volcanic rocks at Brunswick #12 sulphide deposits, N.B., Canada. In: Elliot, I.L., and Fletcher, W.K. (ed.), Geochemical Exploration, 1974. Elsevier, Amsterdam, pp. 279-295.

Goodwin, A.M., 1977. Archean volcanism in Superior Province, Canadian Shield. In: Volcanic Regimes in Canada, Barager, W.R.A., Coleman, L.C., Hall, J.M. (ed.), Geol. Assoc. Can., Spec. Paper No. 16, pp. 205-241.

Gould, D., 1966. Geochemical and mineralogical studies of the granitic gneiss and associated rocks of Western Ardgour, Argyll. Unpubl. Ph.D. Thesis, Univ. Edinburgh.

Govett, G.J.S., 1972. Interpretation of a rock geochemical exploration survey in Cyprus - statistical and graphical techniques. J. Geochem. Explor. v. 1, pp. 77-102.

Govett, G.J.S. and Nichol, I., 1979. Lithogeochemistry in mineral exploration. In: Hood, P.J. (ed.), Geophysics and geochemistry in the search of metallic ores. Geol. Surv. Can., Econ. Geol. Report 31, pp. 339-362.

Govett, G.J.S. and Pantazis, T.M., 1971. Distribution of Cu, Zn, Ni, and Co in the Troodos pillow lava series, Cyprus. Inst. Min. Metall. Trans., Sec. B, v. 80, pp. 1327-1347.

Gustafson, L.B., and Hunt, J.P., 1975. The porphyry copper deposit at El Salvador, Chile. Econ. Geol., v. 70, pp. 857-912.

Hawkes, H.E., and Webb, J.S., 1962. Geochemistry in mineral exploration. Harper and Row Publishers, New York, 415 pp.

Helwig, J.T., and Council, K.A., 1979. (Ed.) SAS users guide, 1979 edition. SAS Institute Statistical Analysis System, SAS Institute Inc., Cary, North Carolina, U.S.A., 650 pp.

Hemley, J.J., and Jones, W.R., 1964. Chemical aspects of hydrothermal alteration with emphasis on hydrogen metasomatism. Econ. Geol., v. 59, pp. 539-569.

Henley, R.W., and Thornley, P., 1981. Low grade metamorphism and the geothermal environment of massive sulphide ore formation, Buchans, Newfoundland. In: Swanson, E.A., Strong, D.F. and Thurlow, J.G. (eds), The Buchans Orebodies: fifty years of mining and geology. Geol. Assoc. Can., Spec. Paper 22, pp. 205-228.

Hinchey, J.P., and Prince, D.R., 1980a. Report on lithogeochemical studies on the Strickland-Porter Fee simple option, Newfoundland, NTS 110/16. Unpubl. Co. Report, Falconbridge Nickel Mines Ltd., 9 pp.

Hinchey, J.P., and Prince, D.R., 1980b. Report on the 1980 drilling program, Strickland-Porter et al. option, Hermitage Flexure, SW Coast Nfld., 110/16. Unpubl. Co. Report, Falconbridge Nickel Mines Ltd., 7 pp.

Hodgson, C.J. and Lydon, J.W., 1977. Geological setting of volcanogenic massive sulphide deposits and active hydrothermal systems: some implications for exploration. Can. Min. and Metall. Bull., v. 70, pp. 95-106.

Hutchison, M.N., and Scott, S.D., 1981. Sphalerite geobarometry in the Cu-Fe-Zn-S system. Econ. Geol., v. 76, pp. 143-153.

Indorf, C., 1981. The Silver Hill zinc deposit and associated deposits, central North Carolina. Econ. Geol., v. 76, pp. 1170-1185.

Ishihara, S., 1974. (Ed.) Geology of Kuroko Deposits. Soc. Min. Geol., Spec. Issue 6, 435 pp.

Ishikawa, et al., 1976. (In Japanese) See Izawa et al., 1978

Izawa, E., 1980. Hydrothermal alteration associated with Kuroko-type mineralization: an example from the Iwami mining district, Shimane, Japan. In: Ridge, J.D. (ed.), IAGOD symposium, 5th: Stuttgart, E., Schweizerbart'sche Verlagsbuchhandlung, pp. 697-707.

Izawa, E., Yoshida, T., Saito, R., 1978. Geochemical characteristics of hydrothermal alteration around the Fukazawa Kuroko Deposit, Akita, Japan. Mining Geol. v. 28, pp. 325-335.

Jolly, W.T., 1980. Development and degradation of Archean lavas, Abitibi area Canada, in light of major element chemistry. Jour. of Pet., v. 21, part 2, pp. 323-363.

Kerlinger, F.N., and Pedhazur, E.J., 1973. Multiple regression in behavioural research. Holt, Rinehart and Winston, N.Y., 534 pp.

Kerr, P.F., 1959. Optical mineralogy: McGraw-Hill Book Company, Inc. Toronto, 442 pp.

Kerrich, R., and Fryer, R.J., 1981. The separation of rare elements from abundant base metals in Archean lode gold deposits: implication of low water/rock source regions. Econ. Geol., v. 76, no. 1, pp. 160-166.

Klovan, J.E., and Billings, C.K., 1967. Classification of geological samples by discriminant function analysis. Bull. Can. Pet. Geol., v. 15, no. 3, pp. 313-330.

Knuckey, M.J., 1975. Geology of the Millenbach copper-zinc orebody, Noranda District, Quebec (abstr.). In: Soc. of Econ. Geol. meeting with AIME, Econ. Geol., vol. 70, no. 1, p. 247.

Koo, J., and Mossman, D., 1975. Origin and metamorphism of the Flin Flon stratabound Cu-Zn sulphide deposit, Saskatchewan and Manitoba. Econ. Geol., v. 70, pp. 48-62.

Koch, G.S., and Link, R.F., 1971. Statistical analysis of geological data. John Wiley and Sons, New York, N.Y., Vols. I and II, 858 pp.

Krumbein, W.C., and Graybill, F.A., 1965. An introduction to statistical models in geology. McGraw-Hill, New York, N.Y., 475 pp.

Kuroda, Y., 1961. Minor elements in metasomatic zones related to a copper-bearing pyrite deposit. Econ. Geol., v. 56, pp. 847-854.

Lambert, I.B., 1976. The McArthur zinc-lead-silver deposit: features, metallogenesis and comparisons with some other stratiform ores. In: Wolf, K.H. (ed.), Handbook of stratabound and stratiform ore deposits. Elsevier, Amsterdam, v. 6, pp. 535-586.

Lambert, I.B., and Sato, T., 1974. The Kuroko and associated ore deposits of Japan: A review of their features and metallogenesis. Econ. Geol., v. 69, pp. 1215-1236.

Langmhyer, F.J., and Paus, P.E., 1968. The analysis of inorganic siliceous materials by atomic absorption spectrophotometry and the hydrofluoric acid decomposition technique, Part 1: The analysis of silicate rocks. Anal. Chem. Acta., v. 43, pp. 397-408.

Large, R.R., 1977. Chemical evolution and zonation of massive sulphide deposits in volcanic terrains. Econ. Geol., v. 72, no. 4, pp. 549-572.

Lavin, O., 1976. Lithogeochemical discrimination between mineralized and unmineralized cycles of volcanism in the Sturgeon Lake and Ben Nevis areas of the Canadian Shield. Unpubl. M.Sc. Thesis, Queen's University, Kingston, Ontario, Canada. 249 pp.

Maxwell, J.A., 1968. Rock and mineral analysis. Interscience, John Wiley and Sons, pp. 394-396.

McBride, D.E., 1976. Tectonic setting of the Tetagouche Group, host to the New Brunswick polymetallic massive sulphide deposits. In: Metallogeny and Plate Tectonics, Strong, D.F., (ed), Geol. Assoc. Can., Spec. Paper 14, pp. 473-485.

McConnell, J.W., 1976. Geochemical dispersion in wallrocks of Archean massive sulphide deposits. Unpubl. M.Sc. Thesis, Queen's University, Kingston, Ontario. 230 pp.

Miyashiro, A., 1973. Metamorphism and metamorphic belts. John Wiley and Sons (New York), 479 pp.

Nichol, I., Bogle, E.W., Lavin, O.P., McConnell, J.W. and Sopuck, V.J., 1977. Lithogeochemistry as an aid in massive sulphide exploration. In prospecting in areas of glaciated terrain, Jones M.J. (ed.), Inst. Min., Met., London, pp. 63-71.

Nie, N.W., Hull, H.C., Jenkins, J.G., Steinbrenner, K., and Bent, D.J., 1975. (ed.). Statistical package for the social sciences 2nd ed., McGraw-Hill Inc., N.Y., 675 pp.

Nilsson, C.A., 1968. Wall rock alteration at the Boliden deposit, Sweden. Econ. Geol., v. 63, pp. 472-494.

O'Driscoll, C.F., and Gibbons, R.V., 1980. Geochronology report, Newfoundland and Labrador, editors of Current Research, Newfoundland Dept. of Mines and Energy, Mineral Development Division, Report 80-1, pp. 143-146.

Oskarsson, N., Sigvaldason, G.E., and Steinthorsson, S., 1982. A dynamic model of rift zone petrogenesis and the regional petrology of Iceland. Jour. of Pet., v. 23, pp. 28-74.

Parry, S., and Hutchinson, R.W., 1981. Origin of a complex alteration assemblage, Four Corners Cu-Zn prospect, Quebec, Canada. Econ. Geol., v. 76, no. 5, pp. 1186-1201.

Payne, J.G., Bratt, J.A., and Stone, B.G., 1980. Deformed mesozoic volcanogenic Cu-Zn sulfide deposits in the Britannia District, British Columbia. Econ. Geol., v. 75, no. 5, pp. 700-721.

Pettijohn, F.J., 1963. Chemical composition of sandstones - excluding carbonate and volcanic sands, chapter 5. In: Fleischer, M., (ed.), Data of geochemistry. U.S. Geol. Surv., Prof. Paper 440-5.

Prince, D., 1977a. Hermitage project, PN 820. Report on the geology and mineral occurrences of the Hermitage Flexure, La Poile to Grey River, south coast, Newfoundland. Unpubl. co. report, Falconbridge Nickel Mines Ltd., 20 pp.

Prince, D., 1977b. Hermitage project, PN 820, preliminary report on the geology and mineral occurrences of the Bay du Nord Group, Partriige Pond to North Bay Pt. section, La Poile River, Newfoundland. Unpubl. co. report, Falconbridge Nickel Mines Ltd., 14 pp.

Prince, D., 1978. Report on the geological, geophysical and geochemical investigations on the Hermitage Flexure project, 1978 season, Part IV, Examination of the Strickland Showing. Unpubl. co. report, Falconbridge Nickel Mines Ltd., 9 pp.

Prince, D., and Briggs, D.N., 1978. Report on the geological, geophysical and geochemical investigations on the Hermitage Flexure Project, 1978 season, Part III: Grid investigation of the area around the Strickland Showings. Unpubl. co. report, Falconbridge Nickel Mines Ltd., 12 pp.

Pwa, U.A., 1977. Regional rock geochemical exploration, Bathurst District, N.B. Unpubl. M.Sc. Thesis, University of New Brunswick, Fredericton, N.B.

Reading, A.L., 1933. Unpublished excerpts from a report on the Cinq Cerf Brook mining property to Burgeo Mines Limited, 8 pp.

Riverin, G., 1977. Wall-rock alteration at the Millenbach mine, Noranda area, Quebec. Unpubl. Ph.D. Thesis, Queen's University, Kingston, 255 pp.

Riverin, G., and Hodgson, C.J., 1980. Wall-rock alteration at the Millenbach Cu-Zn mine, Noranda, Quebec. Econ. Geol., v. 75, p. 424-444.

Roberts, R.G., and Reardon, E.J., 1978. Alteration and ore-forming processes at Matagami Lake mine, Quebec. Can. J. Earth Sci., v. 15, pp. 1-21.

Rose, A.W., Dalberg, R.C., and Keith, M.L., 1970. A multiple regression technique for adjusting background values in stream sediment geochemistry. Econ. Geol., v. 65, pp. 156-165.

Rui, I.J., 1973. Structural control and wall rock alteration at Killingdal mine, central Norwegian Caledonides. Econ. Geol., v. 68, pp. 859-883.

Sakrison, H.C., 1966. Chemical studies of the host rocks of the Lake Dufault mine, Quebec. Unpubl. Ph.D. Thesis, McGill University.

Sangster, D.F., 1972. Precambrian volcanogenic massive sulphide deposits in Canada, a review. Geol. Surv. Can., Paper 72-122, 44 pp.

Sangster, D.F., 1980. Quantitative characteristics of volcanogenic massive sulphide deposits in volcanic centres. Can. Min. Metall. Bull., v. 73, pp. 74-81.

Sangster, D.F., and Scott, S.D., 1976. Precambrian strata-bound massive Cu-Zn-Pb sulphide ores of North America. In: Wolfe, K.H. (ed.), Handbook of Stratabound and Stratiform ores. Elsevier, Amsterdam, pp. 129-222.

Sato, T., 1972. Behaviours of ore-forming solutions in seawater. Mining Geol., v. 22, pp. 31-42.

Sato, T., 1977. Kuroko deposits: their geology, geochemistry and origin. In: Volcanic processes in ore genesis, (Anonymous), Inst. Mining Metallurg., London, pp. 153-161.

Scott, S.D., 1973. Experimental calibration of the sphalerite geobarometer: Econ. Geol., v. 68, pp. 466-474.

Scott, S.D., 1974. Experimental methods in sulphide synthesis. In: Ribbe, R.H. (ed.) Sulphide Mineralogy, Mineral Soc. America, Short Course Notes, v. 1, pp. 1-38.

Scott, S.D., 1976. Application of the sphalerite geobarometer to regionally metamorphosed terrains. Am. Mineral., v. 61, pp. 661-670.

Scott, S.D., 1978. Structural control of the Kuroko deposits of Hokuroku district, Japan. Mining Geol., v. 28, pp. 301-311.

Scott, S.D., 1980. Geology and structural control of Kuroko-type massive sulphide deposits. In: Geol. Assoc. Can. Spec. Paper 20, pp. 705-722.

Scott, S.D., and Barnes, H.L., 1971. Sphalerite geothermometry and geobarometry, Econ. Geol., v. 66, pp. 653-669.

Shirozu, H., 1974. Clay minerals in altered wall rocks of the Kuroko-type deposits. In: Ishihara, S. (ed.), Geology of the Kuroko Deposits. Mining Geology Special Issue No. 6, pp. 303-310.

Simmons, B.D., 1973. Geology of the Millenbach massive sulphide deposit, Noranda, Quebec. Can. Min. Metall. Bull., v. 166, no. 739, pp. 67-68.

Slack, J.F., 1981. Prospecting with tourmaline for stratabound massive sulphide deposits: examples from the Appalachian-Caledonide orogen. Inst. Mining Metallurgy Trans., v. 90, sec. B, pp. B56.

Slack, J.F., and Taylor, B.E., 1980. Tourmalines associated with Appalachian massive sulphide deposits (abs.). Geol. Soc. Amer., Abs. with Pgms., 12, 198, pp. 523.

Smyth, W.R., 1979. Reconnaissance of the Burgeo map area (11P west half), Newfoundland. In: Report of activities for 1978. Gibbons, R.V. (ed.), Newfoundland Dept. of Mines and Energy, Mineral Development Division, Report 79-1, pp. 54-57.

Smyth, W.R., 1980. Reconnaissance geology of White Bear River (11 P/14) and Dollard Brook (11 P/15) map areas. The In: Current research. O'Driscoll, C.F., and Gibbons, R.V., (eds.), Newfoundland Dept. of Mines and Energy, Mineral Development Division, Report 80-1, pp. 89-92.

Snelgrove, A.K., 1935. Geology of the gold deposits of Newfoundland. Dept. of Natural Resources, Geological Section, Bull. 2, 46 pp.

Sopuck, V.J., 1977. A lithogeochemical approach in the search for an area of felsic volcanic rocks associated with mineralization in the Canadian Shield. Unpubl. Ph.D. Thesis, Queen's University, Kingston, Ontario, 400 pp.

Sopuck, V.J., Lavin, O.P., and Nichol, I., 1980. Lithogeochemistry as a guide to identifying favourable areas for the discovery of volcanogenic massive sulphide deposits. Can. Inst. Min. Metal. Bull., v. 73, no. 823, pp. 152-166.

Stackhouse, J.C., 1976. Economic geology of the southwestern Bay du Nord Group, North Bay, Newfoundland. Unpubl. B.Sc. Thesis, Memorial University of Newfoundland, 59 pp.

Stevens, R.K., Strong, D.F., and Kean, B.F., 1974. Do some eastern Appalachian ultramafic rocks represent mantle diapires above a subduction zone? Geology, v. 2, pp. 175-178.

Strong, D.F., Dickson, W.L., O'Driscoll, C.F., Kean, B.F., and Stevens, R.K., 1974. Geochemical evidence for eastward Appalachian subduction in Newfoundland. Nature, 248, pp. 37-39.

Sundblad, K., 1980. A tentative "volcanogenic" formation model for the sediment-hosted Ankarvattnet Zn-Cu-Pb massive sulphide deposit, central Swedish Caledonides, Norq. Geol. Unders., 360, pp. 211-227.

Swinden, H.S., 1981. Economic geology of the western Hermitage Flexure, Newfoundland. In: Current Research, O'Driscoll, C.F. and Gibbons, R.V. (eds.), Nfld. Dept. Mines and Energy, Report 81-1, pp. 80-95.

Tatsumi, T., and Clark, L.A., 1972. Chemical composition of acid volcanic rocks genetically related to formation of the Kuroko deposits. J. Geol. Soc. Japan, v. 78, pp. 191-201.

Thurlow, J.G., 1980. Geology, ore deposits and applied rock geochemistry of the Buchans Group. Unpubl. Ph.D. Thesis, Memorial University of Newfoundland, 314 pp.

Thurlow, J.C., Swanson, E.A., and Strong, D.F., 1975. Geology and lithogeochemistry of the Buchans polymetallic sulphide deposit, Newfoundland. Econ. Geol., v. 70, no. 1, pp. 130-144.

Vokes, F.M., 1969. A review of the metamorphism of sulphide deposits. Earth Sci. Rev., v. 5, pp. 99-143.

Wahl, J.L., Govett, G.J.S., and Goodfellow, W.D., 1975. Anomalous element distribution in volcanic rocks around Key Anacon, Heath Steele, B-zone and Brunswick No. 12 sulphide deposits (abstract), Can. Inst. Min. Met. Bull., v. 68, no. 755, p. 49.

Walford, D.C., and Franklin, J.M., 1982. The Anderson Lake Mine, Snow Lake, Manitoba. In: Precambrian sulphide deposits (H.S. Robinson memorial volume), Hutchinson, R.W., Spence, C.D., and Franklin, J.M. (eds.). Geol. Assoc. Can. Spec. Paper 25, 800 pp.

Wedepohl, K.H., 1969. Composition and abundance of common sedimentary rocks. Chapter 8, In: Wedepohl, K.H., (ed), Handbook of geochemistry, v. 1, Springer-Verlag, New York, 442 pp.

Whitehead, R.E.S., and Govett, G.J.S., 1974. Exploration geochemistry - detection of trace element haloes at Heath Steele Mines (N.B., Canada) by discriminant analysis. J. Geochem. Explor., v. 3, pp. 371-396.

Willan, R.C.R., and Hall, A.J., 1980. Sphalerite geobarometry and trace-element studies on stratiform sulphide from McPhun's Cairn, Loch Fyne, Argyll, Scotland. Inst. Min. Metall., Trans., Sect. B, v. 89, pp. 31-40.

Williams, H., 1979. Appalachian orogen in Canada. Can. Jour. Earth Sci., v. 16, pp. 792-807.

Winkler, H.G.F., 1976. Petrogenesis of metamorphic rocks, 4th edition, Springer-Verlag, New York, 334 pp.

APPENDIX A

SPHALERITE ANALYSES

A.1 Textured red-brown sphalerite as inclusions in pyrite

Slide no.	Point no.	weight % S	Fe	Zn	Total	mole% FeS
W5018D	2	32.50	8.12	59.36	99.98	7.03
W5018D	1	32.16	7.79	59.91	99.86	6.77
W5025	5	32.58	8.16	60.29	101.03	7.01
W5025	4	33.68	8.57	59.11	101.36	7.28
W5025	3	32.96	8.17	59.97	101.10	6.99
W5025	2	32.50	8.26	59.21	99.96	7.15
W5025B	1	32.38	8.18	58.68	99.23	7.00
W5025B	1	32.38	8.03	59.36	99.78	6.97
W5017A	3	31.71	8.72	58.80	99.24	7.63
W5017A	2	31.86	8.71	58.93	99.50	7.60
W5025A	3	32.06	8.14	59.04	99.23	7.11
W5025A	3	32.32	8.36	58.58	99.27	7.29
W5025A	2	32.42	8.46	58.66	99.54	7.35
NR*	NR	32.75	9.12	58.45	100.32	7.85
NR	NR	32.89	8.89	58.28	100.05	7.67
NR	NR	32.87	9.22	57.62	99.70	7.97
NR	NR	32.33	8.70	58.23	99.27	7.58
W5028	4	32.89	8.64	58.67	100.20	7.33
W5028	4	33.11	9.05	59.00	101.15	7.72
W5028	3	31.81	9.30	58.07	99.18	8.13
W5028	1	32.59	8.63	59.19	100.41	7.44

* NR = Not recorded

Appendix A
A.1 continued.

Slide no.	Point no.	weight % S	Fe	Zn	Total	mole% FeS
W5028	6	33.15	9.08	58.36	100.59	7.78
W5075	2	32.53	7.75	59.63	99.92	6.72
W5017B	1	33.08	8.10	59.16	100.34	6.96

A.2 Textured red-brown sphalerite—matrix.

Slide no.	Point no.	weight % S	Fe	Zn	Total	mole% FeS
W5018D	4	32.72	7.89	59.73	100.35	6.8
W5018D	2	33.09	7.54	59.72	100.35	6.5
W5025	3	33.65	8.04	59.87	101.56	6.8
W5025A	NR	33.49	7.84	58.75	100.09	6.7
W5025A	NR	33.08	8.51	59.23	100.82	7.3
W5028	NR	33.59	7.91	60.19	101.70	6.7
W5075	3	33.43	8.40	59,87	101.70	7.1
W5075B	5	32.45	8.35	59.43	100.22	7.2

A.3 Clear red-brown sphalerite—matrix

Slide no.	Point no.	weight % S	Fe	Zn	Total	mole% FeS
W5018D	4	31.85	7.07	59.49	98.41	6.2
W5028	NR	32.99	7.41	59.45	98.86	6.4
W5028	NR	32.94	7.52	59.25	99.71	6.5
W5017B	3	32.59	8.32	59.46	100.36	7.2
W5075B	5	32.30	8.49	58.94	99.73	7.4

Appendix A

A.4 Yellow sphalerite—as inclusions in pyrite

Slide no.	Point no.	weight % S	Fe	Zn	Total	mole% FeS
W5018D	3	31.77	5.25	62.39	99.31	4.6
W5018D	3	31.45	5.30	61.66	98.40	4.7
W5018D	2.5	32.55	5.12	62.54	100.21	4.3
5018D	2	32.29	4.20	63.91	100.41	3.6
5018D	2	32.96	4.48	63.00	100.44	3.9

A.5 Yellow sphalerite as isolated grains in quartz gangue

Slide no.	Point no.	weight % S	Fe	Zn	Total	mole% FeS
W5017A	1	32.29	3.80	63.86	99.95	3.3
W5017A	1	32.02	3.69	64.30	100.02	3.0

APPENDIX B

ANALYTICAL METHODS

B.1 Major elements

All the major elements were determined with the assistance of G. Andrews using a Perkin Elmer 370 Atomic Absorption spectrophotometer. The digestion technique used was similar to that described by Langmhyr and Paus (1968). Exactly 0.1000g of sample was weighed and placed in a polystyrene digestion bottle. Digestion was affected by addition of 5ml of concentrated HF and heating on a water bath for 20 minutes. Samples were subsequently cooled and 50ml of boric acid added to complex undissolved fluorides. The samples were heated again, then diluted with 145ml of distilled and de-ionized water. Standards were prepared in a manner similar to that described by Abbey (1968).

Copper was determined for a selected number of surface samples following the same digestion technique but with an initial sample weight of 0.5000g.

Calcium and magnesium were determined using an air-acetylene flame by adding a lanthanum oxide-HCl solution to suppress interference by aluminum. Phosphorus was determined colourimetrically using a Baush and Lomb Spectronic 21 spectrophotometer using a method similar to that described by Maxwell (1968).

B.2 Trace elements

Trace elements were determined for 128 surface samples using a Phillips 1450 X-Ray fluorescence spectrometer calibrated against international standards. The samples were run as pellets prepared by pressing approximately 10g of rock powder and 1.25g of phenol formaldehyde under 50 MPa pressure in a 40 mm diameter die for 1 minute, then baking at 200°C for 10 minutes.

APPENDIX C

PRECISION ESTIMATES

An estimate of the precision of the analyses was calculated from the differences between duplicates on 17 different samples, as outlined by Gould (1966, p. 49), viz.

if X_1; X_2 = two determinations on a single sample,

$\bar{x}$ = mean of a number of determinations, n, and

s = standard deviation from the mean, then

$$s^2 = \frac{\Sigma(x - \bar{x})^2}{n - 1} = \frac{(x_1 - x_2)^2}{2} \text{ and } s = \frac{x_1 - x_2}{\sqrt{2}}$$

The precision can thus be estimated by averaging $(X_1 X_2)/\sqrt{2}$ for all the pairs of duplicate analyses. The results of this method which compare the analyses of samples run in several different batches to those same samples run in a single batch at the end of the analytical period are presented in Table C.1. Plots of SiO_2 and MnO (Figure C.1a, b) are presented as examples of the correlation between the two sets of data.

A similar statistical comparison was done to examine the compatibility or reproducibility of the analyses done in the Memorial University of Nfld. geochemistry labs (M.U.N. labs) by Atomic Absorption and those done by X-Ray Labs. of Toronto (X-Ray Labs) by X-ray fluorescence (Table C.2).

As expected, the between labs results show an overall larger standard deviation(s) (Table C.2) than the within lab results (Table C.1). However, both sets of precision

Table C.1

Statistical comparison of the analytical results from samples analysed in several batches throughout the analytical period and those same samples analysed in a single batch at the end of the analytical period (See Figure C.1)

Element	$\bar{x}_1$	S_1	$\bar{x}_2$	S_2	$\bar{S}$	R^2	Reg. Coef.	Intercept
SiO_2	68.6	12.1	69.3	11.8	.78	.9901	1.0238	-2.3504
TiO_2	0.82	0.93	0.80	0.93	.03	.9959	1.0017	.0149
Al_2O_3	12.2	3.0	12.2	3.0	.20	.9855	1.0107	-.0744
FeO	5.59	4.99	5.58	5.04	.06	.9996	.9902	.0591
MnO	0.19	0.22	0.17	0.19	.02	.9969	1.1577	-.0035
MgO	2.34	2.78	2.28	2.71	.05	.9998	1.0297	-.0082
CaO	1.42	2.36	1.36	2.36	.08	.9874	.9931	.0706
Na_2O	2.59	1.93	2.68	1.99	.10	.9894	.9652	-.0023
K_2O	3.02	2.66	3.03	2.69	.05	.9987	.9893	.0231
P_2O_5	0.15	0.26	0.25	0.35	.07	.8883	.6972	-.0257
LOI	1.75	1.87	1.38	1.38	.38	.4869	.9499	.4410

$\bar{x}_1$, S_1 = mean and standard deviation of those analyses from samples of several different batches.

$\bar{x}_2$, S_2 = mean and standard deviation of those analyses from duplicate samples analysed in a single batch.

$\bar{S}$ = precision estimate of the method calculated from differences between duplicate analyses (Gould, 1966).

R^2 = measure of how well the regression equation fits the data (single batch plotted vs several batch analyses).

Reg.Coef. = regression coefficient (with the several batch analyses as independent variable in the regression equation).

Intercept = intercept on the y-axis of the regression line.

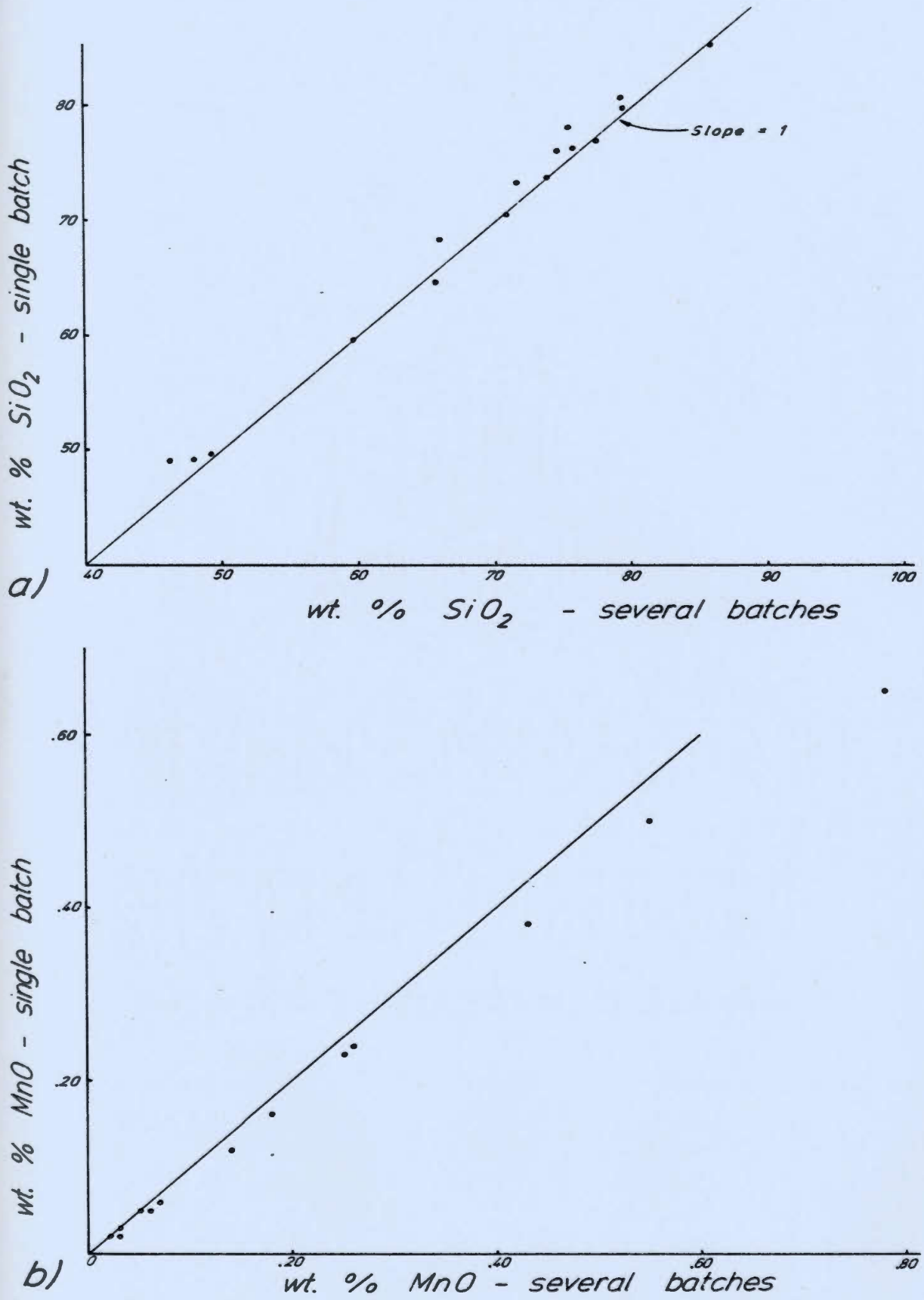

Figure C.1. Comparision of a) wt. % SiO_2 and b) wt. % MnO between single batch analyses and analyses from several batches.

Table C.2

Statistical comparison of the analytical results from samples analysed for major elements by both the Memorial University of Nfld. (M.U.N.) geochemistry lab and X-Ray Labs of Toronto (See Figure C.2)

Element	$\bar{x}_1$	S_1	$\bar{x}_2$	S_2	S	R^2	Reg. Coef.	Intercept
SiO_2	67.7	10.7	67.1	10.7	1.03	.9660	.9839	1.6995
TiO_2	0.89	0.93	0.90	0.91	0.43	.9903	1.0175	-.0305
Al_2O_3	12.1	2.7	12.2	2.8	0.24	.9788	.9517	.5000
FeO	5.95	3.15	6.39	3.45	0.31	.9916	.9098	.1433
MnO	0.11	0.10	0.13	0.11	0.01	.9618	.9127	-.0008
MgO	2.72	2.90	2.65	2.72	0.15	.9848	1.0582	-.0892
CaO	1.33	1.95	1.43	1.86	0.09	.9988	1.0464	-.1603
Na_2O	1.60	1.30	1.62	1.26	0.06	.9942	1.0273	-.0595
K_2O	3.04	1.93	2.90	1.80	0.11	.9955	1.0682	-.0591
P_2O_5	0.15	0.17	0.18	0.19	0.02	.9687	.8815	-.0096
LOI	2.47	1.40	2.31	1.22	0.22	.9277	1.1060	-.0823

$\bar{x}_1$, S_1 = mean and standard deviation of those analysed done by Memorial University of Nfld. geochemistry Lab.

$\bar{x}_2$, S_2 = mean and standard deviation of those analyses done by X-Ray Labs of Toronto.

S = precision estimate of the two data sets (X-Ray Lab and M.U.N. lab) calculated from differences between duplicate analyses (Gould, 1966).

R^2 = measure of how well the regression equation fits the data.

Reg.Coef. = regression coefficient (with the M.U.N. lab data as the independent variable in the regression equation).

Intercept = intercept on the y-axis of the regression equation.

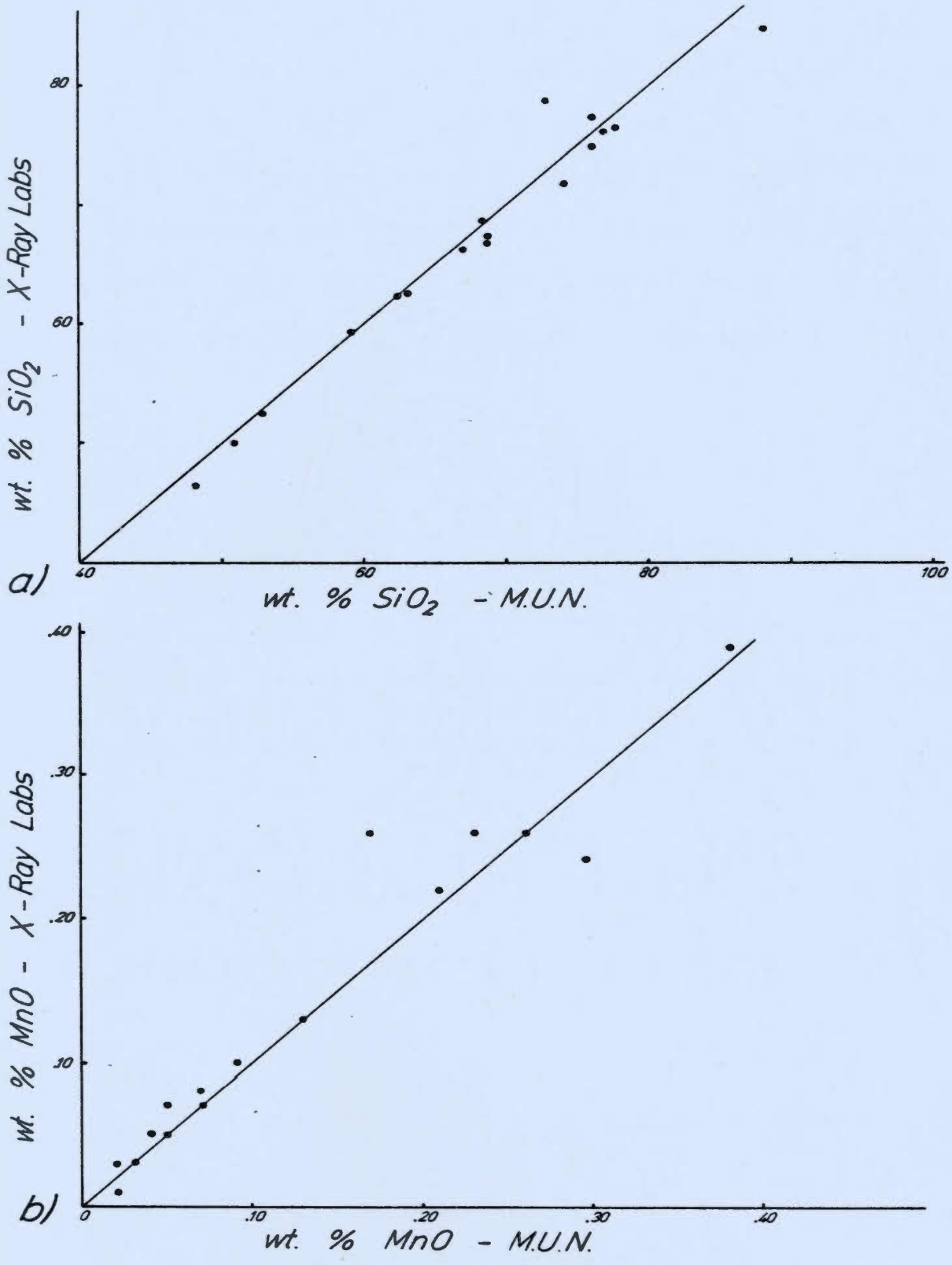

Figure C.2. Comparision of a) wt. % SiO_2 and b) wt. % MnO analyses done by the M.U.N. and X-Ray Labs.

estimates fall well within acceptable ranges of error for all the elements (SiO_2 + 0.78% or + 1.03%, Na_2O + 0.1%, + 0.06%). A statistical comparison of Pb and Zn analyses done by X-Ray Labs of Toronto (using a warm HNO_3-HCl digestion) and by the method outlined above in the M.U.N. labs is presented in Table C.3. Figure C.3 shows plots of the two data sets and the poorer correlation of the Pb data is evident. No regression analysis was done on this data.

Table C.3

Statistical comparison of the analytical results from samples analysed for trace elements by both M.U.N. labs and X-Ray Labs (see Figure C.3)

	Pb	Zn
$\bar{x}_1$	12.0	41
S_1	9.9	35
$\bar{x}_2$	6.6	34
S_2	9.0	31
S	4.5	8.5
n	59	56

$\bar{x}_1$, S_1 = mean and standard deviation of M.U.N. lab analyses.
$\bar{x}_2$, S_2 = mean and standard deviation of X-Ray lab analyses.
S = precision of the results from the two labs calculated from differences between duplicate analyses of the same rocks (Gould, 1966).
n = nos. of duplicate samples.

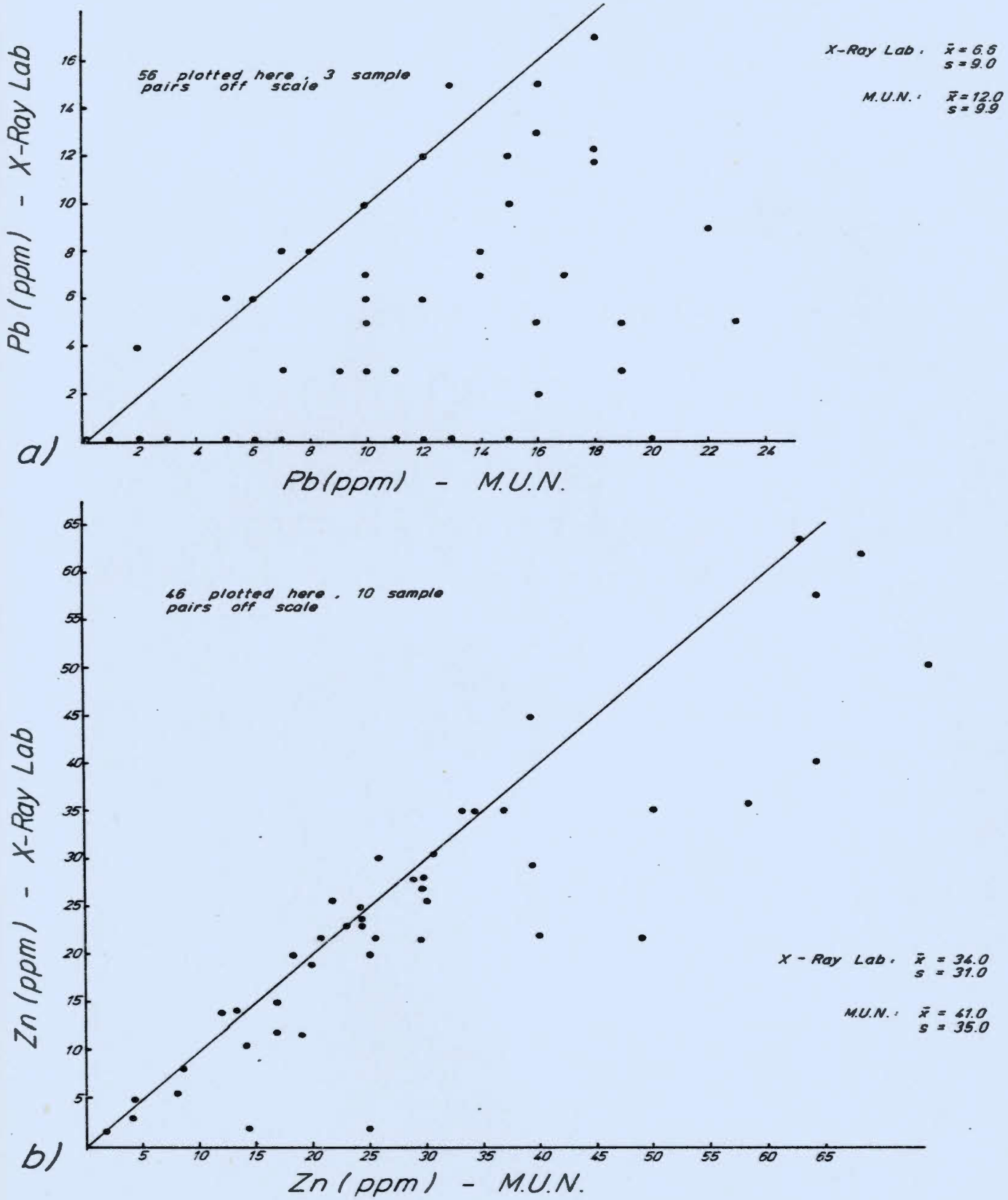

Figure C.3. Comparision of a) Pb and b) Zn analyses done by the M.U.N. and X-Ray Labs.

APPENDIX D

Coding scheme used on the sample description card in the data list:

SAMPLE	11000	- samples collected by Falconbridge personnel are usually prefaced by a 1.
	25009	- samples collected by P. J. Wynne are prefaced by a 2. On the sample location map this sample appears as W5009.
EASTING	+265E	- 265 m east of the OOE baseline
	-1210S	- 1210 m south of the OON baseline
TYPE	1	- surface sample
	2	- diamond drill core sample
DRILLHOLE	160230002	- a hole drilled on the Strickland/Porter fee simple by Falconbridge.
	160200002	- a hole drilled on the claim blocks surrounding the Strickland/Porter fee simple by Falconbridge.
	10009	- a hole drilled by Kopan Developments Ltd. — this appears as K-9 in Figure 6.1, p.
	20010	- a hole drilled by Long Lac Mineral Exploration Ltd. — this appears as L-10 in Figure 6.1, p.113.

LITHOLOGY	LITHCODE	
M:TF	1	- mafic tuff
S#CH	2	- chlorite schist
I:TF	3	- intermediate tuff
I:LT	4	- intermediate lapilli tuff
I:AG	5	- intermediate agglomerate
I:FL	6	- intermediate flow
F:TF	7	- felsic tuff
F:LT	8	- felsic lapilli tuff
F:AG	9	- felsic agglomerate
F:FL	10	- felsic flow
SSLT	11	- siltstone
SSST	12	- sandstone
SHAL	13	- shale
GRAN	14	- granite (Baggs Hill)
D/F:	15	- felsic dyke
D/M:	16	- mafic dyke
CGXX	17	- conglomerate
TFSD	18	- tuffaceous sediment
SEDM	19	- sedimentary rock
CARB	20	- carbonate, carbonate-tremolite
M:LT	21	- mafic lapilli tuff

Appendix D continued

TS/PTS	1	- thin section made
	2	- polished thin section made
ALTERATION	SIL	- silica
	SER	- sericite
	CAR	- carbonate
	ACT	- actinolite
	CHL	- chlorite
	V/QZ	- quartz veins
	FEO	- iron staining
MINERALIZATION	PY	- pyrite
	PR	- pyrrhotite
	SL	- sphalerite
	CP	- chalcopyrite
	GA	- galena
COMMENTS		- usually subordinate lithologies, see LITHOLOGY
	CHER MTX	- cherty matrix
	BASC	- basic rock
	STXX	- sedimentary rock
DEPTH	154.0	- 154.0 m down the hole to the top of the sample
WIDTH	7.6	- a 7.6 m length of core was sampled

SAMPLE	EASTING	NORTHING	TYPE	DRILLHOLE	LITHOLOGY	LITHCODE	TS/PTS	ALTERATION	MINERALIZATI
11000	+ 265E	-1210S	1	0	SSST	12	0		
1323	+ 300E	-1300S	1	0	SSST	12	0		
1324	+ 205E	-1300S	1	0	SSST	12	0		
1325	+ 370E	-1300S	1	0	SHAL	13	0		
1326	+ 175E	-1300S	1	0	SSST	12	0		
13634			2	160230002	I:TF	3	0		
13635			2	160230002	F:LT	8	0		
13636			2	160230002	M:TF	1	0		
13637			2	160230002	F:LT	8	0	SIL SER	
13638			2	160230002	SSLT	11	0		
13639			2	160230001	F:TF	7	0		
13640			2	160230001	M:TF	1	0		
13641			2	160230001	F:LT	8	0		
13642			2	160230001	CARB	20	0	CAR TRE	
13643			2	160230001	SEDM	19	0		
13644			2	20010	F:TF	7	0		
13645			2	20010	I:TF	3	0		
13646			2	20010	F:TF	7	0	SIL SER	
13647			2	20010	I:TF	3	0		
13659			2	10001	M:TF	1	0		
13660			2	10001	F:LT	8	0	SIL SER	
13661			2	10001	SSLT	11	0		
13662			2	10009	F:TF	7	0		
13663			2	10009	F:LT	8	0	SIL SER	
13664			2	10009	SSLT	11	0		
13665			2	20001	M:TF	1	0		
13666			2	20001	I:TF	3	0		
13667			2	20001	F:LT	8	0	SIL SER	

SAMPLE	SiO2	TiO2	Al2O3	FeO	MnO	MgO	CaO	Na2O	K2O	P2O5	LOI	Zr	Sr	Rb	
11000	79.70	.22	7.92	2.79	.04	.79	1.73	1.82	.56	.28	1.31	74	104	26	
1323	85.30	.21	6.11	2.08	.04	.76	.99	1.30	.84	.06	.69				
1324	83.90	.20	7.28	1.27	.03	.48	1.42	2.11	.58	.19	.62				
1325	72.90	.55	13.10	3.79	.04	1.38	1.09	2.34	1.58	.13	2.15				
1326	75.70	.53	9.23	5.53	.02	.97	.76	1.17	1.88	.50	2.92				
13634	58.90	1.83	12.60	9.71	.32	4.89	2.27	3.02	1.13	.51	2.31				
13635	66.00	.73	13.80	5.98	.12	2.74	.33	1.31	2.98	.10	2.85				1
13636	49.00	2.87	12.60	12.80	.29	7.33	5.05	2.57	.27	.74	3.15				
13637	66.00	.52	14.30	4.25	.05	2.76	.28	1.35	3.59	.07	3.00				
13638	67.10	.86	14.10	6.51	.05	2.14	.69	.87	3.86	.16	2.54				
13639	65.90	.85	14.60	5.40	.08	2.26	.49	1.48	3.05	.09	3.31				
13640	48.20	2.95	13.10	13.30	.27	8.92	3.60	1.94	.27	.70	4.46				
13641	68.80	.50	12.42	3.74	.09	3.68	.84	.52	4.32	.06	3.00				1
13642	21.10	.27	5.59	4.08	.50	6.00	26.40	.27	1.18	.09	19.46				1
13643	69.20	.59	13.50	4.18	.03	.93	1.28	1.56	3.37	.29	2.62				
13644	70.30	.60	12.90	6.36	.11	1.62	.30	.92	3.44	.08	2.38				
13645	62.70	.80	13.60	8.62	.28	2.30	1.71	2.40	2.12	.17	2.77				
13646	53.10	2.32	12.10	12.30	.45	5.37	3.42	2.58	.88	.64	4.54				1
13647	60.90	.68	12.40	11.10	.48	4.12	1.06	2.23	2.34	.18	2.08				
13659	52.40	2.29	12.90	10.60	.26	5.89	5.27	2.90	.24	.59	4.38				
13660	67.50	.54	10.60	4.37	.06	1.22	.28	.39	3.89	.07	2.69				7
13661	65.90	.67	16.00	5.44	.03	1.23	1.23	1.86	3.67	.16	2.92				
13662	76.00	.22	10.20	3.77	.08	.70	.31	.32	4.83	.02	1.54				
13663	61.80	.89	16.40	5.86	.05	3.04	1.65	.64	4.39	.16	4.23				
13664	66.20	.59	15.10	5.11	.05	1.24	.79	1.88	3.28	.14	2.46				
13665	47.70	2.78	13.00	12.70	.22	7.63	6.66	1.68	.36	.72	6.23				
13666	61.80	1.30	14.10	7.57	.20	4.60	.93	2.61	1.47	.31	3.77				
13667	67.80	.70	13.40	5.17	.08	1.55	.24	.27	4.37	.07	3.38				5

LITHCODE	TS/PTS	ALTERATION	MINERALIZATION	COMMENTS	DEPTH	WIDTH
12	0			SHAL	.0	.0
12	0				.0	.0
12	0				.0	.0
13	0			SSLT	.0	.0
12	0			SHAL	.0	.0
3	0				6.4	3.8
8	0				17.1	7.7
1	0		Y		31.0	7.5
8	0	SIL SER			45.7	7.6
11	0			SSST	57.6	7.6
7	0				9.0	7.0
1	0				22.0	9.0
8	0				142.0	7.0
20	0	CAR TRF			56.0	4.0
19	0				67.0	8.0
7	0				17.0	7.6
3	0				37.0	7.6
7	0	SIL SER			47.4	7.1
3	0			LITF	61.0	7.6
1	0				77.7	2.0
8	0	SIL SER			79.7	2.0
11	0				81.7	2.0
7	0				69.6	7.6
8	0	SIL SER			152.0	7.6
11	0			SSST	169.0	7.6
1	0				22.2	7.6
3	0				32.0	6.0
8	0	SIL SER		SSLT	46.5	7.6

P2O	K2O	P2O5	LOI	Zr	Sr	Rb	Zn	Cu	U	Th	Ga	Pb	Ni	Y	Ag
.82	.56	.28	1.31	74	104	26	31	12	0	3	10	3	2	29	0
.30	.84	.06	.69				27	20				0			0
.11	.58	.19	.62				12	9				5			0
.34	1.58	.13	2.15				42	20				4			0
.17	1.88	.50	2.92				28	13				3			0
.02	1.13	.51	2.31				200	28				32			0
.31	2.98	.10	2.85				1020	61				40			0
.57	.27	.74	3.15				100	28				0			0
.35	3.59	.07	3.00				79	20				20			0
.87	3.86	.16	2.54				49	21				0			0
.48	3.05	.09	3.31				88	28				18			0
.94	.27	.70	4.46				100	22				0			0
.52	4.32	.06	3.00				1480	67				820			3
.27	1.18	.09	19.46				1280	88				3000			44
.5	1.27	.20	2.62				84	23				22			1
.92	3.44	.08	2.38				73	17				0			0
.40	2.12	.17	2.77				180	220				18			0
.58	.88	.64	4.54				1200	44				180			1
.23	2.34	.18	2.08				500	480				180			1
.90	.24	.59	4.38				98	21				0			0
.39	3.89	.07	2.69				7900	68				6200			4
.86	3.67	.18	2.92				90	27				57			1
.32	4.83	.02	1.54				54	34				13			0
.64	4.39	.16	4.23				67	34				22			0
.88	3.28	.14	2.46				55	28				7			0
.68	.36	.72	6.23				120	18				0			0
.61	1.47	.31	3.77				120	23				10			0
.27	4.37	.07	3.38				5800	140				2040			2

SAMPLE	EASTING	NORTHING	TYPE	DRILLHOLE	LITHOLOGY	LITHCODE	TS/PTS	ALTERATION	MINERALIZATI
13668			2	20001	SHAL	13	0		
13669			2	20003	M:TF	1	0		
13670			2	20003	F:LT	8	0	SIL SER	
13671			2	20003	SHAL	13	0		
13672			2	160230023	F:LT	8	0	SIL	
13673			2	160230023	F:FL	10	0		
13674			2	160230023	I:TF	3	0		
13675			2	160230023	F:TF	7	0		
13676			2	160230023	SEDM	19	0		
17101			2	160230022	F:FL	10	0		
17102			2	160230022	I:TF	3	0		
17103			2	160230022	SSLT	11	0		
17104			2	160230022	I:LT	4	0		
17105			2	160230022	F:LT	8	0		
17106			2	160230022	SSLT	11	0		
17107			2	160230021	SSLT	11	0		
17108			2	160230021	F:LT	8	0		
17109			2	160230021	SSLT	11	0		
17110			2	160230021	I:TF	3	0	ACT	
17111			2	160230021	F:TF	7	0		
17112			2	160230020	SSLT	11	0		
17113			2	160230020	SSLT	11	0		
17114			2	160230020	I:TF	3	0	ACT	
17115			2	160230020	SHAL	13	0		
17116			2	160230020	M:LT	21	0		GA
17117			2	160230020	SSST	12	0		
17118			2	160230019	SSST	12	0		
17119			2	160230019	CARB	20	0	CHL ACT	

SAMPLE	SiO2	TiO2	Al2O3	FeO	MnO	MgO	CaO	Na2O	K2O	P2O5	LOI	Zr	Sr	Rb
13668	63.90	.86	15.50	5.93	.07	1.81	.80	.54	5.12	.14	3.23			
13669	65.30	.73	15.70	5.29	.11	2.42	.40	1.15	4.17	.09	2.92			
13670	61.20	.99	17.90	5.97	.07	1.45	.23	.27	5.55	.09	3.69			
13671	69.50	.63	14.20	5.52	.04	1.51	.62	1.30	3.64	.11	3.15			
13672	73.50	.58	10.10	4.16	.09	.71	.45	.26	5.24	.05	1.54			
13673	88.70	.13	4.80	1.06	.01	.15	.20	.19	3.02	.02	1.46			
13674	54.40	.95	14.80	10.20	.37	6.65	1.63	1.61	2.75	.12	3.54			
13675	64.90	.61	15.70	4.60	.05	2.08	1.03	1.26	4.02	.12	2.77			
13676	67.90	.63	15.50	4.32	.06	1.45	.91	1.64	3.65	.09	2.31			
17101	77.70	.26	10.50	1.80	.02	.23	.22	.23	6.91	.04	.85			
17102	80.80	.22	7.72	4.15	.07	1.00	.50	.17	3.80	.04	1.23			
17103	60.30	.81	18.10	5.66	.06	2.21	.35	.95	4.82	.07	3.38			
17104	49.10	1.81	14.70	10.40	.54	7.35	4.10	1.70	2.21	.45	3.92			
17105	74.40	.23	11.40	2.97	.12	2.02	.69	2.97	2.55	.03	.85			
17106	67.90	.68	14.60	4.60	.05	1.65	.62	1.47	3.42	.10	2.31			
17107	66.20	.69	15.60	6.12	.09	1.55	.42	.96	4.04	.08	1.85			
17108	72.40	.39	12.70	4.31	.08	.98	.30	.27	6.55	.03	1.54			
17109	70.80	.67	12.40	6.37	.13	1.59	.44	.15	4.28	.17	1.62			
17110	68.20	.80	12.30	8.02	.15	2.00	.54	.15	4.90	.27	1.54			
17111	39.50	.45	11.10	8.72	.39	16.20	3.73	.20	1.51	.17	6.46			
17112	64.70	.65	15.90	7.26	.13	1.89	.44	.17	5.43	.07	2.23			
17113	67.20	.59	12.30	8.77	.16	1.95	.42	.13	4.40	.14	1.46			
17114	63.40	.55	11.40	8.66	.18	5.36	1.27	.58	2.59	.08	2.46			
17115	61.20	.91	18.40	6.09	.04	1.52	.35	1.40	4.05	.09	3.38			
17116	48.20	2.61	14.20	12.90	.45	6.98	3.50	1.71	.98	.58	4.23			
17117	61.40	1.01	13.30	8.37	.27	4.98	1.46	2.68	1.63	.23	2.46			
17118	66.90	.70	13.40	6.92	.14	1.75	.55	.20	5.05	.14	1.85			
17119	50.10	.26	10.10	4.16	.36	6.37	10.10	.30	3.53	.13	8.46			

ITHCODE	TS/PTS	ALTERATION	MINERALIZATION	COMMENTS	DEPTH	WIDTH
13	0				60.5	7.0
1	0			I:TF	49.2	7.6
8	0	SIL SER		SSLT	100.3	7.6
13	0			SSLT	120.7	7.6
8	0	SIL			14.0	7.6
10	0				23.0	7.6
3	0			SSLT SSST	60.0	7.6
7	0			SSLT	78.0	6.6
19	0				96.0	7.6
10	0				25.0	7.6
3	0			F:TF SSLT	40.0	7.6
11	0			SHAL	57.0	7.6
4	0				66.0	7.6
8	0				75.0	7.6
11	0			SSST SHAL	89.0	7.6
11	0			TFSD F:TF	18.5	7.6
8	0			SSLT F:TF	46.0	7.6
11	0			SSST F:TF	61.0	7.6
3	0	ACT			69.0	3.0
7	0			I:TF	89.0	7.6
11	0			SSSS T	29.0	7.6
11	0				55.0	7.6
3	0	ACT		F:TF	72.0	6.0
13	0			SSLT	86.0	7.6
21	0		GA	I:TF	99.0	7.6
12	0			SSLT F:TF	106.0	6.0
12	0			SSLT F:TF	61.0	7.6
20	0	CHL ACT		CARB	75.0	1.0

NA2O	K2O	P2O5	LOI	Zr	Sr	Rb	Zn	Cu	U	Th	Ga	Pb	Ni	Y	Ag
.54	5.12	.14	3.23				70	29				7			1
1.15	4.17	.09	2.92				87	32				10			0
.27	5.55	.09	3.69				130	29				18			1
1.36	3.64	.11	3.15				58	28				3			1
.26	5.24	.05	1.54				51	12				6			1
.19	3.02	.02	1.46				180	64				180			1
1.61	2.75	.12	3.54				470	110				62			0
1.26	4.02	.12	2.77				80	26				15			0
1.64	3.65	.09	2.31				72	27				3			0
.23	6.91	.04	.85				29	34				22			0
.17	3.80	.04	1.23				160	22				23			0
.95	4.82	.07	3.38				76	37				10			0
1.70	2.21	.45	3.92				780	74				400			0
2.97	2.55	.03	.85				470	14				120			0
1.47	3.42	.10	2.31				100	23				7			0
.96	4.04	.08	1.85				64	7				0			0
.27	6.55	.03	1.54				52	65				8			0
.15	4.28	.17	1.62				150	57				0			0
.15	4.90	.27	1.54				91	76				4			0
.20	1.51	.17	6.46				650	160				190			2
.17	5.43	.07	2.23				80	28				0			0
.13	4.40	.14	1.46				130	92				0			0
.58	2.59	.08	2.46				150	270				130			2
1.40	4.05	.09	3.38				85	46				6			0
.71	.98	.58	4.23				190	77				18			0
.68	1.63	.23	2.46				140	37				7			0
.20	5.05	.14	1.15				97	430				5			0
.30	3.53	.13	8.46				9999	140				5600			78

294

2 OF 2

SAMPLE	EASTING	NORTHING	TYPE	DRILLHOLE	LITHOLOGY	LITHCODE	TS/PTS	ALTERATION	MINERALIZATI
17120			2	160230019	SSLT	11	0		
17121			2	160230019	SSLT	11	0		
17122			2	160230019	F:LT	8	0		
17123			2	160230019	SSLT	11	0		
17124			2	160230018	F:LT	8	0		
17125			2	160230018	F:LT	8	0		
17126			2	160230018	SHAL	13	0		
17127			2	160230018	F:LT	8	0		SER
17128			2	160230018	SSLT	11	0		
17129			2	160230017	SSLT	11	0		
17130			2	160230017	I:TF	3	0		
17131			2	160230017	SSLT	11	0		
17132			2	160230016	SSLT	11	0		
17133			2	160230016	F:LT	8	0	SIL	
17134			2	160230016	I:TF	3	0		
17135			2	160230016	F:FL	10	0		
17136			2	160230016	SSLT	11	0		
17137			2	160230015	SSLT	11	0		
17138			2	160230015	F:TF	7	0		
17139			2	160230015	M:TF	1	0		ACT
17140			2	160230015	SSLT	11	0		
17141			2	160230014	SSLT	11	0		CHL
17142			2	160230014	I:LT	4	0		
17143			2	160230014	SHAL	13	0		
17144			2	160230014	M:TF	1	0		
17145			2	160230013	F:FL	10	0		
17146			2	160230013	I:TF	3	0		
17147			2	160230013	SSLT	11	0		

SAMPLE	SiO2	TiO2	Al2O3	FeO	MnO	MgO	CaO	Na2O	K2O	P2O5	LOI	Zr	Sr	Rb
17120	58.10	1.05	20.40	6.07	.06	2.00	.49	1.38	4.90	.10	3.54			
17121	65.40	.69	16.00	4.86	.08	2.07	.73	1.75	3.92	.11	2.00			
17122	71.40	.30	10.20	3.00	.13	2.76	1.22	2.45	1.87	.04	1.69			b
17123	65.50	.79	15.70	5.39	.07	1.58	1.44	1.57	3.57	.11	2.15			
17124	64.70	.64	15.20	7.45	.11	1.55	.52	1.26	4.21	.11	1.69			
17125	62.60	.82	16.30	5.70	.06	4.18	1.04	1.57	4.06	.13	2.38			
17126	55.80	1.10	18.00	6.77	.20	3.51	2.11	1.96	3.87	.11	3.08			
17127	70.40	.70	13.80	4.51	.06	1.68	.48	2.37	2.43	.09	2.15			
17128	68.60	.64	14.40	4.55	.08	1.54	1.62	1.57	3.32	.09	2.15			
17129	71.50	.59	12.20	7.08	.11	1.46	.28	.15	4.18	.08	1.54			
17130	63.20	.57	12.00	8.64	.21	5.87	.73	.22	3.71	.09	2.54			
17131	64.00	.74	16.20	5.95	.07	2.38	.61	.73	4.77	.10	2.77			
17132	67.40	.84	12.80	8.36	.15	1.87	.61	.16	3.92	.30	1.77			
17133	76.60	.38	8.77	6.86	.12	.14	.38	.35	3.18	.07	1.38			1
17134	60.70	.89	11.70	13.40	.22	1.94	.70	.33	5.31	.20	2.08			
17135	84.20	.12	5.51	3.60	.08	.52	.37	.21	2.71	.03	.54			
17136	67.10	.53	13.10	5.11	.11	3.45	.97	.76	3.84	.08	2.15			1
17137	71.10	.47	11.80	5.78	.09	1.00	.58	.28	4.36	.24	1.62			
17138	70.10	.55	12.40	6.70	.11	1.41	.36	.14	4.36	.08	1.85			
17139	42.70	.32	8.17	5.02	.34	16.50	5.86	.16	2.86	.16	3.85			9
17140	59.20	.81	14.50	5.93	.13	8.11	.91	.85	4.12	.11	2.62			
17141	67.70	.60	14.00	6.57	.10	1.66	.80	1.74	3.32	.11	1.77			
17142	78.60	.27	7.05	5.95	.10	1.65	.37	.25	1.77	.06	1.54			3
17143	64.30	.73	14.20	7.53	.23	3.22	.82	3.76	1.18	.17	2.08			
17144	50.70	2.76	12.40	13.90	.46	5.01	4.92	2.67	.77	.86	2.92			
17145	73.70	.52	11.60	6.60	.09	1.27	.37	.24	3.93	.09	1.69			
17146	52.00	.53	13.00	8.93	.32	6.90	2.44	.27	4.48	.11	2.92			4
17147	61.20	.99	19.30	6.53	.07	2.20	.73	1.43	4.45	.10	3.31			

1 OF

ITHCODE	TS/PTS	ALTERATION	MINERALIZATION	COMMENTS	DEPTH	WIDTH
11	0			SHAL TFSD	95.0	7.6
11	0			SHAL F:TF	135.0	7.6
8	0			I:LT	149.0	7.6
11	0			SHAL F:TF	157.0	7.6
8	0			SHAL SSLT	21.0	7.6
8	0				59.0	7.6
13	0			SSLT F:LT	86.0	7.6
8	0		SER	TFSD F:LT	113.0	7.6
11	0			TFSD	123.0	7.3
11	0				8.0	6.0
3	0				17.0	7.6
11	0			SSST F:TF	32.0	7.6
11	0			M:TF	7.5	3.2
8	0	SIL		I:TF	17.6	7.6
3	0				22.3	1.9
10	0				30.5	7.6
11	0			SSST	40.3	7.6
11	0			SSST F:TF	16.0	7.6
7	0			M:TF	32.0	7.6
1	0		ACT		39.0	4.0
11	0			SSST	47.0	7.6
11	0		CHL	SSST F:TF	25.6	7.6
4	0				47.0	7.0
13	0			SSLT F:TF	57.6	7.6
1	0				72.3	7.6
10	0				14.0	7.6
3	0			SSLT	26.0	7.6
11	0			SSST	46.0	7.6

Na2O	K2O	P2O5	LOI	Zr	Sr	Rb	Zn	Cu	U	Th	Ga	Pb	Ni	Y	Ag
1.38	4.90	.10	3.54				72	45				10			0
1.75	3.92	.11	2.90				120	33				18			1
2.45	1.87	.04	1.69				6000	39				900			0
1.57	3.57	.11	2.15				110	34				10			0
1.26	4.21	.11	1.69				72	55				0			0
1.57	4.06	.13	2.38				59	42				7			0
1.96	3.87	.11	3.06				340	58				11			0
2.37	2.43	.09	2.15				120	27				20			1
1.57	3.32	.09	2.15				74	28				16			0
.15	4.16	.08	1.54				130	28				16			0
.22	3.71	.09	2.54				910	71				300			6
.73	4.77	.10	2.77				72	40				9			1
.16	3.92	.30	1.77				110	15				0			0
.35	3.18	.07	1.38				1120	19				440			1
.33	5.31	.20	2.08				170	68				30			4
.21	2.71	.03	.54				46	30				3			3
.76	3.84	.08	2.15				1530	220				400			11
.28	4.36	.24	1.62				68	18				8			2
.14	4.36	.08	1.85				68	12				0			2
.16	2.86	.18	3.85				9999	43				5800			64
.85	4.12	.11	2.62				140	35				72			6
1.74	3.32	.11	1.77				88	20				12			2
.25	1.77	.06	1.54				3900	150				3450			3
3.76	1.18	.17	2.08				210	88				140			2
2.67	.77	.86	2.92				260	47				92			1
.24	3.93	.09	1.69				200	24				73			1
.27	4.48	.11	2.92				4300	400				2420			73
1.43	4.45	.10	3.31				76	48				18			5

295

2 OF 2

SAMPLE	EASTING	NORTHING	TYPE	DRILLHOLE	LITHOLOGY	LITHCODE	TS/PTS	ALTERATION	MINERALIZATI
17148			2	160230013	F:LT	8	0		
17149			2	160230013	F:TF	7	0		
17150			2	160230013	F:TF	7	0		
17151			2	160230013	SSST	12	0		
17152			2	160230012	F:TF	7	0		
17153			2	160230012	SSLT	11	0		
17154			2	160230012	I:LT	4	0		
17155			2	160230012	F:LT	8	0		
17156			2	160230012	SSLT	11	0		
17157			2	160230011	M:LT	21	0		
17158			2	160230011	SSST	12	0		
17159			2	160230011	SSLT	11	0		
17160			2	160230011	F:LT	8	0		
17161			2	160230011	SSLT	11	0		
17162			2	160230010	SHAL	13	0		
17163			2	160230010	I:LT	4	0		
17164			2	160230010	F:TF	7	0	CHL	
17165			2	160230010	F:TF	7	0	SER	
17166			2	160230010	F:LT	8	0		
17167			2	160230010	SSLT	11	0		
17168			2	160230009	M:LT	21	0		
17169			2	160230009	SSLT	11	0		
17170			2	160230009	F:LT	8	0		
17171			2	160230009	F:LT	8	0		
17172			2	160230008	F:LT	8	0		
17173			2	160230008	F:TF	7	0		
17174			2	160230008	M:TF	1	0		
17175			2	160230008	F:LT	8	0		

SAMPLE	SiO2	TiO2	Al2O3	FeO*	MnO	MgO	CaO	Na2O	K2O	P2O5	LOI	Zr	Sr	Rb
17148	76.30	.26	11.40	4.33	.15	2.42	.33	2.00	3.03	.03	1.23			
17149	59.60	1.07	17.20	6.42	.12	3.85	1.61	1.73	3.61	.19	2.69			
17150	68.90	.25	10.60	3.15	.16	4.27	1.19	1.65	2.10	.03	2.31			
17151	68.00	.64	15.10	5.10	.02	1.17	1.08	2.12	3.31	.17	2.08			
17152	64.00	.78	16.30	6.85	.11	2.90	.38	.70	3.89	.11	3.23			
17153	68.00	.76	15.70	5.41	.07	1.71	.42	1.51	3.95	.11	1.92			
17154	58.30	1.35	13.70	7.79	.21	7.31	2.47	1.71	1.56	.31	2.92			
17155	67.80	.44	13.60	3.44	.08	2.00	.11	2.77	2.66	.04	2.00			
17156	70.10	.73	14.70	5.03	.05	1.64	.67	1.75	3.22	.08	1.77			
17157	48.00	3.01	12.90	13.50	.35	7.18	5.03	1.81	.43	.78	4.92			
17158	56.80	1.85	13.30	10.90	.46	6.67	1.27	2.42	.78	.52	3.23			
17159	66.20	.95	16.30	6.27	.09	1.71	.34	1.23	4.00	.10	2.31			
17160	66.80	1.16	14.70	6.24	.16	3.51	.90	3.31	2.11	.24	2.08			
17161	68.40	.84	15.80	5.56	.08	1.64	.37	1.33	4.05	.08	2.08			
17162	61.90	.95	19.40	6.50	.04	1.49	.30	1.47	4.14	.09	3.62			
17163	52.20	2.47	13.10	12.20	.54	6.70	4.37	1.45	.77	.56	3.69			
17164	72.50	.24	11.20	3.54	.18	3.57	1.01	1.83	3.29	.03	.85			
17165	73.10	.64	12.90	4.00	.06	1.58	.91	1.34	3.59	.08	1.46			
17166	72.70	.49	11.80	4.01	.17	4.31	1.59	2.13	1.60	.08	1.62			
17167	68.00	.87	16.20	5.52	.07	1.40	.29	1.14	3.92	.08	2.15			
17168	47.30	2.84	13.00	14.90	.89	9.88	2.23	1.08	.72	.73	4.46			
17169	69.70	.78	14.80	5.22	.10	1.83	.47	1.89	3.30	.13	2.54			
17170	68.30	.76	15.90	5.33	.09	2.36	.80	1.74	3.67	.10	1.92			
17171	65.20	.82	16.30	6.30	.16	3.74	.42	1.38	3.11	.12	2.92			
17172	66.20	.71	15.60	6.76	.15	2.00	.38	.47	4.76	.09	2.69			
17173	73.80	.38	11.80	4.22	.08	1.18	.42	.47	3.98	.06	1.62			
17174	47.30	3.18	13.70	14.10	.28	9.50	4.09	1.76	.19	.77	4.31			
17175	65.90	.96	16.30	5.96	.05	2.16	.35	.45	4.95	.11	3.23			

ITHCODE	TS/PTS	ALTERATION	MINERALIZATION	COMMENTS	DEPTH	WIDTH
8	0				66.0	7.6
7	0			SSST SSLT	90.0	7.6
7	0				97.0	4.0
12	0			SSLT TFSD	110.0	7.6
7	0				14.0	7.6
11	0			SSST	35.0	7.6
4	0				51.0	7.6
8	0			F:TF	58.0	6.0
11	0				68.0	7.6
21	0				40.0	7.6
12	0			F:TF M:TF	54.0	7.6
11	0				75.0	7.6
8	0			SSLT F:TF	95.0	7.0
11	0				105.0	4.0
13	0			SSLT	36.0	7.6
4	0				48.0	7.0
7	0	CHL			66.0	7.4
7	M	SER		F:LT	87.0	7.6
8	0			SSLT F:TF	98.0	7.6
11	0				105.0	6.0
21	0				14.0	7.6
11	0				40.0	7.6
8	0			F:TF I:TF	47.0	5.0
8	0			SSLT SHAL	61.0	7.6
8	0			F:TF F:FL	29.6	7.6
7	0			I:TF F:TF	55.0	7.6
1	0			F:LT M:TF	84.8	7.6
8	0				107.0	7.6

a2O	K2O	P2O5	LOI	Zr	Sr	Rb	Zn	Cu	U	Th	Ga	Pb	Ni	Y	Ag
.00	3.03	.03	1.23				100	16				15			1
.73	3.61	.19	2.69				120	32				40			0
1.65	2.10	.03	2.31				5800	42				2500			4
2.42	3.31	.17	2.08				85	26				10			0
.70	3.89	.11	3.23				76	38				16			0
1.51	3.95	.11	1.92				70	28				8			0
1.71	1.56	.31	2.72				330	22				400			0
2.97	2.66	.04	2.00				7200	290				3700			1
1.75	3.22	.08	1.77				150	29				20			0
1.81	.43	.78	4.92				240	22				31			0
2.42	.78	.52	3.23				690	68				46			0
1.23	4.00	.10	2.31				110	42				100			0
3.31	2.11	.24	2.08				340	35				89			0
1.33	4.05	.08	2.08				230	29				60			0
1.47	4.14	.09	3.62				91	44				5			0
1.45	.77	.56	3.69				660	46				390			1
1.83	3.29	.03	.85				110	15				10			0
1.34	3.59	.08	1.46				51	20				10			0
2.13	1.60	.08	1.92				2000	28				220			0
1.14	3.92	.08	2.15				79	28				5			0
1.08	.72	.73	4.46				2060	360				760			0
1.39	3.30	.13	2.54				150	28				61			0
1.74	3.67	.10	1.92				93	29				19			0
1.38	3.11	.12	2.92				660	18				140			1
.47	4.76	.09	2.69				110	33				22			0
.47	3.98	.06	1.62				110	38				25			0
1.76	.19	.77	4.31				96	23				0			0
.45	4.95	.11	3.23				34	26				39			1

2 OF 2

SAMPLE	EASTING	NORTHING	TYPE	DRILLHOLE	LITHOLOGY	LITHCODE	TS/PTS	ALTERATION	MINERALIZATI
17176			2	160230008	SSST	12	0		
17177			2	160230007	I:TF	3	0		
17178			2	160230007	I:TF	3	0		
17179			2	160230007	F:LT	8	0	SIL SER	
17180			2	160230007	M:TF	1	0		
17181			2	160230007	SSST	12	0		
17182			2	160230006	F:TF	7	0	SER SIL	
17183			2	160230006	S:CH	2	0	CHL	
17184			2	160230006	I:TF	3	0	V/OZ	
17185			2	160230006	F:LT	8	0	CHL	
17186			2	160230006	SSST	12	0		
17187			2	160230005	F:TF	7	0	SIL	
17188			2	160230005	I:TF	3	0		
17189			2	160230005	F:TF	7	0		
17190			2	160230005	F:LT	8	0		
17191			2	160230005	SSST	12	0		
17192			2	160230004	I:TF	3	0		
17193			2	160230004	M:LT	21	0		
17194			2	160230004	F:LT	8	0	SIL SER	
17195			2	160230004	SSLT	11	0		
17196			2	160230003	I:TF	3	0		
17197			2	160230003	F:TF	7	0		
17198			2	160230003	M:TF	1	0		
17199			2	160230003	I:LT	4	0	SER	
17200			2	160230003	SSLT	11	0		
17601			2	160230024	SSLT	11	0		
17602			2	160230024	SSLT	11	0		
17603			2	160230024	SSLT	11	0		

SAMPLE	SiO2	TiO2	Al2O3	FeO	MnO	MgO	CaO	Na2O	K2O	P2O5	LOI	Zr	Sr	Rb
17176	66.00	.74	16.30	5.49	.04	1.61	.43	1.47	4.20	.12	2.46			
17177	61.20	1.19	13.40	10.20	.23	3.29	1.17	.87	2.66	.28	3.08			
17178	71.70	.54	11.40	5.70	.11	1.26	.37	.34	3.83	.11	2.00			
17179	72.10	.59	13.10	5.03	.11	1.76	.35	1.61	2.69	.07	2.00			
17180	44.80	2.91	12.60	12.60	.40	7.54	6.28	2.08	.36	.68	4.69			
17181	53.60	2.41	13.80	11.30	.27	7.20	1.09	3.24	.55	.54	3.69			
17182	62.30	.95	15.10	8.02	.26	2.78	1.06	.38	3.53	.18	3.46			
17183	44.50	2.50	14.70	15.20	.72	8.01	2.37	1.35	1.51	.68	4.92			3
17184	52.40	1.20	17.50	9.78	.27	4.99	1.32	.51	4.48	.24	3.77			
17185	71.70	.29	11.10	3.55	.10	2.45	.64	.17	4.87	.05	1.69			1
17186	66.00	.66	16.10	4.91	.04	1.73	.68	1.07	3.77	.10	2.69			
17187	63.50	.79	14.90	7.52	.25	2.73	.74	2.61	2.39	.17	2.62			
17188	53.70	2.04	11.40	15.70	.44	5.62	1.47	.86	1.04	.52	4.00			
17189	51.10	1.21	11.20	7.66	.37	4.45	5.10	1.03	2.31	.27	3.62			
17190	75.20	.19	11.00	2.47	.05	2.56	.33	1.47	3.41	.02	1.23			
17191	70.30	.58	12.90	6.28	.03	1.04	.55	.87	3.25	.13	2.08			
17192	61.60	.61	12.10	11.60	.43	4.10	.92	1.34	2.29	.17	2.08			
17193	45.60	2.78	12.60	11.50	.37	7.83	6.03	1.24	.96	.66	6.31			
17194	73.70	.19	11.10	2.16	.05	3.49	.26	1.49	2.44	.02	2.23			1
17195	67.30	.70	13.90	6.16	.04	1.41	.62	1.14	3.30	.12	2.46			
17196	60.00	1.05	19.60	5.79	.05	1.65	.22	.61	5.18	.08	3.38			
17197	59.90	1.00	17.00	6.58	.09	2.72	.41	1.47	3.66	.14	3.62			
17198	45.60	3.01	12.80	12.70	.40	7.87	5.68	2.02	.47	.66	4.62			
17199	69.70	.65	12.90	4.24	.05	2.79	.54	.73	2.96	.09	3.31			
17200	65.40	.70	15.70	5.07	.03	1.56	.98	2.08	3.15	.12	2.54			
17601	64.00	.85	15.70	5.00	.09	2.14	1.35	3.99	2.72	.16	.93			
17602	61.40	.79	16.90	6.68	.10	1.90	.80	2.56	3.69	.14	1.39			
17603	67.60	.69	13.60	5.74	.11	1.37	.55	.54	4.56	.07	1.62			

LITHCODE	TS/PTS	ALTERATION	MINERALIZATION	COMMENTS	DEPTH	WIDTH
12	0			SHAL CGXX	122.9	7.6
3	0			I:LT I:TF	22.3	7.6
3	0				40.1	7.6
8	0	SIL SER			59.0	7.6
1	0				74.0	6.0
12	0				77.0	3.0
7	0	SFT SIL		I:TF	13.0	7.6
2	0	CHL			30.0	7.4
3	0	V/02		I:LT	48.0	7.6
8	0	CHL		F:TF	68.0	7.6
12	0			SSLT	80.0	7.6
7	0	SIL			15.0	7.6
3	0				26.0	7.6
7	0			F:LT I:LT	38.0	7.6
8	0			I:LT	59.0	7.6
12	0				75.0	6.0
3	0				15.0	7.6
21	0			I:LT	29.0	7.6
8	0	SIL SER		F:TF	46.0	7.6
11	0			SSST	61.0	7.6
3	0				12.0	7.6
7	0				20.0	7.6
1	0				29.0	7.6
4	0	SER			41.0	7.6
11	0			SSST	55.0	7.6
11	0			SSST	36.0	7.6
11	0			SSST F:TF	88.5	7.6
11	0			SSST I:LT	158.9	7.6

Na2O	K2O	P2O5	LOI	Zr	Sr	Rb	Zn	Cu	U	Th	Ga	Pb	Ni	Y	Ag
1.47	4.20	.12	2.46				66	34				3			0
.87	2.66	.26	3.08				270	94				49			0
.34	3.83	.11	2.00				69	180				18			0
1.61	2.69	.07	2.00				83	24				11			0
2.08	.36	.68	4.69				140	21				0			0
3.24	.55	.54	3.69				120	20				8			0
.38	3.53	.18	3.46				940	45				210			2
1.35	1.51	.68	4.92				3220	580				370			0
.51	4.48	.24	3.77				350	400				100			2
.17	4.87	.05	1.69				1720	25				630			1
1.07	3.77	.10	2.69				71	33				9			0
2.61	2.39	.17	2.62				310	39				180			0
.86	1.04	.52	1.00				280	990				20			0
1.03	2.31	.27	3.62				440	67				260			1
1.47	3.41	.02	1.23				110	17				11			0
.87	3.25	.13	2.96				42	20				0			0
1.34	2.29	.17	2.08				310	860				81			2
1.24	.96	.66	6.31				100	24				2			0
1.49	2.44	.02	2.23				1080	17				260			0
1.14	3.30	.12	2.46				48	24				4			0
.61	5.18	.08	3.38				82	61				7			0
1.47	3.66	.14	3.62				86	36				21			1
2.02	.47	.66	4.62				160	25				0			0
.73	2.96	.09	3.31				100	26				20			0
2.00	3.15	.12	2.54				60	30				3			0
3.99	2.72	.16	.93				039	013				01			0
2.56	3.69	.14	1.39				098	014				016			0
.54	4.56	.07	1.62				064	120				020			0

SAMPLE	EASTING	NORTHING	TYPE	DRILLHOLE	LITHOLOGY	LITHCODE	TS/PTS	ALTERATION	MINERALIZATIO
17604			2	160230024	F:TF	7	0		
17605			2	160230024	SSLT	11	0		
17606			2	160230024	F:TF	7	0		
17607			2	160230024	SSLT	11	0		
17608			2	160230024	I:TF	3	0	SER CHL	
17609			2	160230024	SHAL	13	0		
17610			2	160230025	SSLT	11	0		
17611			2	160230025	F:LT	8	0		
17612			2	160230025	SSLT	11	0		
17613			2	160230025	I:TF	3	0		
17614			2	160230025	I:LT	4	0		
17615			2	160230025	F:LT	8	0		
17616			2	160230025	SSLT	11	0		
17617			2	160230025	M:TF	1	0		
17618			2	160230025	SSLT	11	0		
17619			2	160230026	SSLT	11	0		
17620			2	160230026	I:TF	3	0		
17621			2	160230026	F:LT	8	0		
17622			2	160230026	F:TF	7	0		
17623			2	160230026	SSLT	11	0		
17624			2	160230026	F:TF	7	0		
17625			2	160230026	I:TF	3	0		
17626			2	160230026	SSLT	11	0		
17627			2	160230027	SSLT	11	0		
17628			2	160230027	I:LT	4	0		
17629			2	160230027	F:LT	8	0		
17630			2	160230027	F:TF	7	0		
17631			2	160230027	SSLT	11	0		

SAMPLE	SiO2	TiO2	Al2O3	FeO	MnO	MgO	CaO	Na2O	K2O	P2O5	LOI	Zr	Sr	Rb
17604	74.30	.47	11.00	4.35	.07	.87	.38	.01	4.51	.05	1.62			
17605	72.50	.28	13.40	3.49	.06	.67	.16	.13	5.89	.03	1.39			
17606	74.00	.46	11.00	4.33	.07	.89	.37	.02	4.52	.04	1.77			
17607	66.80	.79	14.60	5.98	.13	1.69	.54	.06	5.13	.16	1.77			
17608	59.20	.94	18.40	6.54	.06	2.03	.49	1.30	4.32	.09	3.23			
17609	68.40	.50	12.80	4.77	.15	2.87	.67	2.53	2.20	.05	2.23			
17610	64.30	.88	16.40	5.08	.08	1.70	.26	1.21	4.05	.11	2.62			
17611	63.40	.70	16.30	5.53	.13	1.88	.68	2.54	3.43	.10	1.77			
17612	72.00	.36	13.50	3.12	.04	.55	.18	1.56	3.74	.04	1.62			
17613	58.40	.93	16.00	8.52	.18	4.68	.31	.49	3.50	.10	4.00			
17614	64.10	.70	12.90	7.42	.28	.72	2.44	4.29	1.67	.18	1.85			
17615	60.80	.95	13.70	7.34	.24	5.20	1.34	1.90	2.87	.17	2.77			
17616	65.40	.86	15.30	5.49	.10	1.76	.21	.69	4.49	.10	2.00			
17617	48.40	2.96	12.90	13.40	.30	9.00	3.17	2.10	.25	.66	4.08			
17618	64.40	.72	15.50	4.89	.08	1.79	1.04	.98	4.99	.10	2.08			
17619	69.10	.59	13.50	5.53	.08	1.35	.48	1.45	3.74	.09	1.00			
17620	64.70	.77	13.90	7.16	.20	1.48	1.14	3.67	1.97	.16	1.31			
17621	71.90	.35	11.10	3.02	.11	5.04	.19	1.54	1.70	.04	2.62			
17622	55.10	2.02	15.50	10.10	.29	4.05	2.56	1.86	2.53	.49	4.15			
17623	54.20	1.99	15.20	9.99	.29	3.91	2.52	1.88	2.62	.51	2.85			
17624	66.50	.70	14.60	5.78	.10	1.95	.28	1.35	3.22	.07	2.54			
17625	55.40	1.72	13.00	11.40	.32	6.70	1.20	3.80	.92	.54	3.16			
17626	65.30	.76	15.30	5.94	.04	1.66	.56	1.87	3.06	.14	2.47			
17627	73.10	.48	11.90	3.89	.06	1.01	.56	2.37	2.59	.07	1.00			
17628	58.00	.98	13.80	6.51	.15	8.26	1.91	1.69	1.79	.19	3.77			
17629	67.50	.58	14.10	4.27	.08	3.25	.54	2.13	2.51	.08	2.54			
17630	68.90	.40	12.50	5.97	.18	2.98	.42	2.06	1.96	.06	2.16			
17631	60.80	.97	17.80	5.69	.13	2.27	.33	1.16	4.76	.10	3.00			

LITHCODE	TS/PTS	ALTERATION	MINERALIZATION	COMMENTS	DEPTH	WIDTH	PAGE
7	0				177.6	7.6	
11	0				184.9	6.4	
7	0			I:TF SSLT	198.4	7.6	
11	0			SHAL F:TF	215.5	7.6	
3	0	SER CHL		F:TF	237.7	7.6	
13	0			SSLT	258.1	7.6	
11	0			SSST F:TF	24.0	7.6	
8	0				46.2	6.2	
11	0				86.3	7.6	
3	0			SSLT SSST	111.6	7.6	
4	0				133.5	7.6	
8	0			I:TF	151.6	7.6	
11	0			SSST	167.5	7.6	
1	0			F:LT I:TF	183.7	7.6	
11	0			SSST SHAL	209.0	7.6	
11	0			SSST F:TF	23.8	7.6	
3	0			F:TF	53.4	7.6	
8	0				86.1	7.6	
7	0			F:TF	109.1	7.6	
11	0			SSST I:TF	121.9	5.9	
7	0			I:TF	136.2	7.6	
3	0			I:TF	163.2	7.6	
11	0			SSST	185.6	7.6	
11	0			F:TF	19.7	7.6	
4	0			F:TF I:TF	47.1	7.6	
8	0				83.6	7.6	
7	0			F:LT	115.0	7.6	
11	0			SHAL	134.0	5.0	

Ba20	K20	P205	LOI	Zr	Sr	Rb	Zn	Cu	U	Th	Ga	Pb	Ni	Y	Ag
.01	4.51	.05	1.62				032	020				020			0
.13	5.89	.03	1.39				068	049				008			0
.02	4.52	.04	1.77				039	079				012			0
.06	5.13	.16	1.77				065	042				016			0
1.30	4.32	.09	3.23				170	045				024			0
2.53	2.20	.05	2.23				082	024				016			0
1.21	4.05	.11	2.62				067	037				008			0
2.54	3.43	.10	1.77				031	047				012			0
1.56	3.74	.04	1.62				100	072				024			0
.49	3.50	.10	4.00				160	009				032			0
4.29	1.67	.18	4.85				110	023				020			0
1.90	2.87	.17	2.77				160	046				052			0
.69	4.49	.10	2.00				280	029				088			0
2.10	.25	.66	1.08				140	026				028			0
.98	4.99	.10	2.08				870	027				120			1
1.45	3.74	.09	1.00				038	039				008			0
3.67	1.97	.16	1.31				160	026				028			0
1.54	1.70	.04	2.62				110	017				048			0
1.86	2.53	.49	4.15				710	054				120			0
1.88	2.62	.51	2.85				410	027				130			1
1.35	3.22	.07	2.54				110	130				040			0
3.80	.92	.54	3.16				400	026				080			0
1.87	3.06	.14	2.47				059	031				020			0
2.37	2.59	.07	1.00				038	100				008			0
1.69	1.79	.19	3.77				260	071				044			0
2.13	2.51	.08	2.54				074	025				024			0
2.06	1.96	.06	2.16				530	040				040			0
1.16	4.76	.10	3.00				230	053				136			0

SAMPLE	EASTING	NORTHING	TYPE	DRILLHOLE	LITHOLOGY	LITHCODE	TS/PTS	ALTERATION	MINERALIZATIO
17632			2	160230027	F:LT	8	0		
17633			2	160230027	SSLT	11	0		
17634			2	160230028	F:TF	7	0		
17635			2	160230028	F:TF	7	0		
17636			2	160230028	I:TF	3	0		
17637			2	160230028	I:TF	3	0		
17638			2	160230028	SHAL	13	0		
17639			2	160230028	SHAL	13	0		
17640			2	160230029	SSLT	11	0		
17641			2	160230029	F:TF	7	0		
17642			2	160230029	F:TF	7	0		
17643			2	160230029	F:TF	7	0		
17644			2	160230029	I:LT	4	0		
17645			2	160230029	I:LT	4	0		
17646			2	160230029	F:LT	8	0		
17647			2	160230029	SFDM	19	0		
17648			2	160230030	I:TF	3	0		
17649			2	160230030	F:TF	7	0		
17650			2	160230030	L:LT	4	0		
17651			2	160230030	F:TF	7	0		
17652			2	160230030	I:TF	3	0		
17653			2	160230030	I:LT	4	0		
17654			2	160230030	SSLT	11	0		
17655			2	160230031	SSLT	11	0		
17656			2	160230031	F:LT	8	0		
17657			2	160230031	SSLT	11	0		
17658			2	160230031	F:LT	8	0		
17659			2	160230031	SSLT	11	0		

SAMPLE	SiO2	TiO2	Al2O3	FeO	MnO	MgO	CaO	Na2O	K2O	P2O5	LOI	Zr	Sr	Rb
17632	52.00	1.41	14.80	8.43	.29	9.27	2.67	2.57	.99	.26	4.39			
17633	66.20	.77	14.50	5.97	.04	1.52	.50	.82	3.74	.14	2.47			
17634	76.20	.45	10.80	3.46	.07	.88	.15	1.39	2.56	.05	1.47			
17635	69.70	.77	11.80	6.41	.14	2.04	.54	.22	3.26	.09	2.16			
17636	78.20	.38	8.10	4.58	.10	.73	.54	.00	2.90	.06	1.54			
17637	51.00	2.49	13.60	12.00	.27	4.83	6.47	3.91	.58	.55	1.62			
17638	61.00	.91	17.20	5.74	.09	2.96	.94	.79	4.84	.13	2.62			
17639	70.00	.50	12.20	5.99	.12	2.26	.48	.13	4.04	.06	1.77			
17640	66.10	.66	15.10	5.43	.08	1.59	.78	1.98	3.56	.10	1.47			
17641	72.30	.44	11.40	4.97	.07	1.09	.38	.24	3.68	.06	1.85			1
17642	70.40	.59	13.10	4.30	.06	2.13	.29	.95	3.07	.06	2.39			
17643	69.60	.49	13.80	4.46	.08	1.19	.36	1.18	3.47	.10	2.16			
17644	71.30	.21	12.30	2.86	.14	3.59	.16	1.79	2.43	.02	2.16			
17645	53.40	1.79	13.30	10.30	.45	6.82	2.59	.74	3.46	.47	3.31			
17646	71.40	.11	12.10	2.92	.09	2.21	.28	.06	6.45	.02	1.62			1
17647	65.70	.76	14.70	6.00	.05	1.72	.97	1.02	3.67	.11	2.31			
17648	77.70	.23	10.00	2.59	.05	.66	.31	.00	3.94	.03	1.39			
17649	70.90	.34	13.20	4.09	.08	1.14	.19	.53	4.85	.04	1.62			
17650	52.70	1.67	12.90	12.40	.32	3.49	5.51	3.72	.21	.55	4.23			
17651	59.50	.87	12.00	10.90	.31	2.42	1.47	4.10	.67	.28	4.16			4
17652	61.90	1.10	14.90	8.19	.19	3.35	.88	2.67	1.99	.15	2.62			
17653	73.00	.27	12.00	2.74	.08	3.65	.12	1.53	2.39	.03	2.16			
17654	64.80	.77	15.30	6.27	.04	1.64	.89	1.67	2.97	.16	2.47			
17655	63.30	.69	16.30	5.64	.12	2.04	.93	2.32	3.73	.11	1.47			
17656	77.60	.19	11.00	2.48	.04	.55	.20	.46	3.46	.03	1.54			
17657	66.40	.64	14.70	5.75	.11	1.23	.21	.00	5.32	.10	2.31			
17658	57.30	.64	14.40	6.51	.30	5.16	3.56	.15	5.22	.06	2.31			2
17659	59.50	1.13	15.70	7.32	.16	4.46	.54	2.75	3.01	.14	2.62			

LITHCODE	TS/PTS	ALTERATION	MINERALIZATION	COMMENTS	DEPTH	WIDTH
8	0			I:LT	154.0	7.6
11	0			SHAL	174.2	7.6
7	0				12.6	7.6
7	0			I:TF SSLT	24.0	7.6
3	0			I:LT	33.2	7.6
3	0				46.5	7.6
13	0			SSLT F:LT	59.9	7.6
13	0			SSLT F:LT	73.6	7.6
11	0			F:TF I:LT	12.9	7.6
7	0			SSLT SHAL	31.8	7.6
7	0			I:TF	73.1	7.6
7	0			I:TF	100.6	7.6
4	0			I:TF	138.7	7.6
4	0				149.2	6.9
8	0				163.5	7.6
19	0				178.2	6.0
3	0				39.6	7.6
7	0			I:TF F:LT	57.5	7.6
4	0				77.0	7.6
7	0			F:LT	88.8	7.6
3	0			F:LT	104.6	7.6
4	0			F:LT	140.4	7.6
11	0				170.2	7.6
11	0			SSST SHAL	32.1	7.6
8	0			I:LT SSLT	86.1	7.6
11	0			F:LT	131.9	7.6
8	0			I:TF	156.7	7.6
11	0				184.6	.4

Na2O	K2O	P2O5	LOI	Zr	Sr	Rb	Zn	Cu	U	Th	Ga	Pb	Ni	Y	Ag
2.57	.99	.26	4.39				180	032				060			0
.82	3.74	.14	2.47				058	035				012			0
1.39	2.56	.05	1.47				045	016				008			0
.22	3.26	.09	2.16				110	170				012			0
.00	2.90	.06	1.54				690	510				080			1
3.91	.58	.55	1.62				068	028				012			0
.79	4.84	.13	2.62				120	042				032			0
.13	4.04	.06	1.77				120	028				012			0
1.98	3.56	.10	1.47				043	020				008			0
.24	3.68	.06	1.85				1540	190				064			0
.95	3.07	.06	2.39				081	025				016			0
1.18	3.47	.10	2.16				060	009				008			0
1.79	2.43	.02	2.16				510	007				088			0
.74	3.46	.47	3.31				480	056				192			1
.06	6.45	.02	1.62				1900	007				920			0
1.02	3.67	.11	2.31				065	025				016			0
.00	3.94	.03	1.39				033	006				008			0
.53	4.85	.04	1.62				033	008				008			0
3.72	.21	.55	4.23				130	023				008			0
4.10	.67	.28	4.16				A700	8900				150			13
2.67	1.79	.15	2.62				320	950				092			1
1.53	2.39	.03	2.16				100	026				012			0
1.67	2.97	.16	2.47				68	39				8			0
2.32	3.73	.11	1.47				047	046				004			0
.46	3.46	.03	1.54				021	006				004			0
.00	5.32	.10	2.31				054	140				008			0
.15	5.22	.06	2.31				2000	045				520			3
2.75	3.01	.14	2.62				120	024				016			0

SAMPLE	EASTING	NORTHING	TYPE	DRILLHOLE	LITHOLOGY	LITHCODE	TS/PIS	ALTERATION	MINERALIZATION
17660			2	160230031	F:LT	8	0		
17661			2	160230031	SHAL	13	0		
17662			2	160230032	F:TF	7	0		
17663			2	160230032	F:LT	8	0		
17664			2	160230032	F:LT	8	0		
17665			2	160230032	F:TF	7	0		
17666			2	160230032	I:TF	3	0		
17667			2	160230032	F:TF	7	0		
17668			2	160230032	I:TF	3	0		
17669			2	160230033	F:TF	7	0		
17670			2	160230033	F:TF	7	0		
17671			2	160230033	I:TF	3	0		
17672			2	160230033	I:TF	3	0		
17673			2	160230033	F:TF	7	0		
17674			2	160230033	F:LT	8	0		
17675			2	160230033	I:TF	3	0		
17676			2	160230033	SEDM	19	0		
17677			2	160230033	I:TF	3	0		
17678			2	160230034	F:TF	7	0		
17679			2	160230034	SSLT	11	0		
17680			2	160230034	I:LT	4	0		
17681			2	160230034	SSLT	11	0		
17682			2	160230034	I:LT	4	0		
17683			2	160230034	SSLT	11	0		
17684	+ 630E	-1110S	1	0	F:TF	7	0		
17685	+ 450E	-1100S	1	0	F:TF	7	0		
17686	+ 550E	-1100S	1	0	SSST	12	0		
17687	+ 450E	-1200S	1	0	F:TF	7	0		

SAMPLE	SiO2	TiO2	Al2O3	FeO	MnO	MgO	CaO	Na2O	K2O	P2O5	LOI	Zr	Sr	Rb
17660	70.70	.69	13.40	4.80	.08	1.55	.17	1.36	3.01	.07	2.08			
17661	61.30	1.55	13.30	7.97	.12	3.42	2.72	1.17	2.11	.24	2.70			
17662	90.70	.24	2.80	2.04	.04	.42	.15	.00	.43	.03	.93			
17663	73.30	.37	11.80	3.20	.07	.92	.23	1.04	4.06	.08	1.62			
17664	78.50	.14	9.90	1.97	.04	.35	.05	1.39	3.72	.02	1.16			
17665	67.90	.48	14.70	4.52	.09	1.08	.24	.24	5.29	.09	2.08			
17666	53.70	1.44	13.40	13.20	.38	3.57	3.30	2.25	1.40	.53	2.93			
17667	64.20	.83	15.10	6.05	.11	2.62	.78	1.66	2.94	.09	2.70			
17668	53.70	1.58	16.40	10.20	.37	4.87	1.48	1.56	2.72	.26	3.70			
17669	67.40	.64	14.30	5.81	.10	1.74	.74	2.48	2.75	.12	1.23			
17670	75.90	.40	11.10	3.15	.05	.67	.30	.74	3.40	.04	1.23			
17671	70.70	.50	13.60	4.37	.07	.99	.30	.43	4.40	.05	1.54			
17672	70.50	.53	13.10	4.84	.09	1.28	.20	.51	4.19	.05	1.62			
17673	70.90	.41	13.10	4.26	.09	1.12	.19	.00	5.34	.04	1.39			
17674	78.90	.15	8.90	2.80	.05	.40	.13	.00	4.71	.03	.93			
17675	76.90	.33	9.70	3.78	.07	1.03	.36	.08	4.44	.04	1.16			
17676	62.20	.90	18.90	5.93	.06	1.85	.21	.78	4.62	.09	3.39			
17677	71.60	.58	13.60	4.24	.09	1.34	.24	1.37	3.23	.05	1.70			
17678	66.30	.75	14.30	6.18	.13	1.79	.47	.67	4.14	.10	1.77			
17679	64.20	.74	15.80	5.44	.10	1.98	.65	.91	4.49	.12	2.31			
17680	51.10	1.57	12.40	12.00	.39	3.58	6.74	3.04	.34	.52	5.93			
17681	56.30	1.27	17.30	8.13	.19	3.96	2.43	3.55	1.96	.14	2.77			
17682	73.60	.20	11.30	2.44	.08	3.48	.18	1.72	2.54	.02	1.85			
17683	65.70	.80	16.30	5.71	.05	1.60	.73	.58	4.66	.09	2.54			
17684	73.90	.17	12.60	2.00	.06	1.05	.24	1.88	2.89	.02	2.54			
17685	76.90	.12	10.80	1.91	.03	.37	.00	.07	6.17	.02	1.62			
17686	72.50	.45	12.20	4.54	.09	1.13	.58	2.17	1.96	.04	1.70			
17687	78.50	.12	9.70	1.97	.03	.33	.00	.01	5.80	.02	1.31			

LITHCODE	TS/PTS	ALTERATION	MINERALIZATION	COMMENTS	DEPTH	WIDTH
8	0			I:LT	198.0	7.6
13	0				208.8	5.0
7	0			SSST	38.9	7.6
8	0			I:LT	78.7	7.6
8	0				132.4	7.6
7	0			I:TF	147.3	7.6
3	0			1:LT	164.0	7.6
7	0			SSLT SHAL	176.6	7.6
3	0			F:TF	185.1	7.6
7	0			I:TF SEDM	32.6	7.6
7	0			SEDM	68.7	7.6
3	0				84.0	7.6
3	0			M:TF	107.7	7.6
7	0			I:TF	127.4	7.6
8	0				140.4	7.6
3	0			M:TF	153.0	7.6
19	0				171.7	7.6
3	0				193.4	7.6
7	0				35.6	7.6
11	0			F:TF	35.6	7.6
4	0				68.1	7.0
11	0				76.3	7.6
4	0				105.7	7.6
11	0				137.3	7.6
7	0				.0	.0
7	0				.0	.0
12	0				.0	.0
7	0				.0	.0

Na2O	K2O	P2O5	LOI	Zr	Sr	Rb	Zn	Cu	U	Th	Ga	Pb	Ni	Y	Ag
1.36	3.01	.07	2.08				160	018				012			0
1.17	2.11	.24	2.70				068	020				012			0
.00	.43	.03	.93				023	016				004			0
1.04	4.06	.08	1.62				048	110				008			0
1.39	3.72	.02	1.16				028	019				016			0
.24	5.29	.09	2.08				047	020				012			0
2.25	1.40	.53	2.93				1900	650				1200			3
1.66	2.94	.09	2.70				110	059				024			0
1.56	2.72	.28	3.70				2040	097				520			0
2.48	2.75	.12	1.23				039	012				008			0
.74	3.40	.04	1.23				024	038				008			0
.43	4.40	.05	1.54				036	055				008			0
.51	4.19	.05	1.62				047	046				008			0
.00	5.34	.04	1.39				043	014				012			0
.00	4.71	.03	.93				044	004				020			0
.08	4.44	.04	1.16				040	020				028			0
.78	4.62	.09	3.39				061	032				008			0
1.37	3.23	.05	1.70				560	014				220			0
.67	4.14	.10	1.77				065	041				004			0
.91	4.49	.12	2.31				071	035				008			0
3.04	.34	.52	5.93				130	027				008			0
3.55	1.96	.14	2.77				120	062				020			0
1.72	2.54	.02	1.85				074	010				008			0
.58	4.66	.09	2.54				069	023				012			0
1.88	2.89	.02	2.54				025	001				004			0
.07	6.17	.02	1.62				017	035				000			0
2.17	1.96	.04	1.70				035	007				004			0
.01	5.80	.02	1.31				022	064				024			0

SAMPLE	EASTING	NORTHING	TYPE	DRILLHOLE	LITHOLOGY	LITHCODE	TS/PTS	ALTERATION	MINERALIZATI
17688	+ 550E	-1200S	1	0	SSST	12	0		
17689	+ 450E	-1300S	1	0	SSLT	11	0		
17690	+ 650E	-1200S	1	0	F:TF	7	0		
17691	+ 500E	-1310S	1	0	F:TF	7	0		
17692	+ 600E	-1300S	1	0	F:TF	7	0		
17693	+ 400E	- 800S	1	0	F:TF	7	0		
17694	+ 675E	- 900S	1	0	SSLT	11	0		
17695	+ 650E	-1000S	1	0	F:TF	7	0		
17696	+ 400E	-1000S	1	0	F:TF	7	0		
17697	+ 400E	- 900S	1	0	F:TF	7	0		
17698	+ 550E	- 900S	1	0	F:TF	7	0		
17699	+ 550E	-1000S	1	0	F:TF	7	0		
17700	+ 675E	- 800S	1	0	F:TF	7	0		
18383	+ 550E	- 800S	1	0	SSST	12	0		
1871	- 050W	-0400S	1	0	SHAL	13	0		
1872	+ 065E	-0400S	1	0	S#CH	2	0	CHL	
1873	+ 175E	-0380S	1	0	F:LT	8	0		
1874	+ 010E	-0400S	1	0	SHAL	13	0		
1875	+ 225E	-0200S	1	0	SSST	12	0		
1876	+ 250E	-0400S	1	0	D/F:	15	0		
1877	+ 090E	-0400S	1	0	F:TF	7	0		
1878	+ 060E	-0200S	1	0	I:TF	3	0		
1879	+ 125E	-0200S	1	0	I:TF	3	0		
1880	- 100W	+0200N	1	0	SHAL	13	0		
1881	- 065W	-0200S	1	0	SHAL	13	0		
1882	- 050W	-0200S	1	0	SSLT	11	0		
1883	+ 175E	-0200S	1	0	SSLT	11	0		
1884	+ 220E	+0200N	1	0	SSLT	11	0		

SAMPLE	SiO2	TiO2	Al2O3	FeO	MnO	MgO	CaO	Na2O	K2O	P2O5	LOI	Zr	Sr	Rb
17688	78.50	.31	7.80	5.38	.09	1.24	.35	.85	1.16	.07	1.54			
17689	54.40	1.09	18.20	8.19	.16	3.01	1.89	5.11	3.18	.14	1.23			
17690	78.70	.19	10.30	1.93	.02	.26	.19	3.79	1.13	.01	1.16			
17691	72.90	.25	11.10	4.16	.09	.70	.00	.04	7.61	.02	1.23			
17692	87.70	.19	4.90	1.79	.03	.23	.11	.00	1.51	.01	1.54			
17693	85.80	.52	4.70	2.86	.05	.49	.11	.00	1.28	.03	1.16			
17694	70.40	.75	12.70	4.39	.09	1.36	.59	3.71	2.17	.07	.93			
17695	82.60	.42	6.80	3.53	.05	.61	.00	.00	2.05	.02	1.39			
17696	77.40	.17	11.10	1.75	.03	.19	.03	1.38	5.07	.03	.70			
17697	92.60	.12	2.20	1.57	.03	.20	.00	.23	.64	.01	.70			
17698	75.30	.32	10.00	5.61	.11	1.01	.08	.14	2.66	.02	1.77			
17699	85.40	.38	4.90	3.48	.06	.50	.00	.00	1.60	.01	1.16			
17700	70.50	.88	12.00	4.87	.11	1.36	.63	3.69	1.99	.07	.93			
18383	84.50	.35	5.50	3.73	.06	.62	.00	.00	2.03	.01	.93			
1871	67.90	.85	12.90	4.06	.04	1.35	2.50	3.44	.54	.09	3.00	193	182	22
1872	46.40	3.69	8.62	15.40	.39	7.03	1.37	3.01	.30	.75	4.54	287	62	19
1873	76.00	.78	7.00	4.06	.08	1.89	.52	2.71	1.17	.09	2.31	228	48	66
1874	73.00	.03	12.50	3.57	.03	.82	.85	1.65	2.41	.09	2.00	164	74	152
1875	77.20	.43	16.50	4.48	.07	1.08	.56	2.77	1.48	.06	1.23	126	56	77
1876	79.30	.35	8.81	4.08	.05	.83	.31	2.12	1.97	.04	1.00	84	44	100
1877	89.20	.11	9.06	1.56	.03	.30	.61	.93	1.27	.02	.69	172	29	34
1878	72.30	.15	11.40	2.67	.15	3.48	.37	4.21	.67	.03	1.77	337	37	31
1879	83.30	.13	10.60	1.34	.04	.96	.19	3.72	.42	.01	1.00	232	25	11
1880	70.40	.84	8.18	4.60	.04	1.03	.61	1.22	2.46	.10	3.31	233	81	119
1881	69.40	.79	12.50	4.54	.04	1.15	.65	1.87	1.95	.11	3.31	203	101	90
1882	81.60	.45	11.40	2.43	.02	.74	.49	2.11	1.55	.05	1.38	217	51	74
1883	62.50	.80	9.46	8.69	.26	1.55	2.00	3.32	2.78	.20	.85	898	126	77
1884	78.70	.32	10.30	4.04	.07	.75	.32	2.09	1.43	.04	1.23	83	38	61

LITHCODE	TS/PTS	ALTERATION	MINERALIZATION	COMMENTS	DEPTH	WIDTH
12	0				.0	.0
11	0				.0	.0
7	0				.0	.0
7	0				.0	.0
7	0				.0	.0
7	0				.0	.0
11	0				.0	.0
7	0				.0	.0
7	0				.0	.0
7	0				.0	.0
7	0				.0	.0
7	0				.0	.0
7	0				.0	.0
12	0				.0	.0
13	0				.0	.0
2	0	CHL			.0	.0
8	0				.0	.0
13	0			SSLT	.0	.0
12	0				.0	.0
15	0				.0	.0
7	0				.0	.0
3	0				.0	.0
3	0				.0	.0
13	0				.0	.0
13	0				.0	.0
11	0				.0	.0
11	0				.0	.0
11	0				.0	.0

Na2O	K2O	P2O5	LOI	Zr	Sr	Rb	Zn	Cu	U	Th	Ga	Pb	Ni	Y	Ag
.85	1.16	.07	1.54				042	007				004			0
5.11	3.18	.14	1.23				053	002				008			0
3.79	1.13	.01	1.16				011	001				000			0
.04	7.61	.02	1.23				044	005				012			0
.00	1.51	.01	1.54				008	004				004			0
.00	1.28	.03	1.16				022	013				004			0
3.71	2.17	.07	.93				025	015				004			0
.00	2.05	.02	1.39				018	011				004			0
1.38	5.07	.03	.70				015	006				000			0
.23	.64	.01	.70				013	004				024			0
.14	2.66	.02	1.77				037	012				004			0
.00	1.60	.01	1.16				024	002				000			0
3.69	1.99	.07	.93				034	008				000			0
.00	2.03	.01	.93				030	003				000			0
3.44	.54	.09	3.00	193	182	22	36	29	3	7	18	9	4	27	0
3.01	.30	.75	4.54	287	62	19	130	22	5	6	25	2	0	81	0
2.71	1.17	.09	2.31	228	48	66	40	22	0	7	13	25	0	36	0
1.65	2.41	.09	2.00	164	74	152	22	13	5	12	15	5	0	24	0
2.77	1.48	.06	1.23	126	56	77	26	8	3	12	12	0	2	14	0
2.12	1.97	.04	1.00	84	44	100	26	10	2	8	10	0	0	13	0
.93	1.27	.02	.66	172	29	34	11	27	0	5	5	8	0	41	0
4.21	.67	.03	1.77	337	37	31	390	5	2	13	19	23	0	152	0
3.72	.42	.01	1.00	232	25	11	28	6	1	7	13	12	1	45	0
1.22	2.46	.10	3.31	233	81	119	22	18	4	14	19	0	0	17	0
1.87	1.95	.11	3.31	203	101	90	35	20	4	11	16	17	00	21	0
2.11	1.55	.05	1.38	217	51	74	15	9	1	6	10	0	2	18	0
3.32	2.78	.20	.85	898	126	77	110	7	3	10	25	0	0	129	0
2.09	1.43	.04	1.23	83	38	61	23	9	0	7	11	0	0	12	0

SAMPLE	EASTING	NORTHING	TYPE	DRILLHOLE	LITHOLOGY	LITHCODE	TS/PTS	ALTERATION	MINERALIZATI
1885	+ 130E	+0200N	1	0	I:TF	3	0		
1886	+ 075E	+0200N	1	0	F:TF	7	0		
1887	- 040W	+0200N	1	0	SSLT	11	0		
1888	+ 070E	+0600N	1	0	F:FL	10	0		
1889	+ 225E	+0700N	1	0	SSST	12	0		
1890	- 065W	+0700N	1	0	SSLT	11	0		
1891	- 025W	+0700N	1	0	SHAL	13	0		
1892	- 010W	+0700N	1	0	S*CH	2	0	CHL	
1893	+ 005E	+0400N	1	0	F:TF	7	0		
1894	+ 125E	+0400N	1	0	SSST	12	0		
1895	+ 210E	+0400N	1	0	SSLT	11	0		
1896	- 025W	+0385N	1	0	F:TF	7	0		
1897	+ 130E	+ 600N	1	0	F:LT	8	0		
1898	+ 170E	+0700N	1	0	F:TF	7	0		
1899	+ 070E	+0700N	1	0	F:FL	10	0		
1900	+ 140E	+0700N	1	0	F:TF	7	0		
1901	+ 250E	+0600N	1	0	SSLT	11	0		
1902	+ 060E	+0600N	1	0	SHAL	13	0	SIL	
1903	+ 220E	+0600N	1	0	SSST	12	0		
1904	- 115W	+0600N	1	0	SSLT	11	0		
1905	+ 165E	+0400N	1	0	SSST	12	0		
1906	- 010W	+0575N	1	0	F:LT	8	0		
1907	+ 280E	+0400N	1	0	F:TF	7	0		
1908	+ 235E	+0875N	1	0	SSLT	11	0		
1909	+ 265E	+1000N	1	0	SSLT	11	0		
1910	+ 015E	+1025N	1	0	F:TF	7	0		
1911	- 060W	+0400N	1	0	SHAL	13	0		
1912	+ 165E	+0600N	1	0	F:TF	7	0		

SAMPLE	SiO2	TiO2	Al2O3	FeO	MnO	MgO	CaO	Na2O	K2O	P2O5	LOI	Zr	Sr	Rb
1885	67.70	.68	9.67	7.20	.29	.77	.67	5.19	.48	.15	1.62	789	58	12
1886	60.00	.87	11.70	8.02	.33	3.41	.68	5.84	.31	.12	3.08	225	158	7
1887	84.90	.23	18.00	1.77	.01	.31	.36	1.03	1.95	.34	1.54	72	35	94
1888	84.60	.12	16.30	2.19	.03	.25	.13	.26	3.34	.02	.77	114	11	87
1889	76.10	.43	8.70	3.78	.06	.91	.46	2.91	2.04	.12	1.15			
1890	77.50	.41	8.55	4.94	.04	.85	1.20	2.73	.93	.09	1.23			
1891	67.30	.90	13.30	5.61	.06	1.80	.19	1.57	2.69	.06	3.00			
1892	49.10	3.12	19.40	14.00	.04	9.90	1.10	.79	.53	.72	5.38			
1893	73.40	.17	9.97	2.36	.11	3.72	.33	.99	2.43	.03	2.46	259	56	105
1894	81.50	.28	17.50	4.81	.09	.81	.13	.19	3.06	.04	1.08	180	20	120
1895	60.60	.77	11.00	8.47	.13	2.20	1.16	1.50	3.89	.11	2.38	253	47	140
1896	79.90	.39	14.80	1.74	.01	.50	.13	.44	4.34	.04	1.92	123	28	164
1897	76.20	.15	9.86	2.22	.03	.26	.12	.25	5.14	.02	1.46	225	32	144
1898	76.60	.13	10.80	1.49	.01	.32	.13	.35	7.30	.02	1.00			
1899	80.70	.02	18.18	1.59	.02	.10	.12	.19	5.51	.03	.38			
1900	73.20	.03	9.46	2.81	.03	.26	.12	.32	5.42	.02	1.46			
1901	76.50	.06	10.30	3.54	.06	1.00	.83	2.65	1.62	.06	1.00	97	69	82
1902	74.70	.03	9.67	4.65	.03	.75	1.36	2.32	1.26	.02	2.38	161	83	83
1903	74.30	.07	11.70	3.58	.07	.94	.43	2.90	2.14	.05	1.15	124	40	103
1904	62.30	.16	18.00	6.95	.16	2.11	.55	1.66	3.04	.11	3.54	228	88	149
1905	62.60	.13	16.30	7.19	.13	2.06	.89	1.08	4.39	.10	2.08	165	88	227
1906	78.40	.12	8.70	2.11	.12	3.18	.27	2.96	.44	.02	1.85	289	25	20
1907	82.10	.02	9.55	.74	.02	.17	.13	.38	5.70	.02	1.54	90	42	90
1908	66.70	.10	13.30	6.66	.10	1.95	1.14	2.99	1.62	.08	1.62			
1909	58.80	.88	19.40	4.31	.15	2.19	.60	2.72	4.31	.10	2.23	185	82	156
1910	77.80	.22	9.97	.64	.04	1.12	.25	4.13	.64	.03	1.15			
1911	65.40	.75	17.50	5.65	.02	1.00	.16	.29	5.65	.10	4.23	170	23	279
1912	77.10	.16	11.00	5.54	.03	.52	.13	.61	5.54	.02	1.08	181	51	175

THCODE	TS/PTS	ALTERATION	MINERALIZATION	COMMENTS	DEPTH	WIDTH
3	0				.0	.0
7	0				.0	.0
11	0				.0	.0
10	0				.0	.0
12	0				.0	.0
11	0		SHAL		.0	.0
13	0		F:TF		.0	.0
2	0	CHL			.0	.0
7	0				.0	.0
12	0				.0	.0
11	0		SSST		.0	.0
7	0				.0	.0
8	0				.0	.0
7	0				.0	.0
10	0				.0	.0
7	0				.0	.0
11	0		SSST		.0	.0
13	0	SIL			.0	.0
12	0		TFSD		.0	.0
11	0		SHAL		.0	.0
12	0		BASC		.0	.0
8	0				.0	.0
7	0				.0	.0
11	0		BASC		.0	.0
11	0				.0	.0
7	0				.0	.0
13	0				.0	.0
7	0				.0	.0

Na2O	K2O	P2O5	LOI	Zr	Sr	Rb	Zn	Cu	U	Th	Ga	Pb	Ni	Y	Ag
5.19	.48	.15	1.62	789	58	12	140	8	0	9	22	3	00	112	0
5.84	.31	.12	3.08	225	158	7	110	110	0	14	18	40	0	21	0
1.03	1.95	.34	1.54	72	35	94	2	9	0	2	10	8	0	22	0
.26	3.34	.02	.77	114	11	87	18	8	1	7	6	0	0	41	0
2.91	2.04	.12	1.15				27	15				0			0
2.73	.93	.09	1.23				27	10				0			0
1.57	2.69	.06	3.00				49	15				0			0
.79	.53	.72	5.38				130	16				3			0
.49	2.43	.03	2.46	259	56	105	5800	60	0	81	162	6900	0	72	4
.19	3.06	.04	1.08	180	20	120	74	25	0	41	64	45	0	53	0
1.50	3.89	.11	2.38	253	47	140	84	15	5	14	19	15	0	26	0
.44	4.34	.04	1.92	123	28	164	3	11	4	6	13	7	0	6	0
.25	5.14	.02	1.46	225	32	144	12	9	1	10	12	15	0	42	0
.35	7.30	.02	1.00				18	8				3			0
.19	5.51	.03	.38				50	32				85			0
.32	5.42	.02	1.46				13	9				7			0
2.65	1.62	.06	1.00	97	69	82	28	9	0	4	13	0	5	15	0
2.32	1.26	.02	2.38	161	83	83	27	16	0	4	11	6	0	24	0
2.90	2.14	.05	1.15	124	40	103	22	21	0	9	12	0	3	18	0
1.66	3.04	.11	3.54	228	88	149	58	17	1	12	23	0	10	21	0
1.08	4.39	.10	2.08	165	88	227	63	14	1	6	19	5	8	34	0
2.96	.44	.02	1.85	289	25	20	50	8	3	12	16	3	1	94	0
.38	5.70	.02	1.54	90	42	90	8	8	5	15	6	5	0	34	0
2.99	1.62	.08	1.62				37	10				0			0
2.72	4.31	.10	2.23	185	82	156	57	30	3	12	24	0	12	37	0
1.13	.64	.03	1.15				12	13				13			0
.29	5.65	.10	4.23	170	23	279	2	14	8	13	22	5	0	13	0
.61	5.54	.02	1.08	181	51	175	22	8	4	14	13	10	0	48	0

SAMPLE	EASTING	NORTHING	TYPE	DRILLHOLE	LITHOLOGY	LITHCODE	TS/PTS	ALTERATION	MINERALIZATI
1913	- 135W	+1000N	1	0	SHAL	13	0		
1914	+ 025E	+0875N	1	0	F:TF	7	0		
1915	+ 150E	+0900N	1	0	F:TF	7	0		
1916	- 060W	+1000N	1	0	SSLT	11	0		
1917	+ 185E	+0900N	1	0	F:TF	7	0		
1918	+ 075E	+1000N	1	0	F:TF	7	0		
1919	+ 140E	+1000N	1	0	TFSD	18	0		
1920	+ 025E	+0875N	1	0	SSST	12	0		
1921	- 100W	+0800S	1	0	SSLT	11	0	SIL	
1922	+ 210E	+1000S	1	0	SSST	12	0		
1923	+ 020E	+1000N	1	0	F:TF	7	0		
1924	- 025W	+0800N	1	0	F:TF	7	0	SER /	
1925	- 075W	+0900N	1	0	SHAL	13	0		
1926	+ 025E	+0800N	1	0	F:TF	7	0		
1927	+ 105E	+0900N	1	0	SSLT	11	0		
1928	+ 125E	+0800N	1	0	F:TF	7	0		
1929	+ 250E	+0800N	1	0	SSLT	11	0		
1930	+ 075E	+0800N	1	0	F:FL	10	0		
1931	+ 175E	+0800N	1	0	SSST	12	0		
1932	+ 200E	+0790N	1	0	F:TF	7	0		
1933	+ 065E	+0900N	1	0	F:TF	7	0		
1934	+ 080E	-0700S	1	0	SHAL	13	0		
1935	+ 250E	-0600S	1	0	F:TF	7	0		
1936	+ 115E	- 700S	1	0	F:AG	9	0	CHL	
1937	+ 325E	- 700S	1	0	F:TF	7	0		
1938	+ 375E	-0700S	1	0	F:TF	7	0		
1939	+ 125E	- 700S	1	0	F:TF	1	0		PY
1940	+ 200E	- 700S	1	0	F:TF	7	0		

SAMPLE	SiO2	TiO2	Al2O3	FeO	MnO	MgO	CaO	Na2O	K2O	P2O5	LOI	Zr	Sr	Rb
1913	70.00	.90	14.80	3.16	.06	1.36	.35	1.01	3.16	.16	3.69	183	92	202
1914	78.30	.15	9.86	5.12	.11	.93	.18	.62	5.12	.01	1.08	278	59	62
1915	80.20	.15	10.80	2.60	.01	.30	.14	2.81	2.60	.02	.92			
1916	79.40	.54	8.96	1.01	.04	.09	1.37	2.32	1.01	.04	1.23			
1917	77.00	.22	11.00	2.77	.01	.37	.14	1.89	2.77	.02	1.54			
1918	86.60	.12	5.54	3.57	.00	.08	.12	.22	3.57	.02	.54	151	24	65
1919	80.02	.17	10.70	2.86	.03	.36	.15	2.24	2.86	.02	1.08	174	30	118
1920	77.90	.53	10.20	1.54	.05	1.00	1.10	2.27	1.54	.04	1.38			
1921	83.60	.30	8.97	1.16	.04	.72	1.15	2.06	1.16	.04	.92	387	104	72
1922	71.10	.47	12.40	2.33	.06	1.32	.42	2.83	2.33	.07	1.31			
1923	81.60	.15	9.45	2.06	.00	.27	.19	2.76	1.51	.02	1.62	294	22	50
1924	77.20	.40	10.50	3.01	.02	.42	.44	2.18	2.07	.06	2.08	224	57	107
1925	68.00	.78	16.80	3.77	.03	1.49	.24	1.12	3.93	.06	3.38			
1926	76.10	.24	10.30	3.26	.11	1.23	.23	3.48	1.08	.03	1.54	314	32	51
1927	77.40	.23	9.98	3.92	.05	.64	.15	.15	4.96	.03	1.15			
1928	79.20	.14	8.99	1.26	.01	.18	.12	.33	5.61	.02	1.15	212	44	152
1929	66.70	.75	14.50	6.34	.13	2.25	.71	3.41	2.02	.08	2.15	161	80	91
1930	84.60	.12	5.48	1.67	.01	.22	.12	.20	3.89	.02	.85	122	0	113
1931	79.50	.12	9.95	2.46	.02	.32	.12	.22	3.99	.02	1.77	142	17	155
1932	75.00	.31	11.90	3.50	.05	.71	.31	2.10	2.71	.02	1.38	124	41	150
1933	84.50	.10	5.22	1.24	.02	.11	.11	.18	3.45	.02	.85			
1934	64.70	.81	17.00	4.72	.03	1.25	.16	.19	4.36	.11	3.69			
1935	76.30	.23	9.07	3.19	.05	.30	.13	.31	6.61	.02	.92	342	64	170
1936	74.90	.21	11.00	2.36	.08	1.69	.24	.91	5.65	.03	.85			
1937	71.30	.48	13.50	4.09	.06	1.31	.27	.78	4.25	.05	1.62			
1938	88.60	.35	4.17	2.53	.03	.40	.13	.33	1.13	.03	1.23			
1939	37.90	4.97	18.10	11.20	.34	9.01	5.65	2.81	.70	1.34	6.69			
1940	81.00	.25	9.00	1.18	.01	.18	.26	.31	5.92	.07	.54			

ITHCODE	TS/PTS	ALTERATION	MINERALIZATION	COMMENTS	DEPTH	WIDTH
13	0				.0	.0
7	0			CHER MTX	.0	.0
7	0				.0	.0
11	0			SSST	.0	.0
7	0				.0	.0
7	0				.0	.0
18	0				.0	.0
12	0				.0	.0
11	0	SIL			.0	.0
12	0				.0	.0
7	0				.0	.0
7	0	SER			.0	.0
13	0				.0	.0
7	0				.0	.0
11	0				.0	.0
7	0				.0	.0
11	0				.0	.0
10	0				.0	.0
12	0				.0	.0
7	0				.0	.0
7	0				.0	.0
13	0				.0	.0
7	0				.0	.0
9	0	CHL			.0	.0
7	0				.0	.0
7	0				.0	.0
1	0		PY		.0	.0
7	0				.0	.0

a2O	K2O	P2O5	LOI	Zr	Sr	Rb	Zn	Cu	U	Th	Ga	Pb	Ni	Y	Ag
1.01	3.16	.16	3.69	183	92	202	34	18	4	11	22	5	10	31	0
.62	5.12	.01	1.08	278	59	62	25	11	0	4	9	12	0	13	0
.81	2.60	.02	.92				11	7				2			0
.32	1.01	.04	1.23				24	8				2			0
.89	2.77	.02	1.54				11	8				0			0
.22	3.57	.02	.54	151	24	65	0	7	1	10	6	15	0	34	0
.24	2.86	.02	1.08	174	30	118	20	5	1	10	12	0	0	45	0
.27	1.54	.04	1.38				29	11				0			0
.06	1.16	.04	.92	387	104	72	30	12	4	13	12	0	0	62	0
.63	2.33	.07	1.31				42	5				0			0
.76	1.51	.02	1.62	294	22	50	2	9	1	8	17	13	0	87	0
.18	2.07	.06	2.08	224	57	107	12	12	1	10	18	7	0	21	0
1.12	3.93	.06	3.38				30	14				16			0
3.48	1.08	.03	1.54	314	32	51	35	9	5	15	12	6	1	98	0
.15	4.96	.03	1.15				37	5				0			0
.33	5.61	.02	1.15	212	44	152	0	8	2	7	12	12	0	32	0
3.41	2.02	.08	2.15	161	80	91	62	32	1	9	15	0	9	25	0
.20	3.89	.02	.85	122	0	113	14	8	0	9	4	6	0	22	0
.22	3.99	.02	1.77	142	17	155	10	8	3	14	13	0	0	37	0
.10	2.71	.02	1.38	124	41	150	27	16	3	10	13	0	1	24	0
.18	3.45	.02	.85				8	12				19			0
.19	4.36	.11	3.69				28	18				3			0
.31	6.61	.02	.92	342	64	170	39	22	4	13	10	34	0	49	0
.91	5.65	.03	.85				150	7				59			0
.78	4.25	.05	1.62				39	5				0			0
.33	1.13	.03	1.23				15	22				0			0
2.81	.70	1.34	6.69				130	15				5			0
.31	5.92	.07	.54				1	10				27			0

303

SAMPLE	EASTING	NORTHING	TYPE	DRILLHOLE	LITHOLOGY	LITHCODE	TS/PTS	ALTERATION	MINERALIZATI
1941	+ 275E	- 700S	1	0	F:TF	7	0		
1942	+ 365E	-0600S	1	0	F:TF	7	0		
1943	+ 215E	- 600S	1	0	F:TF	7	0		
1944	+ 140E	-0600S	1	0	S#CH	2	0	CHL	
1945	+ 075E	-0575S	1	0	F:TF	7	0		
1946	+ 050E	-0590S	1	0	SSST	12	0		
1947	- 015W	-0600S	1	0	SSST	12	0		
1948	+ 325E	-1000S	1	0	F:TF	7	0		
1949	+ 275E	- 900S	1	0	SSLT	11	0		
1950	+ 225E	-1000S	1	0	SSLT	11	0		
1951	+ 350E	-0800S	1	0	F:TF	7	0		
1952	+ 350E	-0975S	1	0	F:TF	7	0		
1953	+ 350E	-0850S	1	0	F:TF	7	0		
1954	+ 225E	- 900S	1	0	SSLT	11	0		
1955	+ 325E	-0800S	1	0	F:TF	7	0		
1956	+ 220E	- 800S	1	0	F:TF	7	0	FEO	
1957	+ 125E	- 800S	1	0	F:TF	7	0		
1958	+ 055E	-0775S	1	0	SSST	12	0		
1959	+ 050E	-0900S	1	0	SSLT	11	0		
1960	+ 175E	-1000S	1	0	F:TF	7	0		
1961	+ 180E	-0800S	1	0	TFSD	18	0		
1962	+ 290E	-1000S	1	0	SHAL	13	0		
1963	+ 400E	-1375S	1	0	SHAL	13	0		
1964	+ 775E	-1400S	1	0	I:TF	3	0		
1965	+ 460E	-1390S	1	0	SHAL	13	0		
1966	+ 550E	-1380S	1	0	F:TF	7	0		
1967	+ 780E	-1500S	1	0	SSST	12	0		
1968	+ 725E	-1400S	1	0	F:TF	7	0		

SAMPLE	SiO2	TiO2	Al2O3	FeO	MnO	MgO	CaO	Na2O	K2O	P2O5	LOI	Zr	Sr	Rb
1941	83.70	.14	7.04	3.00	.07	.61	.19	.00	2.89	.03	.77			
1942	78.70	.20	9.62	1.87	.03	.31	.15	1.32	4.66	.02	.77			
1943	62.90	2.02	11.90	11.60	.34	2.89	1.98	1.28	1.49	.53	1.85			
1944	54.80	2.24	9.60	17.80	.39	4.50	.47	.61	.66	.52	5.85	193	28	44
1945	72.40	.23	12.40	2.50	.07	3.98	.28	2.04	2.52	.02	2.08			
1946	74.80	.57	10.00	5.38	.02	.81	.23	.92	2.43	.08	2.69	187	28	157
1947	88.40	.09	6.38	.86	.00	.20	.41	2.36	.71	.14	1.23	33	36	29
1948	79.70	.18	8.79	2.01	.07	1.16	.60	3.25	.65	.02	1.23			
1949	52.50	1.21	18.60	8.98	.29	7.41	1.37	4.45	.79	.17	3.62			
1950	78.90	.48	8.53	3.09	.03	.69	1.34	2.59	.23	.12	1.54			
1951	86.30	.53	5.60	2.93	.05	.48	.13	.15	1.72	.02	1.38	329	5	80
1952	76.80	.16	10.10	2.60	.04	.39	.15	1.95	3.29	.02	1.46			
1953	75.20	.18	11.70	2.66	.05	.67	.18	.44	5.42	.05	1.54			
1954	60.10	1.20	19.80	6.50	.05	2.01	.29	.57	4.44	.09	3.38			
1955	76.30	.15	10.40	2.24	.03	.47	.12	.25	5.53	.01	1.46	167	28	154
1956	78.90	.22	10.00	1.32	.02	.13	.21	.46	6.88	.02	.23			
1957	82.80	.12	7.29	1.59	.05	.91	.19	.04	4.32	.02	1.00			
1958	71.80	.55	13.50	3.71	.04	1.29	.43	2.36	2.50	.09	2.62	208	57	137
1959	69.60	.49	13.50	3.90	.02	.84	.47	1.65	3.53	.14	2.46			
1960	73.30	.38	12.40	2.81	.04	.65	1.08	3.00	1.88	.03	1.31			
1961	76.60	.69	13.10	7.38	.15	1.25	.68	4.71	.42	.12	1.77	850	96	19
1962	64.50	.86	15.70	4.54	.03	1.36	1.73	2.42	2.60	.07	2.85			
1963	68.50	.63	13.80	5.82	.03	1.33	.93	1.67	1.96	.10	3.38			
1964	50.50	1.36	17.20	8.98	.21	6.62	3.88	4.92	.89	.10	2.77			
1965	70.50	.71	13.20	3.61	.04	1.49	.97	3.67	1.30	.03	2.15			
1966	77.60	.22	9.62	1.93	.04	.37	.20	.27	6.13	.02	.92			
1967	48.70	2.30	14.60	11.80	.28	5.52	7.86	3.26	1.47	.34	1.23			
1968	77.60	.16	11.10	1.47	.05	.43	.38	.84	6.26	.02	.46			

LITHCODE	TS/PTS	ALTERATION	MINERALIZATION	COMMENTS	DEPTH	WIDTH
7	0				.0	.0
7	0				.0	.0
7	0			M:TF	.0	.0
2	0	Chl			.0	.0
7	0				.0	.0
12	0				.0	.0
12	0				.0	.0
7	0				.0	.0
11	0				.0	.0
11	0				.0	.0
7	0				.0	.0
7	0				.0	.0
7	0				.0	.0
11	0				.0	.0
7	0				.0	.0
7	0	Fld			.0	.0
7	0				.0	.0
12	0			SHAL	.0	.0
11	0			SHAL	.0	.0
7	0				.0	.0
18	0				.0	.0
13	0				.0	.0
13	0				.0	.0
3	0				.0	.0
13	6			F:TF	.0	.0
7	0				.0	.0
12	0				.0	.0
7	0				.0	.0

Na2O	K2O	P2O5	LOI	Zr	Sr	Rb	Zn	Cu	U	Th	Ga	Pb	Ni	Y	Ag
.00	2.89	.03	.77				44	6				4			0
1.32	4.66	.02	.77				13	38				0			0
1.28	1.49	.53	1.85				260	17				0			0
.61	.66	.52	5.85	193	28	44	170	610	0	8	18	3	0	32	0
2.04	2.52	.02	2.08				100	7				11			0
.92	2.43	.08	2.69	187	28	157	23	18	4	6	14	0	0	11	0
2.36	.71	.14	1.23	33	36	29	5	12	0	1	6	4	0	41	0
3.25	.65	.02	1.23				37	8				2			0
1.45	.79	.17	3.62				190	31				11			0
2.59	.23	.12	1.54				30	14				0			0
.15	1.72	.02	1.38	329	5	80	25	14	0	5	8	0	2	11	0
1.95	3.29	.02	1.46				13	7				3			0
.44	5.42	.05	1.54				28	14				10			0
.57	4.44	.09	3.38				65	12				2			0
.25	5.53	.01	1.36	167	28	154	23	7	5	17	11	0	0	38	0
.46	6.88	.02	.23				2	6				11			0
.04	4.32	.02	1.00				27	6				9			0
2.36	2.50	.09	2.62	208	57	137	35	13	1	9	17	0	0	21	0
1.65	3.53	.14	2.16				17	18				4			0
3.00	1.88	.03	1.31				41	8				5			0
4.71	.42	.12	1.77	850	96	19	140	9	1	10	22	0	0	124	0
2.42	2.60	.07	2.85				36	24				10			0
1.67	1.96	.10	3.38				38	28				2			0
1.92	.89	.10	2.77				56	68				0			0
3.67	1.30	.03	2.15				56	68				18			0
.27	6.13	.02	.92				35	17				5			0
3.26	1.47	.34	1.23				55	32				0			0
.84	6.26	.02	.46				18	20				18			0

SAMPLE	EASTING	NORTHING	TYPE	DRILLHOLE	LITHOLOGY	LITHCODE	TS/PTS	ALTERATION	MINERALIZATIO
1969	+ 730E	-1500S	1	0	M:TF	1	0	ACT	
1970	+ 610E	-1380S	1	0	F:TF	7	0		
1971	+ 575E	-1500S	1	0	F:AG	9	0		
1972	+ 500E	-1380S	1	0	F:FL	10	0		
1973	+ 625E	-1500S	1	0	F:TF	7	0		
1974	+ 700E	-1700S	1	0	F:AG	9	0		
1975	+ 740E	-1700S	1	0	I:TF	3	0		
1976	+ 760E	-1700S	1	0	I:TF	3	0		
1977	+ 840E	-1600S	1	0	M:TF	1	0	ACT	
1978	+ 610E	-1700S	1	0	F:TF	7	0		
1979	+ 650E	-1630S	1	0	I:TF	3	0		
1980	+ 550E	-1620S	1	0	SHAL	13	0		
1981	+ 725E	-1615S	1	0	I:TF	3	0		
1982	+ 800E	-1600S	1	0	F:TF	7	0		
1983	+ 575E	-1700S	1	0	F:TF	7	0		
1984	+ 660E	-1700S	1	0	F:TF	7	0		
1989	+ 120E	-1100S	1	0	SSST	12	0		
1990	+ 290E	-1100S	1	0	F:TF	7	0		
1991	+ 200E	-1100S	1	0	SHAL	13	0		
1992	+ 170E	-1100S	1	0	SHAL	13	0		
1993	+ 365E	-1100S	1	0	F:TF	7	0		
1994	+ 260E	-1100S	1	0	SSST	12	0		
1995	+ 075E	-1100S	1	0	SHAL	13	0	V/07	
1996	+ 225E	-1210S	1	0	SSST	12	0		
1997	+ 175E	-1200S	1	0	SHAL	13	0		
1998	+ 350E	-1210S	1	0	F:TF	7	0		
1999	+ 100E	-1200S	1	0	I:TF	3	0		
25009	+ 585E	+ 100N	1	0	D/M:	16	0		

SAMPLE	SiO2	TiO2	Al2O3	FeO	MnO	MgO	CaO	Na2O	K2O	P2O5	LOI	Zr	Sr	Rb
1969	53.40	2.57	13.10	12.30	.32	3.92	6.15	3.13	.64	.72	1.15			
1970	77.00	.32	10.30	2.37	.06	.69	.23	2.32	2.56	.04	1.23			
1971	73.50	.30	11.00	3.73	.06	.46	.13	.23	6.55	.03	1.62			
1972	73.50	.28	11.10	2.75	.07	.39	.15	.33	8.06	.03	1.08			
1973	75.10	.26	10.30	2.00	.05	.24	.20	.14	8.09	.03	.46			
1974	71.20	.22	13.20	2.55	.10	2.23	.32	5.01	1.98	.02	1.08			
1975	55.00	1.56	15.70	9.20	.12	3.13	.99	6.16	1.20	.19	3.00			
1976	49.10	1.76	14.90	10.20	.20	5.91	9.33	3.65	.55	.19	1.15			
1977	52.10	2.91	14.50	13.60	.33	4.30	6.76	3.16	.58	.84	1.31	352	138	19
1978	76.80	.91	9.95	2.02	.08	2.60	.36	3.14	1.19	.02	1.54			
1979	49.10	1.95	14.80	10.90	.30	6.97	6.24	3.73	1.51	.16	1.54	140	178	67
1980	66.70	.80	12.10	7.93	.03	.81	.17	.57	2.99	.19	4.23	210	44	129
1981	50.00	1.82	14.20	10.50	.22	7.76	6.93	4.01	.50	.19	2.15	140	152	15
1982	68.80	.92	12.50	5.14	.09	1.34	.86	3.96	2.23	.18	1.69	308	61	76
1983	82.70	.17	6.64	1.66	.02	.05	.14	.26	4.42	.02	1.23			
1984	73.90	.19	10.80	2.19	.11	1.88	.46	1.52	5.71	.02	.92			
1989	75.40	.58	11.00	3.49	.08	1.02	.97	2.50	1.94	.07	.92			
1990	82.40	.21	8.37	1.00	.00	.44	.13	1.00	2.35	.02	1.54			
1991	76.10	.24	11.10	2.50	.04	.67	1.37	3.31	1.14	.03	.85			
1992	71.20	.82	14.00	3.53	.03	.88	.32	.84	3.19	.10	3.38	200	136	81
1993	83.90	.10	5.30	5.24	.09	.90	.23	.14	1.28	.05	1.31			
1994	74.10	.44	11.20	4.73	.03	.91	.95	2.25	1.54	.09	2.54			
1995	53.30	1.21	21.90	7.27	.14	2.30	.17	2.28	3.82	.10	3.69			
1996	74.60	.25	12.60	2.56	.07	1.13	2.39	2.87	1.25	.04	.38			
1997	72.70	.78	12.50	4.25	.05	1.43	1.63	2.06	1.45	.12	2.23	200	140	81
1998	86.90	.18	6.67	.66	.00	.30	.15	.31	2.27	.02	1.08	53	28	86
1999	74.90	.61	11.40	3.71	.09	1.13	1.25	3.04	1.62	.08	1.00	224	117	70
25009	50.00	1.74	14.40	9.75	.26	6.99	10.00	2.69	.93	.15	.92			

LITHCODE	TS/PTS	ALTERATION	MINERALIZATION	COMMENTS	DEPTH	WIDTH
1	0	ACT			.0	.0
7	0				.0	.0
9	0				.0	.0
10	0				.0	.0
7	0				.0	.0
9	0				.0	.0
3	0				.0	.0
3	0				.0	.0
1	0	ACT			.0	.0
7	0				.0	.0
3	0				.0	.0
13	0				.0	.0
3	0				.0	.0
7	0				.0	.0
7	0				.0	.0
7	0				.0	.0
12	0			TFSD	.0	.0
7	0				.0	.0
13	0			SSST	.0	.0
13	0				.0	.0
7	0				.0	.0
12	0				.0	.0
13	0	V/QZ			.0	.0
12	0			TFSD	.0	.0
13	0				.0	.0
7	0				.0	.0
3	0				.0	.0
16	0				.0	.0

Na2O	K2O	P2O5	LOI	Zr	Sr	Rb	Zn	Cu	U	Th	Ga	Pb	Ni	Y	Ag
3.13	.64	.72	1.15				51	9				0			0
2.32	2.56	.04	1.23				22	80				6			0
.23	6.55	.03	1.62				22	24				3			0
.33	8.06	.03	1.08				28	14				6			0
.14	8.09	.03	.46				19	16				8			0
5.01	1.98	.02	1.08				59	8				0			0
6.16	1.20	.19	3.00				120	28				3			1
3.65	.55	.19	1.15				17	70				5			0
3.16	.58	.84	1.31	352	138	19	55	18	4	9	23	5	0	88	0
3.14	1.19	.02	1.54				47	8				3			0
3.73	1.51	.16	1.53	140	178	67	54	27	3	1	18	0	26	44	0
.57	2.99	.19	4.23	210	44	129	20	15	2	9	16	3	0	14	0
1.01	.50	.19	2.15	140	152	15	36	32	0	3	19	0	19	42	0
3.96	2.23	.18	1.69	309	61	76	45	13	2	8	16	0	0	45	0
.26	4.42	.02	1.23				3	35				40			0
1.52	5.71	.02	.92				47	8				2			0
2.50	1.94	.07	.92				36	16				0			0
1.00	2.35	.02	1.54				0	13				9			0
3.31	1.14	.03	.85				68	8				7			0
.84	3.19	.10	3.38	200	136	81	22	22	3	9	16	7	0	29	0
.14	1.28	.05	1.31				140	93				270			0
2.25	1.54	.09	2.54				38	31				3			0
2.28	3.82	.10	3.69				68	32				7			0
2.97	1.25	.04	.38				78	12				20			0
2.06	1.45	.12	2.23	200	140	81	44	15	3	8	16	5	0	31	0
.31	2.27	.02	1.08	53	28	86	6	13	4	4	8	8	0	5	0
3.04	1.62	.08	1.00	224	117	70	35	14	2	11	16	12	5	32	0
2.69	.93	.15	.92												

SAMPLE	EASTING	NORTHING	TYPE	DRILLHOLE	LITHOLOGY	LITHCODE	TS/PTS	ALTERATION	MINERALIZATI
25010	+1025E	+ 040N	1	0	F:FL	10	1		
25012	+ 725E	+ 175N	1	0	GRAN	14	1		
25030			2	160230006	SSLT	11	1	SER	
25031			2	160230006	M:TF	1	0		CP PR
25033			2	160230006	I:TF	3	0		
25035			2	160230006	F:LT	8	0	SER	
25036			2	160230006	I:TF	3	1	CHL SER	
25037			2	160230006	F:TF	7	0		
25038			2	160230006	SSLT	11	1	SER	
25039			2	20010	SSLT	11	1	SER	
25040			2	20010	F:TF	7	1	SER	PY PR
25042			2	20010	M:TF	1	0		PR
25045			2	20010	SSLT	11	0	CHL SER	
25046			2	160230003	I:TF	3	1		
25047			2	160230003	M:TF	1	0	ACT CHL	PY
25048			2	160230003	F:TF	7	0	SER	PY
25049			2	160230003	SSLT	11	0	SER	PY
25051			2	160230003	I:LT	4	1		PY
25052			2	160230001	SSLT	11	1	SER	PY
25053			2	160230001	M:TF	1	1	ACT CHL	
25055			2	160230001	F:TF	7	0		
25056			2	160230001	F:TF	7	0	SER	SL
25061			2	160230001	SSLT	11	0		PY
25062			2	160230002	F:TF	7	0	SER	PY
25063			2	160230002	F:TF	7	1	SER	PY
25064			2	160230002	M:TF	1	0	CHL CAR	PY
25065			2	160230002	F:LT	8	0	SER	PY
25066			2	160230002	SSLT	11	0	SER	PY

SAMPLE	SiO2	TiO2	Al2O3	FeO	MnO	MgO	CaO	Na2O	K2O	P2O5	LOI	Zr	Sr	Rb
25010	79.70	.17	10.40	.90	.05	.33	.44	4.69	.76	.03	.43			
25012	69.10	.39	16.40	2.65	.03	.93	.45	4.93	3.44	.15	1.52			
25030	61.80	.70	17.70	6.13	.07	1.84	.49	1.10	4.92	.58	3.33			
25031	49.60	2.24	10.80	17.96	.65	7.04	1.90	.70	.75	.56	5.15			
25033	57.80	.63	19.30	6.52	.16	4.42	.31	.19	5.62	.05	4.14			
25035	77.90	.14	10.40	2.66	.09	1.58	.10	2.17	2.47	.00	1.39			
25036	71.10	.30	12.70	3.19	.14	3.15	.17	3.20	3.54	.56	1.47			
25037	62.10	.88	17.70	5.47	.05	2.07	.43	.89	6.32	.60	3.27			
25038	63.00	.53	16.90	5.68	.04	1.78	.24	2.44	3.72	.50	3.02			
25039	73.90	.41	8.70	4.08	.07	1.16	.16	.54	3.18	.41	1.46			
25040	72.60	.69	11.60	4.76	.05	1.18	.11	.43	4.03	.29	2.32			
25042	61.40	.96	10.90	13.83	.37	4.84	1.13	.91	1.40	.09	3.17			
25045	64.50	.61	12.80	8.25	.38	2.85	.74	3.03	2.82	.63	1.58			
25046	65.40	.24	15.00	6.24	.08	3.39	.28	2.25	2.89	.63	3.41			
25047	48.00	2.76	12.50	12.66	.33	5.89	6.13	3.38	.12	1.30	5.20			
25048	71.00	.19	13.10	1.28	.03	3.30	.18	1.31	3.11	.04	3.37			
25049	65.00	1.03	14.80	7.16	.06	2.79	.87	1.30	3.26	.20	2.93			
25051	71.50	.50	14.10	3.51	.05	1.19	.51	3.46	2.28	.09	1.35			
25052	64.30	.45	16.00	5.80	.07	2.90	.54	2.54	3.71	.94	3.13			
25053	48.40	2.79	13.10	13.23	.19	9.57	3.22	2.68	.06	1.78	4.69			
25055	76.90	.35	9.60	3.55	.08	1.81	.15	.68	3.74	.08	1.78			
25056	76.70	.26	6.50	2.26	.13	2.91	3.19	.47	1.66	.02	3.68			
25061	67.80	.58	15.00	4.84	.02	1.29	.56	2.48	4.14	1.13	2.36			
25062	64.80	.53	17.50	6.04	.06	1.94	.20	.74	5.32	.46	3.46			
25063	71.90	.16	12.50	2.83	.12	4.07	.31	5.04	.76	.55	1.93			
25064	46.60	2.78	12.20	12.44	.40	8.36	5.33	2.73	.58	1.44	5.31			
25065	64.70	.48	15.60	5.39	.04	2.29	.06	1.34	4.99	1.21	3.44			
25066	65.00	.77	14.40	6.66	.05	2.05	.25	1.41	4.20	.62	2.50			

1 OF

LITHCODE	TS/PTS	ALTERATION	MINERALIZATION	COMMENTS	DEPTH	WIDTH
10	1				.0	.0
14	1				.0	.0
11	1	SER			14.7	.1
1	0		CP PR		26.4	.2
3	0				30.9	.3
8	0	SER			36.6	.3
3	1	CHL SER			48.9	.3
7	0				70.2	.4
11	1	SER			87.0	.1
11	1	SER			21.3	.2
7	1	SER	PY PR		26.1	.1
1	0		PR		37.2	.2
11	0	CHL SER			63.0	.1
3	1			F:TF SSLT	13.3	.2
1	0	ACT CHL	PY		24.3	.2
7	0	SER	PY		33.7	.3
11	0	SER	PY		45.6	.3
4	1		PY		58.5	.2
11	1	SER	PY	TFSD	7.8	.2
1	1	ACT CHL			17.8	.2
7	0				43.3	.2
7	0	SER	SL		51.5	.3
11	0		PY		63.0	.1
7	0	SER	PY		11.5	.2
7	1	SER	PY		7.2	.3
1	0	CHL CAR	PY		29.4	.2
8	0	SER	PY		43.6	.3
11	0	SER	PY		52.3	.2

Na2O	K2O	P2O5	LOI	Zr	Sr	Rb	Zn	Cu	U	Th	Ga	Pb	Ni	Y	Ag
1.69	.76	.03	.43												
4.93	3.44	.15	1.52												
1.10	4.92	.58	3.33												
.70	.75	.56	5.15												
.19	5.62	.05	4.11												
2.17	2.47	.00	1.39												
3.20	3.54	.56	1.47												
.89	6.32	.60	3.27												
2.44	3.72	.50	3.02												
.54	3.18	.41	1.46												
.43	4.03	.29	2.32												
.91	1.40	.09	3.17												
3.03	2.82	.63	1.56												
2.25	2.89	.63	3.41												
3.38	.12	1.30	5.20												
1.31	3.11	.04	3.37												
1.30	3.26	.20	2.93												
3.46	2.28	.09	1.35												
2.54	3.71	.94	3.13												
2.68	.06	1.78	4.69												
.68	3.74	.08	1.78												
.47	1.66	.02	3.68												
2.48	4.14	1.13	2.36												
.74	5.32	.46	3.46												
5.04	.76	.55	1.93												
2.73	.58	1.44	5.31												
1.34	4.99	1.21	3.44												
1.41	4.20	.62	2.50												

SAMPLE	EASTING	NORTHING	TYPE	DRILLHOLE	LITHOLOGY	LITHCODE	TS/PTS	ALTERATION	MINERALIZAT
25068			2	160230014	SSLT	11	0	CHL CAR	
25069			2	160230014	F:TF	7	1		
25070			2	160230014	I:TF	3	0		
25071			2	160230014	I:TF	3	0	CHL	PY SL GA
25071			2	160230014	M:TF	1	0	CHL	PY SL GA
25073			2	160230014	M:TF	1	0	CHL	PY
25074			2	160230014	M:TF	1	1	CHL CAR	PY
25077			2	160230026	F:TF	7	0	SER	
25078			2	160230026	I:TF	3	0	CHL	PY SL
25080			2	160230026	I:FL	6	1	CAR SER	
25081			2	160230026	F:TF	7	1	SER	
25082			2	160230026	M:TF	1	0	ACT	PR
25085			2	160230026	I:TF	3	1	CHL SER	PY
25086			2	160230026	M:TF	1	0	CHL CAR	
25087			2	160230026	SSST	12	1	CHL SER	
25088			2	160230026	SSLT	11	1	SER	PY
25090			2	160230016	SSST	12	1		
25091			2	160230016	I:TF	3	0	CHL	
25092			2	160230016	F:FL	10	1		
25093			2	160230016	SSLT	11	1	SIL	
25094			2	20001	M:TF	1	1	CHL CAR	
25095			2	20001	F:FL	10	0		
25096			2	20001	F:TF	7	1	SER	SL
25098			2	20001	F:LT	8	1	SER	PY
25100			2	20001	SSLT	11	1	SER	
26203	+ 605E	+ 835N	1	0	GRAN	14	1		
26204	+ 700E	+ 650N	1	0	GRAN	14	1		
26205	+ 700E	+ 750N	1	0	GRAN	14	1		

SAMPLE	SiO2	TiO2	Al2O3	FeO	MnO	MgO	CaO	Na2O	K2O	P2O5	LOI	Zr	Sr	Rb
25068	62.40	.77	16.50	6.32	.08	1.98	.62	3.63	3.19	.99	2.32			
25069	75.40	.34	10.20	4.13	.07	1.20	.68	2.80	2.43	.69	1.28			
25070	76.50	.32	11.00	3.32	.06	.90	.71	3.66	2.17	.55	1.17			
25071	70.40	.31	9.30	9.24	.15	1.26	1.89	.43	1.76	.07	2.75			
25071	70.40	.31	9.30	9.24	.15	1.26	1.89	.43	1.76	.07	2.75			
25073	48.40	2.37	11.80	12.51	.36	4.72	6.66	2.63	.69	.58	6.27			
25074	44.90	2.57	11.70	12.31	.43	5.22	7.19	3.02	.82	.74	8.35			
25077	76.90	.31	10.70	3.58	.05	.93	.43	2.43	2.82	.11	1.14			
25078	71.80	.36	10.90	7.60	.12	1.37	.23	1.71	1.96	.11	1.95			
25080	67.30	.61	11.80	6.96	.20	1.38	1.72	4.76	.95	.68	2.02			
25081	75.10	.16	10.80	2.06	.09	4.53	.12	3.51	.96	.69	2.17			
25082	48.60	2.78	12.70	13.40	.35	6.24	4.22	3.97	.38	.79	3.33			
25085	73.10	.20	10.80	6.76	.18	2.36	.21	2.42	1.95	.70	2.01			
25086	49.10	2.84	11.80	12.04	.50	7.52	8.36	2.98	.22	1.03	2.85			
25087	35.20	.17	4.10	1.48	.55	20.30	17.55	.51	.23	.48	19.94			
25088	65.70	.80	17.00	5.47	.03	1.64	.16	1.94	3.95	.32	2.87			
25090	72.80	.55	11.10	6.13	.10	1.42	.16	1.16	4.05	1.11	1.47			
25091	58.80	.84	12.30	12.60	.19	1.94	.50	.20	6.71	.16	2.37			
25092	84.20	.16	5.90	4.49	.06	.50	.14	.46	3.38	.44	.84			
25093	64.60	.55	16.00	5.19	.07	2.53	.40	.97	5.28	.55	2.97			
25094	43.80	2.37	11.30	11.83	.28	7.35	9.40	1.59	1.42	.60	9.33			
25095	76.00	.30	11.70	1.78	.06	.96	.58	6.08	.05	.10	.75			
25096	81.70	.10	7.10	1.44	.02	.51	.22	.02	3.97	.01	1.27			
25098	64.70	.64	15.40	5.35	.06	1.88	.54	1.63	4.73	.12	3.61			
25100	70.00	.62	13.20	6.32	.04	1.65	.21	.88	4.21	.10	2.25			
26203	77.90	.19	11.70	1.83	.04	.04	.07	3.97	4.11	.01	.15			
26204	78.90	.13	11.70	1.31	.02	.05	.13	4.13	3.92	.00	.20			
26205	78.30	.20	11.60	1.70	.03	.13	.26	4.41	3.34	.01	.25			

LITHCODE	TS/PTS	ALTERATION	MINERALIZATION	COMMENTS	DEPTH	WIDTH
11	0	CHL CAR		SHAL	11.7	.2
7	1				24.4	.2
3	0			SSST	29.8	.3
3	0	CHL	PY SL GA		45.3	.3
1	0	CHL	PY SL GA		45.3	.3
1	0	CHL	PY		63.9	.3
1	1	CHL CAR	PY		72.9	.3
7	0	SER			13.8	.3
3	0	CHL	PY SL	SSLT	43.3	.3
6	1	CAR SER			49.5	.2
7	1	SER			72.3	.3
1	0	ACT	PR		106.5	.3
3	1	CHL SER	PY		127.8	.3
1	0	CHL CAR			150.9	.2
12	1	CHL SER			127.8	.3
11	1	SER	PY		177.1	.2
12	1			SSLT	11.1	.2
3	0	CHL			21.5	.2
10	1			F:FL STXX	26.0	.2
11	1	SIL		SSLT	11.1	.2
1	1	CHL CAR			17.5	.2
10	0				22.5	.3
7	1	SER	SL		36.4	.2
8	1	SER	PY		49.9	.2
11	1	SER			56.4	.2
14	1				.0	.0
14	1				.0	.0
14	1				.0	.0

Na20	K20	P205	LOI	Zr	Sr	Rb	Zn	Cu	U	Th	Ga	Pb	Ni	Y	Ag
3.63	3.19	.99	2.32												
2.80	2.43	.69	1.28												
3.66	2.17	.55	1.17												
.43	1.76	.07	2.75												
.43	1.76	.07	2.75												
2.63	.69	.58	6.27												
1.02	.82	.74	8.35												
2.43	2.82	.11	1.14												
1.71	1.96	.11	1.95												
4.76	.95	.68	2.02												
3.51	.96	.69	2.17												
3.97	.38	.79	3.11												
2.42	1.95	.70	2.01												
2.98	.22	1.03	2.85												
.51	.23	.48	19.94												
1.94	3.95	.32	2.87												
1.16	4.05	1.11	1.47												
.20	6.71	.16	2.37												
.46	3.38	.44	.84												
.97	5.28	.55	2.97												
1.59	1.42	.60	9.33												
6.08	.05	.10	.75												
.02	3.97	.01	1.27												
1.63	4.73	.12	3.61												
.88	4.21	.10	2.25												
3.97	4.11	.01	.15												
4.13	3.92	.00	.20												
4.41	3.34	.01	.25												

307

SAMPLE	EASTING	NORTHING	TYPE	DRILLHOLE	LITHOLOGY	LITHCODE	TS/PTS	ALTERATION	MINERALIZATI
26206	+ 700E	+1050N	1	0	GRAN	14	1		
26207	+ 700E	+ 950N	1	0	GRAN	14	1		
26208	+ 700E	+ 850N	1	0	GRAN	14	1		
26209	+ 900E	+ 850N	1	0	GRAN	14	1		
26210			2	160230009	M:TF	1	1	CHL CAR	
26211			2	160230009	SSLT	11	1		PY
26212			2	160230009	F:FL	10	0		
26215			2	160230009	F:TF	7	0	SER	PY
26218			2	160230009	SSLT	11	0		
26219			2	160230019	F:TF	7	1		
26220			2	160230019	F:TF	7	1		
26224			2	160230019	SSLT	11	1		
26225			2	160230019	SHAL	13	1		PY
26226			2	160230019	F:TF	7	1	SER	
26233			2	160230019	F:LT	8	1		
26234			2	160230019	F:FL	10	2		SL
26236			2	160230019	SSLT	11	1		
26237	+ 350E	+1400N	1	0	F:TF	7	1		
26238	+ 525E	+1400N	1	0	F:FL	10	1	SER	
26239	+ 670E	+1400N	1	0	SSLT	11	1	SER	
26240	+ 720E	+1260N	1	0	GRAN	14	1		
26243	+ 345E	- 210S	1	0	F:FL	10	1		
26244	+ 535E	- 250S	1	0	I:TF	3	1	SER	
26245	+ 550E	- 310S	1	0	F:FL	10	1		
26246	+ 650E	- 200S	1	0	SSST	12	0	SER	
26247	+ 915E	- 200S	1	0	F:TF	7	1	SER	
26248	+ 925E	- 400S	1	0	F:FL	10	0		
26249	+ 875E	- 400S	1	0	I:TF	3	1	ACT	

SAMPLE	SiO2	TiO2	Al2O3	FeO	MnO	MgO	CaO	Na2O	K2O	P2O5	LOI	Zr	Sr	Rb
26206	78.70	.27	11.50	1.78	.03	.11	.28	4.17	3.54	.01	.28			
26207	77.70	.12	11.70	1.98	.04	.07	.14	4.20	3.44	.01	.26			
26208	78.10	.22	11.30	1.40	.03	.06	.58	3.18	3.31	.03	.74			
26209	79.00	.10	10.30	.95	.02	.05	.91	5.39	.47	.01	.72			
26210	50.90	2.63	12.90	12.86	.57	9.06	1.69	1.82	.26	.62	4.69			
26211	57.30	1.03	15.10	8.16	.12	7.14	1.42	3.98	1.06	.16	3.66			
26212	77.50	.27	11.80	1.85	.03	.74	.38	5.94	.33	.03	.51			
26215	71.00	.21	11.60	3.13	.16	6.24	.15	3.97	.64	.01	2.59			
26218	64.90	1.00	16.30	5.80	.06	1.57	.11	.55	5.03	.03	2.52			
26219	73.00	.40	12.70	5.07	.10	1.20	.37	2.67	3.04	.01	1.09			
26220	49.80	.37	26.30	6.52	.06	1.49	.11	.17	9.52	.01	4.26			
26224	64.90	.53	13.40	4.89	.10	5.68	1.33	.92	2.77	.05	3.29			
26225	60.80	.76	19.20	5.94	.04	1.46	.18	1.17	5.34	.05	3.67			
26226	62.90	.65	17.70	6.08	.07	1.91	.13	.23	5.38	.06	3.53			
26233	67.30	.28	12.40	3.43	.22	5.75	1.74	3.00	3.39	.02	1.50			
26234	79.30	.01	19.70	1.50	.03	.93	.30	4.75	.16	.05	1.20			
26236	67.70	.70	15.50	5.23	.05	1.71	.54	1.29	4.09	.13	2.56			
26237	79.70	.11	10.50	1.63	.03	.49	.05	.45	5.87	.08	.75			
26238	72.30	.15	9.50	1.19	.03	.41	.35	2.32	2.73	.01	.92			
26239	72.60	.56	13.90	4.31	.07	1.66	1.46	4.17	1.62	.08	.73			
26240	82.10	.10	10.50	.27	.01	.04	.04	5.96	.17	.06	.06			
26243	78.00	.20	10.60	2.31	.05	.40	.00	.61	7.43	.03	.33	333	077	133
26244	71.20	.78	12.30	5.06	.11	1.40	.47	3.86	2.26	.10	1.08	267	057	088
26245	74.70	.20	12.00	1.40	.04	.37	.11	1.20	8.40	.04	1.32	269	057	106
26246	69.30	.63	14.70	5.25	.14	1.89	.93	3.19	3.00	.17	1.26	151	074	113
26247	74.10	.16	14.00	1.31	.02	.44	.37	6.00	1.48	.39	.71	134	094	058
26248	76.70	.13	11.50	1.18	.02	.15	.05	2.11	7.27	.54	.41	169	026	173
26249	70.90	.34	14.90	3.59	.05	.65	.40	5.49	2.32	.76	1.14	319	040	093

LITHCODE	TS/PTS	ALTERATION	MINERALIZATION	COMMENTS	DEPTH	WIDTH
14	1				.0	.0
14	1				.0	.0
14	1				.0	.0
14	1				.0	.0
1	1	CHL CAR		F:LT	6.7	.3
11	1		PY		19.5	.2
10	0				48.4	.2
7	0	SER	PY		58.2	.3
11	0			SHAL	67.2	.3
7	1			SSST	5.1	.3
7	1				37.6	.3
11	1			SSLT	74.1	.3
13	1		PY		90.3	.3
7	1	SER		I:TF	100.6	.3
8	1				108.0	.3
10	2		SL		147.9	.3
11	1			CGXX	155.4	.3
7	1				.0	.0
10	1	SER		F:TF	.0	.0
11	1	SER			.0	.0
14	1				.0	.0
10	1				.0	.0
3	1	SER		SSST	.0	.0
10	1				.0	.0
12	0	SER			.0	.0
7	1	SER			.0	.0
10	0				.0	.0
3	1	ACT		GRAN	.0	.0

Na2O	K2O	P2O5	LOI	Zr	Sr	Rb	Zn	Cu	U	Th	Ga	Pb	Ni	Y	Ag
4.17	3.54	.01	.28												
4.20	3.44	.01	.26												
3.18	3.31	.03	.74												
5.39	.47	.01	.72												
1.82	.26	.62	4.69												
3.98	1.06	.16	3.66												
5.94	.33	.03	.51												
3.97	.64	.01	2.59												
.55	5.03	.03	2.52												
2.67	3.04	.01	1.09												
.17	9.52	.01	4.26												
.92	2.77	.05	3.29												
1.17	5.34	.05	3.67												
.23	5.38	.06	3.53												
3.00	3.39	.02	1.50												
4.75	.16	.05	1.20												
1.29	4.09	.13	2.56												
.45	5.87	.08	.75												
2.32	2.73	.01	.92												
1.17	1.62	.08	.73												
5.96	.17	.06	.06												
.61	7.43	.03	.33	333	077	133	0020	06	4	15	16	005	000	100	
3.86	2.26	.10	1.08	267	057	088	0044	02	3	12	13	007	010	057	
1.20	8.40	.04	1.32	269	057	106	0021	18	0	17	13	32	0	057	
3.19	3.00	.17	1.26	151	074	113	0063	20	5	10	17	007	005	018	
6.00	1.48	.39	.71	134	094	058	0011	02	2	05	14	002	000	023	
2.11	7.27	.54	.41	169	026	173	0	6	3	17	13	003	000	045	
5.49	2.32	.76	1.14	319	040	093	0020	08	0	04	15	001	000	022	

2 OF 2

SAMPLE	EASTING	NORTHING	TYPE	DRILLHOLE	LITHOLOGY	LITHCODE	TS/PTS	ALTERATION	MINERALIZATIO
26250	+ 650E	- 400S	1	0	I:TF	3	0		
26261	+ 580E	- 380S	1	0	F:FL	10	1		
26251	+ 580E	- 380S	1	0	F:FL	10	0		
26252	+ 475E	- 410S	1	0	I:TF	3	1	SER	
26253	+ 320E	- 415S	1	0	F:LT	8	1	SER	
26254	+ 015E	+1800N	1	0	F:FL	10	1		
26255	+ 250E	+1800N	1	0	SSLT	11	0	SER	
26256	+ 380E	+1800N	1	0	GRAN	14	1		
26257	+ 475E	+1800N	1	0	F:FL	10	1	SER	
26258	+ 530E	+1800N	1	0	SSST	12	1	SER	
26259	+ 725E	+1800N	1	0	D/F:	15	1		
26260	+ 640E	+1600N	1	0	I:TF	3	1	SER	
26261	+ 400E	+1600N	1	0	GRAN	14	0		
26262	+ 100E	+1600N	1	0	SSLT	11	0	SER	
26263	- 050W	+1620N	1	0	F:TF	7	0	FEO	
26264	- 115W	+1400N	1	0	SSLT	11	1		
26265			2	160230031	SSLT	11	0	SER	
26266			2	160230031	SSST	12	0	SER	
26267	+1350E	- 800S	1	0	D/M:	16	1	ACT	
26268	+1480E	- 775S	1	0	F:TF	7	0		
26269	+1580E	- 800S	1	0	F:FL	10	1		PY
26270	+1865E	- 780S	1	0	F:FL	10	1		
26271	+1800E	- 600S	1	0	F:TF	7	1	SER	PY
26272	+1650E	- 600S	1	0	F:FL	10	0		
26273	+1575E	- 600S	1	0	D/M:	16	0	ACT	
26274	+1520E	- 600S	1	0	F:FL	10	1		
26275	+1475E	- 600S	1	0	SHAL	13	0		
26276	+1240E	- 600S	1	0	F:TF	7	0	SER	

SAMPLE	SiO2	TiO2	Al2O3	FeO	MnO	MgO	CaO	Na2O	K2O	P2O5	LOI	Zr	Sr	Rb
26250	70.90	.63	12.90	5.29	.12	1.47	.48	3.67	2.76	.49	1.11	233	066	120
26251	79.10	.23	12.90	1.85	.09	.73	1.15	3.43	2.20	.02	.86			
26251	79.10	.23	12.90	1.85	.09	.73	1.15	3.43	2.20	.02	.86	288	130	058
26252	67.40	.60	16.90	4.08	.12	.60	.68	3.85	4.52	.06	1.18	193	093	200
26253	76.20	.21	11.90	2.50	.05	.44	.01	1.07	6.50	.05	.98	106	033	195
26254	82.40	.00	9.50	.63	.02	.74	.12	5.00	.00	.03	.67	263	048	000
26255	68.10	.59	15.30	5.14	.10	2.10	.60	2.37	3.36	.16	1.81	188	065	125
26256	77.50	.40	11.50	3.31	.06	1.02	.35	3.69	1.51	.07	1.03	111	056	061
26257	81.80	.00	8.80	.44	.02	.13	.01	1.11	5.91	.39	.47	082	038	095
26258	75.60	.26	11.20	3.50	.10	1.16	.19	2.64	2.80	.13	1.01	112	051	111
26259	80.60	.20	11.40	.81	.02	.43	.39	4.89	1.31	.03	.45			
26260	73.10	.69	13.40	2.48	.04	1.55	1.03	5.92	.99	.11	.49	200	083	032
26261	77.20	.13	12.10	.71	.02	.23	.00	.74	8.86	.05	.36	113	050	140
26262	62.60	.70	16.50	5.82	.12	2.24	.66	3.67	2.78	.12	1.77	156	083	113
26263	79.00	.16	10.70	1.55	.02	1.31	.24	4.05	.83	.02	1.08	316	040	031
26264	79.50	.18	9.70	2.01	.02	.61	.50	2.94	1.46	.00	1.17			
26265	63.80	.77	16.60	5.69	.10	2.23	.83	3.16	3.11	.14	1.89			
26266	75.80	.35	11.50	4.08	.07	1.12	.40	3.75	2.25	.60	.88			
26267	49.20	1.67	14.60	10.32	.23	7.85	7.91	2.25	.72	.27	1.90	128	153	064
26268	81.10	.18	10.80	.63	.01	.21	.36	5.20	.77	.04	.46	143	063	030
26269	77.50	.11	12.00	.81	.02	.44	.27	4.04	4.68	.41	.27	112	083	129
26270	79.70	.12	10.30	1.28	.01	.15	.15	.25	6.64	.00	.57	193	019	201
26271	69.40	.34	15.40	4.09	.06	2.33	1.15	2.87	.84	.04	2.04	090	072	084
26272	76.00	.14	13.00	1.06	.02	.42	.48	2.96	6.31	.03	.15	138	033	163
26273	48.90	1.16	14.20	9.21	.20	11.10	8.80	2.34	1.26	.12	1.99	084	148	068
26274	76.60	.10	12.70	1.07	.02	.42	.06	5.34	2.40	.03	.46	123	032	085
26275	66.60	.25	19.80	2.95	.02	.95	.02	.87	4.38	.00	3.77	208	075	183
26276	63.30	.76	16.70	4.91	.08	2.33	2.36	3.73	2.24	.14	1.79	275	131	112

1 OF

ITHCODE	TS/PTS	ALTERATION	MINERALIZATION	COMMENTS	DEPTH	WIDTH
3	0			SEDM	.0	.0
10	1			F:TF	.0	.0
10	0				.0	.0
3	1	SER			.0	.0
8	1	SER			.0	.0
10	1			F:TF	.0	.0
11	0	SER			.0	.0
14	1			TFSD	.0	.0
10	1	SER			.0	.0
12	1	SER			.0	.0
15	1				.0	.0
3	1	SER		SSLT	.0	.0
14	0				.0	.0
11	0	SER			.0	.0
7	0	FEO			.0	.0
11	1			SHAL	.0	.0
11	0	SER			16.5	.3
12	0	SER			51.9	.3
16	1	ACT			.0	.0
7	0				.0	.0
10	1		PY		.0	.0
10	1				.0	.0
7	1	SER	PY		.0	.0
10	0				.0	.0
16	0	ACT			.0	.0
10	1				.0	.0
13	0				.0	.0
7	0	SER			.0	.0

Na20	K20	P205	LOI	Zr	Sr	Rb	Zn	Cu	U	Th	Ga	Pb	Ni	Y	Ag
3.67	2.76	.49	1.11	233	066	120	0052	70	4	11	14	012	004	019	
3.43	2.20	.02	.86												
3.43	2.20	.02	.96	288	130	058	0197	18	4	23	20	164	000	074	
3.85	4.52	.06	1.18	193	093	200	0357	18	2	07	21	095	000	031	
1.07	6.50	.05	.98	106	033	195	0027	42	4	10	10	004	000	041	
5.00	.00	.03	.67	263	048	000	0019	04	3	11	15	011	000	077	
2.32	3.36	.16	1.81	188	065	125	0056	14	4	15	19	003	009	024	
3.69	1.51	.07	1.03	111	056	061	0023	02	1	09	12	002	003	014	
1.11	5.91	.39	.47	082	038	095	0011	02	3	17	11	009	000	039	
2.64	2.80	.13	1.01	112	051	111	1442	92	6	25	28	654	001	027	
4.89	1.31	.03	.45												
5.92	.99	.11	.49	200	083	032	0015	02	1	06	15	000	011	033	
.74	8.86	.05	.36	113	050	140	0013	02	6	21	10	008	000	062	
3.67	2.78	.12	1.77	156	083	113	0080	06	0	07	18	001	009	012	
4.05	.83	.02	1.08	316	040	031	0038	02	1	12	12	006	000	088	
2.94	1.46	.00	1.17												
3.16	3.11	.14	1.89												
3.75	2.25	.60	.88												
2.25	.72	.27	1.90	128	153	064	0126	08	0	00	17	011	052	041	
5.20	.77	.04	.46	143	063	030	0008	02	3	16	10	024	000	056	
4.04	4.68	.41	.27	112	083	129	0014	06	4	21	10	024	000	067	
.25	6.64	.00	.57	193	019	201	0020	06	2	17	16	009	000	081	
2.87	.84	.04	2.04	090	072	084	0055	06	0	25	16	015	003	017	
2.96	6.31	.03	.15	138	033	163	0014	02	8	22	16	013	000	082	
2.34	1.26	.12	1.99	084	148	068	0089	02	0	00	15	005	228	024	
5.34	2.40	.03	.46	123	032	085	0013	02	7	20	17	18	2	057	
.87	4.38	.00	3.77	208	075	183	0034	20	4	11	27	017	000	023	
3.73	2.24	.14	1.79	275	131	112	0102	24	2	16	26	080	001	033	

309

2 OF 2

SAMPLE	EASTING	NORTHING	TYPE	DRILLHOLE	LITHOLOGY	LITHCODE	TS/PTS	ALTERATION	MINERALIZATIC
26277	- 260W	- 020S	1	0	SSLT	11	1	SIS	
26278	- 350W	000	1	0	SSLT	11	0	SIS	
26279	+ 690E	- 800S	1	0	SSLT	11	0		
26280	+ 900E	- 800S	1	0	F:TF	7	0		
26281	+1025E	- 780S	1	0	F:TF	7	0		
26283	+1050E	- 800S	1	0	F:FL	10	0	SIL	
26284	+1125E	- 800S	1	0	M:TF	1	0	ACT	
26285	+1140E	600S	1	0	F:TF	7	0		
26286	+ 935E	- 600S	1	0	F:TF	7	0		
26287	+ 880E	- 600S	1	0	F:TF	7	0		
26288	+ 825E	- 600S	1	0	SSLT	11	0		
26289	+0420E	-0600S	1	0	F:TF	7	0		
26290	- 225W	+ 200N	1	0	SSLT	11	0		
26291	300N	+ 200N	1	0	SSST	12	0		
26292	+1380E	-1200S	1	0	D/F:	15	1		
26293	+1460E	-1200S	1	0	D/M:	16	1		
26294	+1510E	-1200S	1	0	I:TF	16	0		
26295	+1675E	-1200S	1	0	F:FL	10	0		
26296	+1810E	-1190S	1	0	M:TF	1	1		
26297	+1900E	-1200S	1	0	F:FL	10	0		
26298	+1900E	-1000S	1	0	D/M:	16	0	ACT	
26299	+1800E	-1000S	1	0	F:FL	10	0		
26300	+1685E	-1000S	1	0	I:FL	6	0		
28201	+1500E	- 980S	1	0	D/M:	16	0		
28202	+1450E	-1000S	1	0	SHAL	13	0		
28203	+ 700E	-1200S	1	0	F:TF	7	0		
28204	+ 850E	-1200S	1	0	I:TF	3	0		
28205	+ 930E	-1200S	1	0	F:FL	10	1		

SAMPLE	SiO2	TiO2	Al2O3	FeO	MnO	MgO	CaO	Na2O	K2O	P2O5	LOI	Zr	Sr	Rb	
26277	73.50	.19	12.70	1.13	.02	.35	.34	2.94	6.26	.08	2.32	305	061	093	0
26278	73.20	.68	12.40	3.98	.09	1.59	.29	3.05	1.40	.08	1.24	194	178	069	0
26279	45.30	.86	20.10	17.30	.30	3.92	.80	3.97	3.60	.11	2.44	290	074	165	0
26280	73.70	.46	13.60	1.88	.03	.90	.96	4.76	2.32	.11	.46	171	145	061	0
26281	75.60	.71	11.00	4.44	.05	.97	.29	.83	3.20	.16	1.84	211	034	155	0
26283	78.60	.20	11.80	.60	.02	.14	.22	.51	9.38	.13	.38	226	047	175	0
26284	49.40	3.08	13.80	13.77	.39	4.48	4.17	2.11	3.10	.83	2.29	363	113	164	0
26285	62.70	.70	19.60	4.22	.11	1.44	.19	1.11	5.55	.11	2.85	265	034	256	0
26286	76.40	.19	12.20	1.82	.02	.22	.38	2.74	4.43	.01	.81	292	049	112	0
26287	77.00	.17	11.10	1.96	.02	.27	.08	.35	6.96	.01	.82	165	022	190	0
26288	73.50	.82	12.20	4.36	.08	1.54	.52	4.57	.95	.33	1.14	276	056	038	0
26289	78.90	.15	11.80	1.88	.04	.49	.08	1.28	4.94	.00	1.30	079	030	181	0
26290	55.10	1.12	21.30	6.83	.16	2.48	1.07	2.55	3.83	.13	3.52	274	160	161	0
26291	74.60	.64	12.10	4.05	.09	1.54	1.09	2.30	1.58	.12	1.83	198	131	071	0
26292	75.90	.11	12.80	1.54	.02	.20	.11	4.31	4.16	.02	.37	208	027	097	0
26293	51.90	1.50	15.20	8.32	.18	8.67	9.17	2.57	.08	.19	1.87	109	200	001	0
26294	49.20	1.26	16.60	8.72	.14	9.10	7.26	3.00	2.15	.13	1.78	086	176	136	0
26295	75.40	.21	12.60	1.43	.03	.34	.48	3.49	5.33	.02	.36	124	033	185	0
26296	52.30	1.03	23.30	7.83	.16	3.18	.66	1.06	5.95	.07	3.57	193	047	206	0
26297	79.60	.20	11.50	.89	.02	.18	.42	1.98	4.80	.00	.62	214	031	169	0
26298	49.70	1.20	17.00	8.86	.14	8.45	9.14	3.35	.29	.12	1.90				
26299	79.50	.09	11.90	.94	.06	.33	1.68	1.00	3.91	.05	1.05				
26300	74.60	.67	11.00	4.43	.12	1.97	1.08	3.35	.47	.16	1.43				
28201	50.50	1.19	16.60	8.29	.13	9.02	8.33	3.64	.16	.13	2.06				
28202	64.40	.20	18.40	4.41	.03	1.34	.14	1.00	3.91	.14	3.84				
28203	74.40	.34	12.20	2.78	.06	.40	.09	.27	8.70	.01	.55	422	041	232	
28204	70.40	.32	12.30	6.55	.12	1.79	.38	2.26	4.14	.02	.99	075	050	175	
28205	79.20	.16	10.50	1.32	.02	.15	.00	.43	7.64	.08	.37	150	039	190	

LITHCODE	TS/PTS	ALTERATION	MINERALIZATION	COMMENTS	DEPTH	WIDTH
11	1	SER			.0	.0
11	0	SER			.0	.0
11	0				.0	.0
7	0				.0	.0
7	0				.0	.0
10	0	SIL			.0	.0
1	0	ACT			.0	.0
7	0				.0	.0
7	0				.0	.0
7	0				.0	.0
11	0			F:TF	.0	.0
7	0			F:LT	.0	.0
11	0			SHAL	.0	.0
12	0			I:TF	.0	.0
15	1				.0	.0
16	1				.0	.0
16	0			SSLT	.0	.0
10	0				.0	.0
1	1				.0	.0
10	0			F:TF	.0	.0
16	0	ACT			.0	.0
10	0			F:TF	.0	.0
6	0				.0	.0
16	0				.0	.0
13	0				.0	.0
7	0			I:TF	.0	.0
3	0				.0	.0
10	1			F:TF	.0	.0

Na2O	K2O	P2O5	LOI	Zr	Sr	Rb	Zn	Cu	U	Th	Ga	Pb	Ni	Y	Ag
2.94	6.26	.08	2.32	305	061	093	0059	18	4	13	16	009	007	021	
3.05	1.40	.08	1.24	194	178	069	0044	16	0	17	14	019	001	021	
3.97	3.60	.11	2.44	290	074	165	0122	10	7	19	32	009	003	016	
4.76	2.32	.11	.46	171	145	061	0013	04	0	12	16	009	000	053	
.83	3.20	.16	1.86	211	034	155	0024	16	4	08	14	005	000	019	
.51	9.38	.13	.38	226	047	175	0003	02	6	19	05	000	000	072	
2.11	3.10	.83	2.29	363	113	164	0134	36	0	00	23	016	000	086	
1.11	5.55	.11	2.85	265	034	256	0069	10	6	26	29	013	000	020	
2.74	4.43	.01	.91	292	049	112	0008	04	1	15	18	005	000	067	
.35	6.96	.01	.82	165	022	190	0011	04	2	18	14	003	000	037	
4.57	.95	.33	1.13	276	056	038	0023	00	2	12	13	004	010	054	
1.28	4.94	.00	1.30	079	030	181	0014	06	5	11	13	005	000	037	
2.55	3.83	.13	3.52	274	160	161	0085	14	5	18	26	018	011	031	
2.30	1.58	.12	1.83	198	131	071	0047	12	2	09	14	009	003	020	
4.31	4.16	.02	.37	208	027	097	0024	04	5	24	20	014	000	059	
2.57	.08	.19	1.87	109	200	001	0065	08	0	04	14	009	102	035	
3.00	2.15	.13	1.78	086	176	136	0089	06	0	00	18	004	162	029	
3.49	5.33	.02	.36	124	033	185	0035	02	7	26	18	008	000	122	
1.06	5.95	.07	3.57	193	047	206	0112	34	5	21	33	018	038	025	
1.98	4.80	.00	.62	214	031	169	0064	00	11	19	18	008	000	083	
3.35	.29	.12	1.90												
1.00	3.91	.05	1.05												
3.35	.47	.16	1.43												
3.64	.16	.13	2.06												
1.00	3.91	.14	3.84												
.27	8.70	.01	.55	422	041	232	35	4	2	16	15	10	00	83	
2.26	4.14	.02	.99	075	050	175	78	6	0	06	14	01	01	21	
.43	7.64	.08	.37	150	039	190	10	0	1	13	08	04	00	50	

SAMPLE	EASTING	NORTHING	TYPE	DRILLHOLE	LITHOLOGY	LITHCODE	TS/PTS	ALTERATION	MINERALIZATI
28206	+ 930E	-1200S	1	0	F:TF	7	0		
28207	+1050E	-1200S	1	0	SSST	12	0		
28208	+1080E	-1100S	1	0	F:TF	7	0	FEO	
28209	+1225E	-1100S	1	0	F:LT	8	0		
28210	+1225E	- 990S	1	0	F:LT	8	0		
28211	+ 810E	-1000S	1	0	SSST	12	0		
28212	+ 725E	-1100S	1	0	F:LT	8	0		
28213	- 130W	+ 400N	1	0	SHAL	13	0		
28214	- 250W	+ 400N	1	0	F:LT	8	2		AS
28215	- 340W	- 200S	1	0	I:TF	3	0		
28216	- 320W	- 260S	1	0	SHAL	13	0	SER	
28217	- 250W	- 400S	1	0	I:TF	3	0		
28218	- 350W	- 400S	1	0	I:TF	3	1	SER FEO	
28219	- 275W	- 600S	1	0	I:TF	3	0	SER	
28220	- 210W	- 600S	1	0	SHAL	13	0		
28221			2	160230031	I:TF	3	1	SER	
28222			2	160230031	SSLT	11	0		
28223			2	160230031	F:TF	7	1	SER	
28225			2	160230031	SSLT	11	2		PY
28227			2	160230031	SHAL	13	1	SER	PY
28228			2	160230031	SSLT	11	1	SER	PY
28229			2	160230031	F:TF	7	1	SER	PY
28230			2	160230031	I:TF	3	0		PY
28231			2	160200002	I:LT	4	1	SER	
28232			2	160200002	I:LT	4	1		
28233			2	160200001	I:LT	4	1	SER	
28236			2	160200001	I:TF	3	1		
28237			2	160200002	SHAL	13	0	SER	

SAMPLE	SiO2	TiO2	Al2O3	FeO	MnO	MgO	CaO	Na2O	K2O	P2O5	LOI	Zr	Sr	Rb
28206	77.30	.12	9.30	2.76	.05	.50	.12	.36	6.00	.05	.61	123	046	143
28207	73.00	.62	11.30	4.24	.09	1.38	.62	3.76	1.95	.19	.51	227	060	094
28208	68.80	.60	15.40	3.69	.06	1.37	.40	3.29	2.55	.05	2.44			
28209	66.50	.80	16.90	4.09	.07	1.70	.78	1.91	3.64	.00	2.61			
28210	66.50	.84	15.20	6.00	.09	1.42	.69	2.15	3.06	.22	2.98			
28211	85.60	.38	4.70	3.71	.05	.79	.18	.58	.65	.02	.97			
28212	74.20	.26	14.30	1.80	.02	.15	.16	3.99	3.37	.06	.77	122	055	125
28213	60.60	.99	18.60	7.12	.16	2.33	.39	1.90	3.60	.12	4.14	204	065	154
28214	70.90	.69	13.60	4.12	.11	1.42	1.85	3.40	1.61	.21	1.53	276	183	085
28215	76.30	.40	11.40	3.91	.06	1.42	.87	2.56	1.43	.04	1.53	202	105	056
28216	69.60	.76	13.40	5.00	.06	1.63	.39	1.79	2.71	.12	3.13	204	077	106
28217	66.70	.80	15.50	4.78	.11	1.49	.75	3.62	1.91	.05	1.93	431	126	090
28218	73.30	.93	10.80	3.82	.06	1.41	1.05	2.44	1.34	.05	1.88			
28219	75.40	.60	11.30	3.82	.05	1.42	.54	2.24	1.69	.04	1.87	193	074	069
28220	59.50	.88	19.70	7.17	.16	2.29	.37	1.03	4.45	.08	3.78	195	060	183
28221	76.90	.24	12.80	2.88	.04	.71	.18	1.58	3.80	.06	1.51			
28222	66.60	.76	16.70	5.54	.09	1.78	.25	1.61	4.43	.15	2.67			
28223	76.40	.13	11.50	3.25	.07	.87	.24	.63	5.65	.02	1.26			
28225	47.70	1.10	15.80	9.41	.61	12.71	1.17	.30	6.18	.17	3.72			
28227	62.10	.91	18.90	5.76	.06	.70	.12	.99	6.48	.70	3.47			
28228	62.80	.33	18.30	6.15	.05	1.82	.15	.29	5.73	.18	2.76			
28229	77.40	.09	10.20	2.41	.11	1.77	.21	4.23	1.14	.20	.94			
28230	47.50	2.70	12.60	13.25	.24	7.98	5.97	1.00	.65	.88	3.97			
28231	63.50	.88	14.70	6.19	.32	4.26	1.04	3.35	3.72	.21	1.39			
28232	66.30	.65	15.30	5.00	.08	1.78	.78	2.63	3.52	.14	1.86			
28233	64.20	.65	15.50	5.13	.18	3.16	.84	3.13	4.43	.18	1.65			
28236	66.30	.68	16.20	5.31	.08	1.78	.89	2.54	3.94	.09	2.07			
28237	60.00	.99	20.00	6.14	.06	1.76	.20	.73	5.42	.15	3.79			

LITHCODE	TS/PTS	ALTERATION	MINERALIZATION	COMMENTS	DEPTH	WIDTH
7	0				.0	.0
12	0			I:TF	.0	.0
7	0	FED			.0	.0
8	0				.0	.0
8	0				.0	.0
12	0				.0	.0
8	0				.0	.0
13	0				.0	.0
8	2		AS		.0	.0
3	0			SSST	.0	.0
13	0	SER			.0	.0
3	0				.0	.0
3	1	SER FED		SSST	.0	.0
3	0	SER		SSST	.0	.0
13	0				.0	.0
3	1	SER		SSLT	77.7	.3
11	0				96.6	.3
7	1	SER			115.0	.3
11	2		PY		147.9	.3
13	1	SER	PY		156.3	.3
11	1	SER	PY		163.9	.3
7	1	SER	PY		188.8	.3
3	0		PY		206.1	.2
4	1	SER			14.8	.3
4	1				50.4	.3
4	1	SER		I:LT	7.9	.1
3	1			I:LT	104.8	.2
13	0	SER			63.6	.3

Na2O	K2O	P2O5	LOI	Zr	Sr	Rb	Zn	Cu	U	Th	Ga	Pb	Ni	Y	Ag
.36	6.00	.05	.61	123	046	143	21	8	3	13	08	00	00	23	
3.76	1.95	.19	.51	227	060	094	64	0	1	10	12	04	07	36	
3.29	2.55	.05	2.44												
1.91	3.64	.00	2.61												
2.15	3.06	.22	2.98												
.58	.65	.02	.97												
3.99	3.37	.06	.77	122	055	125	12	0	1	10	15	02	00	51	
1.90	3.60	.12	4.14	204	065	154	80	18	7	18	24	20	09	22	
3.40	1.61	.21	1.53	276	183	085	41	14	0	09	16	18	02	36	
2.56	1.43	.04	1.53	202	105	056	41	8	3	10	13	07	05	22	
1.79	2.71	.12	3.13	204	077	106	59	9	3	12	18	13	00	22	
3.62	1.91	.05	1.93	431	126	090	53	10	2	19	16	13	14	45	
2.44	1.34	.05	1.88												
2.24	1.69	.04	1.87	193	074	069	44	8	1	11	12	44	05	20	
1.03	4.45	.08	3.78	195	060	183	78	4	2	15	25	19	12	24	
1.58	3.80	.06	1.51												
.61	4.43	.15	2.67												
.63	5.65	.02	1.26												
.30	6.18	.17	3.72												
.99	6.48	.70	3.47												
.29	5.73	.18	2.76												
4.23	1.14	.20	.74												
1.00	.65	.88	3.97												
3.35	.72	.21	1.49												
2.63	.52	.14	1.86												
3.13	4.43	.18	1.65												
2.51	3.94	.09	2.07												
.73	5.42	.15	3.79												

2 OF 2

SAMPLE	EASTING	NORTHING	TYPE	DRILLHOLE	LITHOLOGY	LITHCODE	TSZETS	ALTERATION	MINERALIZATIO
28238			2	160200002	SSLT	11	1	SER	
28239			2	160200001	I:LT	4	1	SER	PY
28240			2	160200001	I:TF	3	1		
28241	+9999E	-9999S	1	0	F:TF	7	1		
28242	+1175E	+ 850N	1	0	I:TF	3	0		
28243	+ 100E	- 550S	1	0	M:TF	1	0		
6802	- 050W	- 500S	1	0	SHAL	13	0		
6803	000	- 500S	1	0	SSLT	11	0		
6804	+ 030E	- 500S	1	0	SSLT	11	0		
6805	+ 085E	- 480S	1	0	F:LT	8	0		
6806	+ 125E	- 525S	1	0	M:TF	1	0	CHL	
6808	+ 270E	- 500S	1	0	TFSD	18	[illegible]		
6809	- 080W	- 300S	1	0	SHAL	13	0		
6810	- 045W	- 300S	1	0	SSLT	11	0		
6811	+ 075E	- 280S	1	0	F:TF	7	0		
6812	+ 125E	- 285S	1	0	F:FL	10	0		
6813	+ 200E	- 300S	1	0	F:FL	10	0		
6814	+ 250E	- 300S	1	0	SSST	12	0		
6815	+ 300E	- 300S	1	0	SSLT	11	0		
6816	+ 225E	- 100S	1	0	F:LT	8	0		
6817	+ 175E	- 100S	1	0	SSLT	11	0		
6818	+ 115E	- 100S	1	0	I:TF	3	0		
6819	+ 075E	- 100S	1	0	F:TF	7	0		
6820	000	- 100S	1	0	SSLT	11	0		
6821	- 050W	- 100S	1	0	SSLT	11	0		
6822	- 075W	- 100S	1	0	SHAL	13	0		
6823	- 075W	000	1	0	SHAL	13	0		
6824	- 050W	000	1	0	SSLT	11	0		

SAMPLE	SiO2	TiO2	Al2O3	FeO	MnO	MgO	CaO	Na2O	K2O	P2O5	LOI	Zr	Sr	Rb
28238	67.00	.87	14.60	4.94	.25	2.42	1.42	4.34	3.18	.19	1.92			
28239	66.50	.82	16.30	5.22	.13	1.96	.85	2.17	3.78	.14	.77			
28240	65.30	.94	16.40	5.76	.08	1.92	.96	2.10	3.28	.13	2.40			
28241	77.00	.26	11.00	1.17	.01	.18	.00	.19	8.20	.03	.45			
28242	73.20	.28	12.20	3.91	.06	.50	.07	.24	8.56	.07	.72			
28243	63.90	.63	11.40	10.41	.35	3.96	.40	2.57	1.51	.18	2.66			
6802	70.90	.88	14.10	4.51	.06	1.53	1.93	3.38	.60	.09	2.48			
6803	85.00	.17	6.92	1.33	.02	.37	1.48	2.21	.60	.66	1.54			
6804	88.50	.12	4.34	1.98	.02	.53	.37	1.34	.28	.05	1.12			
6805	66.10	.68	12.60	9.32	.43	2.54	.24	3.69	1.24	.16	2.42			
6806	52.70	3.34	13.30	14.30	.30	5.27	2.29	2.11	1.23	.58	3.64			
6808	76.80	.41	11.00	3.43	.05	.70	.14	2.48	2.37	.04	1.33			
6809	61.50	.93	17.90	6.89	.13	2.13	.73	2.46	2.55	.11	3.08			
6810	78.10	.49	10.20	2.61	.04	.86	.85	3.15	1.37	.07	1.24			
6811	78.70	.27	10.50	3.36	.11	1.45	.06	2.67	1.89	.04	1.48			
6812	82.00	.12	8.85	1.50	.11	1.72	.26	3.84	.52	.02	1.22			
6813	91.20	.06	3.07	2.69	.03	.26	.00	.65	.75	.02	1.09			
6814	76.60	.40	10.80	3.31	.05	.83	.25	2.58	2.38	.06	1.11			
6815	77.40	.72	10.10	4.31	.10	1.13	.88	3.37	1.33	.07	.75			
6816	75.40	.40	11.10	3.86	.06	.88	.27	3.06	2.54	.07	1.13			
6817	67.00	.76	13.20	7.73	.25	1.31	1.91	3.04	2.22	.17	1.62			
6818	68.80	1.38	9.91	7.49	.23	4.58	1.34	1.35	.23	.31	3.78			
6819	76.70	.13	10.10	1.40	.04	.53	.00	.14	7.24	.02	.99			
6820	79.50	.42	8.33	3.39	.03	.82	.10	.43	2.66	.07	1.52			
6821	75.60	.48	11.50	3.18	.03	1.19	.40	2.30	2.36	.09	1.65			
6822	69.00	.89	14.20	4.35	.05	1.19	.19	.91	3.31	.07	3.85			
6823	66.00	.91	15.50	5.11	.08	1.40	2.24	2.92	1.33	.12	3.75			
6824	78.70	.46	9.57	3.29	.02	.93	.26	1.77	1.88	.09	1.68			

LITHCODE	%S/PTS	ALTERATION	MINERALIZATION	COMMENTS	DEPTH	WIDTH
11	1	SER			82.5	.3
4	1	SER	PY		57.3	.3
3	1				131.5	.3
7	1				.0	.0
3	0				.0	.0
1	0				.0	.0
13	0				.0	.0
11	0			SSST	.0	.0
11	0			SSST	.0	.0
8	0				.0	.0
1	0	CHL			.0	.0
18	0				.0	.0
13	0				.0	.0
11	0				.0	.0
7	0				.0	.0
10	0				.0	.0
10	0				.0	.0
12	0				.0	.0
11	0				.0	.0
8	0			SSST	.0	.0
11	0			SHAL	.0	.0
3	0				.0	.0
7	0				.0	.0
11	0				.0	.0
11	0				.0	.0
13	0				.0	.0
13	0				.0	.0
11	0				.0	.0

Na2O	K2O	P2O5	LOI	Zr	Sr	Rb	Zn	Cu	U	Th	Ga	Pb	Ni	Y	Ag
4.34	3.18	.19	1.92												
2.17	3.78	.14	.77												
2.10	3.28	.13	2.40												
.19	8.20	.03	.45												
.24	8.56	.07	.72												
2.57	1.51	.18	2.66												
3.38	.60	.09	2.48												
2.21	.60	.66	1.54												
1.34	.28	.05	1.12												
3.69	1.24	.16	2.42												
2.11	1.23	.58	3.64												
2.48	2.37	.04	1.33												
2.46	2.55	.11	3.08												
3.15	1.37	.07	1.24												
2.67	1.88	.04	1.48												
3.84	.52	.02	1.22												
.65	.75	.02	1.09												
2.58	2.38	.06	1.11												
3.37	1.33	.07	.75												
3.06	2.54	.07	1.13												
3.04	2.22	.17	1.62												
1.85	.23	.31	3.78												
.14	7.24	.02	.99												
.93	2.66	.07	1.52												
2.30	2.36	.09	1.65												
.91	3.31	.07	3.85												
2.92	1.33	.12	3.75												
1.77	1.88	.09	1.68												

SAMPLE	EASTING	NORTHING	TYPE	DRILLHOLE	LITHOLOGY	LITHCODE	TS/PTS	ALTERATION	MINERALIZATIO
6825	- 015W	000	1	0	F:TF	7	0		
6826	+ 060E	000	1	0	F:FL	10	0		
6827	+ 080E	000	1	0	F:FL	10	0		
6828	+ 135E	000	1	0	I:TF	3	0		
6829	+ 215E	000	1	0	F:TF	7	0		
6830	+ 240E	+ 100N	1	0	SSLT	11	0		
6831	+ 200E	+ 100N	1	0	SSST	12	0		
6832	+ 140E	+ 100N	1	0	I:TF	3	0		
6833	+ 075E	+ 100N	1	0	F:FL	10	0		
6834	+ 035E	+ 100N	1	0	F:FL	1	0		
6835	- 025E	+ 100N	1	0	SSLT	11	0		
6836	- 100W	+ 100N	1	0	SHAL	13	0		
6837	- 125W	+ 300N	1	0	SHAL	13	0		
6838	- 075W	+ 300N	1	0	SSLT	11	0		
6839	+ 030E	+ 300N	- 1	0	F:TF	7	0		
6840	+ 110E	+ 300N	1	0	F:FL	10	0		
6841	+ 175E	+ 300N	1	0	SSST	12	0		
6842	+ 210E	+ 300N	1	0	SSST	12	0		
6843	+ 280E	+ 300N	1	0	F:FL	10	0		
6844	+ 275E	+ 500N	1	0	F:FL	10	0		
6845	+ 225E	+ 500N	1	0	SSLT	11	0		
6846	+ 175E	+ 500N	1	0	F:TF	7	0		
6847	+ 125E	+ 500N	1	0	SSLT	11	0		
6848	+ 075E	+ 525N	1	0	F:FL	10	0		
6849	000	+ 500N	1	0	F:TF	7	0		
6850	- 090W	+ 500N	1	0	SHAL	13	0		

SAMPLE	SiO2	TiO2	Al2O3	FeO	MnO	MgO	CaO	Na2O	K2O	P2O5	LOI	Zr	Sr	Rb
6825	88.70	.21	4.31	1.13	.02	.63	.02	.10	1.45	.02	1.48			
6826	77.50	.15	11.60	1.81	.05	.81	.09	3.43	2.26	.03	1.25			
6827	78.50	.10	9.74	3.62	.03	.34	.05	.41	4.52	.02	2.15			
6828	68.30	.72	13.10	5.86	.31	2.68	1.19	3.78	2.33	.18	1.10			
6829	83.70	.20	5.98	2.69	.06	.63	.83	1.40	.85	.04	.66			
6830	73.00	.41	11.80	4.67	.06	1.13	.29	3.01	2.30	.06	1.38			
6831	74.10	.40	12.80	3.79	.03	1.02	.20	2.88	2.57	.05	1.37			
6832	69.20	.74	13.20	6.51	.32	1.08	1.42	3.98	1.43	.17	1.22			
6833	78.90	.13	10.30	1.45	.02	.18	.00	.16	7.43	.02	.97			
6834	53.40	3.03	14.80	11.70	.35	4.92	3.01	2.86	.32	.93	5.16			
6835	75.10	.44	11.70	3.44	.03	.88	.32	1.91	2.78	.06	2.41			
6836	72.60	.85	12.60	4.13	.03	1.19	.17	1.02	3.03	.19	3.08			
6837	62.50	.99	17.90	6.76	.15	2.08	.67	1.54	3.52	.12	3.45			
6838	78.90	.42	9.47	2.61	.02	.65	.04	1.54	2.08	.07	2.18			
6839	73.20	.57	13.10	3.61	.07	2.15	.37	5.62	.18	.08	1.89			
6840	67.90	.70	13.00	7.08	.36	1.45	.56	4.84	.21	.17	2.17			
6841	64.20	.71	14.90	9.38	.12	2.06	.33	1.58	3.92	.10	2.48			
6842	76.80	.44	10.30	4.64	.02	.89	.12	2.15	1.88	.06	1.62			
6843	64.50	.17	17.60	.68	.01	.09	.00	.81	13.00	.02	.99			
6844	79.40	.10	8.25	1.50	.02	.22	.00	.29	6.28	.02	.85			
6845	73.80	.48	12.10	4.99	.07	1.29	.49	2.27	3.03	.09	1.35			
6846	76.90	.11	10.50	2.18	.04	.36	.00	.05	5.86	.02	1.47			
6847	70.60	.57	11.40	7.95	.14	1.56	.29	.19	4.14	.09	1.85			
6848	76.50	.56	11.00	3.67	.09	1.68	.84	3.97	.31	.05	1.60			
6849	81.20	.13	8.36	2.08	.12	3.59	.82	3.61	1.46	.02	1.91			
6850	87.70	.41	7.49	2.09	.03	.62	.30	1.81	1.06	.07	1.50			

ITHCODE	TS/PTS	ALTERATION	MINERALIZATION	COMMENTS	DEPTH	WIDTH
7	0				.0	.0
10	0				.0	.0
10	0			F:TF	.0	.0
3	0				.0	.0
7	0				.0	.0
11	0			SHAL	.0	.0
12	0				.0	.0
3	0				.0	.0
10	0				.0	.0
1	0				.0	.0
11	0				.0	.0
13	0				.0	.0
13	0				.0	.0
11	0				.0	.0
7	0				.0	.0
10	0				.0	.0
12	0				.0	.0
12	0				.0	.0
10	0				.0	.0
10	0				.0	.0
11	0				.0	.0
7	0				.0	.0
11	0				.0	.0
10	0				.0	.0
7	0				.0	.0
13	0				.0	.0

Na2O	K2O	P2O5	LOI	Zr	Sr	Rb	Zn	Cu	U	Th	Ga	Pb	Ni	Y	Ag
.10	1.45	.02	1.46												
3.43	2.26	.03	1.25												
.41	4.52	.02	2.15												
3.78	2.33	.18	1.10												
1.40	.85	.04	.66												
3.01	2.30	.06	1.38												
2.88	2.57	.05	1.37												
3.98	1.43	.17	1.22												
.16	7.43	.02	.97												
2.86	.32	.93	5.16												
1.91	2.78	.06	2.41												
1.02	3.03	.19	3.08												
1.54	3.52	.12	3.45												
1.54	2.08	.07	2.18												
5.62	.18	.08	1.89												
4.84	.21	.17	2.17												
1.58	3.92	.10	2.48												
2.15	1.88	.06	1.62												
.81	13.00	.02	.99												
.29	6.28	.02	.85												
3.27	3.03	.09	1.35												
.05	5.86	.02	1.47												
.19	4.14	.09	1.85												
3.97	.31	.05	1.60												
3.61	1.46	.02	1.91												
1.81	1.06	.07	1.50												

Legend

1	Felsic flows
2	Felsic tuff
3	Felsic lapilli tuff
4	Felsic agglomerate
5	Intermediate flows
6	Intermediate tuff
7	Intermediate lapilli tuff
8	Mafic tuff
9	Chlorite schist
10	Sandstone
11	Siltstone
12	Shale
	Quartz - graphite rock
14	Baggs Hill Granite
15	Felsic dykes
16	Mafic dykes

Symbols

Geological boundary (defined, approximate, assumed, gradational, geophysically inferred

Bedding (horizontal, inclined, vertical, overtu tops direction)

Schistosity (horizontal, inclined, vertical)

S_1

S_2

Lineation (drag fold axis, mineral or elonga clast)

Fault (assumed, arrows show relative movei

Swamp

Major lithology, subordinate lithology

Geology by Falconbridge Nickel personnel (1979), with additions P.J. Wynne (1980).

1 / OF

Note: This is a list of lithologies only and the order has no stratigraphic significance.

ZONES OF MINERALIZATION

B BOG ZONE

BF BISON FAULT ZONE

SOON

imate,
inferred)

l, overturned,

tical)

or elongate

ve movement)

gy 2, 1

Nickel Ltd.
ditions by

2 OF

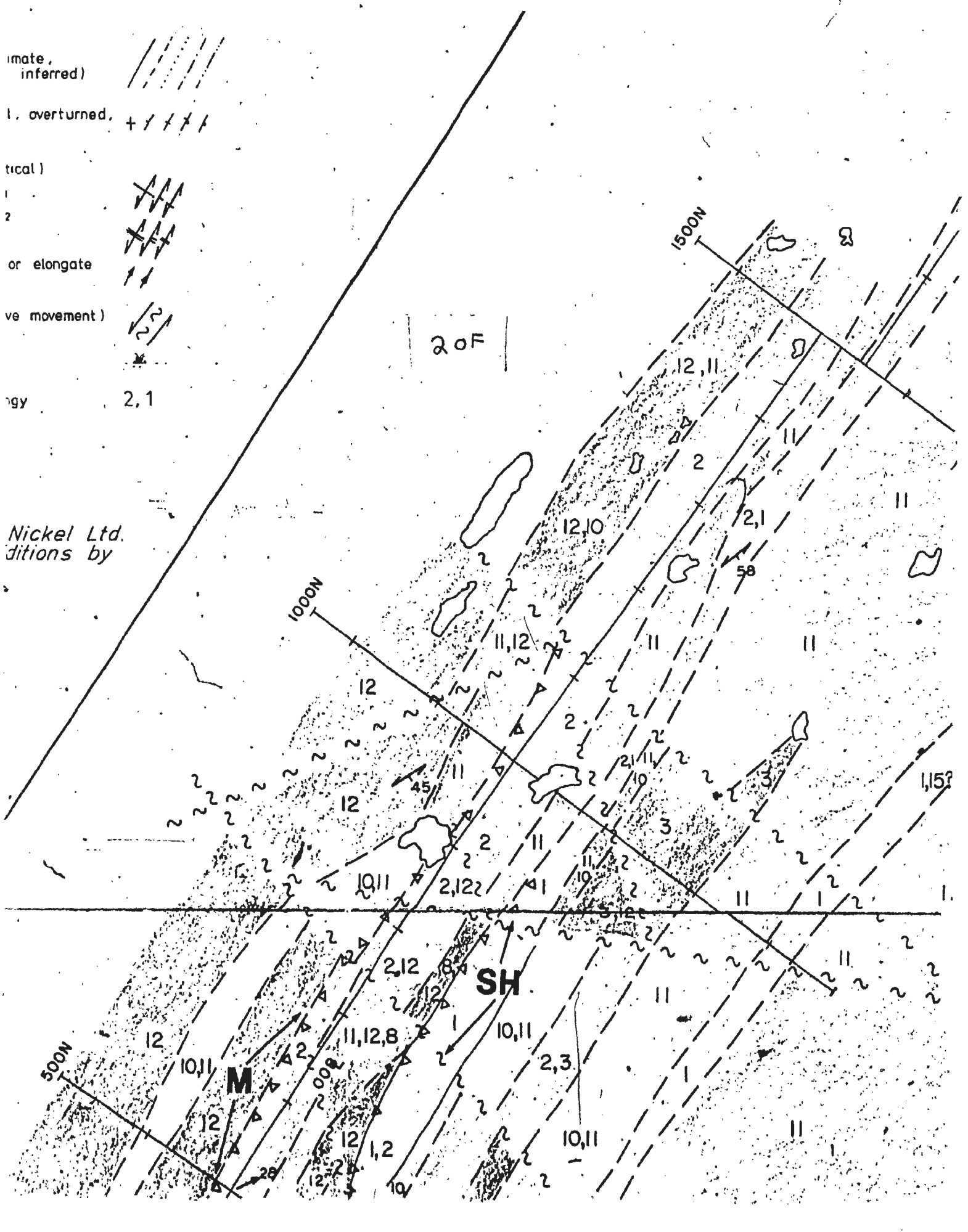

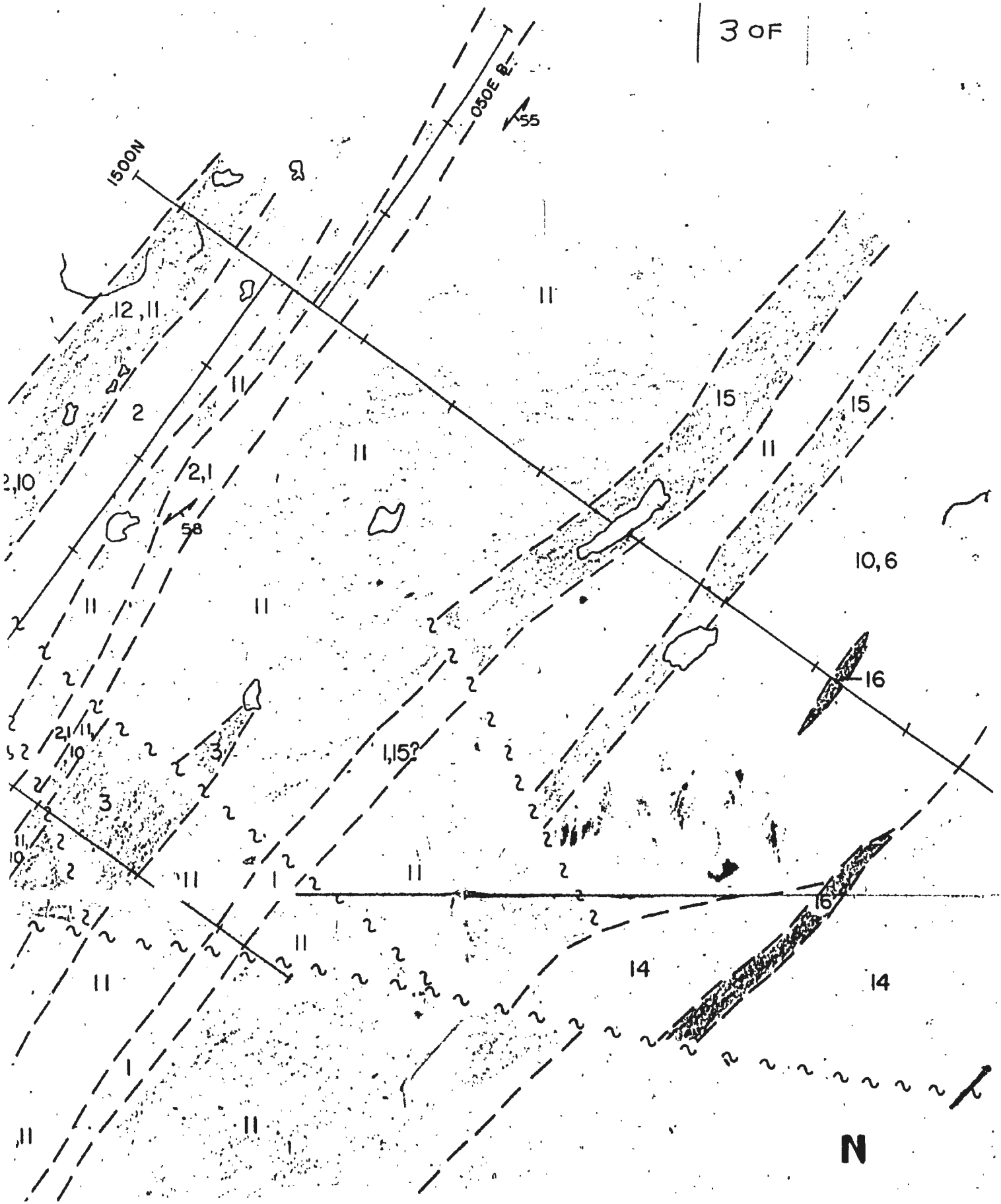
050E
55
1500N
12, 11
11
2
11
15
15
11
2,10
2,1
58
10, 6
11
11
16
2,1
10
3
1,15?
3
11
1
11
16
11
14
14
1
11
11
N

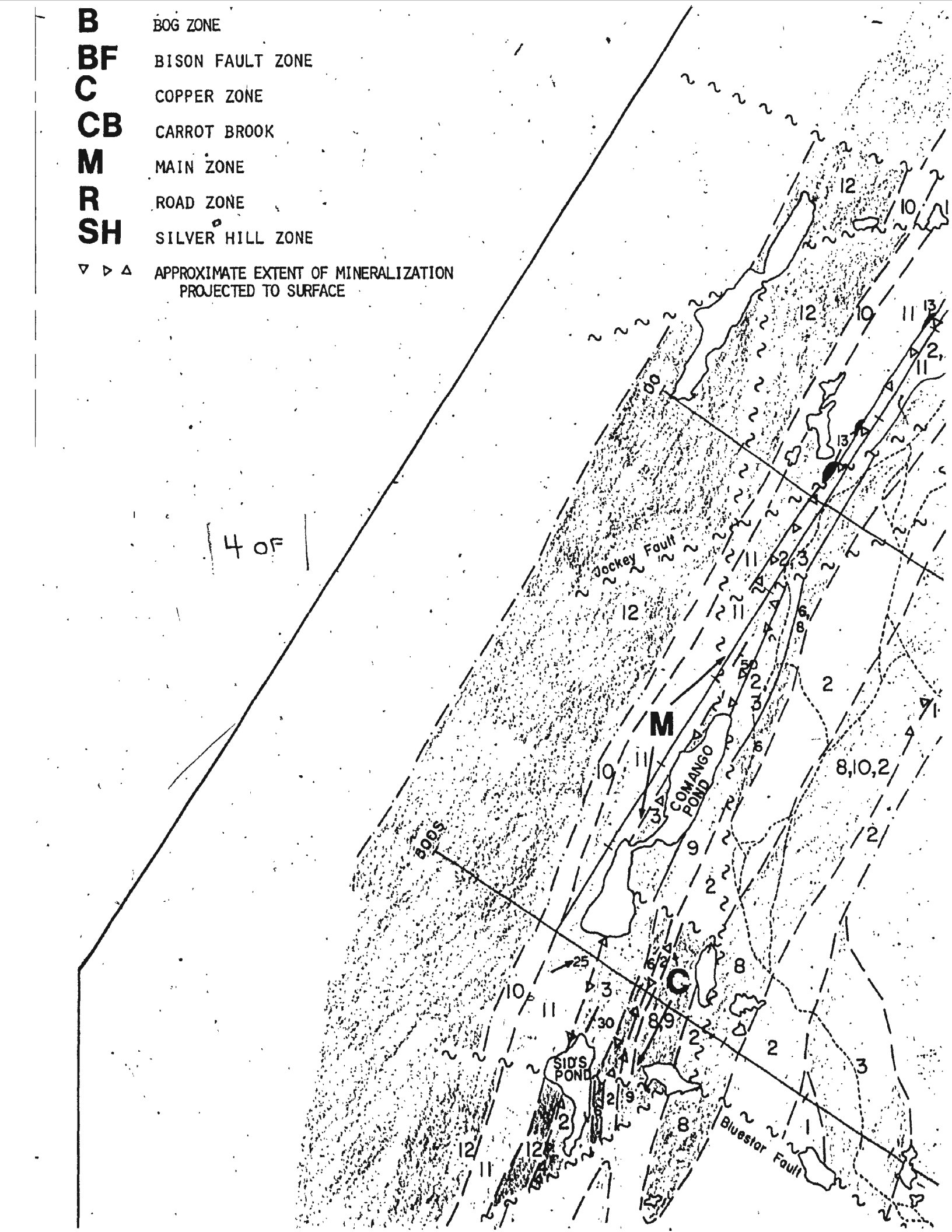
B BOG ZONE
BF BISON FAULT ZONE
C COPPER ZONE
CB CARROT BROOK
M MAIN ZONE
R ROAD ZONE
SH SILVER HILL ZONE
APPROXIMATE EXTENT OF MINERALIZATION PROJECTED TO SURFACE
4 OF
Jockey Fault
M
COMANGO POND
800S
C
SID'S POND
Bluestar Fault

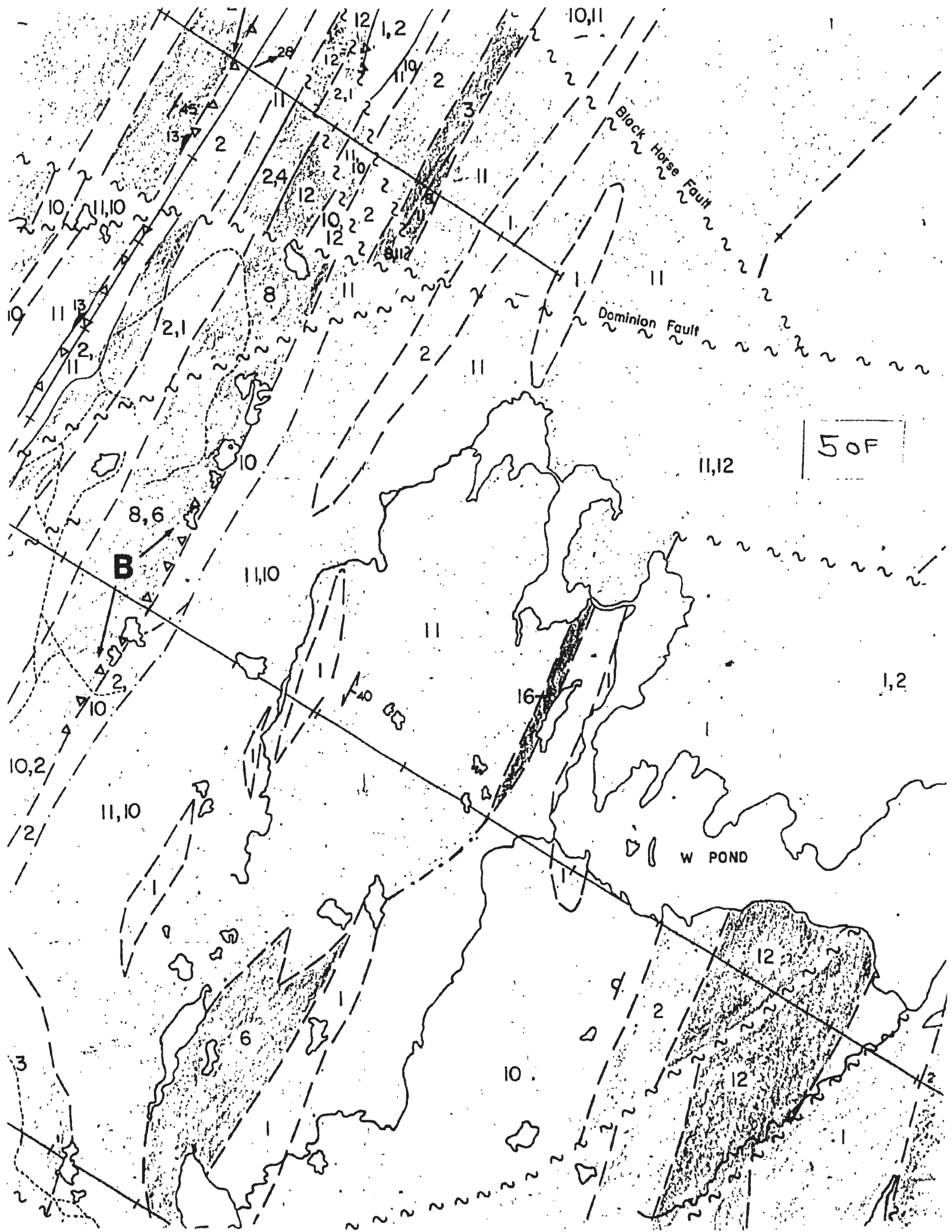
Black Horse Fault
Dominion Fault
5 OF
B
W POND

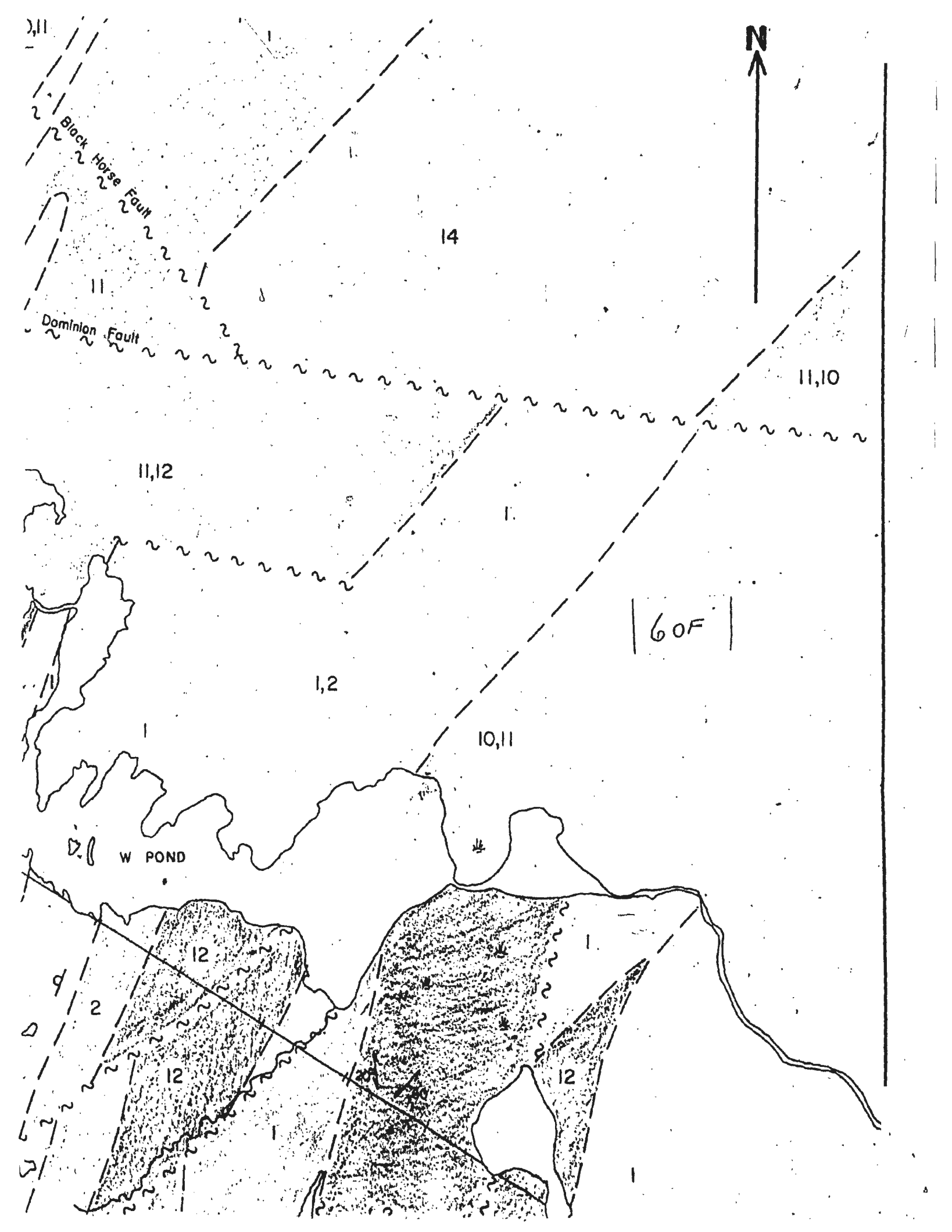
N
Block Horse Fault
Dominion Fault
14
11
11,10
11,12
1,2
10,11
60F
W POND
12
12
12
1
2

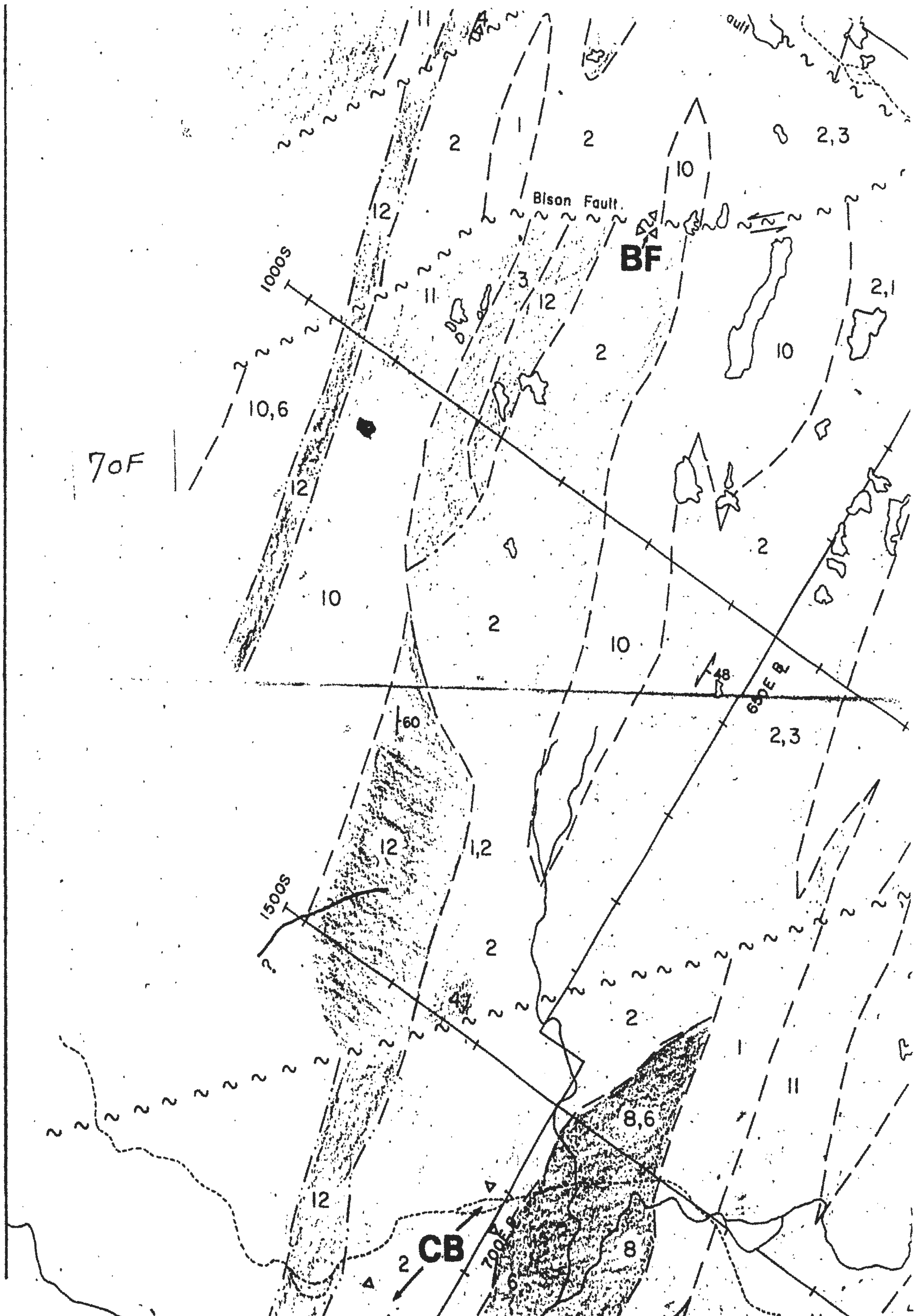

Bison Fault
BF
CB
1000S
1500S
70F
10,6
12
10
2
1
3
11
2,3
2,1
1,2
8,6
8
6
60
48
47

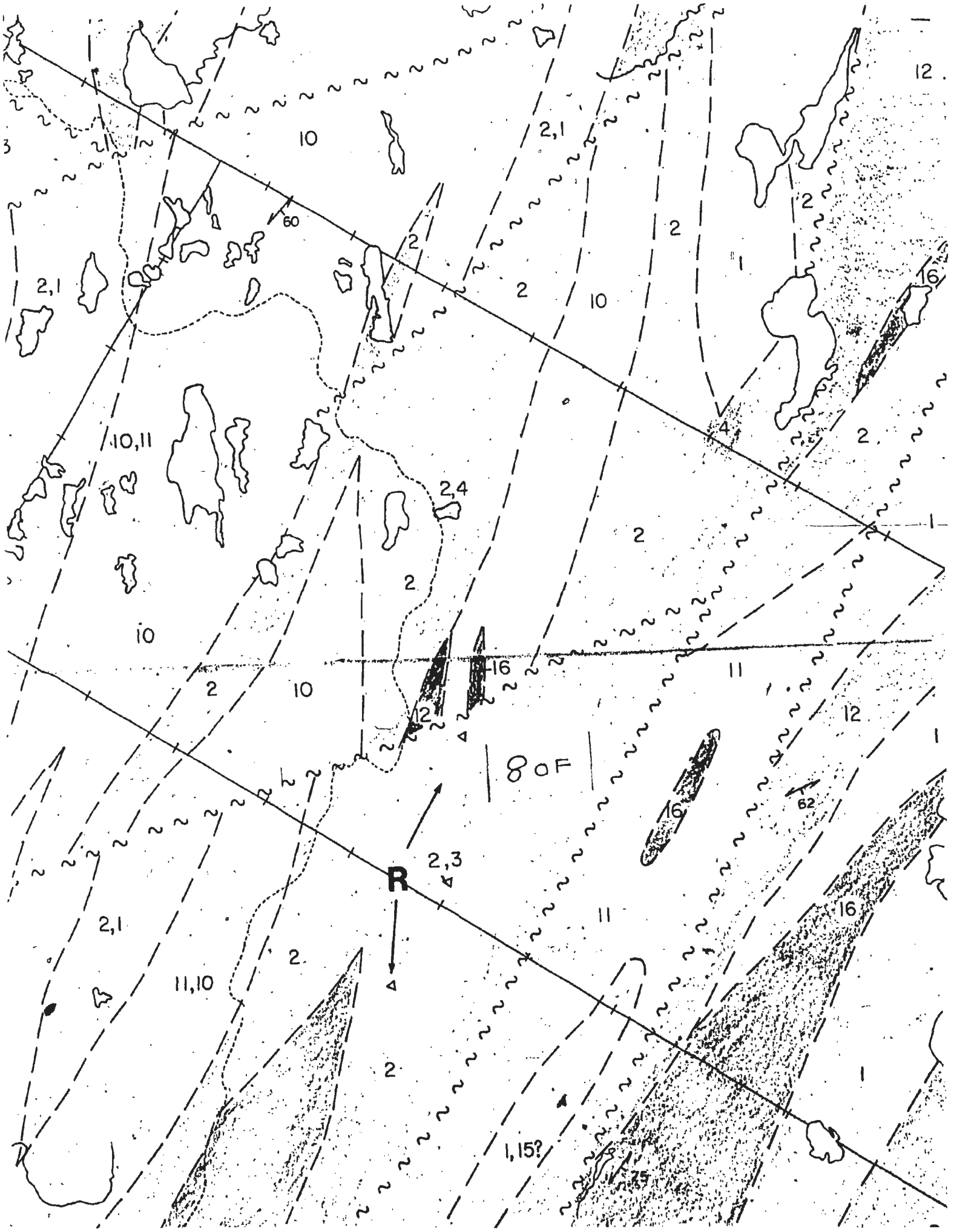
10
2,1
60
2
2
2
10
2,1
2
16
10,11
4
2
2,4
2
2
10
16
11
2
10
12
12
8 OF
16
62
2,3
R
2,1
11
16
2.
11,10
2
1,15?
25

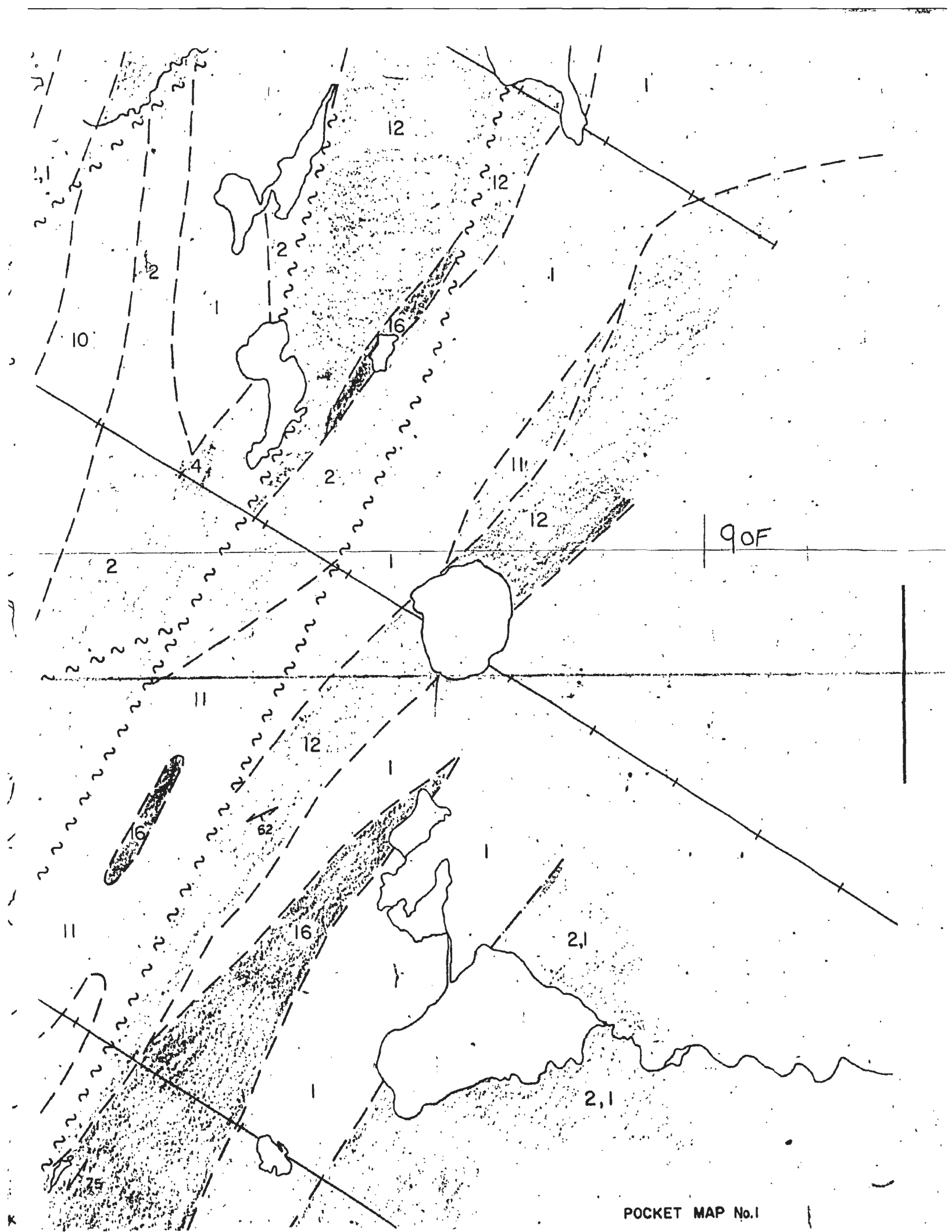
12
12
2
2
10
16
4
2
11
12
9 OF
1
12
16
62
16
2,1
2,1
25
POCKET MAP No.1

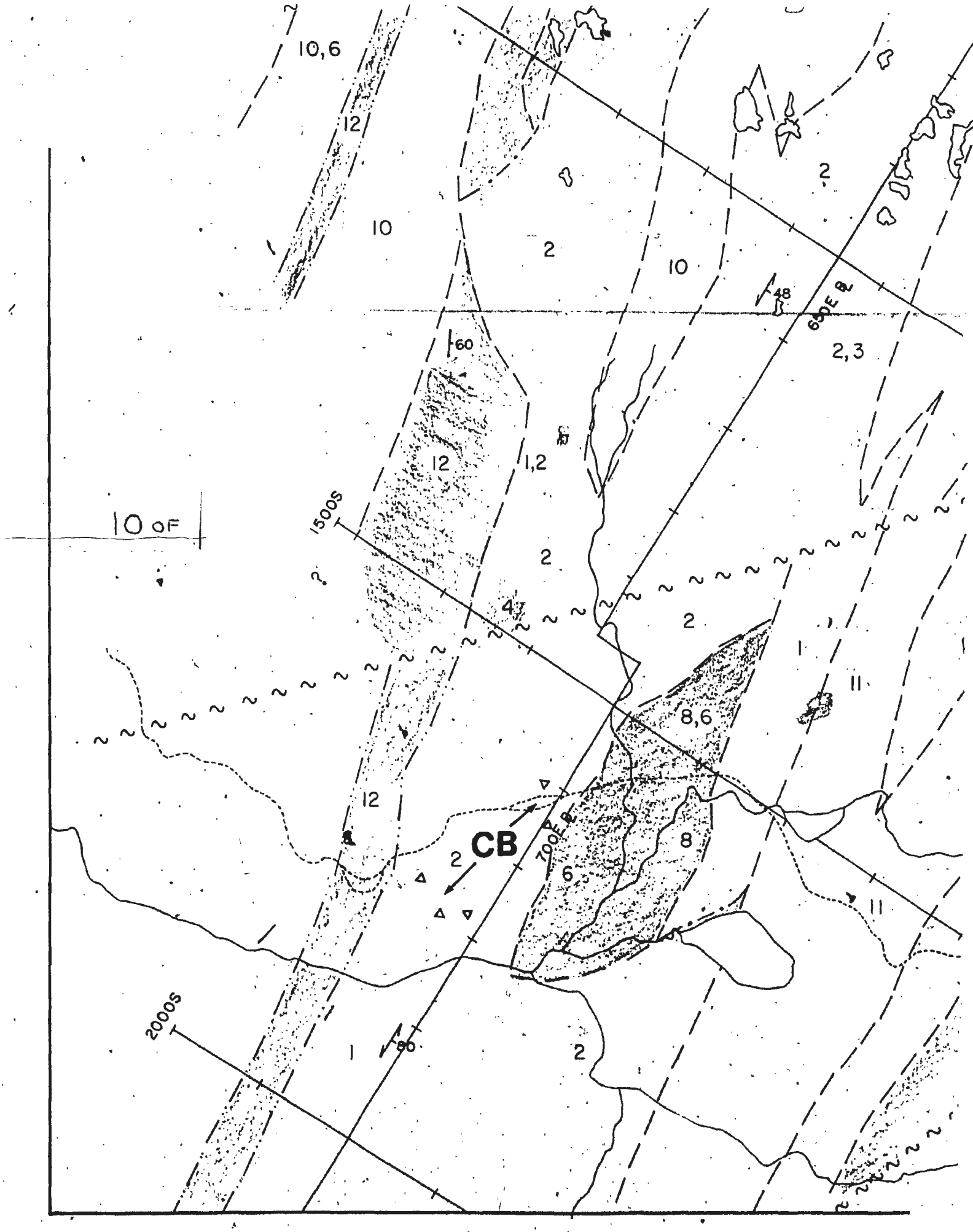
10,6
12
10
2
10
2
48
60E
2,3
60
12
1,2
10 OF
1500S
2
4
2
1
11
8,6
12
CB
2
70E
8
6
11
2000S
1
90
2

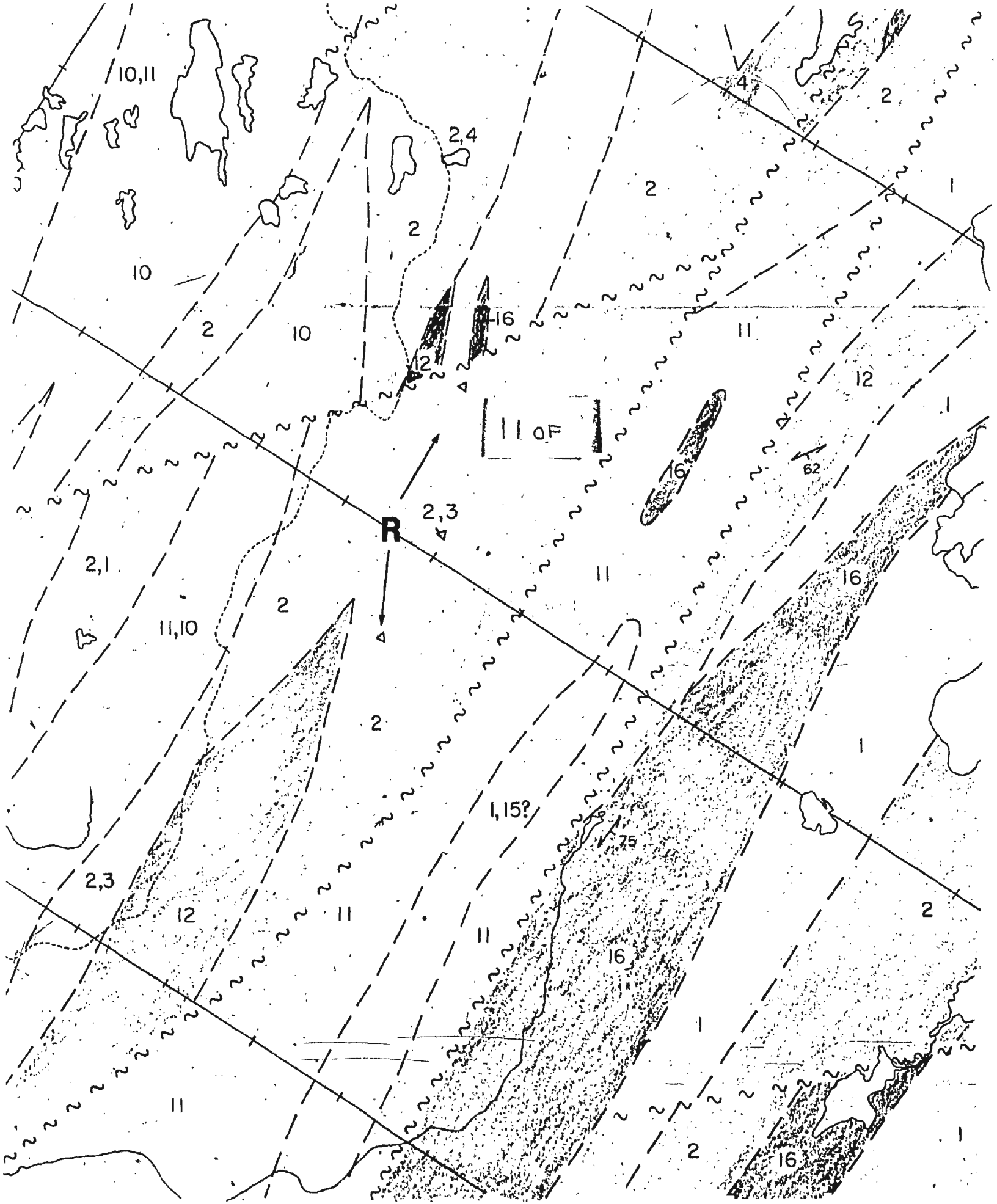
10,11
2,4
2
4
2
1
10
2
10
16
11
12
12
1
11 OF
62
16
R
2,3
2,1
11
16
11,10
2
2
1
1,15?
75
2,3
12
11
11
16
2
1
2
16
1

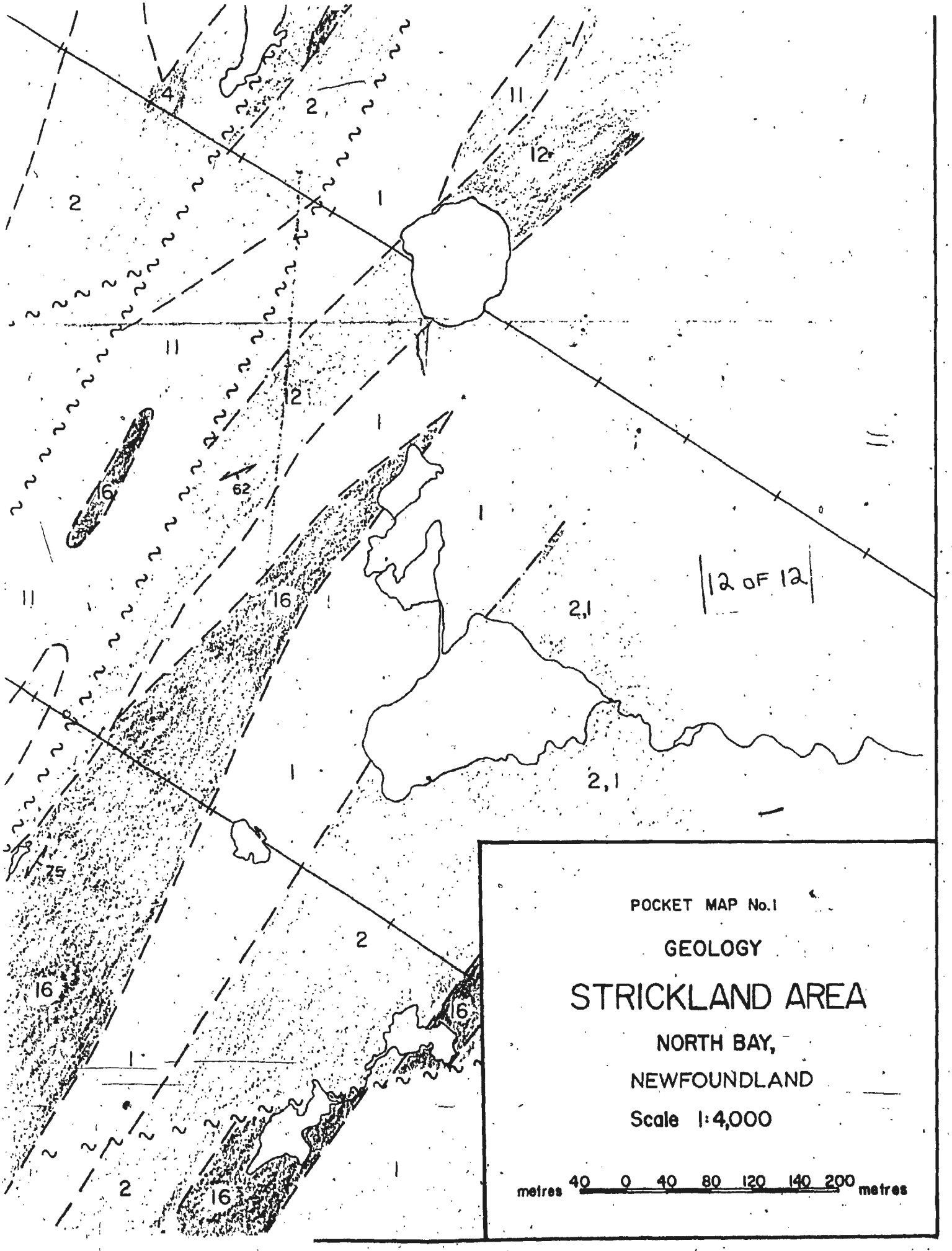
12 OF 12
POCKET MAP No.1
GEOLOGY
STRICKLAND AREA
NORTH BAY,
NEWFOUNDLAND
Scale 1:4,000
metres 40 0 40 80 120 140 200 metres

Symbols

•975	Sample collected by Falconbridge personnel
•W8205	Sample collected by P.J. Wynne
C.B. 1020	Claim Block 1020
WP □ →	Witness Post
V.1, F.33, PFS	Volume 1, Folio 33, Porter Fee Simple
V.1, F.34, SFS	Volume 1, Folio 34, Strickland Fee Simple

[1 OF]

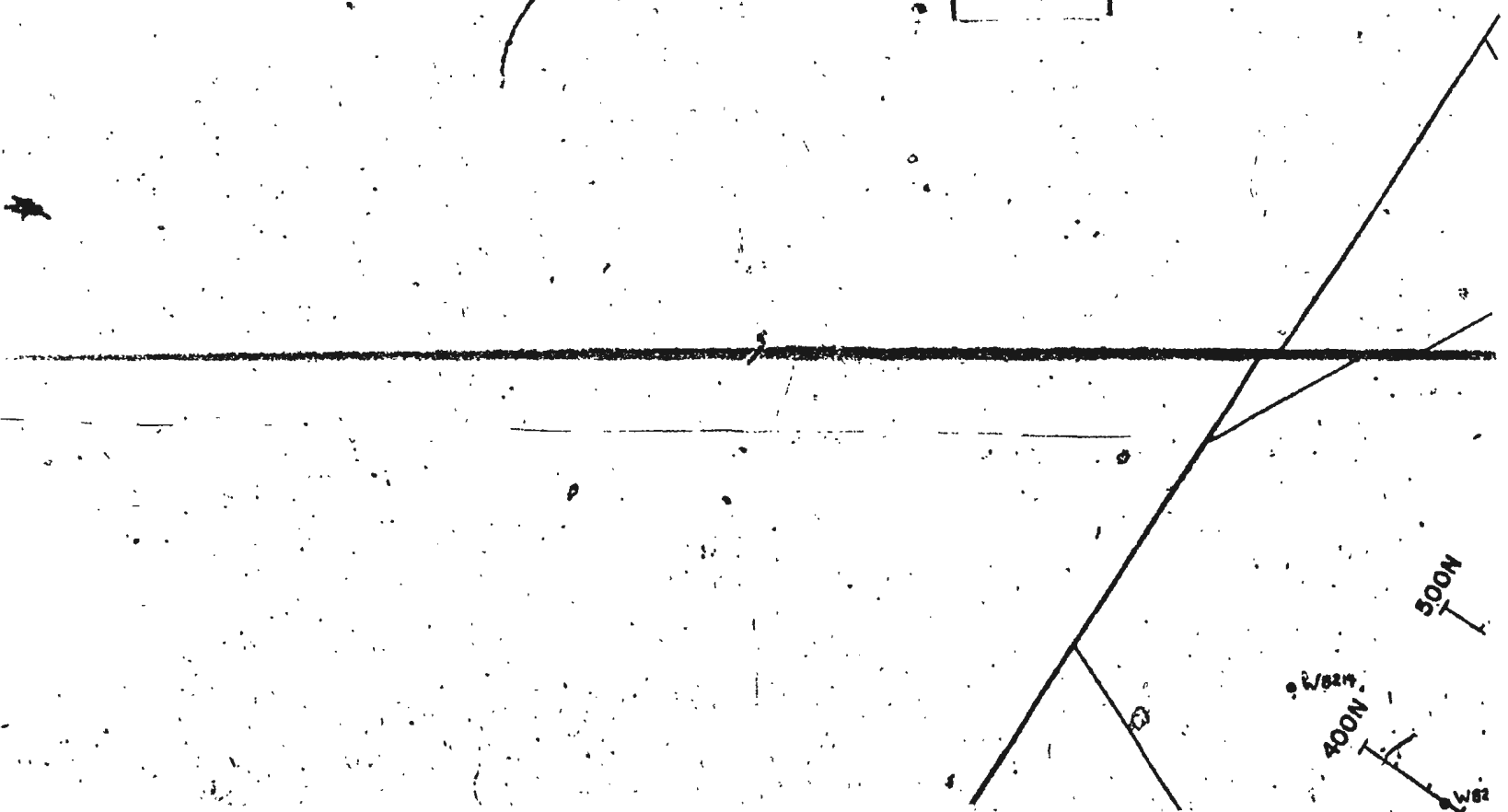

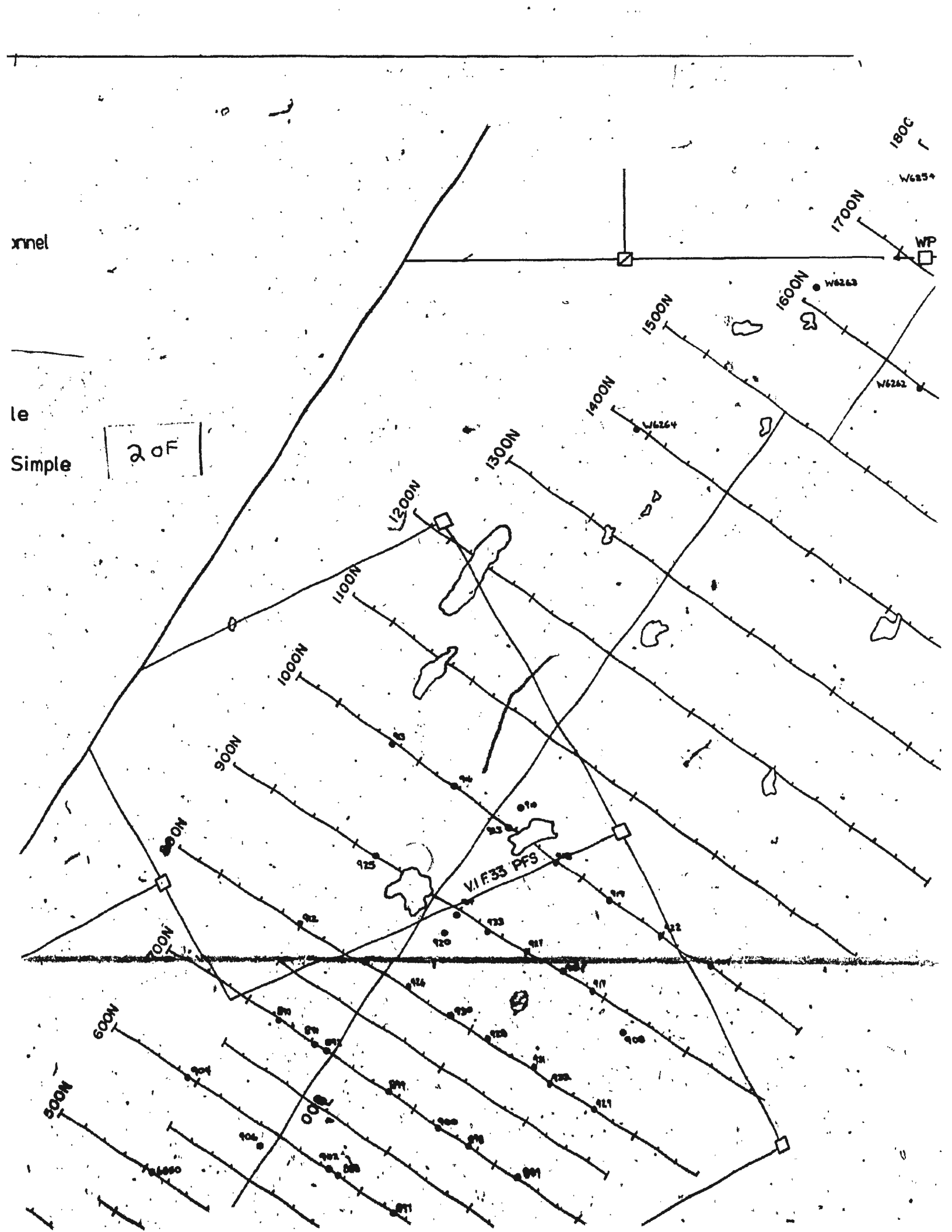
xnnel
le
Simple
2 OF
1700N
WP
1600N
W6263
1500N
W6262
1400N
W6264
1300N
1200N
1100N
1000N
900N
800N
700N
600N
500N
V/F 33 PFS

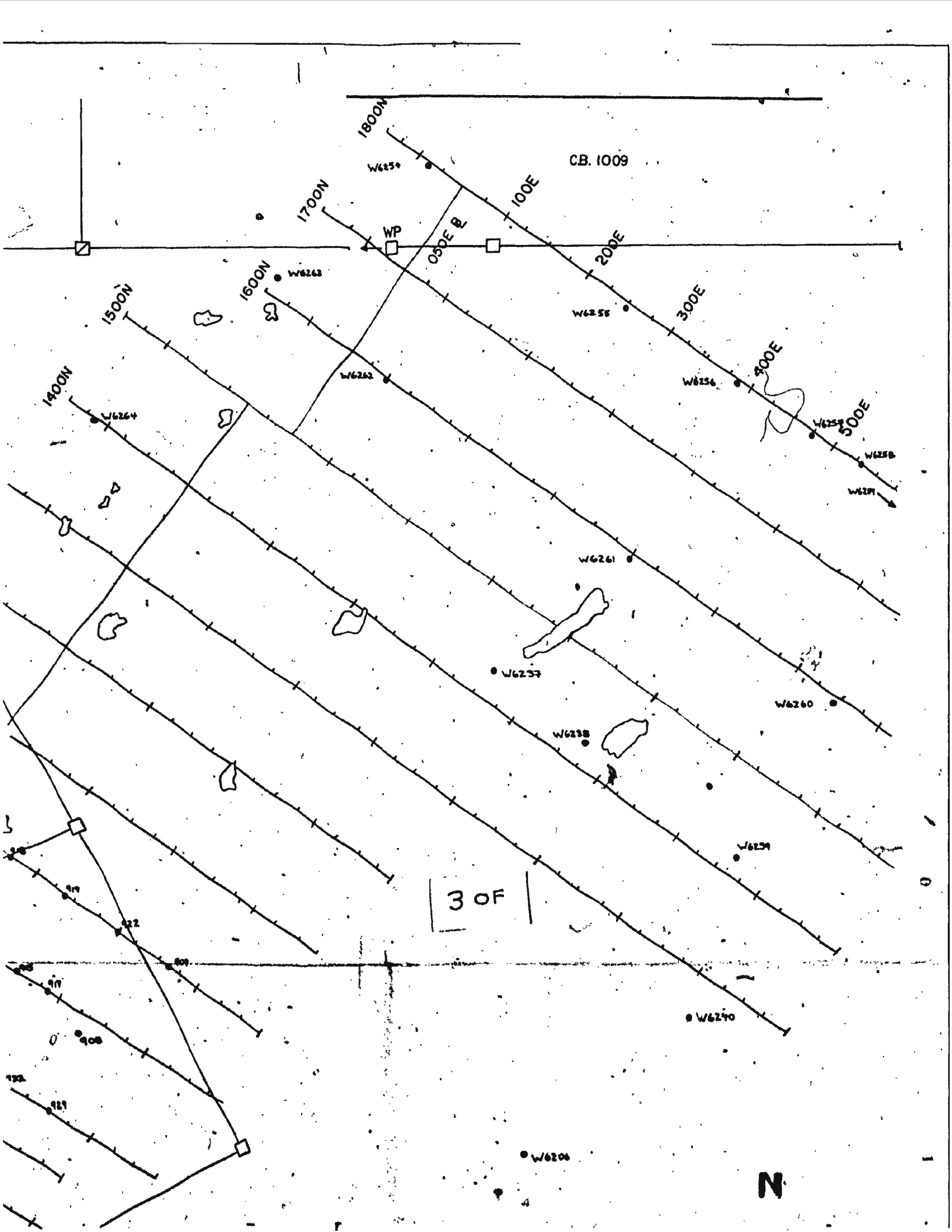
CB. 1009
1800N
1700N
1600N
1500N
1400N
100E
200E
300E
400E
500E
050E B
WP
W6254
W6255
W6256
W6258
W6259
W6261
W6260
W6257
W6238
W6239
W6240
W6206
W6262
W6263
W6264
3 OF
N

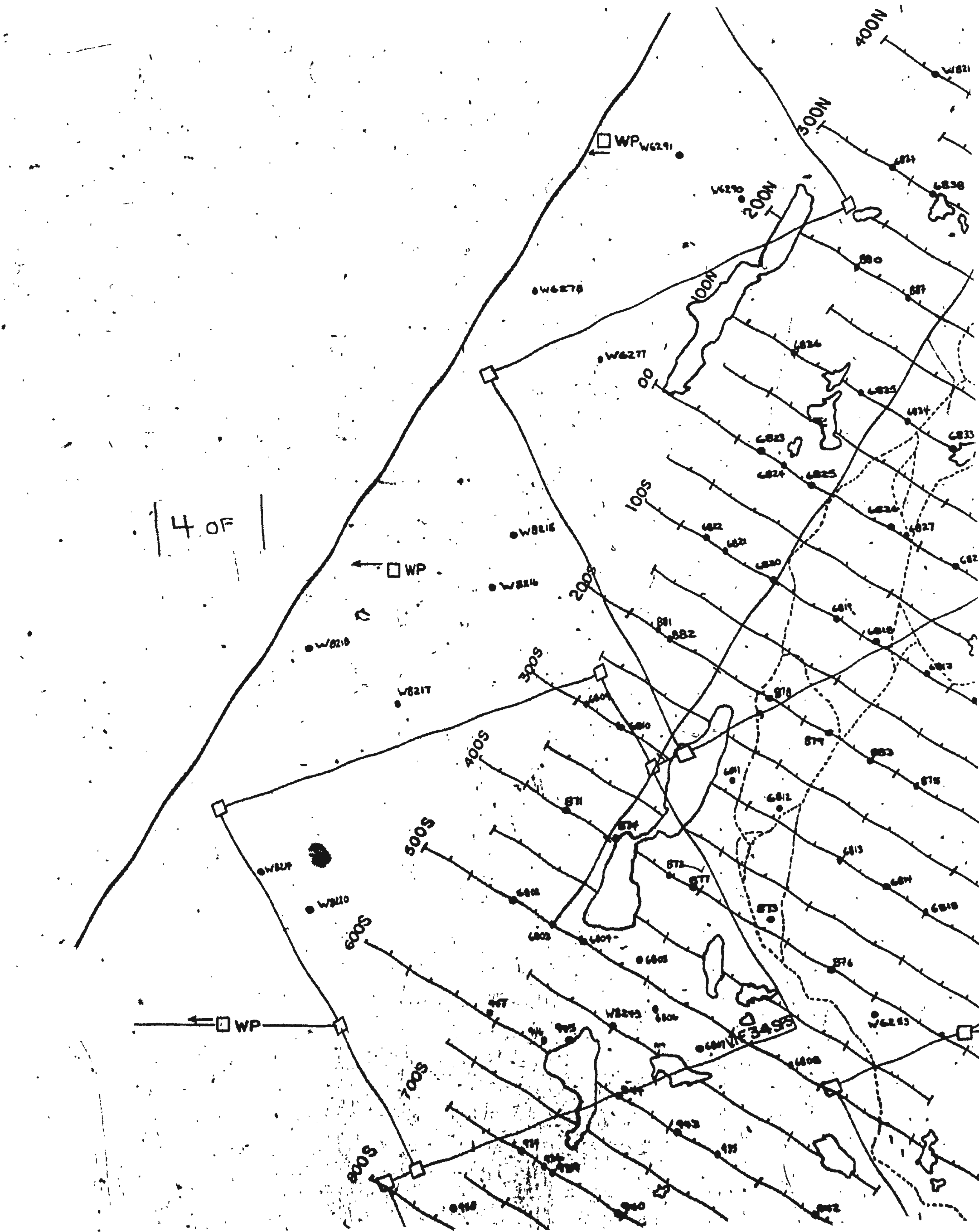
4 OF
WP
W6291
WP
WP
400N
300N
200N
100N
00
100S
200S
300S
400S
500S
600S
700S
800S
W6290
W6278
W6277
W8215
W8214
W8217
W8220
882
878
875
876
6827
6813

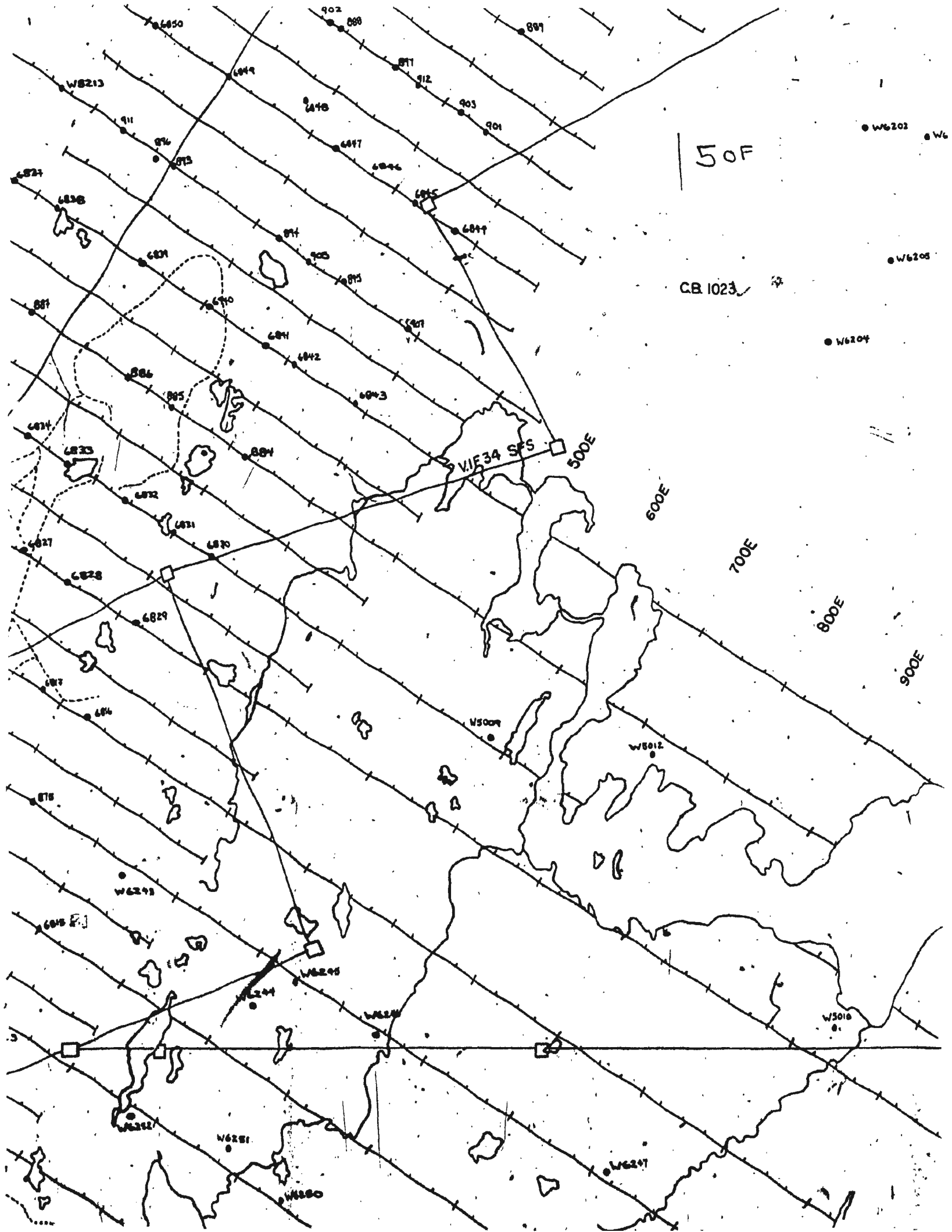
5 OF
C.B. 1023
V.I.E 34 SES
500E
600E
700E
800E
900E
W6202
W6205
W6204
W5009
W5012
W5010
W6243
W6245
W6244
W6246
W6252
W6251
W6250
W6247

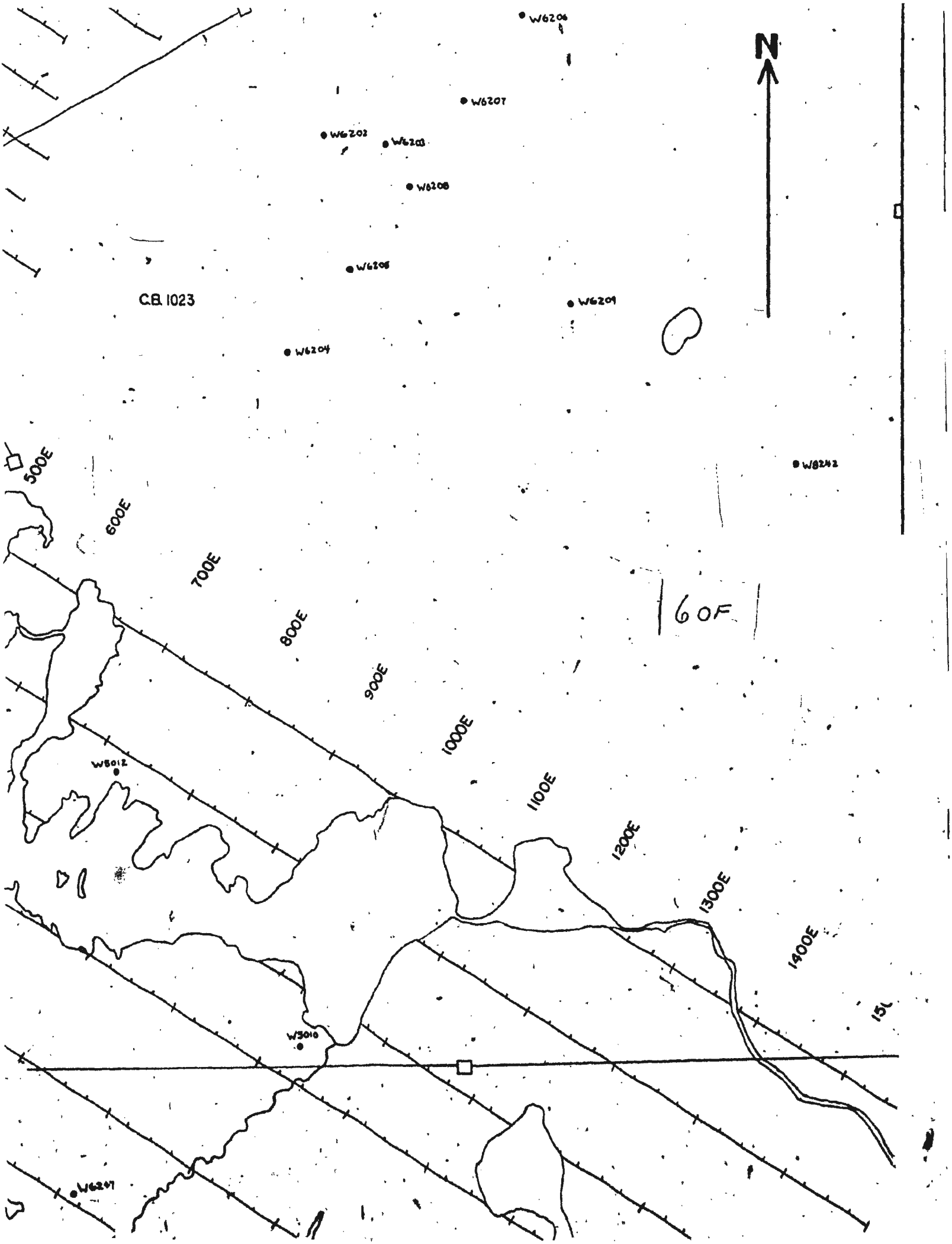
W6206
N
W6207
W6202
W6203
W6208
W6205
C.B. 1023
W6209
W6204
W8242
500E
600E
700E
800E
900E
1000E
1100E
1200E
1300E
1400E
1500
W5012
W3010
W6241

60F

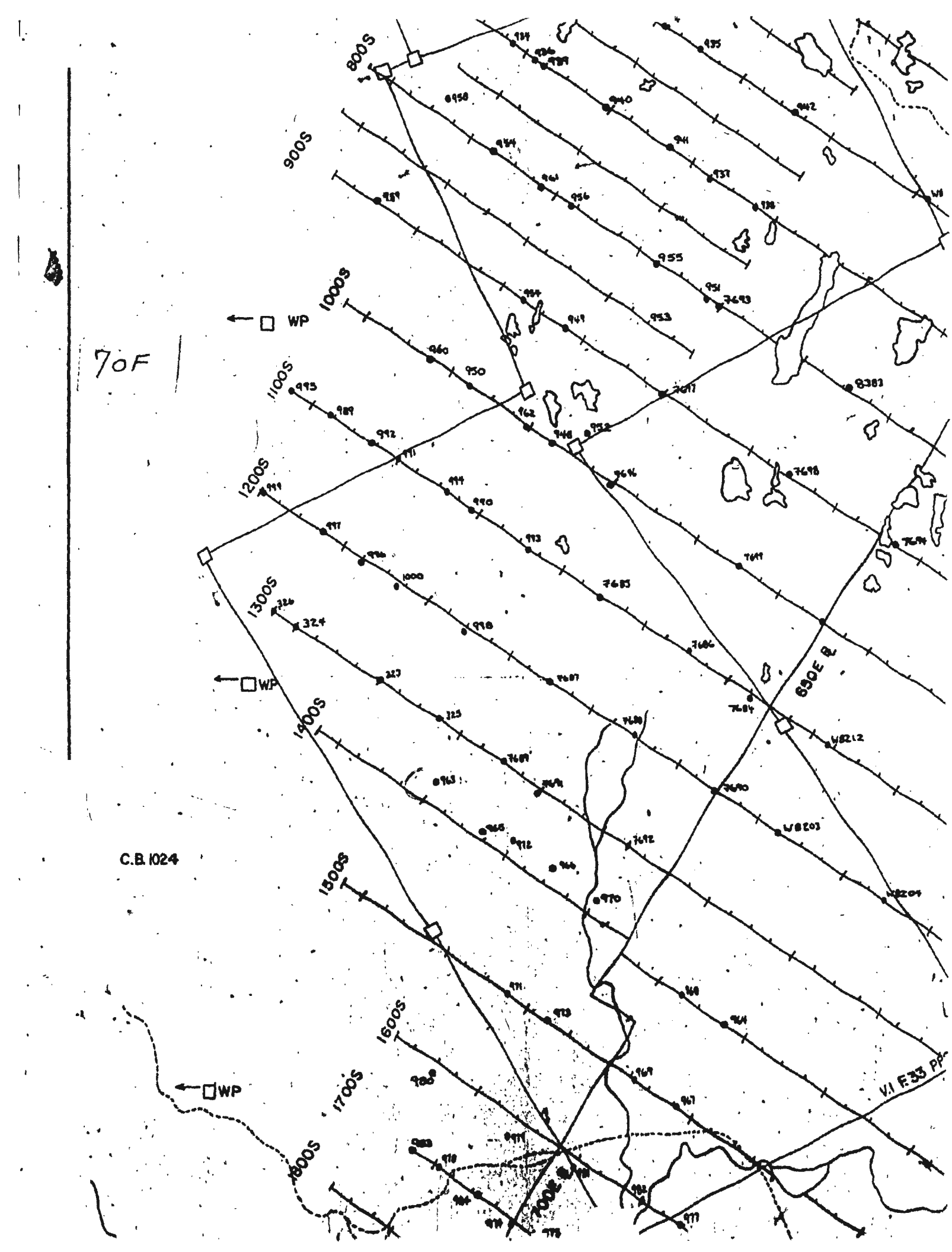
7 OF
800S
900S
1000S
1100S
1200S
1300S
1400S
1500S
1600S
1700S
1800S
WP
WP
WP
650E
C.B. 1024
V.I F.33 PP

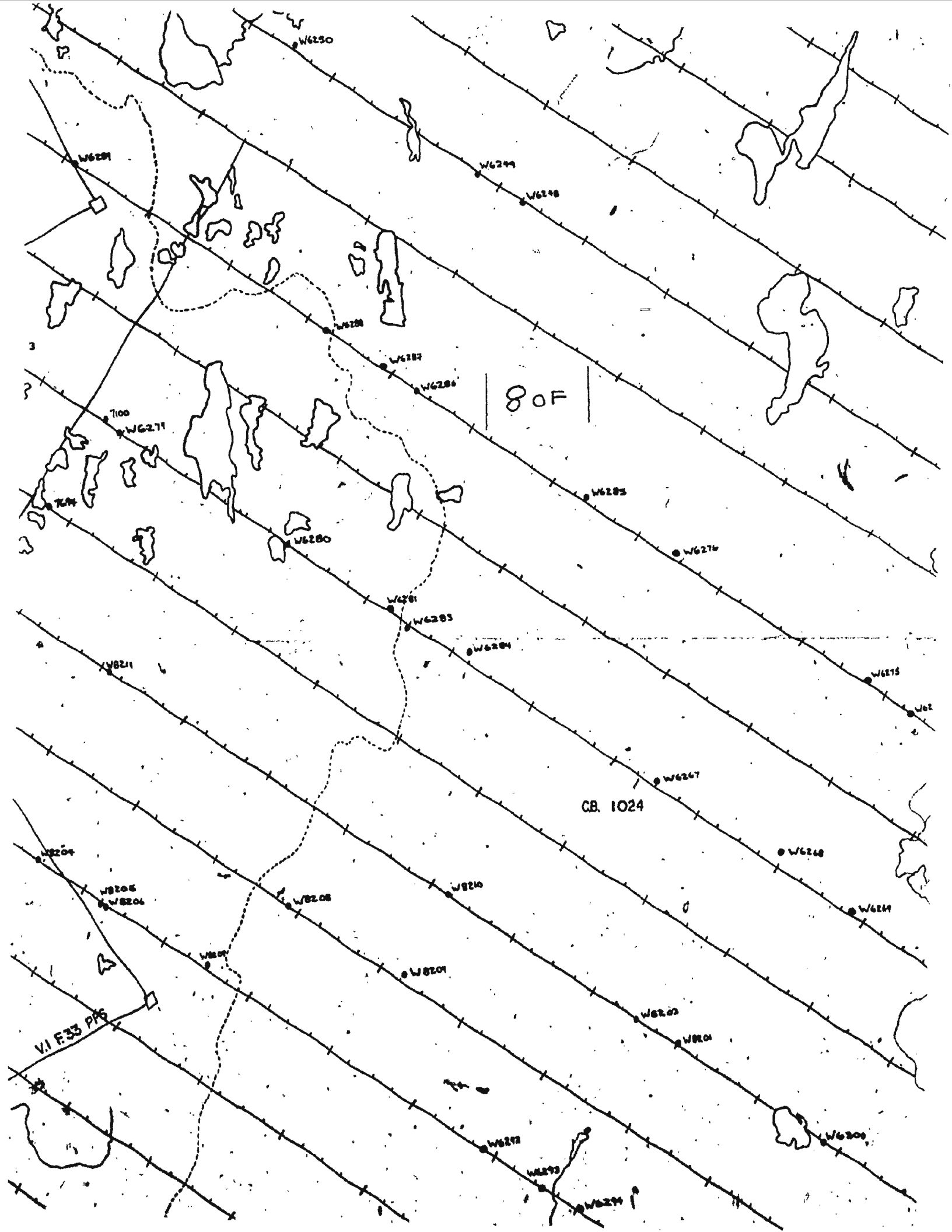
W6250
W6249
W6248
W6291
W6288
W6287
W6286
8 OF
7100
W6279
W6285
W6276
W6280
W6281
W6283
W6284
W6275
W6211
W6247
CB. 1024
W6268
W6269
W8204
W8206
W8205
W8208
W8210
W8201
W8202
W8201
V.I F.33 PPG
W6272
W6273
W6274
W6300

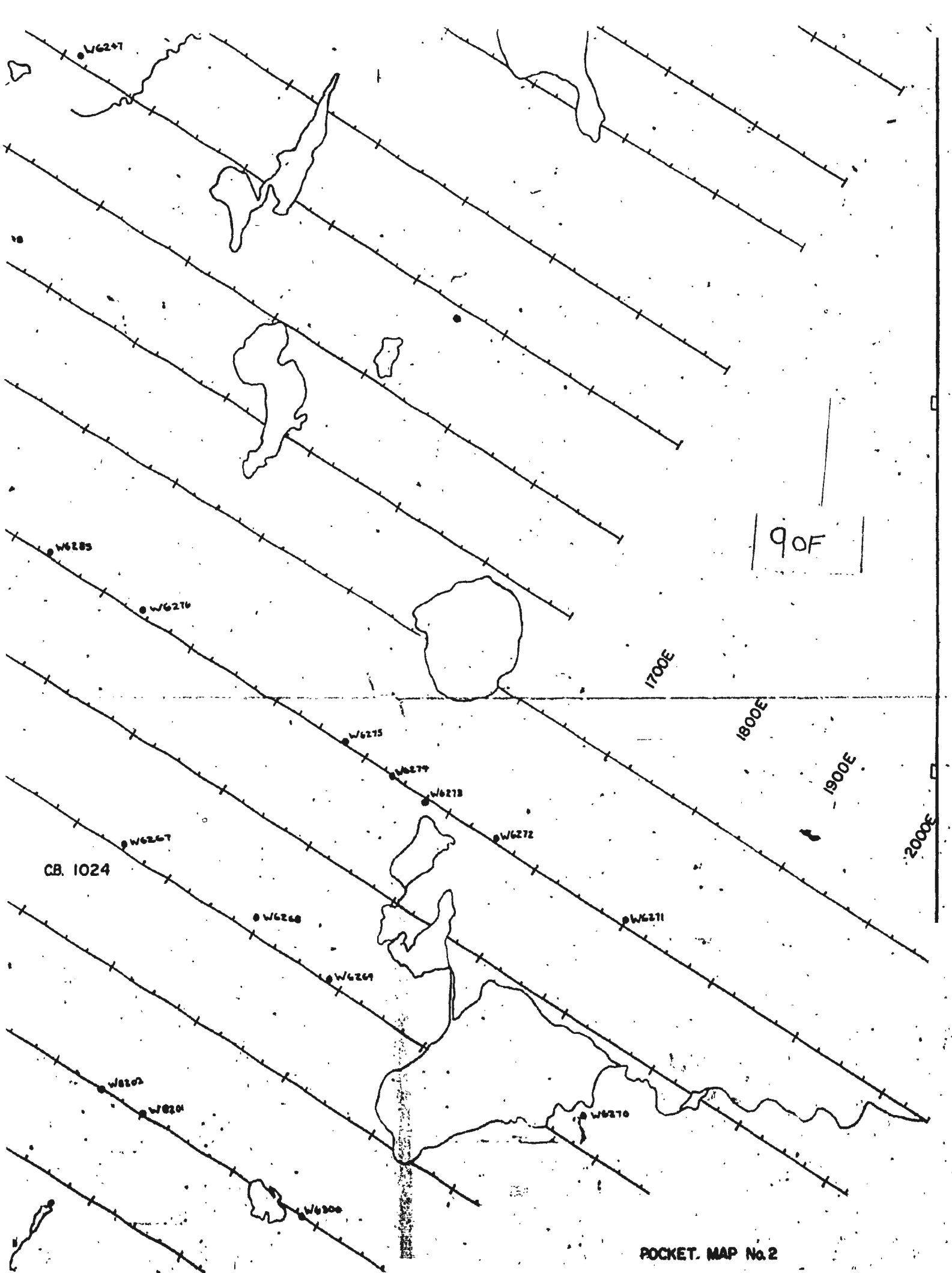

POCKET. MAP No. 2

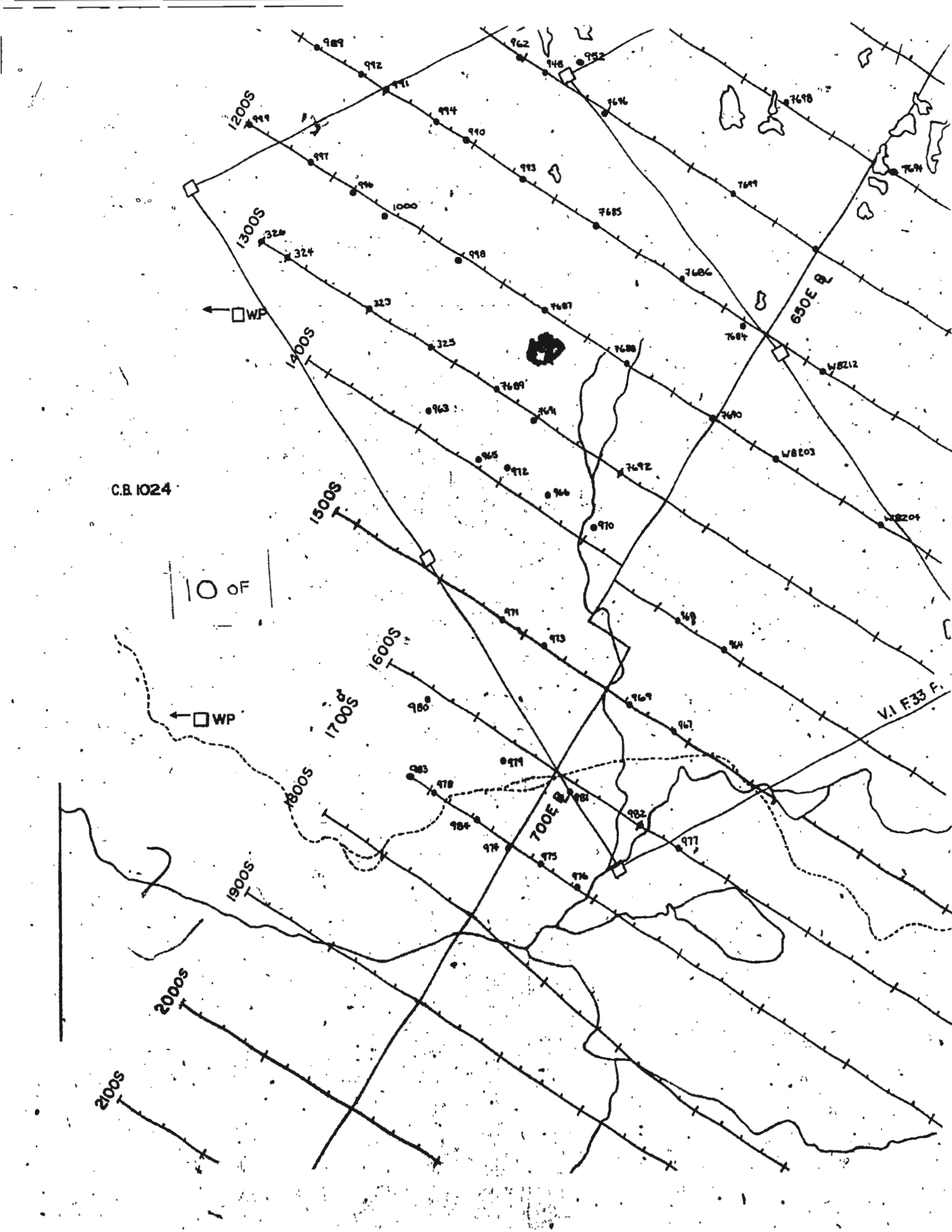
1200S
1300S
1400S
1500S
1600S
1700S
1800S
1900S
2000S
2100S
650E
700E
WP
WP
C.B. 1024
10 OF
V.I F.33 F.

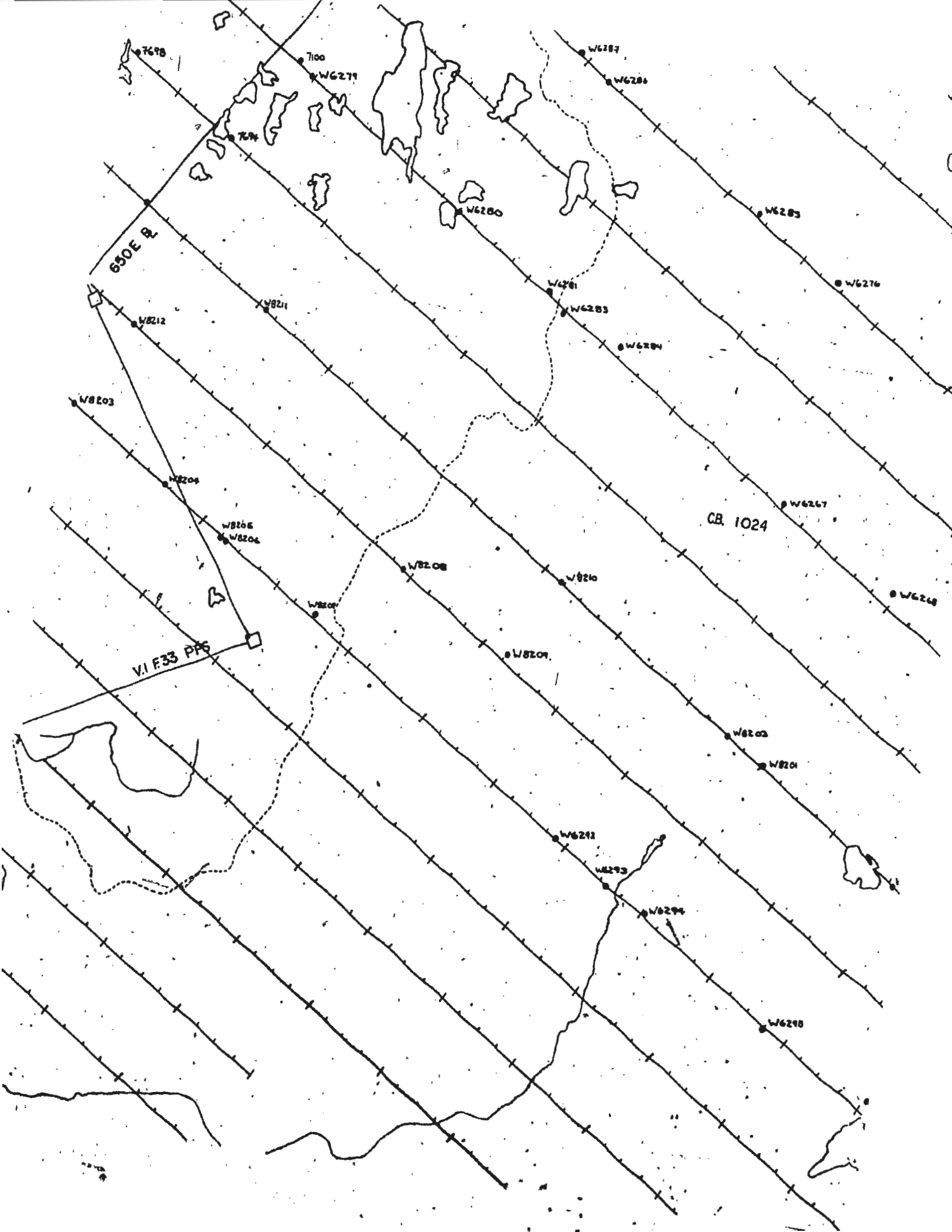
7098
7100
W6279
7094
W6280
W6287
W6286
W6283
W6276
W6281
W6283
W6284
W6267
W6268
650E
W8211
W8212
W8203
W8204
W8205
W8206
W8208
W8210
W8209
W8202
W8201
W6292
W8293
W6294
W6298
CB. 1024
V.I F33 PP6

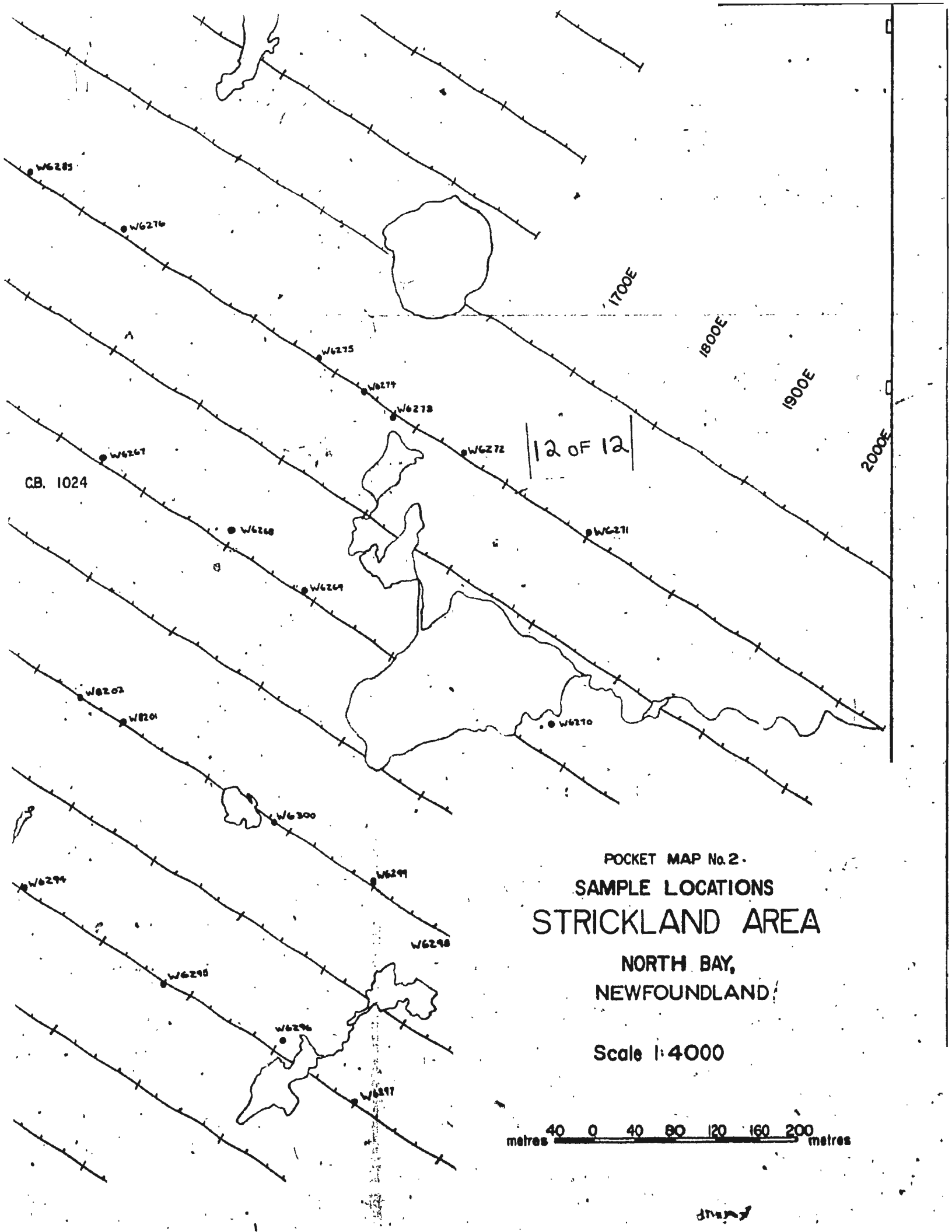

POCKET MAP No. 2.

SAMPLE LOCATIONS

STRICKLAND AREA

NORTH BAY,

NEWFOUNDLAND

Scale 1:4000

metres 40 0 40 80 120 160 200 metres